

UNIVERSITY OF CAPE TOWN

HOT-THERMISTOR SPIROMETRY FOR THE ARTIFICIAL
VENTILATION OF INFANTS

by

Timothy John Hughes

A thesis submitted in fulfil-
ment of the requirements for
the degree of Ph.D.

The University of Cape Town has been given
the right to reproduce this thesis in whole
or in part. Copyright is held by the author.

The copyright of this thesis vests in the author. No quotation from it or information derived from it is to be published without full acknowledgement of the source. The thesis is to be used for private study or non-commercial research purposes only.

Published by the University of Cape Town (UCT) in terms of the non-exclusive license granted to UCT by the author.



Figure P.0

Hot-thermistor spirometer being used for testing whether the tracheotomised infant can maintain an adequate ventilation level without assistance.

I hereby declare that the contents of the accompanying thesis "Hot thermistor spirometry for the Artificial Ventilation of infants" is completely my own work in concept and execution except for the mechanical design of the flow sensor assembly which was developed jointly with D. Ijams and J. North who contributed as much to the design as myself.

Signed by candidate

T.J. HUGHES, Pr.Eng.

23rd December 1981.

CONTENTS

	<u>Chap.</u>	<u>Page</u>
Acknowledgements		(i)
Abstract		(ii)
Introduction	0	1
Units, Terminology, Abbreviations, Symbols	1	17
Infant Flowmeter : Infant Parameters and Technical Requirements during Artificial Ventilation	2	22
Flow Measurement and Spirometry	3	38
Hot-Thermistor Spirometry	4	60
Design of Flow-Sensor Assembly	5	99
Measuring the Work of Ventilation and the Respiratory System Impedance	6	105
Evaluation of the Hot-Thermistor Spirometer/Flowmeter	7	128
Selection and Evaluation of Pressure Transducer	8	145
Evaluation of Respiratory Impedance Analyser	9	148
<hr/>		
Appendix A - Calculating Peak Expiratory Flow Rate (V_{exp}) and Gas Trapping in Controlled Ventilation		167
Appendix B - A New Technique for Use with the Method of Forced Oscillations : Measuring Resistance and Reactance from Power Measurements		171
Appendix C - Correcting Volumes for Temperature and Vapour Pressure Changes		174
Appendix D - Multipliers and Linearisation		175
Appendix E - Pressure Transducer Amplifier		179
Appendix F - Flowmeter Circuits		184
Appendix G - Impedance Analyser Circuits		190
Appendix H - Problems in the Artificial Venti- lation of Infants - A Popular View		196
Appendix I - Respiratory Analyser Test Waveforms and Results		197
References		206
Bibliography		230

Detailed Contents

	<u>Page</u>
Acknowledgements	(i)
Abstract	(ii)
<u>Chapter 0 : Introduction</u>	1
0.1 A Beginning	
0.1.1 Hot-Thermistor Anemometry	
0.2 Pulmonary Function Monitoring	
0.3 A Clinical Emphasis	
0.4 A Clinical Requirement	
0.4.1 Flow Measurement	
0.4.2 Optimal Artificial Ventilation	
0.4.3 Choosing Ventilator Settings	
0.5 Modelling and Measuring the Mechanical Properties of the Respiratory System	
0.6 The Work of Ventilation and Measurements of Respiratory Impedance	
0.7 The Objectives of this Thesis	
<u>Chapter 1 : Units, Terminology, Abbreviations and Symbols</u>	17
1.1 Units : S.I. versus "medical" units	
1.2 Terminology Spirometer, Respirometer, Pneumotachograph, Flowmeter	
1.3 Abbreviations and Symbols	
1.3.1 Abbreviations and Subscripts	
1.3.2 Symbols	
<u>Chapter 2 : Infant Flowmeter : Infant Parameters and Technical Requirements during Artificial Ventilation</u>	22
2.0 Introduction	
2.1 Respiratory Parameters in Infants	
2.2 Infant Flowmeter/Spirometer : Specification and Requirements	
2.2.1 General Requirements	
2.2.2 Measured Quantities	
2.2.3 Required Accuracy and Its Specifications	
2.3 Conclusions and Comments	
<u>Chapter 3 : Flow Measurement and Spirometry</u>	38
3.0 Introduction	
3.1 A Review of Measurement Techniques	
3.1.1 Plethysmography	
3.1.2 Collection Techniques	
3.1.3 Turbine and Rotating Vane Flowmeters	
3.1.4 Flow-Resistance Flowmeters	
3.1.5 The Fluidic Flowmeter	
3.1.6 The Corona Discharge Mass Flowmeter	
3.1.7 Vortex Flowmeters	
3.1.8 Ultrasonic Flowmeters	
3.1.9 Hot-Wire and Hot-Thermistor Anemometer/Spirometers	
3.2 Conclusions	

Chapter 4 : Hot-Thermistor Spirometry

60

4.1	Heat-Transfer Equations
4.2	Constant-Temperature Anemometry
4.3	Temperature Compensation
4.4	Linearisation Techniques
4.5	Thermistors
4.6	Hot-Thermistor or Hot-Wire Spirometer?
4.7	Frequency Response
4.8	Thermistor Spirometry : More Detailed Aspects of This Work
4.8.1	New Temperature-Compensation Techniques
4.8.2	New Linearisation Techniques
4.8.3	Complete Flowmeter System
4.8.4	Flow-Sensing Threshold
4.9	Summary and Conclusions

Chapter 5 : Design of Flow-Sensor Assembly

99

- 5.0 Design of Flow-Sensor Assembly

Chapter 6 : Measuring the Work of Ventilation and the Respiratory System Impedance

105

6.0	Introduction
6.1	Modelling the Ventilator
6.2	Respiratory Power and the Work of Ventilation
6.3	Measuring Respiratory Impedance - A Review
6.3.1	Static Measurements
6.3.2	Sampling Techniques
6.3.3	Loop-Flattening and Related Techniques
6.3.4	The Method of Forced Oscillations and Other Phase-Angle Methods
6.3.5	Respiratory Impedance from Work or Power Measurements
6.4	Measuring Respiratory Impedance - This Work
6.4.1	Problems with the Method of Forced Oscillations
6.4.2	Measuring Respiratory Resistance and Compliance from Measurements of Respiratory Power
6.4.3	Sampling for Measuring Respiratory Resistance and Compliance
6.5	Summary and Conclusions

Chapter 7 : Evaluation of the Hot-Thermistor Spirometer/Flowmeter

128

7.1	Test Methods
7.2	Results and Discussion
7.2.1	Accuracy and Linearity
7.2.2	Temperature Effects
7.2.3	Humidity and Condensation
7.2.4	Effects of Gas Mixtures and Vapours
7.2.5	Entrance Effects
7.2.6	Long-Term Stability
7.3	Clinical Evaluation
7.3.1	Reliability
7.3.2	Clinical Utility of the Hot-Thermistor Flowmeter
7.4	Suggested Improvements to the Hot-Thermistor Flowmeter based on Clinical Experience and Testing
7.5	Conclusions

Detailed Contents (Contd)

	<u>Page</u>
<u>Chapter 8 : Selection and Evaluation of Pressure Transducer</u>	145
8.0 Selection and Evaluation of Pressure Transducer	
8.1 Summary and Conclusions	
<u>Chapter 9 : Evaluation of Respiratory Impedance Analyser</u>	148
9.0 Introduction	
9.1 Laboratory Tests	
9.1.1 Lung and Airways Simulator	
9.1.2 Mechanical Simulation	
9.1.3 Electrical Simulation	
9.1.4 Calculations	
9.2 Results	
9.3 Discussion	
9.3.1 Sampling Point	
9.3.2 Accuracy	
9.3.3 Clinical Evaluation	
9.4 Conclusions	
<u>Appendix A :</u>	167
Calculating Peak Expiratory Flow Rate and Gas Trapping in Controlled Ventilation	
<u>Appendix B :</u>	171
A New Technique for Use with the Method of Forced Oscillations : Measuring Resistance and Reactance from Power Measurements	
<u>Appendix C :</u>	174
Correcting Volumes for Temperature and Vapour Pressure Changes	
<u>Appendix D :</u>	175
Multipliers and Linearisation	
<u>Appendix E :</u>	179
Pressure Transducer Amplifier	
E.1 Statham Instruments Model P 23 db Pressure Transducer	
E.2 Instrumentation Amplifier	
<u>Appendix F :</u>	184
Spirometer/Flowmeter Circuits	
<u>Appendix G :</u>	190
Impedance Analyser Circuits	
<u>Appendix H :</u>	196
Problems of Infant Ventilation - a Popular View	
<u>Appendix I :</u>	197
Respiratory Analyser Test Waveforms	
References	206
Bibliography	230

Key words : infant, monitoring, spirometry, pneumotachography, anemometry, constant temperature, thermistor, respiratory impedance, respiratory compliance, respiratory resistance, work of ventilation.

Artificial ventilation of an infant's lungs, either during anaesthesia or during respiratory insufficiency, poses special problems not encountered with adults. These problems are associated with the infant's small tidal volume, the small lung-chest compliance, the high airways resistance and the low gas flow rates. Difficulties in optimising infant ventilation are compounded by the still widespread use of adult ventilators and even adult tubing and fittings, which are unsatisfactory for infant use.

This thesis describes equipment and techniques which were developed for use in monitoring mechanical aspects of artificial ventilation and optimising ventilation procedures. A strong emphasis is placed on the clinical applicability of the techniques and clinical applications are discussed.

A new temperature-compensated hot-thermistor anemometer/spirometer was developed because the wide variety of spirometers described previously for measuring respiratory volumes and volume flow rates were unsatisfactory for routine use in monitoring infant ventilation. The principles of hot-thermistor spirometry were investigated both theoretically and experimentally to develop new temperature-compensation techniques and to predict the effect of gas composition changes on spirometer calibration. New electronic circuits were developed which greatly simplify the construction of temperature-compensated hot-thermistor anemometers and extend the dynamic range of flow rates that can be measured.

The new spirometer/flowmeter can measure instantaneous flow rates from approximately 50 ml/minute to above 50 litres/minute. Accuracy is within 5 percent of reading over a 200 : 1 dynamic range above 0.45 litres/minute. The spirometer measures average volume flow rate (minute ventilation) to an accuracy of 5 percent under most

conceivable conditions of clinical usage and with the (iii) lowest minute ventilation levels likely in infants (300 ml/min). Humidity and common anaesthetic gasses and vapours have only a small effect on spirometer calibration, except for nitrous oxide which requires a switched correction factor to compensate for the resultant under-estimation of flow rate.

New theoretical techniques were developed for use with the hot-thermistor spirometer for monitoring the mechanical properties of the infant's chest/lungs and measuring the work of ventilation. Unlike conventional techniques for measuring the mechanical driving point impedance of the respiratory system, the new techniques are based on measurements of mean respiratory power and mean squared flow rate and offer theoretical and practical advantages over conventional techniques. One of the new techniques was implemented in hardware and compared in laboratory and clinical tests with the classical "zero crossing" sampling technique first described by Neergaard and Wirz. The new technique was found to be more accurate and reproducible and less susceptible to artifacts than the classical sampling technique.

A new theoretical technique for respiratory impedance measurement using the method of forced oscillations was developed but this technique was not tested practically.

INTRODUCTION

0.1 A Beginning

My interest in the artificial ventilation of infants arose from a request for help from Consultant Anaesthetists at the Red Cross War Memorial Children's Hospital in Cape Town in late 1976. They wished to measure the tidal volume (volume/breath) of artificially ventilated infants so that they could eliminate trial-and-error methods of ventilator adjustment. Gas-flow measuring devices (spirometers, respirometers) are often used during anaesthesia for monitoring ventilation levels in adults, but these devices (usually turbine flowmeters) are inaccurate and unreliable when used for infants owing to the infant's small tidal volume (neonate : 15 ml./breath). Even without the use of a flowmeter correct ventilation in adults is much easier to maintain than it is in infants.

The problem of controlling ventilation in infants is made more difficult by the still widespread use of adult ventilators and fittings [1], which are mostly unsuitable for infant use [2]. Volume-cycled ventilators in theory offer accurate control of ventilation. In practice the "compressible volume" of the ventilator, humidifier and tubing, may absorb an appreciable proportion of the volume delivered by the ventilator [3][1][4]. Any flow sensor must, therefore, sense flow in circuit as it enters (or leaves) the patient rather than flow as it leaves the ventilator. The ventilator circuit near the patient offers a very harsh environment for flow sensing with high humidity, rapid temperature variation (inspiration to expiration), widely varying gas and vapour mixtures

(sometimes flammable) and water from condensation. In addition, the flow regime is often transitional from laminar to turbulent so that the gas velocity profile across the tubing is easily affected by factors such as water accumulation or bending of the tubing close to the sensor.

Various techniques were considered for measuring volume and volume flowrate. One of the most important aspects was that the technique chosen had to be one which would unobtrusively fit in with a wide range of standard anaesthetic and intensive care unit procedures. It was also important that the flow sensor should not change the infant's respiratory requirements by increasing respiratory deadspace or adding appreciable flow resistance. Although the mean volume flowrate required for ventilating infants ranges from about 300 ml/min to 6 L/min the peak instantaneous flows can be as high as 49 L/min depending on ventilator and inspiratory/expiratory ratio (Keuskamp in [4]). Flowmeters should thus, ideally, be able to operate with an acceptable accuracy over a dynamic range in excess of 160 : 1.

For monitoring ventilation the reproducibility of the measurement and reliability of the equipment is probably of more importance than the absolute accuracy. This is because the normal nomograms used for estimating ventilatory requirements are accurate to within only 7 percent for adults while their accuracy for infants is even lower [5].

0.1.1 Hot-Thermistor Anemometry

My previous experience, using local heat clearance for estimating blood perfusion flow in tissue [6][7], indicated that the related technique of constant-temperature hot-thermistor anemometry could form the basis for a sufficiently sensitive infant spirometer. A number of problems had to be overcome before a practical

hot-thermistor spirometer was produced. In the process new techniques for temperature compensating and linearising hot-thermistor anemometers were developed. The temperature compensation technique is particularly simple and has the advantage of allowing inspiratory and expiratory gas temperatures to be monitored. This is useful for optimising humidification so that respiratory heat and water losses are minimised without the hazard of scalding the patient.

Constant-temperature hot-thermistor anemometry involves measuring the power required to maintain a self-heated thermistor at constant resistance and hence constant temperature. Forced convection past the thermistor increases the rate of cooling and hence the heating power required to maintain the thermistor at constant temperature. This increase in heating power is a non-linear function of gas velocity and hence must be linearised before it can be processed to yield volumes or average volume flowrate. The linearising technique developed in this thesis is unusual but particularly simple to implement. The performance of the new lineariser compares favourably with complex techniques used previously.

The theoretical basis of hot-thermistor anemometry was developed to predict the effect of varying gas mixtures and temperature on flowmeter calibration.

0.2 Pulmonary Function Monitoring

While investigating techniques for measuring tidal volume and flowrate it was realised that a much wider variety of practical clinical problems related to optimising ventilation required a suitable flow sensor.

Two general fields were considered :

- (i) Monitoring gas exchange function of the cardio-pulmonary system. This requires additional automated gas-analysis measurements.

- (ii) Monitoring mechanical properties of the patient's lungs/chest/abdomen and the work of ventilation. This requires additional pressure measurements.

Both of these general areas have potential for optimising ventilation procedures and detecting incipient problems. During work on this thesis there has been an increasing interest in comprehensive automated monitoring of this sort [8][9][10][11], but the clinical utility and cost benefit have yet to be demonstrated [8]. Pulmonary function testing in small infants has attracted far less attention than in adults [12][1][13]. Pulmonary function tests on adults are carried out routinely in most large hospitals but, in general, infant testing is done for research purposes only. This probably stems from the greater technical difficulties and the fact that simple techniques requiring patient co-operation cannot be used on infants [12][1]. For routine use on infants it is thus necessary to be able to automate the measurement techniques reliably.

Polgor [12] has discussed quite fully the possible clinical applications of pulmonary function tests for children and infants. Some of his suggestions are worth quoting and paraphrasing here, in particular those relating to surgery : "It should be routine to evaluate respiratory functions in all patients scheduled for cardio-pulmonary operations and in all others with questionable pulmonary status who are undergoing major surgery. Tests may be required, before, during and after surgery : prior to surgery for indicating or contraindicating surgery and for estimating the immediate risk of surgery; during surgery for assuring adequate ventilation, for guiding the surgeon in the execution of the operative plan by testing the functional effects of the procedures and for predicting the ventilatory assistance needed in the post-operative phase; after surgery for indicating and controlling supportive measures of ventilation and for detecting complications. The method of measurement under

these circumstances depends on technical feasibility. The ideal situation requires permanent equipment in the respective areas for routine measurements of pulmonary functions according to the needs in various diseases." (Condensed from [12].)

I decided not to pursue automated gas-exchange function testing because, although potentially of very great benefit to patient management, it necessitates a large increase in cost and complexity. Monitoring the mechanics of breathing is less complex and does not require as much hardware or maintenance support. In addition such equipment could be useful for training clinicians to optimise mechanical aspects of ventilation using less sophisticated equipment. For example, many of the mechanical aspects can be assessed qualitatively by inspecting the instantaneous flowrate waveform and watching the ventilator's pressure gauge. Providing quantitative information can aid the process of learning to use this visual information.

0.3 A Clinical Emphasis

Much work in biomedical engineering does not receive the acceptance it deserves because the clinical significance and clinical applications of the work are not emphasised. This often stems from the uncompromising engineering or mathematical approach taken by the biomedical engineer. This emphasis on engineering, almost to the exclusion of medicine, severely handicaps the acceptance and utilization of the work. In a similar way mundane, practical matters related to the clinical situation are probably more important than anything else in determining the success of clinical instrumentation. These environmental and human engineering aspects ultimately determine the success or failure of the instrumentation but are often neglected.

In this thesis I have tried to strike a balance between emphasizing clinical applications on the one hand and engineering and theoretical aspects on the other. To make the clinical aspects more cohesive I have separated them from engineering aspects where possible. Descriptions of clinical practice are included to justify the engineering approach taken and to place the work in perspective for the reader with no clinical experience.

Wilson and Bone ([8] p 431) in a recent (1980) review commented on respiratory monitoring techniques :

"Special scrutiny should be applied to two areas in assessing the potential value Can this technique provide the information it claims in a reliable manner, under usual clinical conditions? and Of what value to patient management are the data produced? The presentation of more data than can be assimilated can contribute to incorrect clinical decisions. This factor is too often ignored in assessing the utility of new measurements."

Smith, in his well-known book on infant anaesthesia [14] cautioned :

"Any added manouvre or device carries its own risk and also divides the anaesthetist's attention."

These human engineering aspects were dealt with and assessed by spending considerable time in the clinical environment both before and after developing hardware. A small but important part of this thesis discusses critically some of these hardware aspects in the light of clinical experience.

0.4 A Clinical Requirement

Artificial ventilation is necessary during anaesthesia for surgery but it is also extremely important postoperatively and during respiratory insufficiency.

"Respiratory insufficiency is now the major cause of post-traumatic and postoperative death." (Peters,1972) [15]

"Respiratory failure (in congenital heart disease) is a serious and frequent complication in the lower age groups ventilatory support is likely to become of increasing importance as the age of corrective surgery is lowered." (Battersby,1974) [4]

Okmian commented that where ventilation levels are not monitored :

"The unusually large reduction in total (respiratory) compliance which could be recorded in connection with surgical manipulations may thereby endanger maintenance of adequate ventilation to the child." [16]

Half of the chronic diseases of childhood are related to respiratory disease while it accounts for 75 percent of all problems seen in neonates and 25 percent of all admissions to paediatric hospitals. [13] This high incidence of respiratory disease, combined with some of the physiological and anatomical differences between adults and infants, explains why acute respiratory failure is common in infants, especially in the first year of life [13]. Artificial ventilation is used in the treatment of respiratory failure only when other support measures such as supplementary oxygen have failed. This is because even under ideal conditions artificial ventilation has a number of undesirable side effects, it can be iatrogenic [4] and is difficult to control :

"The main problem in artificial ventilation of the newborn is how to predict, control and achieve an optimal alveolar ventilation." (Mattila) [17]

Problems of ventilator therapy for infants including ethical and legal aspects have even been aired in the popular press. (See Appendix H.)

0.4.1 Flow Measurement

Although paediatric surgery and anaesthesiology are relatively young specialities [3], it has long been realised that there is "clearly a need not only for specially designed ventilators but also for ventilation-measuring equipment suitable for children", (Mushin, Mapleson, Lunn) [2]. The requirements for new apparatus have been known for a considerable time:

"Apparatus scaled to size, which adds no deadspace, demands no work, which is used at the right ambient temperature, which is accurate, and let it be added which does not exist!" (Cross, 1965) [18]

A recent (1980) independent market survey showed that in the (generally less demanding) adult spirometer market "there is a substantial negative attitude to lung function-testing spirometers." These were said to exhibit "constant breakdowns despite fantastic expense and a proliferation in the market place of expensive and inaccurate devices!" [19]

Hilberman suggested in 1977 that "the next critical step" for intraoperative monitoring is :

"a concerted effort to develop flow and gas sensors that are convenient to use, light weight, and do not interfere with the important airway manipulations of the anaesthesiologist." [11]

He cautioned that "it is not certain that such devices will be easy to introduce once built" primarily due to the small number of "catastrophes" encountered by an anaesthetist during his career and thus little pressure for the introduction of such devices. He also commented that "confirmation of the value of the instrumentation is likely to depend upon demonstrating that undesirable events are reduced in frequency, and that the devices perform reliably and safely without providing misinformation to their user." [11]

In a review of a number of cases of cardiac arrest during anaesthesia hypoventilation was found to be the single most important contributory factor accounting for about 40 percent of cases. [20]

0.4.2 Optimal artificial ventilation involves delivering sufficient oxygen to the alveoli in such a way that correct tissue oxygenation results with a minimum of undesirable side effects. Ventilation requirements are thus determined not only by metabolic requirements but by cardiac function and lung gas-exchange function. For example, gross cardiac or circulatory pathology may limit achievable tissue oxygenation even with very high levels of alveolar ventilation. Under these circumstances hypoventilation may be unavoidable since any further increase in ventilation could rupture the lungs. Any hypoventilation and the associated tissue hypoxia may permanently damage tissue with high metabolic requirements and limited oxygen reserves, especially the brain. This has led to a greater emphasis on not just patient survival but intact patient survival :

"Before commencement of (respiratory) therapy during the treatment or in the weaning period the patient's brain may undergo hypoxic periods which result in permanent cerebral damage. The object of the therapy is to protect the patient against such hypoxic episodes and to guarantee intact survival."

Mattila (1974)[17]

Even mild hypoventilation adversely affects cellular function owing to the resultant respiratory and metabolic acidosis which may ultimately precipitate cardio-respiratory failure especially in neonates (Stern in [4]).

Hyperventilation is also potentially hazardous, particularly in long-term ventilation and with high inspired oxygen concentrations. Hyperventilation generally results in excessive carbon dioxide elimination which causes respiratory alkalosis, tetany, hypokalemia and depression of (spontaneous) respiratory drive. Ventilation levels are often assessed by measuring carbon dioxide elimination since many of the side effects of

incorrect ventilation are related to incorrect carbon dioxide elimination. Setting ventilation levels in this manner by measuring end expired CO₂ levels is prone to a variety of technical errors [4] and can also lead to hypoventilation in the presence of abnormal ventilation/perfusion ratios [4][8]. With the increased use of long-term ventilation " the limited value of Pa CO₂ measurements must be recognised. Even when they are combined with O₂ saturation measurements, Pa CO₂ measurements cannot predict the onset of hypoxemia and marked atelectasis." (Hedley-Whyte [196])

Direct arterial blood sampling with blood gas analysis has a number of problems for assessing ventilation in infants. It has about twice as many undesirable sequelae as in older patients [4]. In addition "some patients require artificial ventilation when fatigue appears regardless of the results of blood gas determinations. in older infants and children such (blood gas) determinations are misleading if the sampling technique distresses the patient and increases oxygen needs." Brown [13].

"Excessive ventilation may occur more often than is realised when artificial respiration is maintained in an anaesthetised patient for longer periods of time and may contribute to operative and postoperative morbidity and mortality." (Smith [14])

In hyperventilation, with high inspired oxygen concentrations, oxygen toxicity also has a variety of potentially damaging effects e.g. lung damage, anaemia, and blindness in preterm infants.

Cardiac function is adversely affected by the increased intrathoracic pressure during artificial ventilation which compresses the heart, increases pulmonary vascular resistance and interferes with venous return. [21] The higher pressures also cause gradual long-term damage to the lungs impairing mechanical and gas-exchange function. [21][4] This damage makes

weaning from the ventilator more difficult the longer the patient remains connected to the ventilator.

The maintenance of "correct" ventilation in infants is particularly critical as:

"There is a greater need for individualised calculation of respiratory volume for children than for adults. In addition the demand for accuracy in these calculations becomes greater the smaller the tidal volume is." (Okmian [3])

Smith has stressed the difficulty and variability encountered in ventilating infants :

"Trial and error may be the only clinical way to choose a respirator for a patient and each patient is for some reason different and success in one case may be followed by failure in the next." [14]

It has been suggested [11] that artificially ventilated black patients are at significantly higher risk than white patients since in these patients even gross hypoxia and changes in peripheral perfusion cannot be detected by skin colour changes. Respiratory monitoring is thus even more important in a country like South Africa with a large black population.

0.4.3 Choosing Ventilator Settings

Ventilation waveforms and airways pressures are known to affect cardio-pulmonary function. Exactly what ventilator settings, airways pressures, and flow waveforms optimise ventilation, minimising side effects for a particular patient with particular lung properties, is still under debate. [22][4][23][24][25][26][27][28]

During artificial ventilation the mechanical properties of the lungs/chest, particularly the lung compliance, is thought to change owing to the gradual development of atelectasis which is normally reversible by periodic hyperinflation. [16] Because of the many interrelated variables i.e. type of ventilator, ventilator

settings, patient connections and patient cardio-pulmonary function, no consensus exists as to how "ideal" ventilation should be performed. Only very carefully controlled experiments like those of Lindahl [22] can ultimately determine "ideal" ventilator settings and waveforms for different patients. Monitoring changes in the mechanical properties of the lungs does form an objective basis for choosing ventilator settings and allows some monitoring of the effects of different ventilator settings, particularly in long-term ventilation where gradual damage to the lungs may occur.

0.5 Modelling and Measuring the Mechanical Properties of the Respiratory System

The mechanical properties of the respiratory system are frequently modelled using a linear, single compartment, lumped element equivalent circuit. (See figure 0.1 [29][30][31][32])

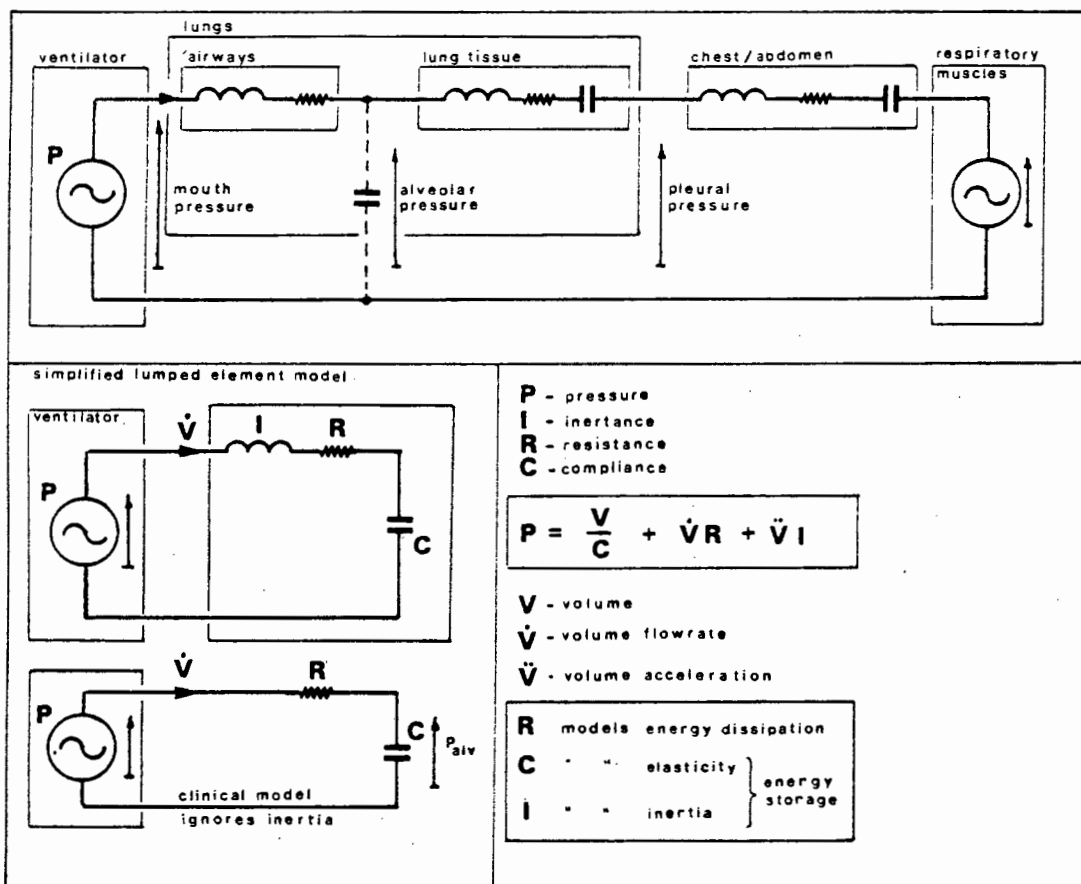


FIG.0.1 Mechanical/electrical models of the respiratory system

Electrical network theory can then be used to analyse mechanical aspects of ventilation. This lumped element, linear representation is a fairly gross approximation to the respiratory system, which is distributed, non-linear, hysteretic and exhibits differences from inspiration to expiration [30][29][33]. However, this model has proved extremely useful as a qualitative tool for describing mechanical aspects of respiration, for diagnostic purposes and for use in controlling artificial ventilation [12][29][21][197]. Parameters of more complex models are sometimes calculated [32][34] but for routine clinical use, in optimising ventilation, it is doubtful whether the added complexity is justified, or that the more complex model will be readily accepted by the clinician. Non-linearities are smallest and the simple model is thus most accurate for quiet, steady respiration in healthy individuals at rest [35]. The model is far less accurate under a variety of other conditions : for large tidal volumes, at high respiratory rates, for forced respiratory manoeuvres, at varying levels of lung inflation and in respiratory disease [29][12][32]. During quiet respiration in infants the model is probably less accurate than it is for adults, as airways closure occurs within the range of normal tidal ventilation in infants [13]. Sometimes non-linear effects are included in the model by making the airways resistance (figure 0.1) a function of flow rate [29(iii)(vi)]. However, for clinical use, especially for controlled ventilation, the most widely used model is the simplest, first-order model.

Measuring the mechanical properties of the respiratory system often involves calculating the constants of a linear model such as figure 0.1 from measurements of pressure, flow rate and/or volume. Some techniques require patient co-operation and are thus not suitable for use on infants or in anaesthesia. Other techniques use the normal ventilation waveforms or superimpose a small high frequency sinewave

on top of the normal respiratory waveform. This latter technique "the method of forced oscillations" is essentially similar to measuring the "small signal driving point impedance" of an electrical network or device. Forced oscillations is a particularly attractive technique, as it makes no assumptions about linearity and can actually be used to investigate the variation of mechanical impedance (and hence non-linearity) at different levels of lung inflation during the normal respiratory cycle.

Different measurement techniques often give rise to different values for the same mechanical quantities. These differences are sometimes related to instrumentation but are usually related to fundamental assumptions which are only approximations : e.g. system linearity, no inspiratory/expiratory differences, sinusoidal breathing waveforms etc.

Hot-thermistor flowmeters, as used in this thesis, are inherently not direction sensitive, which complicates their use in measuring the mechanical properties of the respiratory system.

0.6 The Work of Ventilation and Measurements of Respiratory Impedance

In respiratory and cardiac diseases the work of ventilation may increase to become a substantial proportion of the patient's metabolic requirements. This can ultimately contribute to respiratory failure directly through increased oxygen requirements or indirectly through fatigue. Therefore the work of ventilation is a useful parameter for determining whether ventilatory assistance is required or for detecting changes in the patient's status (e.g. Pulmonary oedema will tend to increase the work of ventilation.) Post operatively, particularly after thoracic surgery, the work of ventilation is increased, often requiring extended ventilatory support. Measuring the work performed by the ventilator on the patient's respiratory system during controlled ventilation in surgery is one possible technique for predicting

what ventilatory support is required post operatively. During weaning from the ventilator measurements of work performed by the ventilator on the patient's respiratory system allow an objective assessment of the support being given to the patient and may simplify setting the ventilator to synchronise with the patient. In this thesis the work of ventilation was normalised per unit of respired gas volume to allow comparison between patients of different sizes or between measurements on the same patient at different ventilation levels.

Previously many researchers have measured respiratory impedance, but it is only relatively recently that analogue multipliers and digital techniques have allowed respiratory power and the work of ventilation to be measured directly in a simple way. Prior to this approximate techniques were commonly used. One such technique assumes sinusoidal breathing waveforms and calculates the work of ventilation using electrical network theory and the measured values of respiratory impedance (normally from measured values of a first-order model). This process was reversed in this thesis and a new technique was developed for calculating respiratory compliance and resistance based on mean power and mean squared flow measurements. Unlike the approximate techniques for estimating the work of ventilation which assume sinusoidal respiratory waveforms, this new technique for measuring respiratory impedance only assumes a linear respiratory model. In the case of gross respiratory system non-linearity the derived values are still important from a ventilation point of view, as they still retain a physical and physiological significance; that is the compliance depends on the average energy stored in the respiratory system, while the resistance depends on the average energy dissipated in the respiratory system over a respiratory cycle. This appears to be a significant advantage over conventional measurement methods, especially as repeatability is good because mean values are utilised rather than one or two discrete samples.

0.7 The Objectives of this Thesis

In the broadest terms the objectives of this thesis were :

- (i) to develop a practical infant flowmeter/spirometer suitable for general clinical use in optimising ventilation procedures;
- (ii) to develop reliable techniques for automatically monitoring the mechanical properties of the respiratory system specifically for optimising ventilation;
- (iii) to assess the reliability of these methods in a clinical context.

CHAPTER 1

1. Units, terminology, abbreviations and symbols1.1 Units : S.I. versus "medical" units.

I have used S.I. units where possible in this thesis, but, for reasons of clinical acceptability and safety, I have conformed to medical practice and used "medical" , non-S.I., units where these are widely used. For example, ventilator pressure gauges are invariably calibrated in centimeters of water (cm H₂O), and it would seem strange to refer to the pressure in a water-filled positive end expiratory pressure (PEEP) bottle in Pascals rather than centimeters of water.

For reasons of clinical acceptability I have used the following "medical" units :

<u>Measurement</u>	<u>Symbol</u>	<u>Units</u>
compliance	C	litres/cm water
flow resistance	R	cm water/litre/sec
inertance	I	cm water/litre/(second) ²
pressure	P	cm of water
volume flow rate	V	litres/minute (LPM) or litres/second

For force, work and power I have used S.I. units.

I have tried to avoid using medical terminology which is confusing, e.g. "elastic resistance" used medically instead of compliance.

Another problem related to units and symbols is the electro-mechanical analogy, widely used for modelling the respiratory system. Confusion may arise because, although an electrical network is usually drawn, only some of the symbols used for the electrical components correspond to those normally used in electrical texts for the same components. The issue is further confused because some of these symbols correspond to other quantities in electrical practice, e.g. I is used for inertance in medical texts,

and for current in electrical texts; V is used for voltage electrically, and volume medically with P (pressure) replacing voltage. I have used the medical terms and symbols in this thesis, except in appendix B, where I have defined and used the electrical symbols to allow comparison with standard texts on electrical theory.

Conventional electrical symbols compared with electro-mechanical (medical) symbols used in this thesis :

Electrical		Electro-mechanical	
Measurement	Symbol	Measurement	Symbol
capacitance	C	compliance	C
charge	Q	volume	V
current	I	flow rate	V
inductance	L	inertance	I
power		power	
resistance	R	resistance	R
voltage	V	pressure	P
work		work	

1.2 Terminology

Spirometer, respirometer, pneumotachograph, flowmeter

Strictly speaking, a (re)spirometer is a device that measures respiratory gas volumes. The term pneumotachograph (or pneumotachygraph) is often used to mean a particular type of respiratory gas velocity sensor using a linear resistance flow sensor. The term is sometimes qualified to indicate other gas velocity sensors (e.g. ultrasonic pneumotachograph). Usually gas velocity sensors are calibrated in terms of volume flow rate, knowing the cross-section of the tube through which the gas flows. Volume can then be derived by integration of the instantaneous flow rate signal. Under these circumstances, it is difficult to decide which term to use for a particular instrument which may be performing a variety of roles. I have tended to use the words flowmeter and spirometer. Spirometer is used because one of the primary quantities of interest is the mean respiratory flow rate or "minute."

volume" ("minute ventilation")- conventionally the expired volume measured during a one-minute period and corrected to standardised conditions of temperature and vapour saturation.

Artificial ventilation (respiration) encompasses both controlled ventilation (respiration) where the patient's respiratory rate and tidal volume are determined solely by the ventilator and assisted ventilation where the patient's own respiratory efforts are assisted by the ventilator. Assisted ventilation often makes use of triggered ventilators which start a respiratory cycle when they sense the patient's spontaneous inspiratory effort. Synchronizing the ventilator ventilator and patient during assisted ventilation is often more difficult in infants than in adults. Manual ventilation is performed by the anaesthetist using a flexible rubber bag which is compressed by hand to inflate the patient's lungs.

1.3 Abbreviations and symbols.

The major abbreviations and symbols used in this thesis are listed below. Most symbols are defined in the text when they are first used and two additional summaries are cited in specialised sections. (See figure 4.1 and appendix B.)

1.3.1 Abbreviations and subscripts

Abbreviations

BTPS represents	body temperature and pressure saturation
BPM "	breaths per minute (respiratory rate)
et. tube "	endotracheal tube or endotracheal connector
CPAP "	continuous positive airways pressure
e.c.g.	electro cardiogram.
FRC	functional residual capacity
FS	full scale

Abbreviations (Contd)

I.C.	represents	inspiratory capacity
I.C.U.	"	intensive care unit
LPM	"	litres per minute
PEEP	"	positive end expiratory pressure
RMS	"	root mean square
VC	"	vital capacity

Subscripts

A and Alv	represent	alveolar
dyn	"	measured under dynamic conditions
end. insp.	"	measured at the end of inspiration
exp.	"	measured during expiration
insp.	"	measured during inspiration
pk	"	peak
tot.		total
vent.		of the ventilator or ventilator circuit

1.3.2 Symbols

C	represents	compliance (usually of the total respiratory system unless specified otherwise)
or C_{tot}		
C_p	"	specific heat at constant pressure
d	"	sensor diameter (hot-thermistor)
f	"	respiratory rate
g		acceleration due to gravity
G_r	"	Grashof number
h	"	heat transfer coefficient
I/E	"	inspiratory-expiratory ratio
k	"	thermal conductivity
L	"	characteristic dimension

Symbols (Contd)

N_u	"	Nusselt number
P_r	"	Prandtl number
RC	"	respiratory system time constant
R	"	resistance
$R_{tot.}$	"	total respiratory system resistance
R_{th}	"	thermistor resistance
T_a	"	ambient temperature
T_m	"	film temperature
T_s	"	sensor temperature (hot thermistor)
U	"	fluid velocity
V	"	volume
\dot{V}	"	volume flow rate (= dV/dt)
\ddot{V}	"	volume acceleration (= d^2V/dt^2)
\bar{V}	"	mean volume flow rate
\hat{V}	"	peak flow rate
V_A or \dot{V}_{alv}		alveolar ventilation in one minute (i.e. excluding anatomical deadspace)
V_D	represents	dead space
V_E	"	expired volume per minute
V_{th}		voltage across thermistor
Z		impedance

β	represents	coefficient of thermal expansion
ϕ	"	diameter
ΔT	"	temperature difference sensor to ambient (hot-thermistor)
μ	"	dynamic viscosity
ρ	"	density

CHAPTER 2

2. Infant Flowmeter : Infant Parameters and Technical Requirements during Artificial Ventilation

2.0 Introduction

A recent review of ultrasonic pneumotachographs noted that there are no accepted standards for the performance of pneumotachographs [36]. Some laboratory lung-function testing spirometers for specific tests have a standardised specification [37][38]. The requirements for different applications vary widely. The most stringent requirements are in oxygen consumption measurements, where accuracies of ± 0.02 percent may be desirable [36].

This section develops a specification for a less demanding application : monitoring ventilation levels in neonates and infants (up to say three years of age) during artificial ventilation. To develop this specification infant respiratory parameters during artificial and spontaneous ventilation were first reviewed.

2.1 Respiratory Parameters in Infants

Fully comprehensive, reliable estimates of infant respiratory parameters, both in health and disease, are generally lacking [1][12][13]. More comprehensive data exist for neonates than for older infants. Figure 2.1 summarises ventilation parameters likely to occur during spontaneous and controlled ventilation of normal infants. Most of these values were obtained from summaries in the literature. Peak expiratory and mean inspiratory flowrates in controlled ventilation were obtained by calculation using the theory developed in appendix A. Where no significant "gas trapping" occurs at the end of expiration, appendix A shows that peak expiratory flow rates are determined by total respiratory time constant and tidal volume. If we assume

Parameter	Age		Neonate		1 Year	3 Years	Comment	Source
	Preterm	1 week	Preterm	1 week				
Spontaneous Ventilation								
IC (ml)		75			260	530	Estimated from IC = FRC	
VC (ml)		141			475	910		
V _T (ml)		17			78	112		
\dot{V}_e (ml/min)	300	550			1 775	2 460	"Minute volume"	[13]
\dot{V}_A (ml/min)		385			1 245	1 760		[12]
V _D (ml)		5			22	32		[14]
f (breaths/min)		28 to 47			24	22		[1]
\hat{V} (insp. or exp.) L/min		exp. 2.2 insp. 2.9			10		Neonatal crying $\hat{V}_{exp} = 6$ to 9 L/min	[13][198][40]
C _{tot} (ml/cm H ₂ O)	0.41 to 4.2	5			16	32	Lung + thorax (thorax highly compliant)	[12]
R _{tot} (cm H ₂ O/L/sec)	43 to 118	26 to 68			13	10	(Lung + airway + thorax), increases with V	[14][17]
R _{tot.C} tot (sec)	0.05 to 0.15	0.15 to 0.33			0.21	0.32	Respiratory time constant	[12][4]
Controlled Ventilation								
Et. tube ϕ (mm)	2.5	3			4	4.5 to 5		[4]
Et. tube R (@ 5 LPM)	60 to 145	40 to 80			18 to 36	8 to 20	Resistances increase substantially with flowrate; this tends to reduce	[199]
Et. tube R (@ 20 LPM)	>> 145	60 to 140			> 36	> 20	calculated max. \dot{V}_{exp}	[200]
Et. tube connection R (@ 5 LPM)	30 to 50	20			9	2		
R.C (incl. Et.t + fitting)	0.15 to 0.5	0.24 to 0.6			0.4 to 0.6	0.6	R estimated from above resistances	
\dot{V}_{exp} (L/min)	4.3 to 1.3	7.6 to 1.9			11.9 to 7.9	11.3	V _T = spontaneous V _T (above)	Calculated
\dot{V}_{insp}	0.9	1.68			5.6	7.4	I/E = 0.5	See Appendix A
Max \dot{V}_{exp} (L/min)	21.5 to 6.4	21 to 8.4			39 to 26	53	V _T = IC, I/E = 0.5. (\dot{V}_{exp} will be lower in reality. See text.)	
\dot{V}_{insp}	4.5	7.4			18	35		

Figure 2.1 Estimates of Pulmonary Parameters in Infants. From Literature and by Calculation and Interpolation.

that the maximum tidal volume that can be safely achieved during controlled ventilation is approximately equal to the inspiratory capacity, then we can calculate the maximum possible peak expiratory flow rate. These flow rates will tend to be unrealistically high, owing to the rapid increase in airways and et. tube resistance at high flow rates, which was not taken into account in the calculation. According to Mushin, patient resistance may increase to about four times normal at 20 L/min [2]. The total resistance, including et. tube and fittings used in calculating the respiratory time constant, was estimated by assuming that the et. tube replaces approximately 40 percent of the infant's respiratory resistance. This value was chosen as neonates are obligatory nose breathers, but oro-tracheal tubes bypass the nasal resistance and replace some of the upper airways resistance. Nasotracheal tubes increase total resistance and time constant still further. In pulmonary disease respiratory resistance can be substantially increased (e.g. Bronchiolitis ($R > 300 \text{ cm H}_2\text{O/L/sec}$), asthma). This is shown by the table below which lists ANSI standard parameters to simulate infant lungs for testing paediatric and neonatal ventilators :

R	20*	50	200	1 000	cm H ₂ O/L/sec
C	1	3	10*		ml/cm H ₂ O
R.C	0.5	1	2		sec
(ANSI 79.7 - 1976) Neonatal lung-simulator characteristics					
* recommended for paediatric modelling [39]					

Keuskamp also quotes resistance values of 500 cm H₂O/L/sec or more as occurring in intubated infants with values of 200 to 500 cm H₂O/L/sec being common in neonates [4]. In these high-resistance patients the time constant may easily rise to four or five times normal, reducing peak expiratory flow rates proportionately. In some diseases low values of compliance occur (e.g. respiratory distress syndrome, or with pulmonary oedema). In some of these low-compliance patients respiratory time constant could be as low as the lowest value quoted for preterm infants.

A noteworthy aspect of controlled ventilation in infants is the large increase in respiratory resistance contributed by the ventilation tubes and fittings and the very small diameter et. tubes which are prone to blockage from lung secretions. Peak flow rates in spontaneous ventilation usually occur during inspiration, but in controlled ventilation peak flow rates are much higher and often occur during expiration [17], although this depends on ventilator settings. Very short inspiratory times can lead to very high peak inspiratory flow rates, and certain ventilators produce inspiratory waveforms with short-duration high-flowrate peaks. Figure 2.2 from Keuskamp [4] illustrates this well, with peak flowrates as high as 49 L/min with quite modest average ventilation rates.

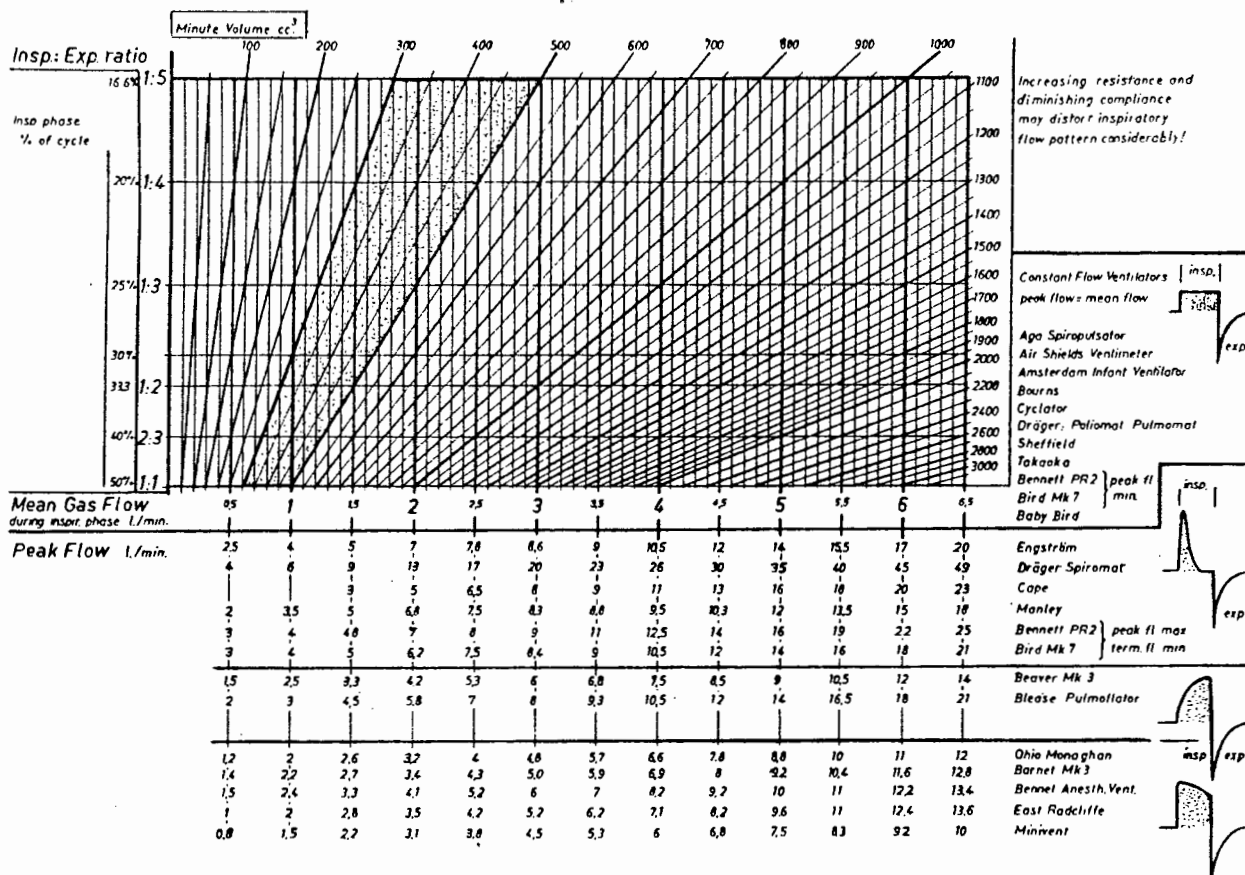


FIGURE 2.2 Influence of I/E ratio on mean gas flow. The stippled area represents the average minute volume of a newborn. The peak flow during the inspiratory phase is measured in different ventilators. As an example, with a minute volume of 500 cu. cm. and an I/E ratio of 1:3, a mean flow of 2 liters per minute is required. The peak flow of a constant-flow machine will be 2 liters per minute. The peak flow of an Engström ventilator or a Dräger Spiromat will be 7 liters per minute or 13 liters per minute, respectively. [4]

Clinical experience using the spirometer equipment developed in this thesis confirmed that high peak flow rates above 40 L/min do occur with some ventilators. Munson showed that (spontaneous) peak flow rates increase by up to 100 percent during "light" anaesthesia compared with the "awake" values. In infants below one year these peaks are as high as 19 L/min [40]. Peak flow rates in infants above one year could exceed 28 L/min [40]. With increasing levels of anaesthesia the peak flow rates decrease to below "awake" levels.

Comparing figure 2.1 with figures 2.2 and 2.3 shows that flow in et. tubes will often be turbulent for at least part of the respiratory cycle, especially in controlled ventilation with the higher peak flow rates. In the patient's upper airways flow is probably turbulent at even lower values of Reynolds' number than would be expected on a theoretical basis [41]. This is important since turbulence changes the velocity profile across the airway from parabolic, under laminar flow conditions, to approximately flat under fully developed turbulence. Turbulence increases the work of ventilation by causing resistance to increase rapidly with increasing flow rate.

Et. Tube Diameter (mm)	Flowrate for $R_e = 2\ 100$ (L/min)	Flowrate for $R_e = 6\ 000$ (L/min)	$R_e = \frac{4 \bar{V} \rho}{\pi \phi \mu}$ R_e - Reynolds' number ϕ - diameter ρ - density μ - viscosity \bar{V} - mean vol. flowrate
2.5	3.7	10	
3	4.4	13	
4	5.9	17	
5	7.3	21	
6	8.8	25	

Figure 2.3 Transition from laminar to turbulent flow occurs between Reynolds' numbers of 2 000 and 6 000. Owing to entrance effects, wall roughness, fluid accumulations, bends, etc., turbulence in et. tubes will tend to be well developed at the lower Reynolds' numbers. Flowrates encountered in infant ventilation (figures 2.1,2.2) span this transition from laminar to turbulent flow.

2.2 Infant Flowmeter/Spirometer : Specification and Requirements

2.2.1 General Requirements

Safety is the overriding requirement. The equipment must not supply dangerous misinformation to the user. In particular, in the event of faults or systematic errors, the equipment should underestimate volume measurements, so that, if the error passes undetected, the operator will tend to hyperventilate the patient. (Hyperventilation is less dangerous than hypoventilation.) For the same reason no range switch should be provided, since hypoventilation could result from reading the wrong scale.

The equipment should also be reliable and stable, under clinical conditions, without requiring frequent recalibration. Provision should be made to allow easy testing by the user.

An instantaneous flow rate signal for display and analysis should be available.

The apparatus should not interfere with normal clinical procedures or patient management. It should be readily adaptable to as wide a range of clinical situations as possible.

The sensor should be sterilizable, either by autoclaving or by gas sterilization. It should also be washable in commercial "dip sterilizing" solutions. Alternatively, the sensor should be disposable.

The sensor should offer no explosion hazard with any combination of flammable anaesthetic gas and vapour mixtures, even under internal fault conditions.

The most flammable mixture likely to be encountered is a 12 percent ether/oxygen mixture. [42]

The sensor should operate correctly under the wet, high humidity conditions in the ventilator circuit.

Sensor Placement is far more important in infant ventilation than it is in adult ventilation, owing to the infant's low respiratory compliance and high resistance.

Measuring gas volume leaving the ventilator can lead to a gross (and dangerous) overestimation of patient ventilation, since this volume is shared between the "compressible volume" (compliance) of the ventilator circuit and the patient. It is not unusual for only a small fraction of the volume leaving the ventilator to enter the infant [3][1]. This is particularly true when adult ventilators and tubing are used on infants and during anaesthesia where additional plumbing, vapourisers, CO₂ absorbers, humidifiers etc. increase the circuit compliance. Sensing gas flow leaving the ventilator circuit suffers from the same errors, unless the circuit is modified by adding valves to separate out patient expiratory flow. This is undesirable as it changes standard plumbing, adds substantial flow resistance and is not suitable for use with all ventilator circuits.

By sensing flow at the entrance of the patient's et. tube, flow to or from the patient can be accurately determined without modifying the ventilator circuit. However, this makes flow-sensor construction more difficult, since it must not interfere with patient manipulations or increase the patient's respiratory requirements.

A small sensor size which does not cause the patient connector to protrude forward from the patient's

face is essential, since the surgeon's normal manipulations during thoracic surgery encroach on the face area in infants.

Sensor Deadspace

Barth [43] suggested a value of less than 1 ml is necessary for an infant pneumotachograph. This corresponds to approximately 20 percent of normal deadspace or six percent of tidal volume in a full-term infant (figure 2.1). It would thus necessitate a six percent increase in ventilation at constant respiratory rate. An even smaller deadspace is desirable since preterm infants will tend to have a smaller tidal volume.

Sensor Flow Resistance

During spontaneous or assisted ventilation an increase in the work of ventilation caused by the added sensor resistance is undesirable. In controlled ventilation also, a substantial increase in resistance is undesirable, since it necessitates extended expiratory times and higher peak inspiratory pressures. In healthy infants the work of ventilation is only a few percent of the patient's overall metabolic requirements [14], so that quite a large increase in the work of ventilation is not significant. In pulmonary disease, however, the work of ventilation may be a substantial proportion of the infant's metabolic requirements, making any increase in the work of ventilation during spontaneous ventilation significant. A flow sensor's resistance is often specified in terms of pressure drop at peak flow rate. Plaut [44] suggested 12 cm H₂O at 200 L/min for an adult pneumotachograph for monitoring purposes. Elsewhere he suggested a value of five to ten percent of respiratory resistance. [44] Barth [43] suggested 0.5 cm H₂O at 18 L/min for an infant pneumotachograph. Linear flow resistance ("Fleisch") pneumotachographs sense a pressure drop of 1.5 cm H₂O at peak flow rate. [45]. However, the overall pressure across these transducers is often more than ten times this value [46]. Considering the very large total (patient + et.tube) resistances encountered in infants

(figure 2.1) a resistance producing 4 cm H₂O at 20 L/min is probably acceptable. This will correspond to approximately 10 to 20 percent of the overall intubated patient resistance at 20 L/min for the larger infants and considerably less for the smaller infants (figure 2.1).

Pressure Plaut suggests a flowmeter should withstand pressures up to 150 cm H₂O without leaks or damage [36]. This is probably unnecessarily high, since most infant ventilators have an absolute maximum pressure limit of between 60 cm H₂O and 100 cm H₂O [17]. Airways pressures greater than 70 cm H₂O are seldom used in artificial ventilation, since lung damage may occur with alveolar pressures above 70 cm H₂O [21]. In neonates alveolar pressures above 35 cm H₂O may cause damage [17], but the neonate's high flow resistance often necessitates much higher peak airways pressures which are not transmitted to the alveoli.

2.2.2 Measured Quantities

Tidal Volume or Minute Volume ?

From a physiological point of view it is desirable to measure and control alveolar ventilation during artificial ventilation [14]. Unfortunately, no simple technique exists to measure this directly by spirometry. Tidal volume and average total ventilation (minute volume) can both be measured directly. Which of these two quantities is more useful to the anaesthetist? Neither shows an advantage for the calculation of alveolar ventilation, since both still require an estimate of deadspace and a measurement of respiratory rate. Tidal volume measurements can help guard against hyperinflation of the lungs. However, minute volume measurements are probably less prone to errors of interpretation and are thus more reliable for setting ventilation levels and detecting errors. This is particularly true at low respiratory rates, often favoured in infant ventilation [14], when minute volume is a closer approximation to alveolar ventilation than it is at high rates.

Variations in Measured Quantities

Measured values of volume or volume flow rate should, ideally, be corrected to standardised conditions of pressure, temperature and humidity. The standardised conditions are body temperature (37°C), 1 atmosphere pressure and fully saturated with water vapour at 37°C . These conditions are termed "Body Temperature and Pressure Saturated" (BTPS) [12]. From Boyle's law volume changes arising from pressure changes in the ventilator circuit are unlikely to exceed 5 percent ($P = 55 \text{ cm H}_2\text{O}$) and will commonly be one to two percent. A flowmeter that is calibrated (at 37°C) in terms of volume flow rate but senses mass flow rate, automatically corrects for temperature and pressure changes. It still needs correction for changes in water vapour content at different temperatures. Other devices that sense volume at a particular temperature and pressure require correction for all three factors. Errors from temperature and vapour pressure are usually considered together, with the inherent assumption that measured volumes are saturated with water vapour at the measurement temperature. This is usually true during ventilation, since inspired gas is normally humidified to 80 percent saturation and expired gas is 100 percent saturated. At 20°C (the lowest temperature likely ever to be encountered), volume change from temperature and humidity is - 9.07 percent compared with the volume at BTPS [12]. Making a correction for this automatically may not be desirable, since periodic calibration or testing with a super syringe then requires a correction factor. If no correction were performed in this calibration, it could lead to mild hypoventilation. On the other hand, in a manually corrected device, if no manual correction is made for temperature, this leads to a safer condition of mild hyperventilation in all cases. A flow sensor should incorporate a gas temperature sensor to allow manual correction for temperature and monitoring of inspired temperatures. Measuring expired gas volumes does not guarantee conditions of BTPS, since, unless

the inspired gases are also at body temperature, heat exchange with the et. tube during inspiration, and then during expiration, reduces expired gas temperature below body temperature [4]. Under "typical" conditions of ventilation inspired gas will be heated and humidified at 30° to 35° C, making inspired gas volumes appear up to 4.5 percent smaller than BTPS conditions. Other factors can cause differences between expired and inspired volumes :

In infant ventilation non-cuffed et. tubes are used, and it is considered good practice to allow a small gas leak past the et. tube to prevent tissue necrosis [14][13]. Inspired volumes measured entering the et. tube include this leak component. For most infants this leak will be very small, since the flow resistance of the leakage path will be very high compared with patient resistance. (The leakage path has a very small cross section and we know resistance increases very rapidly with decreasing cross section.) However, in infants with very large respiratory system resistances and very low compliance, this error may be appreciable, since in these patients ventilation pressures will be high and tidal volumes small. Leakage during expiration will be very small owing to the low et. tube pressure. Another difference between average inspired and expired volumes may arise from the fact that the respiratory exchange quotient (REQ) is usually slightly less than one. If we assume steady state conditions, with REQ = 0.8 and an expired carbon dioxide concentration of four percent, then :

$$\text{inspired volume } V_{\text{insp}} = \left(\frac{0.04}{0.8} + 0.96 \right) V_{\text{exp}}$$

and

$$\frac{V_{\text{insp}}}{V_{\text{exp}}} = 1.01$$

i.e. a difference in volumes of only 1 percent.

2.2.3 Required Accuracy and Its Specifications

Accuracy specifications in commercial flowmeters (for adults) are often limited to a blanket "% accuracy", which, without further qualification, often means percentage of full-scale deflection (% FSD) at constant temperature and constant flow rate in air. Errors at average levels, well below maximum flow rate, could thus be large, although within specification. Similarly, some devices specify a correction factor for sinusoidal flow waveforms, thus indicating the device has a poor dynamic response and is likely to be inaccurate with the decidedly non-sinusoidal flow waveforms encountered in controlled ventilation. Errors from changes in gas composition, temperature etc. may give rise to different errors for different devices, depending on the flow-sensing technique. Specifications seldom include zero stability, minimum detectable flow rate or indicate how temperature, humidity and gas composition affect these factors or overall accuracy. Linearity specifications should state whether the quantity is a best straight-line fit to the output, or whether it is the best straight line passing through zero ("zero-based linearity"). The latter can be a much more demanding specification and gives a better indication of performance. Differences in flow sensitivity from forward to reverse may occur, especially where nearby bends or fittings make the velocity profile across the bore of the flow sensor unstable. These "entrance effects" are a particular problem where the flow sensor is close to a right-angled connector. As a result of this problem deadspace specifications of commercial flowmeters are often meaningless, since transducers may require a substantial length of straight tubing upstream and downstream for reasonable accuracy, and the minimum achievable deadspace then includes this additional volume.

Plaut, after reviewing commercial ventilation-

monitoring flowmeters, specified that an accuracy-linearity of \pm five percent, with a repeatability of two percent and a minimum sensitivity of $\frac{1}{4}$ percent FSD, was acceptable for an adult flowmeter [36]. Barth specified, for an infant flowmeter for use with gas analysis equipment (a more stringent requirement), \pm one percent of reading or 15 ml/min, whichever is the greater, up to 18 L/min FSD [43]. 15 ml/min corresponds to \pm three percent of 450 ml/min, which is the lowest mean flow rate (inspiration plus expiration) likely to be encountered (if we assume I/E = 2, minute ventilation = 300 ml/min minimum). Barth was not consistent, as he also specified in the same publication, that an accuracy of one percent of FSD (i.e. \pm 180 ml/min or \pm 40 % of 450 ml/min) was an acceptable accuracy [43]. Various adult flowmeters claim accuracies of three to five percent at high flow rates [47][48][49][50]. Keuskamp specified that an ideal volume-cycled ventilator should deliver the preset volume to an accuracy of \pm ten percent [4]. Hall came to the conclusion that a Wright (turbine) spirometer with errors up to 35 percent of reading was sufficiently accurate for adult ventilation monitoring! [51]

Considering that respiratory requirements using conventional nomograms cannot be estimated to a very high accuracy (error \geq \pm 7 percent) even in normal infants [5], the design objectives of figure 2.4 were adopted for the infant flowmeter/spirometer.

Repeatability of measurements is important to ensure that, once correct ventilation levels have been established by blood gas analysis or other techniques, changes in ventilation can be accurately monitored and controlled.

The effects of temperature/humidity and different gas mixtures on the flow measurements should be known and simple to correct, so that repeatability is not

REQUIREMENTS		COMMENTS
Accuracy (instantaneous V + minute ventila- tion)	$\pm 5\%$ of reading or 45 ml/min, whichever is the greater, from 450 ml/min to 25 L/min (at 37°C) $\pm 10\%$ of reading from 25 L/min to 50 L/min (at 37°C)	Minimum average flow rate never less than 450 ml/min For ventilators producing high peak flow rates
Resolution	22 ml/min	5 % of 450 ml/min
Sensing Threshold	45 ml/min	10 % of 450 ml/min
Zero Drift	Within 45 ml/min from 20 to 40°C	10 % of 450 ml/min
Repeatability	$\pm 3\%$ under constant conditions	Accurately maintain ventilation
Frequency Response	0 to 20 Hz within $\pm 4\%$	For monitoring mechanical properties of respiratory system
Warm-up Time	< 2 min to $< 5\%$ of final value	
Long-Term Stability	$< 1\%$ /month	Calibration 4 times /year
Gas Mixtures	Inspired + expired gases, N ₂ O to 65 %, O ₂ to 100 %, Halothane, CO ₂ up to 12 %, H ₂ O vapour to 100 % sat.	Ideally insensitive to changes in composition or simple to correct
Safety	No explosion hazard with O ₂ / 12 % ether	Most explosive mixture likely to be encountered
Temperature	Ideally reads volume at temperature to simulate classical wet-seal spirometer	For simple testing reads same volume as calibrated syringe
Minute Ventilation Display	Range : 0 - 7 L/min Response time : 8 to 15 secs.	Analogue display for "at a glance" reading

Figure 2.4 Infant Flowmeter/Spirometer Technical Requirements
(See text for sensor physical requirements)

degraded. Total additional errors from this source should not exceed, say, five percent.

Barth suggested a bandwidth of 100 Hz is required for an infant pneumotachograph [43]. McCall found the harmonic content of a variety of forced and normal breathing patterns in adults seldom exceeded 20 Hz and was normally below 4 Hz [52]. In infants respiratory rates are higher than in adults and during controlled ventilation the amplitude of harmonics is likely to be higher, owing to the rapid changes in flow rate as valves open and close. McCall pointed out that the frequency response requirements for volume measurements (by integration of the flow waveform) are far less demanding than at first would appear, since the amplitude of each of the harmonics is reduced by a factor $1/\text{harmonic number}$ by the integration process [52]. From McCall's data the amplitude of the 10th harmonic was never more than nine percent of the fundamental in tidal breathing, which would thus result in an error of 0.9 percent, if it were ignored in measuring volume. Higher harmonics will contribute even smaller errors, since their amplitudes are smaller and the harmonic number higher. For infants, with maximum respiratory rate 1.5 Hz (90 BPM), each of the frequency components above 15 Hz would thus contribute less than one percent to tidal volume measurements. However, for measuring the mechanical properties of the respiratory system, a bandwidth in excess of 20 Hz is probably desirable to preserve waveshape and amplitudes.

2.3 Conclusions and Comments

In comparison with an adult, the infant's respiratory system is characterised by a higher flow resistance (especially when intubated) and a lower compliance. The respiratory time constant in infants is not markedly different from the value in adults. However, in a number of infant diseases the time constant is increased substantially.

During the controlled ventilation of infants peak flow rates often occur which are very much higher than in spontaneous ventilation. These peaks are often of short duration with low mean flow rates and small tidal volumes. A flow sensor must thus be capable of operating over a wide dynamic range.

Many manufacturers of adult flowmeter/spirometers do not fully specify the accuracy of their equipment. This may well be as a result of the poor performance of many devices [53][51]. Apart from inherent instrument errors under ideal conditions, there are a variety of other potential sources of error which depend on the particular conditions of use. Poor performance of these devices has led to a widespread dissatisfaction amongst users [19].

To achieve wider user acceptance flow sensor accuracy should be fully specified, significant sources of error should be documented, and these errors should, ideally, be easy to correct. For ventilator usage, significant flowmeter errors should result in an under-estimation of flow rate, so that the anaesthetist will hyperventilate the patient if no corrections are made.

The requirements in infant spirometry for controlled ventilation are made extremely difficult by the environmental conditions in the ventilator circuit and by the requirement to sense flow at the patient's endotracheal tube.

Repeatability of flow measurements is of greater importance than very high absolute accuracy. High repeatability ensures that, once a level of ventilation has been chosen for an infant, this level can be monitored and maintained, and trial-and-error methods of adjustment are eliminated.

CHAPTER 3

3. Flow Measurement and Spirometry3.0 Introduction

Many different techniques have previously been used for measuring respiratory volumes and volume flowrates. This section discusses the applicability of a variety of these, and other flow measurement techniques, to monitoring ventilation in infants. For comparison, some of the problems of hot-thermistor spirometry are introduced, although these are dealt with in greater depth later.

To directly compare different flow-measurement techniques, it is necessary to assess how the accuracy of each technique is degraded by clinical conditions of usage and by the skill of the operator.

It was pointed out previously (section 2.2) that the dynamic requirements for a device measuring volume are less critical than for a device measuring flow rate. Thus a device measuring volume with acceptable accuracy may yield an inaccurate flow rate signal when flow rate is derived by differentiating the volume signal. Some techniques for measuring volume are thus unsuitable for deriving instantaneous flow rate. For the full range of applications in controlling ventilation, it is desirable to be able to measure/derive both volume and instantaneous flow rate from a single measuring technique.

3.1 A Review of Measurement Techniques3.1.1 Plethysmography

Total-body plethysmography involves enclosing the patient in a rigid airtight box, so that the

patient's airways are coupled to the box's exterior. Using Boyle's law, pressure variations within the box reflect volume displaced by the patient's chest during respiration. Figure 3.1 shows one version of the body plethysmograph which has been used for infants. System calibration using a syringe is required for each patient.

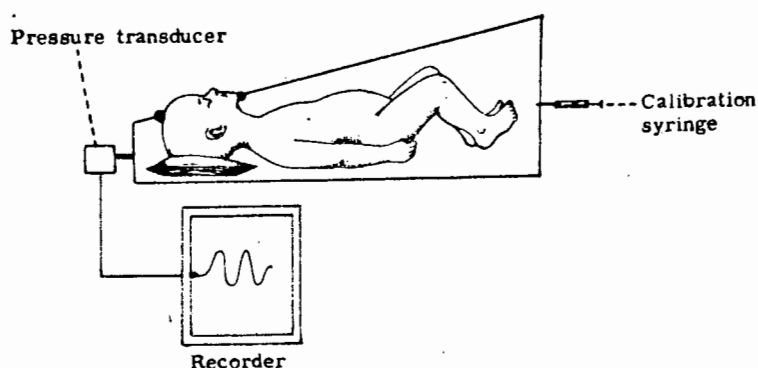


Figure 3.1 The Cross Body Plethysmograph [35]

Although the body plethysmograph has been widely used for respiratory investigations in infants, it has only a moderate accuracy (± 10 percent), after careful calibration at the patient's respiratory rate. [54][55][4] Errors arise from : leaks at low frequencies, temperature changes of the enclosed gas causing gas expansion and hence zero drift, and an amplitude response which varies with respiratory rate, since gas compression changes from isothermal at very low frequencies to adiabatic at higher frequencies. Some of these errors can be reduced by connecting a spirometer or pneumotachograph to an additional port in the side of the plethysmograph and directly measuring the displaced volume entering or leaving this port [56]. This latter technique has a very poor frequency response, unless a pressure transducer is used to measure the very small pressure changes, which now occur in the box, and these are added as a correction to the pneumotachograph signal [56][57].

The respiratory jacket (figure 3.2) replaces the sealed box by an inflatable rubberised jacket, which is prone to movement artifacts.

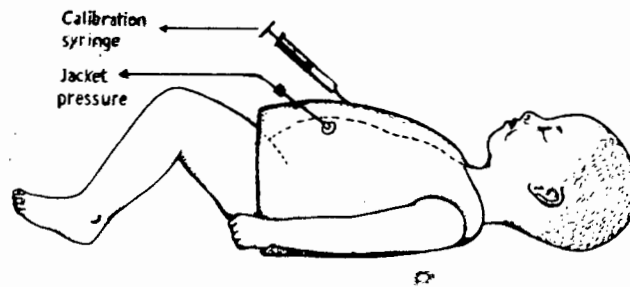


Figure 3.2 Respiratory Jacket [58]

Both the "body box" and the jacket interfere too much with normal nursing and clinical procedures for monitoring applications, particularly during surgery!

Reverse Plethysmography (figure 3.3) places the patient outside the rigid plethysmograph container and again measures respired volumes entering or leaving the container by pressure changes in the container [59].

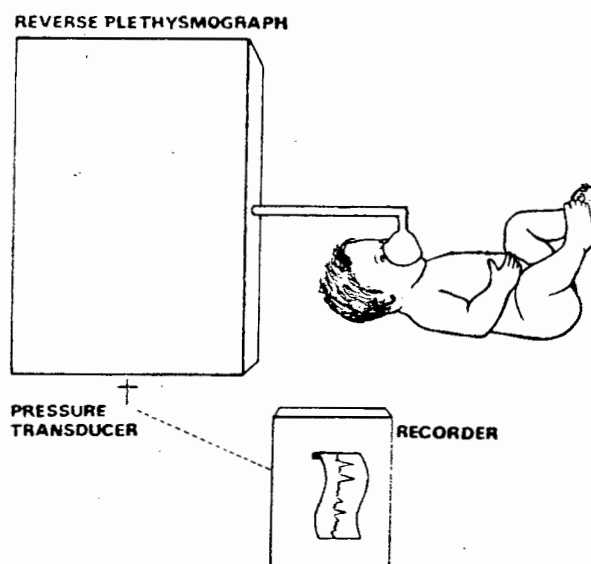


Figure 3.3 Reverse Plethysmograph [59]

Errors are the same as in conventional plethysmography with the additional problems of CO_2 and water vapour accumulations. Individual calibration at the patient's

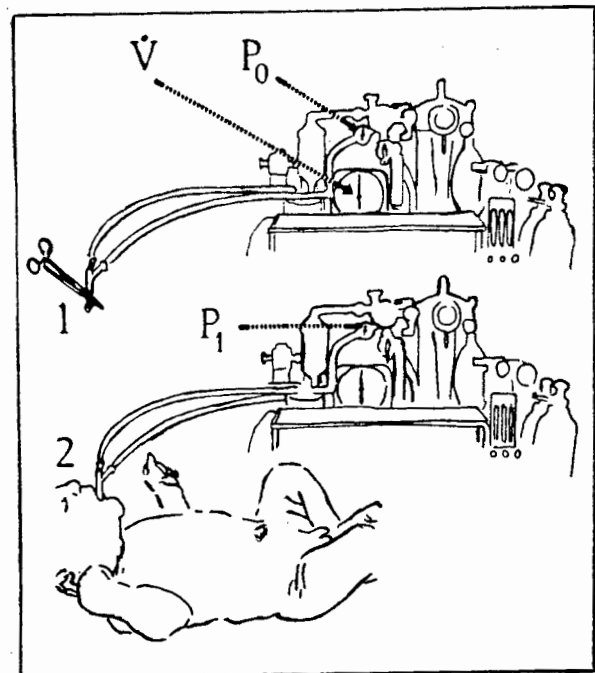
respiratory rate is still necessary [4] and mask or et. tube leaks must be controlled. Normally reverse plethysmography can be used only during spontaneous ventilation. However, Okmian has described an ingenious technique (the "two pressure method"), which uses an Engström ventilator both as ventilator and reverse plethysmograph [60][3]. The two pressure method (figure 3.4) involves first calibrating the reverse plethysmograph (= ventilator + circuit compressible volume), using a gasmeter and pressure gauge, and then calculating tidal volume from end inspired pressure. Claimed accuracy using this technique to measure infant tidal volumes is between approximately three and nine percent. [23].

FIG. 3.4 - Two-pressure method. The tidal volume (\dot{V}_T ml) is calculated from the minute volume (\dot{V} ml/min) obtained from the gasometer; the two pressures recorded by manometer, P_0 (tracheal connection closed) and P_1 (with the patient connected); and the adjusted frequency (f) according to the formula

$$V_T = (P_0 - P_1) \frac{\dot{V}}{f \cdot P_0}$$

The calculation is simplified for unaltered respirator adjustment since the ratio

$\frac{\dot{V}}{f \cdot P_0}$ is practically constant.



Disadvantages of the two pressure method are that :
 it requires the use of a particular ventilator, leaks must be controlled, it requires individual calibration and calculation, an instantaneous flow-rate signal cannot be derived, errors arise from changes in compressible volume (e.g. from switching in a vapouriser or gradual loss of water from a humidifier), it cannot be used with CPAP

as circuit compliance is then usually non-linear, manual ventilation by bag cannot be monitored.

Impedance plethysmography measures the electrical impedance (essentially resistance) of the chest at a frequency of approximately 100 k Hz [61][62]. Respiratory volume changes of the chest cause resistance changes between the measurement electrodes. Some other spirometry technique must be used for initial calibration. The impedance technique is not accurate, particularly in respiratory disease, and consequently it is normally used qualitatively without calibration and often just as an apnoea alarm [4][63]. It is unreliable during thoracotomy and suffers from cardiac artifacts under most conditions of usage.

3.1.2 Collection Techniques

Collection techniques for measuring respiratory volumes can offer the highest accuracy of any spirometry technique. This results from the fact that conditions for collection can be carefully controlled and humidity and temperature corrections are thus easier to apply to measured volumes. In controlled ventilation of infants the normal problems of ventilator compressible volume severely limit accuracy, unless a valve system is placed near the patient on both the inspiratory and expiratory connections. A valve system has a variety of problems, including increased flow resistance, which is undesirable in assisted ventilation, and leaks, which are particularly significant for the small tidal volumes in infants.

Spirometers of this type are sometimes coupled into the ventilator circuit using an ingenious bag-in-box technique with a gas bias flow to stop gas accumulating in the spirometer, while allowing inspiratory and expiratory volumes to be continuously monitored [64].

The wet-seal spirometer exists in a variety of forms [62][12]. Figure 3.5 shows a classical "Benedict-Roth" cylindrical bell spirometer. Gas entering or leaving the counterbalanced bell, from beneath, displaces it vertically. This displacement (\propto volume) is frequently registered by a potentiometer coupled to the counterweight pulley, rather than by a pen and kymograph.

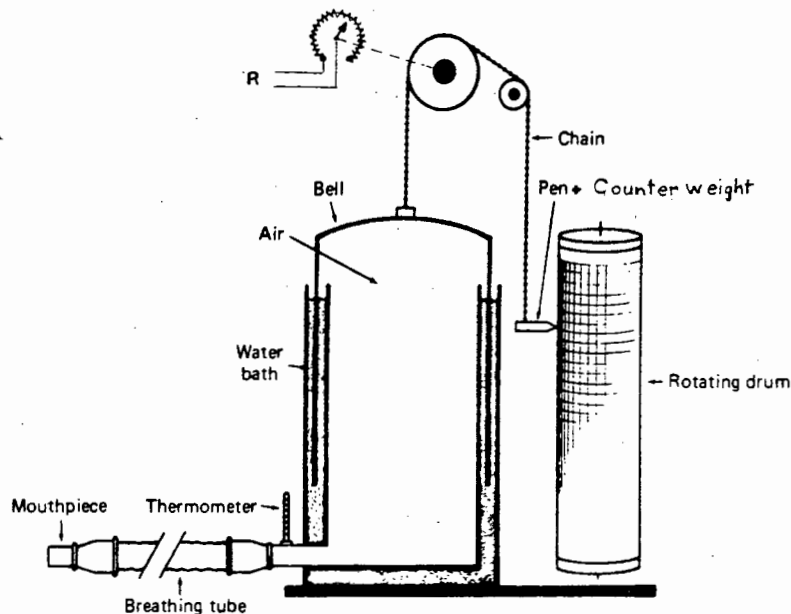


Figure 3.5 Wet-Seal Benedict-Roth Spirometer

The dynamic performance of this type of spirometer is limited by : inertia of the bell/counterweight, water displacement by the gas and the "gas compression volume" of the spirometer, which is variable. The instantaneous flow rate signal derived from the volume signal is thus inaccurate at higher frequencies. Typical amplitude response is within two percent up to 0.6 Hz with the spirometer bell resonance at 1.6 Hz for a small light-weight bell spirometer [62]. Other workers have claimed that a somewhat higher performance can be achieved with an accuracy of \pm one percent up to two Hz [53].

The dry-seal spirometer (figure 3.6) replaces the water seal by a bellows or other flexible seal.

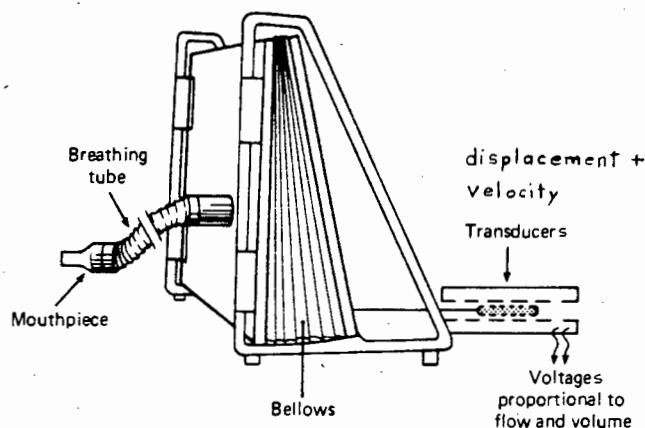


Figure 3.6 The "Wedge" spirometer shown here is an example of one type of dry-seal spirometer. Dynamic performance of dry-seal spirometers is generally slightly better than wet-seal types, but the accuracy is lower, owing to the flexible seal and factors such as humidity and temperature, which are not as well controlled.

A "Douglas Bag" (large weather balloon) is often used in a two-step collection and measurement process, in conjunction with a wet-seal spirometer. This allows larger volumes than can be accommodated in the spirometer to be collected during a timed period and then measured [12]. This technique is useful where extremely high accuracies are required.

Dry gasmeters, similar to those used for domestic gas, have been used for collecting expired volumes [62], but are considered to be too inaccurate for the small volumes from infants [12]. Over a 10 : 1 dynamic range Hill claims an accuracy of two percent is possible in a well-maintained adult meter. This accuracy is achieved only after a few cycles of the mechanism [62]. Water condensation is a problem, causing over reading as water fills the unit's bellows, and frequent maintenance is required [62].

One of the most widely used ventilation monitoring spirometers for adults is the rotating vane "Wright Respirometer" [65] shown in figure 3.7 :

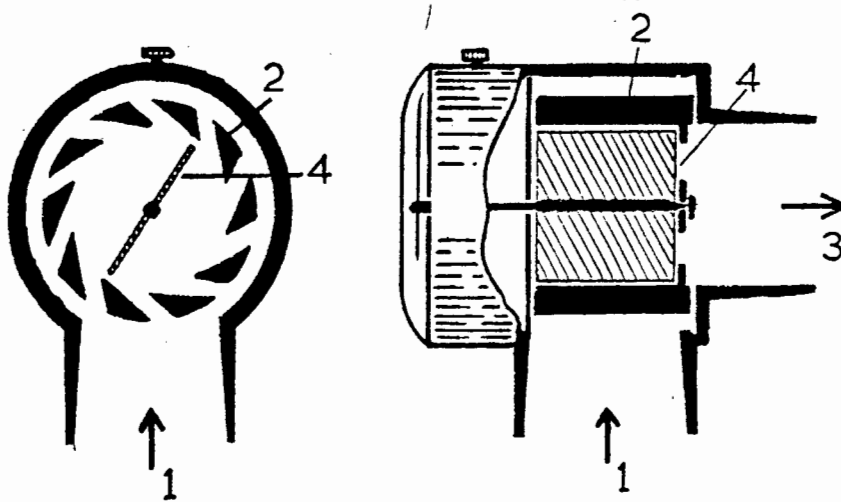


Diagram of the Wright ventilation meter.

- | | |
|--|---|
| 1. Gas inlet | 3. Gas outlet |
| 2. Stator ring with ten tangential slots | 4. Two-bladed rotor running in jewelled bearings. |

Figure 3.7 The Wright Rotating Vane Spirometer

Gas passing through a set of tangential slots strikes the low inertia vane (turbine) causing it to rotate. A gear train coupled to the vane drives the pointer across a dial calibrated in terms of volume. "Electronic" versions of the Wright spirometer detect vane rotation optically or capacitively and count rotations digitally [66][67]. An advantage of this type of meter is its insensitivity to changes in gas composition and humidity, although gradual water accumulations from a nebuliser can cause dangerous over reading (+ 25 per cent in two hours). [67] The Wright spirometer senses gas flowing in a single direction by use of the tangential slots and asymmetrical port system (figure 3.7) This gives rise to an error which depends on whether flow reversal is rapid or not, since the vane tends to (coast) overrun when flow reversal is slow [67]. A variety of other turbine systems are available commercially for monitoring ventilation [21], some of which are bidirectional [53].

Turbine flowmeters suffer from a number of problems: inertia limits the dynamic performance, leading to grossly inaccurate instantaneous flow-rate signals, with errors from 25 to 45 percent [53], turbine meters are often calibrated for sinusoidal waveforms at 20 breaths/min [67] resulting in under-reading at lower frequencies and overreading at higher frequencies [67][53], bearing friction causes static errors to increase rapidly below 7 L/min, with errors reaching 100 percent (sticking/stalling), somewhere between 1.5 and 3.5 L/min, depending on the particular sample of meter [67][51][66][68]. A digital linearisation ("look-up table") technique has been suggested for low flow rates [66] but this requires each particular sensor to be calibrated at a number of flow rates, and large errors will still result for small infants, whose peak flow rates will exceed sensing threshold only for a short part of the respiratory cycle. In long-term use water and contamination cause increasing bearing friction or even seizure [68], so that linearisation does not justify the added cost and complication. Bushman showed that, despite the apparently poor performance of turbine flowmeters, an accuracy of approximately ± 6 percent could often be expected when monitoring adult expiratory tidal volumes [68]. He found that, in controlled ventilation, the high peak instantaneous flow rates that occur at the beginning of expiration apparently improve accuracy, since, under identical conditions, but monitoring inspiration (no high initial peak flow), errors from -12 to -75 percent occurred [68]. During spontaneous respiration expiratory flow waveforms tend to be similar to inspiratory waveforms with no initial high peak flow rate. Thus, even for adults, this could result in measurement errors of up to 25 percent during spontaneous respiration. In contrast, Cox found high peak instantaneous flow rates caused an electronic Wright flowmeter to overestimate tidal

volumes by up to 12 percent [67].

Considering all the potential sources of error, particularly the high flow-sensing threshold, it is not surprising that Mushin came to the conclusion that ventilation monitoring in infants cannot be performed with a Wright respirometer [2].

3.1.4 Flow-Resistance Flowmeters

A variety of flowmeters sense instantaneous volume flow rate by measuring the differential pressure across a flow obstruction (resistance). Flowmeters of this type can have an excellent dynamic performance and have been widely used for respiratory studies. In routine clinical use for ventilation monitoring they suffer from a variety of problems.

Pressure sensing poses a problem for all flowmeters of this type. To minimise flow resistance a pressure drop of at most a few centimetres of water should occur across the flow sensor. Pressure transducers to sense such low pressures are large, expensive and fragile. The relatively large common-mode ventilator pressures will not normally be applied differentially to the pressure transducer, but, in the event of one coupling tube becoming disconnected or blocked (kinking, water etc), an overload of five to fifty times full scale will be applied to the transducer. This will either destroy the transducer, or cause large zero shifts and hysteresis [69], since few transducers can withstand more than two to five times full-scale pressure. Partial transducer damage is particularly hazardous, as this could pass unnoticed and lead to incorrect ventilation. In long-term monitoring it is difficult to guarantee that water will not enter pressure tappings and cause erratic or erroneous readings or even transducer damage [69][70][71]. Flowmeter dynamic range is limited by the zero stability of the pressure transducer and amplifier. If we wish to achieve a 150 to 1 dynamic range in the flowmeter (see flowmeter

technical requirements), and accept a ten percent error at minimum flow rate, then the pressure transducer must have a zero stability of better than ± 0.07 percent of full scale. One technique which is used industrially to achieve this level of performance, without frequent manual zeroing, is to automatically zero the transducer periodically using a system of solenoid valves and a digital zeroing system [72]. Hewlett Packard have made provision for a similar (soft-ware based) auto-zeroing technique in their model 43704A flow sensor when this is computer controlled. [73]

All flow-resistance flowmeters tend to be sensitive to entrance effects, making in situ calibration essential [74]. Short flow-straightening sections are normally built into the sensor to try to reduce sensitivity to entrance conditions. Where entrance conditions are not the same on both sides of the transducer, sensitivity varies from forward to reverse. The flow-straightener sections of these sensors tend to make their dead-space quite large.

Linear Resistance flowmeters (figure 3.8) develop laminar flow through a bundle of fine capillary tubes ("Fleisch pneumotachograph") [75], or through a fine mesh screen ("Lilly pneumotachograph") [76], to produce a differential pressure directly proportional to flow rate. Reynolds' numbers must be kept low (less than 300) within the transducer to ensure laminar flow and hence a linear pressure-flowrate relationship [77].

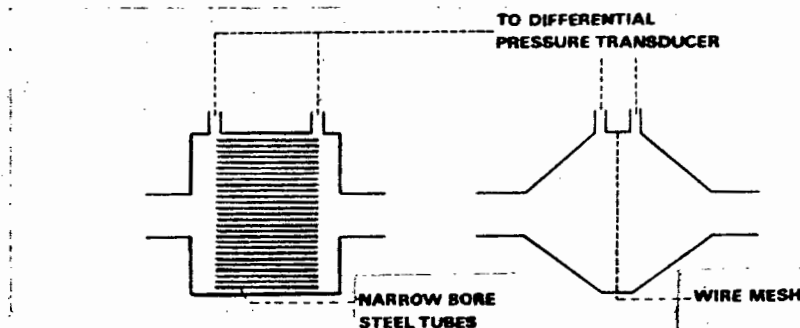


Figure 3.8 Linear resistance flowmeters have been extensively applied to respiratory investigations. "Fleisch" type at left. "Lilly" type at right.

The screen sensor has a very wide bandwidth and good phase response (limited by pressure sensing system), and is less sensitive to upstream geometry than the capillary tube sensor [74][46]. In contrast, the capillary tube sensor has better linearity, but can exhibit a 10° phase error at 10 Hz, despite an amplitude response within a few percent to 30 Hz [74][46]. Most linear flow resistance sensors are calibrated near full scale and are assumed linear at low flow rates. However, Finucane showed that substantial non-linearity of seven to fourteen percent can occur at either low or high flow rates, depending on sensor upstream geometry [74]. This makes in situ calibration over the full range of flow rates necessary [74]. Because of stability problems and the requirement for frequent calibration [12] a special "pneumotachograph calibrator" is available commercially [78].

Figure 3.9 summarises a variety of sources of variability and error in measurements made with linear resistance sensors. The biggest problems for infant use are the limited dynamic range, the large deadspace, and the dangerous errors which result from water accumulations. One attempt has been made to overcome the deadspace problem by incorporating the sensor into a Rees/Ayre's T-piece, but this still increased deadspace of the T-piece from 2 ml to 4 ml [79]. A bias flow can be added through an additional tapping in the pneumotachograph to eliminate the effect of deadspace. However, the stability of this bias flow adds to the flowmeter's low-level noise and limits the dynamic range. A bias flow also adds a potential leakage point, an additional sampling line, and it is not suitable for use in circle absorber systems.

Turbulent flowmeters place a flow resistance in the flow path which ensures turbulence over the range

EFFECT	ERROR	COMMENT	REF.
GAS MIXTURES		Calibrated in air. Scale factor is directly proportional to gas viscosity	
100% oxygen	+ 9.6% (+ 11%)		[80] [70]
75% N ₂ O, 25% O ₂	- 20% (- 12.8%)		[81] [71]
insp/exp difference	< 2%	Viscosity change due to expired CO ₂	[80]
UPSTREAM GEOMETRY CHANGES			
non-linearity	7 to 14%	Calibration in situ can "spread" error reducing max error	[74]
insp/exp difference	7 to 14%	Cannot spread error so easily if geometries differ on each side of probe	[74]
nearby valve	5%		
"jetting"	-4%	Mismatched sensor and upstream tubing diameter	[70]
WATER CONDENSATION	-4 to 43%	Water blocks capillary tubes/screen Dangerous over estimation of ventilation Sensor heater stops condensation but will not evaporate water blown in from adjacent tubing	[70]
TEMPERATURE			
gas expansion + vapour pressure	0.6%/°C	Correction to BTPS Same as for wet-seal spirometer (See appendix C) plus additional 0.17%/°C	[78]
viscosity change	+ 0.17%/°C	Sensor heater causes some drift which is flow-rate dependent	
DYNAMIC RANGE	10 : 1 to 100 : 1	Limited by pressure transducer zero stability (1% FSD stability 10 : 1 0.1% FSD stability 100 : 1 for a 10% error at minimum flow and assuming all other errors negligible)	
DEADSPACE versus PEAK FLOWRATE		Fleisch) 00 - 6 to 9 L/min - 1.7 ml infant) 0 - 18 to 27 L/min - 4.7 ml sizes) 1 - 60 to 90 L/min - 15 ml Compromise between deadspace and peak flow that can be sensed without appreciable non-linearity	[45]
ACCURACY achievable clinically	+ 4% to + 5% + 10%	Fleisch type under "ideal" well-controlled conditions of use (short-term monitoring)	[82] [83]
		Infant screen type in mask	[55]
DRIFT	2 to 8% (in 1/2 hr)		[46]
	±10% (in 1 hr)	Usually within 5%, Zero drift a problem (depends on pressure transducer + amplifier)	[21]

Figure 3.9 Problems in Flow Measurement using Linear Resistance Sensors

of flow rates encountered by the flowmeter. Under these conditions the differential pressure across the resistance is proportional to the velocity squared. Linearisation is then required, using a square root extraction circuit or digital look-up table. Advantages of these sensors are : easy manufacture, low sensitivities to both water accumulation (error 0 to 4 percent) and upstream entrance conditions. Disadvantages are : a poor signal-to-noise ratio, large deadspace (2.5 ml for infants), very limited dynamic range, very large flow resistances above full scale, and large over-estimation of gas flow rate in the presence of nitrous oxide [70][71]. The turbulent flowmeter is most sensitive to changes in gas density and less sensitive to changes in viscosity [70], although Saklad [71] claims equal (but opposite) sensitivities. The large over-estimation of flow rate in the presence of nitrous oxide with these devices is undesirable and hazardous for use during anaesthesia.

Turbulent flowmeters, such as orifice plates, have been widely used industrially and their limited dynamic range (typically only 5 : 1) is well known [84][72]. The dynamic range is limited by the pressure transducer zero drift, which is magnified by the square root operation. For a hypothetical pressure transducer which achieves a 50 : 1 dynamic range with a linear resistance flowmeter, the dynamic range with a turbulent sensor will be only 5 : 1. This problem is well illustrated by Saklad's orifice plate respirometer, with long warm-up times (15 min) and drift up to 16 percent within a four-hour period after zero adjustment [71].

A variety of other flowmeters sense a differential pressure which varies as the square of the velocity.

These include the Pitot tube, the flow nozzle, the venturi and the target meter [72][85]. They all suffer from the same problems of dynamic range as the turbulent flowmeter. The Siemen's "servo" ventilators use a target meter consisting of a force transducer (strain gauged cantilever beam) attached to a disc situated in the centre of the gas stream. Because of the dynamic range limitation, it can be used only for measuring high volume flow rates of adults and the measurement also includes system compressible volume.

The flexural iris flowmeter replaces a fixed orifice by a thin metal iris with a central orifice so arranged that the blades of the iris flex, increasing the effective area of the orifice with increasing flow rate [72].

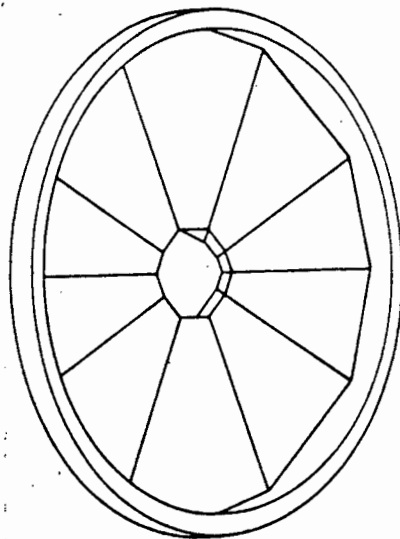


Figure 3.10 Flexural Iris acts as a Variable-Size Orifice Plate

This technique, patented by National Semiconductor, linearises the pressure-flow relationship of the orifice, increasing the achievable dynamic range. It has recently been applied to adult respiratory monitoring by Osborn with apparently only occasional problems from water contamination [8]. For infant respiratory monitoring, this may be the best of the flow-resistive techniques yet developed, but a number of the problems mentioned

previously still remain, especially the high sensitivity to nitrous oxide.

3.1.5 The fluidic flowmeter (figure 3.11) measures the pressure developed in a differential pressure tapping by a gas jet which is deflected by the gas flow being measured.

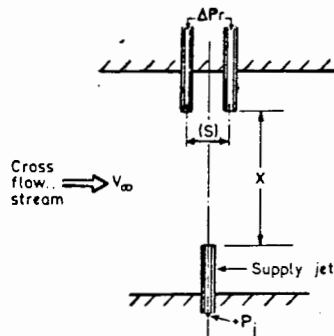


Figure 3.11 Fluidic Flowmeter Senses Bidirectional Flow with Differential Pressure Transducer and Cross-Flow Jet

Parker has described a substantially modified planar version of this device which achieves a 70 : 1 dynamic range and overcomes some of the very serious limitations of earlier designs [86]. The design would require substantial modification for the low flowrates encountered in infants. Difficulties with reliable differential pressure sensing discussed above, contamination, and also a large deadspace may still pose further problems for infant use.

3.1.6 The corona discharge mass flowmeter, used industrially, appears ideal for respiratory monitoring, as it ensures true mass flow rate, independent of velocity profile, with a very high accuracy ($\approx \pm 0.1\%$ FSD) and with a fast response time (< 1 ms) [87]. Unfortunately, the high voltages involved, the sensitivity to humidity and the generation of ozone (which is poisonous) appear to make it unsuitable for respiratory monitoring.

3.1.7 Vortex Flowmeters

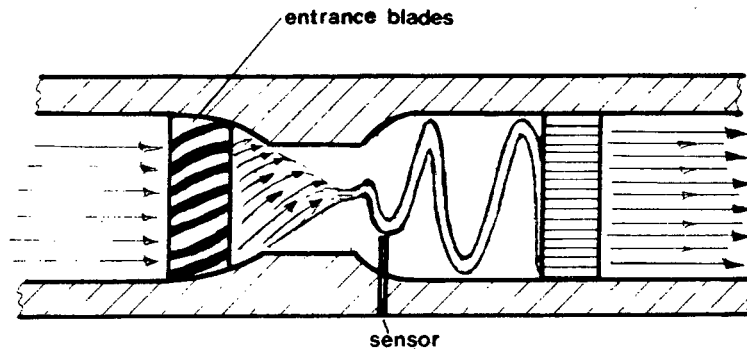
The moving fluid in the vortex flowmeter creates fluid dynamic oscillations with the oscillation frequency proportional to flow rates.

Three types are used industrially :
vortex shedding, vortex precession ("swirl meter")
and fluidic oscillation ("Coanda meter"). (See figure 3.12)
[88][89]

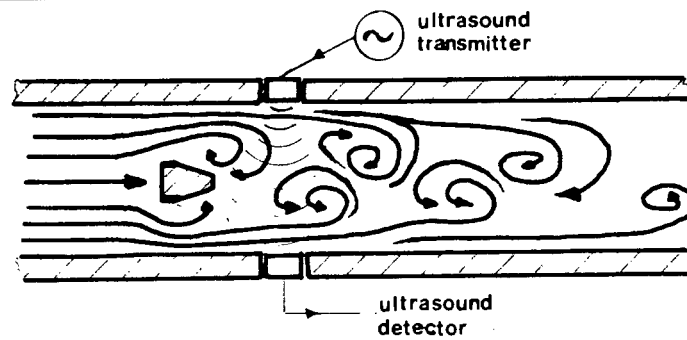
At high Reynolds' numbers ($> 20\ 000$) accuracy and repeatability can be within ± 0.5 percent over a wide dynamic range and independent of fluid physical properties [90][89]. However, at the generally lower Reynolds' numbers encountered in respiratory measurements (see section 2.1), accuracy decreases until oscillations become unpredictable and cease somewhere in the transitional flow region ($Re = 2\ 000$ to $5\ 000$) [91][89]. A flow-straightening section of greater than ten diameters is required upstream from the sensor, making the deadspace of these devices unacceptable for infant use. When measuring instantaneous flow rate the oscillation frequencies are low, even at adult respiratory flow rates. This severely restricts the frequency response over most of the respiratory cycle.

Two vortex flowmeters have been produced commercially for adult respiratory monitoring. The Bourns vortex-shedding flowmeter has a sensing threshold of 5 L/min and a claimed accuracy of ± 3 percent [92]. It uses an ingenious dual vortex-shedding system to achieve a bidirectional response [92]. The Aga (Coanda effect) fluidic spirometer claims an accuracy of ± 5 percent, but has a display resolution ± 10 ml for tidal volume. It has a relatively high flow resistance and no sensing threshold is specified [49].

Vortex precession flowmeters are claimed to operate to slightly lower Reynolds' numbers than the

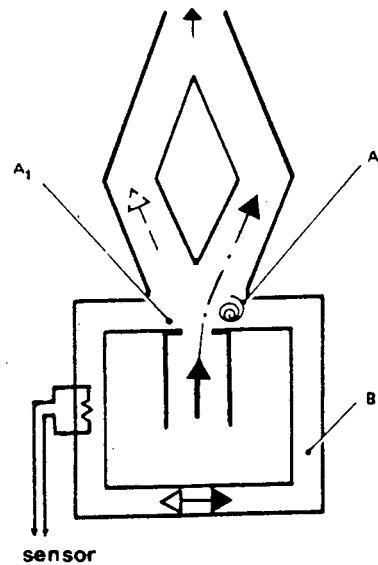


VORTEX PRECESSION FLOWMETER (swirl meter).



VORTEX SHEDDING FLOWMETER.

Working principle: The gas enters at the black arrow in the center. According to the Coanda effect, the gas stream adheres to the wall of one outflow channel only, follows this channel only, thereby giving rise to a sub-atmospheric pressure (due to vortex formation) on the same side (A2). Through the control channel (B) a pressure gradient will be set up between A1 and A2, which will force the gas stream to switch to the other outflow channel, where once again a vortex is formed. With the switching of the gas stream between A1 and A2 there will be a continuous oscillation with the passage of a fixed volume of gas for every oscillation. An electric transducer, consisting of a heated platinum wire located inside control channel B, issues oscillation impulses to an electronic counter



FLUIDIC (Coanda) FLOWMETER.

FIG. 3.12

other two vortex types [89] but they have not yet been applied to respiratory monitoring. However, for infant use, the flow sensing threshold is still likely to be too high, the deadspace too large and contamination and flow resistance may pose problems. (See figure 3.12)

3.1.8 Ultrasonic Flowmeters

Ultrasonic flowmeters measure changes in gas velocity by measuring the corresponding changes in transit time of sound as it passes through the moving gas stream. The transit time of sound through the gas stream depends, not only on gas velocity, but also on other factors, including temperature and gas composition [36][43]. By making measurements of both upstream and downstream transit times, the measurements of gas velocity can, in theory, be made independent of gas composition and temperature. In practice it has not been possible to make measurements totally independent of these factors, although other problems, such as poor zero stability, have been overcome [36][44][93]. A recent review of ultrasonic respiratory flow measurement techniques noted that the available commercial ultrasonic pneumotachographs have been withdrawn from the market because of technical problems [36]. The authors also found that, despite considerable development, ultrasonic pneumotachographs cannot at present be used for quantitative measurements [36].

Barth's detailed interim report on the development of an ultrasonic infant flowmeter [43] should be consulted in conjunction with Plaut and Webster's review [36] for more detailed information on the problems involved with these techniques.

3.1.9 Hot-Wire and Hot-Thermistor Anemometer/Spirometers

Hot-wire and hot-thermistor anemometers infer gas velocity from measurements of the convective heat loss from an electrically heated temperature sensor (thermistor or wire) placed in the gas flow. Normally the electrical

heating power required to maintain the sensor at a constant temperature higher than the ambient gas temperature is measured [94]. This heating power, controlled by a feedback bridge circuit to maintain the sensor temperature constant, increases approximately as the square root of the gas velocity (King's law), making linearisation of the signal necessary [95]. Accuracy under controlled conditions can be within two percent of reading over a wide dynamic range ($\geq 100 : 1$), with a wide bandwidth and with a high signal-to-noise ratio [97][98][94].

For measurements of volume flow rate through a tube a slightly different calibration/linearisation is required to account for changes in the velocity profile with flow rate, since velocity is sensed at a single point. Variable entrance effects can also change the velocity profile, causing additional errors. To reduce this problem, industrial flow sensors of this type are sometimes placed in an orifice to ensure turbulence and thus a flat, more repeatable velocity profile. Dynamic ranges of up to 1000 : 1 are claimed for "mass flowmeters" of this type [97]. Unfortunately, an orifice will tend to increase flow resistance too much for a respiratory flow sensor.

Gas composition can affect accuracy when large changes in gas thermal conductivity occur. For normal respiratory gas and vapour mixtures this additional error is small, except for nitrous oxide mixtures where errors of -15% to -20% can occur. (See section 4.8) The latter would result in the safer error of hyperventilation if uncorrected.

Gas temperature changes affect measurements in two ways : by changing gas density and hence thermal conductivity and by changing the temperature difference between sensor and gas. A temperature compensation technique must thus be incorporated to eliminate these errors which can be very large over the clinical

temperature range [53]. By arranging to correct for the second source of error alone, volumes are automatically corrected to body temperature and pressure (i.e. mass flow measurement).

Heated flow sensors are prone to contamination which reduces their sensitivity to flow. Fine wire sensors are particularly prone to this problem and can even be contaminated by dust particles in the air which become "baked" onto the probe [94][97][99].

For infant respiratory monitoring hot-wire/thermistor anemometry is attractive for its very wide dynamic range, good frequency response, low flow resistance and high sensitivity at low flow rates. However, a variety of problems exist for designing a practical instrument. These are related to :

- temperature compensation,
- sensitivity to nitrous oxide,
- the fact that sensors are not direction sensitive,
- sensor contamination,
- sensor entrance effects and dead space,
- complex linearisation techniques, and
- complex mechanical construction.

Hot-wire anemometers have previously been applied to respiratory testing [53][47] and adult ventilation monitoring [100]. Hot-thermistor anemometers have also been applied to lung-function tests [53][101][48] and adult ventilation monitoring [102][103]. Most of these flowmeters were not accurate at the low flow rates and tidal volumes encountered in infants, and a number were even inaccurate at high flow rates : Visick found that the Bird thermistor spirometer "was grossly inaccurate at tidal volumes less than 350 ml" and overestimated flow rate by 35 percent at 5.7 L/min. At higher flow rates it was more accurate but overestimated in oxygen

by 10 percent and underestimated in 100 percent nitrous oxide by 22 percent [102]. Cox found accuracies of ± 10 percent for high flow rate forced manoeuvres using a thermistor spirometer [101]. However, the device was subsequently withdrawn from the market [53]. Fitzgerald found gross drift of 12 to 25 percent from day to day and errors of up to 40 percent for both a thermistor and a hot-wire spirometer used for measuring forced manoeuvres. He concluded that "the devices were advertised and sold without adequate specifications or clinical trial" [53]. Appel claimed an accuracy of ± 5 percent for a thermistor flowmeter above 12 L/min with additional errors up to 3.5 percent for temperature changes [103]. He did not quote measurements below 12 L/min or for different gas mixtures. A number of recent commercial devices for measuring high flow rate forced manoeuvres claim accuracies of about 5 percent [48][47] but have not been tested independently. Of all of the hot-wire respiratory flowmeters developed so far, the recent work of Kann, using an expensive commercial lineariser, achieved the highest performance with a claimed clinical accuracy of 5 to 10 percent from 12 L/min to 0.33 L/min. Inspiratory/expiratory sensitivity difference was an additional 5 percent [100].

Size and deadspace of all of these flowmeters was much too large for infant use.

3.2 Conclusion

Existing spirometry equipment is unsuitable for the demanding application of routine respiratory monitoring in infants.

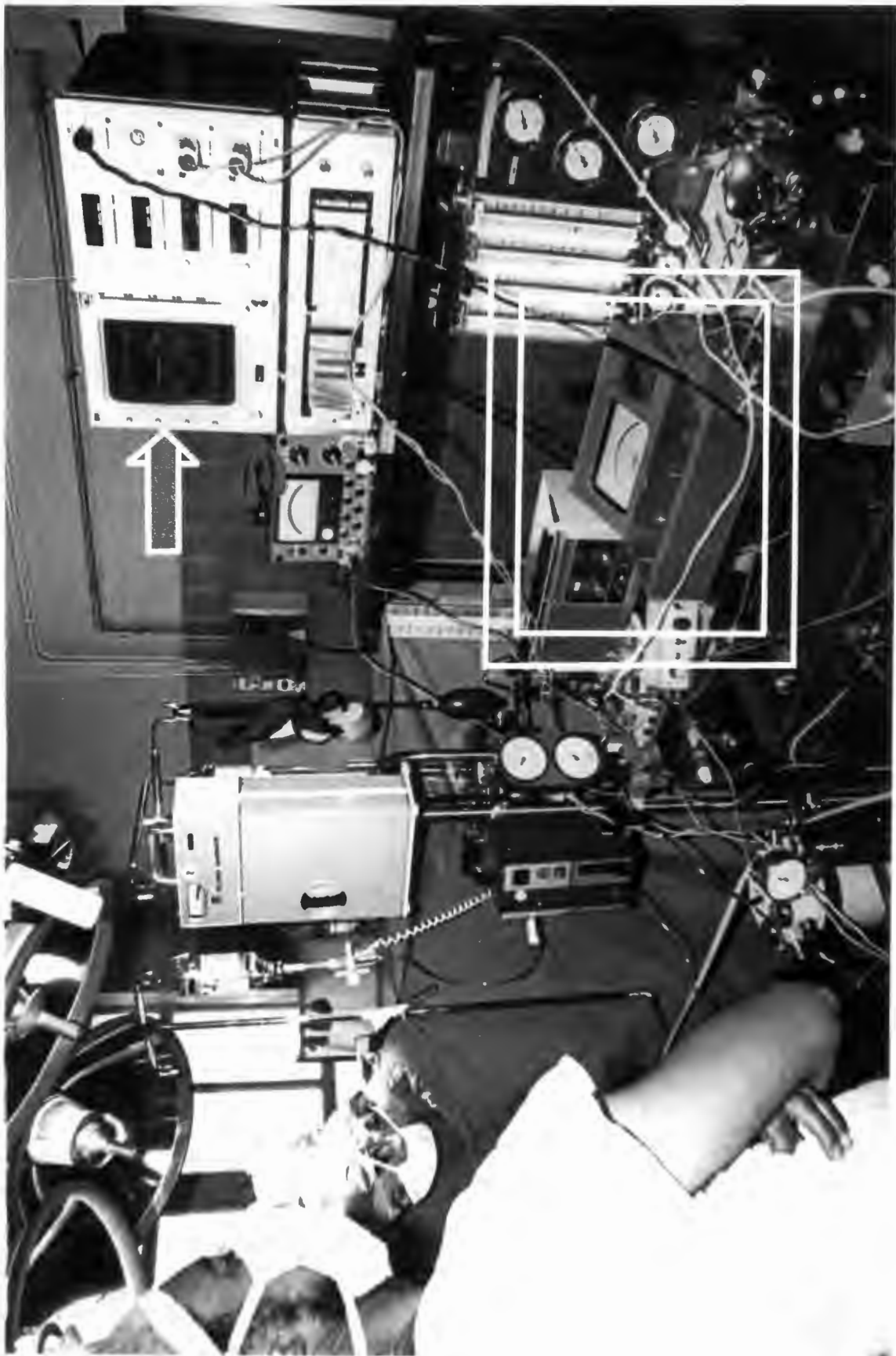


Figure P 4.1

Flowmeter (framed) in use for monitoring ventilation during surgery. Instantaneous flow rate waveform (arrow) displayed on theatre memory display.

4. Hot-Thermistor Spirometry

The previous section briefly introduced the hot-wire and hot-thermistor anemometer/spirometer. This section develops the theory of the hot-thermistor anemometer and describes the design of the hot-thermistor spirometer developed in this thesis.

4.1 Heat-Transfer Equations

Since the pioneering theoretical and experimental work on hot-wire anemometers by King in 1914 [95], numerous investigators have studied the transfer of heat from slender cylinders (wires) to a fluid medium. Most of this work aimed to extend the theoretical and practical basis for hot-wire anemometry. Hot-thermistor anemometers are physically different from slender hot wires in that they measure heat transfer from minute thermistor beads to the fluid. This situation is closer to that for heat transfer from a sphere to the fluid, although a substantial amount of heat is also transferred to the fluid through the thermistor's fine wire leads. (This can be inferred from changes in the thermal time constant of identical bead thermistors mounted with different lead lengths. See [104].) Relatively few studies of heat transfer from spheres have been published. Kramers found that the non-dimensional equations describing heat transfer from a sphere were similar to those describing heat transfer from a cylinder [105]. For the purposes of the discussion which follows it is assumed that the non-dimensional equations describing heat transfer from the thermistor bead may be approximated by using either Kramers' equations or the equations for hot-wire probes. This is a reasonable assumption, as other workers use almost identical equations for hot-film sensors with a variety of geometries [106][107]. Even in the case of hot-wire sensors the equations are approximations which are used qualitatively and fitted to experimental data [94].

$$\text{Prandtl Number} : P_r = \frac{C_p \mu}{k}$$

$$\text{Nusselt Number} : N_u = \frac{h L}{k}$$

$$\text{Reynolds' Number} : R_e = \frac{L U \rho}{\mu}$$

$$\text{Grashof Number} : G_r = \frac{L^3 \rho^2 g \Delta T \beta}{\mu^2}$$

where :

U - fluid velocity

C_p - specific heat at constant pressure (fluid)

ρ - density (fluid)

μ - dynamic viscosity (fluid)

k - thermal conductivity (fluid)

h - heat-transfer coefficient (sensor to fluid)

g - acceleration due to gravity

T_a - ambient temperature (fluid)

T_s - sensor temperature

T_m - film temperature = $\frac{(T_s - T_a)}{2}$

ΔT - $(T_s - T_a)$

L - characteristic dimension (sensor)

β - coefficient of thermal expansion (fluid)

V_{th} - sensor voltage

R_{th} - sensor resistance

d - sensor diameter (for sphere)

Figure 4.1 Definition of Non-Dimensional Parameters and Symbols. Equations using non-dimensional parameters are used to generalise the description of heat transfer from a heated flow sensor to the surrounding fluid.

Fig. 4.1 defines the non-dimensional parameters used to characterise heat transfer from flow sensors [108]. At high fluid velocities (forced convection) the Nusselt number N_u is a function of the Prandtl number P_r , which describes viscous/thermal properties of the fluid, and the Reynolds' number R_e , which describes inertial and viscous forces. At low velocities, in either mixed or natural ("free") convection, the Grashof number G_r , which describes gravitational (buoyancy) effects, must also be included [109][110].

Since the early work of King [95], and for conditions of forced convection, most investigators have fitted their experimental heat transfer data to an equation which can be written in the form :

$$N_u = A + B R_e^n \quad \dots \quad \dots \quad \dots \quad 4.1$$

where A and B are constants with A approximately 0.3 to 0.5, B approximately 0.4 to 0.7 and the exponent n has a value between 0.45 and 0.5 [111][110][94][112].

This equation is sometimes expressed as :

$$N_u = A(P_r)^w + B(P_r)^m(R_e)^n \quad \dots \quad \dots \quad 4.2$$

where A and B are new constants also of the order of 0.5 and the exponent w is approximately 0.2 to 0.33 with m approximately 0.33. [105][107][106]

Kramers' [105] corresponding formulation for spheres under conditions of purely forced convection was :

$$N_u = 2 + 1.3(P_r)^{0.15} + 0.66(P_r)^{0.31}(R_e)^{0.5} \quad \dots \quad 4.3$$

The fluid properties that determine N_u , P_r and R_e depend strongly on temperature [113][108] Most workers evaluate them at a fixed "mean film temperature" T_m (see figure 4.1) but even this is an approximation, with some workers using a variety of reference temperatures.

Experimentally determined values for the constants A and B depend slightly on film temperature. An additional factor to account for this is sometimes included in the heat transfer equation :

$$N_u \left(\frac{T_m}{T_a} \right)^p = A + B (R_e)^n \quad \dots \quad \dots \quad \dots \quad \dots \quad 4.4$$

[112][110][94]

For wire sensors this variation reflects end support effects, including axial heat conduction to the wire supports, since for very slender sensors p tends to 0 [110]. For more common lower aspect ratio wires p. is typically 0.7.

End effects do not seem to have been investigated for thermistor sensors. To minimise these effects leads should be as fine as possible and should be soldered to the supports as far from the thermistor bead as is practical. From 4.4 it follows that end effects are undesirable as they reduce the sensitivity to flow and increase the sensitivity to ambient temperature fluctuations. For long, fine thermistor leads which are in the gas stream, the heat transfer coefficient h in the Nusselt number (see figure 4.1) will be larger than expected, due to the larger effective surface area for heat transfer. However, if the thermistor's leads are short, end effects may lead to the requirement for a substantial temperature loading factor similar to that for short wire sensors (equation 4.4).

It is common to define the heat transfer coefficient h, and hence Nusselt number, in terms of the electrical heating power and sensor surface area. For a spherical sensor (using symbols from figure 4.1) :

$$h = \left(\frac{v_{th}^2}{R_{th}} \right) \frac{1}{\pi d^2} \left(\frac{1}{\Delta T} \right)$$

and

$$N_u = \frac{v_{th}^2}{R_{th} \cdot \pi \cdot d \cdot \Delta T \cdot k} \quad \dots \quad \dots \quad 4.5$$

Substituting this into Kramers' equation 4.3 for spheres,

$$V_{th}^2 = R_{th} \pi d \Delta T \cdot k (2 + 1.3 (P_r)^{0.15} + 0.66 (P_r)^{0.31} \left(\frac{d\rho}{\mu} \right)^{0.5} U^{0.5}) \quad \underline{4.6}$$

Thus, for constant gas properties and sensor temperature (resistance),

$$V_{th}^2 = \Delta T (C + D U^{0.5}) \quad \dots \quad \dots \quad \dots \quad \underline{4.7}$$

This is identical to the normal "King's Law" relationship for cylinders with C and D constants dependent on gas properties and sensor physical size.

For wire sensors, the exponent of U which "best fits" experimental King's Law data, has been investigated by numerous workers, with most workers now using a value of 0.45 rather than 0.5 [109][110][94][112][114]. To fit data to a wide range of velocities, this exponent is sometimes chosen to be larger than 0.45 at low velocities and smaller at high velocities [115]. At very low velocities, in the mixed convection range, equations like 4.6 and 4.7 need additional correction until an absolute limit to sensing is set by natural convection fluctuations [109]. At very low flow rates a simple King's Law relationship like 4.7 overestimates the sensor voltage [105].

4.2 Constant-Temperature Anemometry

Constant-Current or Constant-Temperature Operation?

Early hot-wire anemometers were operated with a constant heating current. Voltage changes across the sensor then reflected changes in temperature produced by changes in forced convection. More recently semiconductor amplifiers, with a sufficiently low voltage noise and drift, have allowed the construction of reliable constant-temperature anemometers (see figure 4.2).

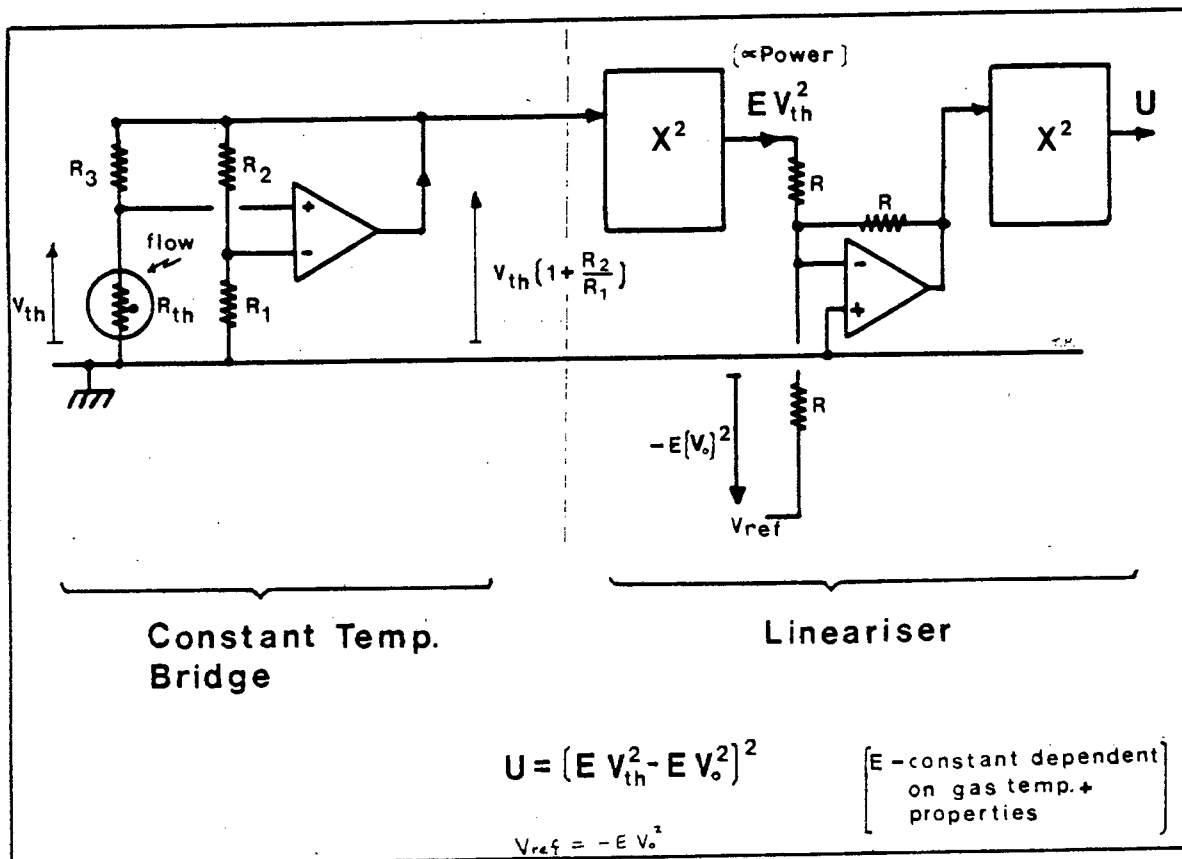


Figure 4.2 : Simplified Constant-Temperature Thermistor Anemometer and Lineariser

Feedback around the bridge circuit adjusts the heating power to the thermistor to maintain its resistance and hence temperature constant. When power is applied positive feedback through R_3 and R_{th} causes the amplifier output to rise to a level at which thermistor heating reduces the positive feedback to match the negative feedback through R_2 and R_1 . A hot-wire anemometer is similar, except for the bridge circuit, which would have the input leads to the amplifier interchanged to accommodate the wire's positive resistance temperature coefficient.

Constant-temperature anemometers have now almost entirely replaced constant-current anemometers, since they extend the sensor bandwidth, are simpler to linearise and temperature compensate, have a wider dynamic range and do not suffer from probe "burn-out" at low velocities [97][94].

4.3 Temperature Compensation

Changes in ambient gas temperature give rise to errors in the measured velocity of a simple anemometer like that shown in figure 4.2. These errors arise directly from the change in T and indirectly from changes in gas properties with film temperature changes. Fig. 4.3 shows that the Prandtl number differs by less than ± 0.7 percent for common respiratory gasses at a fixed temperature of 66°C and that P_r varies with temperature by less than 0.1 percent/ $^\circ\text{C}$. These small variations can be neglected in the heat transfer equation 4.6, especially since P_r 's exponent is less than one. Rewriting equation 4.6 by grouping P_r and other factors independent of temperature into two new constants A, B , we have :

$$U = \left(\frac{\mu}{\rho}\right) \left(\frac{B \cdot V_{th}^2}{\Delta T \cdot k} - A\right)^2 \quad \dots \quad \dots \quad \dots \quad 4.8$$

Evaluating μ, ρ and k at film temperature T_m , provides the closest fit to experimental data [116]. Sensitivity to changes in ambient temperature is thus lower than would be the case if these properties depended only on ambient temperature.

To assess the errors produced by a change in temperature (and/or gas properties), we rewrite equation 4.8, for the conditions at calibration, subscript 1, and for the new conditions, subscript 2. This results in an apparent change of velocity from U to U_{app} , although the velocity is constant at a value U :

$$\text{Calibration : } U = \left(\frac{\mu_1}{\rho_1}\right) \left[\frac{B \cdot V_{th1}^2}{\Delta T_1 k_1} - A\right]^2 \quad \dots \quad \dots \quad 4.9$$

$$\text{New conditions : } V_{th2}^2 = \left[\left(\frac{\rho_2}{\mu_2}\right)^{0.5} U^{0.5} + A \frac{\Delta T_2 \cdot k_2}{B} \right]^2 \quad \dots \quad 4.10$$

Units Gas	k Thermal Conductivity $W.m^{-1}.k^{-1}$	μ Viscosity mPa.sec	C_p Specific Heat $J.Kg^{-1}.k^{-1}$	ρ Density $Kg.m^{-3}$	Pr Prandtl Number at 66°C	$(Pr)_F$ (Pr) ^{0.33} at 66°C	Pr Prandtl Number at 25°C	$\frac{\rho}{\mu}$ $Kg.m^{-3}.Pa^{-1}.s^{-1}$
Air	0.0287	0.0205	994	1.023	0.710	0.893	0.718	49902
O ₂	0.0293	0.0232	915	1.136	0.725	0.899	0.752	48965
N ₂	0.0285	0.0198	1015	0.993	0.705	0.891	0.712	50151
N ₂ O	0.0203	0.0166	875	1.572	0.716	0.896	0.752	94698
67 % N ₂ O + 33 % O ₂	0.0233	0.0188	888	1.428	0.717	0.896	0.741	75957
50 % N ₂ O + 50 % O ₂	0.0248	0.0199	895	1.354	0.718	0.896	0.737	68040

Figure 4.3 Gas properties evaluated at a film temperature $T_f = (102 + \frac{30}{2}) = 66^\circ C$ and 750 mm Hg pressure. Values are based on calculation and interpolation from data in reference [113]. (Errors in N₂O data from [113] have been corrected.) The values for N₂O/O₂ mixtures were obtained by linear interpolation using the data for each gas separately. (Reference [117] discusses more accurate calculation techniques for gas mixtures.)

The anemometer interprets equation 4.10 using calibration equation 4.9 :

$$U_{\text{app}} = \left(\frac{\mu_1}{\rho_1} \right) \left[\frac{\Delta T_2 \cdot k_2}{\Delta T_1 \cdot k_1} \left(\left(\frac{\rho_2}{\mu_2} \right)^{0.5} U^{0.5} + A \right) - A \right]^2 \dots \quad 4.11$$

which can be rewritten :

$$U_{\text{app}} = \left[\left(\frac{\Delta T_2 \cdot k_2}{\Delta T_1 \cdot k_1} \right) \left(\frac{\rho_2}{\rho_1} \right)^{0.5} \left(\frac{\mu_1}{\mu_2} \right)^{0.5} U^{0.5} - A \left(\frac{\mu_1}{\rho_1} \right)^{0.5} \left(1 - \frac{\Delta T_2 \cdot k_2}{\Delta T_1 \cdot k_1} \right) \right]^2 \dots \quad 4.12$$

The first term in the right-hand side of equation 4.12 can be interpreted as changing the scale factor and the second term as shifting the zero setting.

Density is inversely related to absolute temperature. Thus we evaluate the gas properties at film temperatures T_1 and T_2 using :

$$\frac{\rho_2}{\rho_1} = \frac{T_1}{T_2} \quad \dots \quad \dots \quad \dots \quad 4.13$$

Over a limited temperature range we can estimate changes in thermal conductivity [118] and viscosity in both air and oxygen using :

$$\frac{k_1}{k_2} = \left(\frac{T_1}{T_2} \right)^{0.81} \quad \text{and} \quad \frac{\mu_1}{\mu_2} = \left(\frac{T_1}{T_2} \right)^{0.81} \quad \dots \quad 4.14$$

(for $273^\circ < T < 373^\circ \text{K}$, based on data in [113].)

For nitrous oxide mixtures equation 4.14 is not sufficiently accurate and the exponent of temperature must be increased. For 100 percent N_2O the exponent increases to 1 for viscosity and 1.19 for thermal conductivity (based on data in [113]).

Substituting 4.13 and 4.14 into 4.12 allows us to calculate the apparent change in velocity produced by a change in temperature :

$$U_{app} = \left[\frac{\Delta T_2}{\Delta T_1} \left(\frac{T_2}{T_1} \right)^{0.81} \left(\frac{T_1}{T_2} \right)^{0.5} \left(\frac{T_1}{T_2} \right)^{0.4} U^{0.5} - A \left(\frac{\mu_1}{\rho_1} \right)^{0.5} \left(1 - \frac{\Delta T_2}{\Delta T_1} \left(\frac{T_2}{T_1} \right)^{0.81} \right) \right]^2 \dots \dots 4.15a$$

$$= \left[\frac{\Delta T_2}{\Delta T_1} \left(\frac{T_2}{T_1} \right)^{0.81} \left(\frac{T_1}{T_2} \right)^{0.9} U^{0.5} - A \left(\frac{\mu_1}{\rho_1} \right)^{0.5} \left(1 - \left(\frac{\Delta T_2}{\Delta T_1} \right) \left(\frac{T_2}{T_1} \right)^{0.81} \right) \right]^2 \dots \dots 4.15b$$

Equation 4.15b shows that for complete temperature compensation three temperature correction terms may have to be considered. The largest changes are produced by the ΔT terms, since ΔT_1 and ΔT_2 are normally much less than film temperatures T_1 and T_2 .

An ingenious, though complex, three-term temperature compensation scheme has been described by Chevray [118]. He assumed that equations like 4.14 may be adequately represented by a linear function of temperature over a limited temperature range, but neglected to include the effects of viscosity in the theoretical derivation. The latter probably does not materially affect the technique, since constants can be adjusted to account for the small additional changes. He apparently adjusted these constants empirically when calibrating the system. An unheated wire sensor was used with a multiplier, a divider and a square-root circuit to correct for changes in ΔT . (Figure 3 in the original paper appears to be in error, since a squaring circuit should be included after the divider.) Chevray used an additional commercial flow lineariser, including three logarithmic amplifiers, to compensate for the remaining temperature dependent film properties while simultaneously linearising the output.

A simpler, more popular technique tries to maintain

sensor temperature at a constant ΔT above ambient by including the temperature sensor as part of the bridge circuit. This eliminates ΔT dependence but doubles film temperature changes and corresponding gas property changes. Adjusting the compensation to allow a slight change in ΔT can probably reduce this temperature dependence over a limited temperature range. One problem in using this technique involves minimising dissipation and thus flow sensitivity of the temperature sensor at the same time as providing correct temperature compensation. With thermistors a high-resistance temperature-compensation thermistor eliminates dissipation problems, but the temperature sensor generally has a different resistance-temperature coefficient from the flow sensor. The high resistance is also more prone to shorting by water condensation. Adjusting temperature compensation is extremely tedious with this technique, since adjusting temperature compensation changes ΔT and hence the required temperature compensation.

Grahn [119] has described a simple bridge modification which minimises temperature-sensor dissipation while using identical thermistors for flow sensing and temperature correction (figure 4.4) However, this technique increases the amplifier noise gain, and is very tedious to set up because the three pre-set bridge controls all interact.

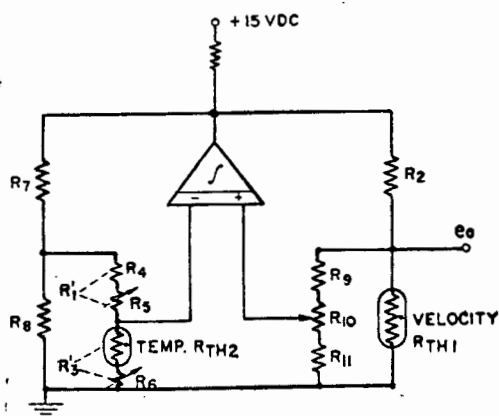


Figure 4.4 Constant-Temperature Difference Thermistor Bridge Circuit due to Grahn [119]. All three pre-set controls interact making setting up difficult.

Appel [103] used a separate temperature correction bridge (figure 4.5) to maintain a constant temperature difference. This produced errors, over a 20°C to 39°C range, of -3.7 percent to 3.5 percent, which he attributed to imperfect output from the temperature bridge. It

seems likely that film temperature changes also contributed to this error.

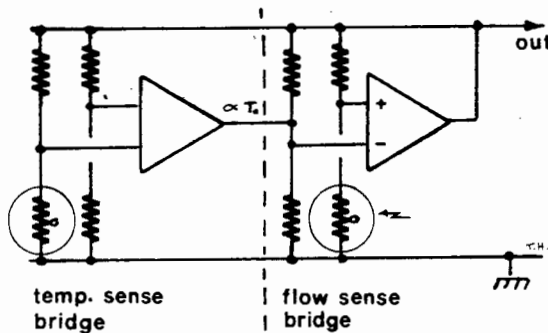


Figure 4.5 Principle of the Constant-Temperature Difference Bridge due to Appel [103]

Sakao [120] has described a temperature-compensation technique using two constant-temperature bridge circuits, both placed in the gas flow but operated at different temperatures. He measured the difference in heating power required by each sensor (figure 4.6).

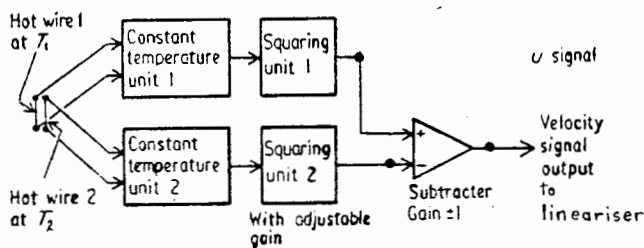


Figure 4.6 Dual Constant-Temperature Bridge Temperature-Compensation Technique due to Sakao [120]

This eliminates the direct ΔT dependence but only partially compensates for sensor film temperature changes. Sakao presented insufficient experimental data to evaluate the technique over a wide range of conditions but the technique may be sufficiently accurate over a limited temperature range for respiratory monitoring. Sakao's technique is attractive since it requires no temperature compensation adjustments and condensation will not occur on either sensor. Disadvantages are an increase in the quantity of circuitry required and practical problems of sensor placement so that thermal wakes do not cause interference between the sensors.

An unusual temperature-compensation technique which corrects for ΔT changes as well as zero shifts produced by film temperature changes has been described

by Zanker [121]. By placing two constant-temperature sensors symmetrically on either side of an orifice plate the two sensors sense different velocities. Taking the ratio of the outputs of the two bridges provides a signal which only has a scale factor error dependent on gas property changes with film temperature. The system is mechanically symmetrical so that bi-directional flow sensing can be implemented. The dynamic range is limited by the orifice plate's high flow resistance.

Grahn [122] has described a technique for constructing a direction-sensing blood velocity sensor using two constant-temperature difference bridges similar to figure 4.4. The two flow sensors are arranged physically so that one sensor is partially shielded from fluid flow in one direction while the second sensor is shielded from flow in the other direction. The difference between the linearised outputs of the two sensors yields a bi-directional flow signal. Although not specifically designed by Grahn for temperature-compensation, this technique would automatically correct for zero shift caused by film property changes from gas composition or temperature changes, while the constant ΔT circuitry corrects for the direct temperature dependence. The only remaining temperature effect is the film property dependence which affects scale factor. A careful evaluation of equation 4.15b shows that this scale factor dependence is very small $(\propto (\frac{T_2}{T_1})^{0.09})$ and, if necessary, this correction can probably be included in the ΔT correction calibration.

The only apparent disadvantages of using a technique similar to Grahn's are the complex setting up required, the complex sensor construction and the large quantity of circuitry for two sensors and linearisers. To investigate and simplify the technique a new sensor based on Grahn's work but with a different mechanical form (figure 4.7) and different temperature compensation was constructed.

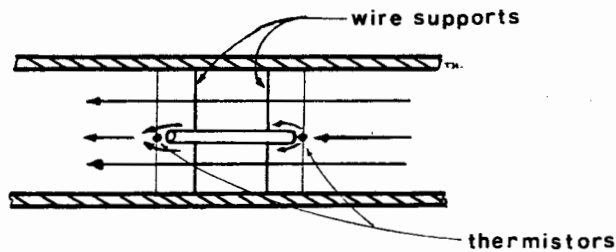


Figure 4.7 Experimental Direction-Sensitive Flow Sensor.
Coaxial perspex rod shields whichever sensor is downstream from the gas flow. Measured difference in sensor outputs yields directional zero-corrected signal.

To simplify the electronics the difference between the squared bridge voltages was measured. The signal was then fed into a final squaring circuit for linearisation. Two problems were encountered :

- (i) Condensation on the central coaxial shield was periodically blown onto the sensors causing erratic sensor output; and
- (ii) it was extremely difficult to match forward and reverse sensitivities precisely, probably owing to small mounting and sensor differences.

This technique was abandoned as the sensor is relatively complex to construct, the condensation problem is difficult to overcome, and the quantity of electronics required is large. Nevertheless, this technique remains attractive, since it is shown below that the major error produced by gas composition changes is a zero shift, and this technique produces an accurate zero correction. Using a zero-correction sensor totally shielded from the flow would not give as accurate a correction, since heat transfer under only natural convection has a different sensitivity to changes in gas properties.

The relationship between gas velocity U and the sensor voltage V_{th} of a constant-temperature anemometer is non-linear. We can rewrite the normal King's Law relationship (4.7) using the fact that the bridge voltage V_b is proportional to V_{th} :

$$U = (B V_b^2 - A)^n \quad \dots \quad \dots \quad 4.16$$

where $n = 2$ and A, B are constants for constant ambient conditions. This leads directly to the widely used linearisation technique shown in figure 4.2. Bruun [123] has shown that A can be determined at zero velocity (where $V_b = V_o$, thus $A = V_o^2$), without appreciably degrading accuracy, although equation 4.16 is not applicable to very low velocities. For highest accuracy Bruun found A should be about $0.9 V_o^2$ for his sensors [115]. He also promoted the idea of a universal calibration law for probes of similar construction [123][115][124]. Using a universal law implies that, once the precise form of an equation like 4.16 has been determined experimentally for one probe, applying this linearisation to physically similar probes requires adjustment only of zero and scale factor - the shape of the curve remains the same. This method of using a single analytical function for linearisation of more than one sensor is important, as it eliminates tedious, costly calibration procedures.

An equation like 4.16 with a fixed exponent n linearises the anemometer over a maximum range of 30 : 1 at low velocities [123]. At "high" velocities the linear range can be less than 5 : 1 [123]. To linearise an anemometer over a wider dynamic range a more complex system than figure 4.2 must normally be used. A digital system using either an analytic function (polynomial) or look-up table could be used for linearisation, but

the required system resolution (for A/D, D/A etc) makes this costly. (A signal-to-noise ratio of 37 dB and a 200 : 1 dynamic range implies a resolution of 13 to 14 bits.) One commercial pulmonary function tester apparently [48] uses this approach for measuring flow volume loops but it does not operate in real time and does not operate over as wide a dynamic range.

Linearisers have previously used two approaches : Linear piecewise approximations [103][125][126] or an analytical function approximation, using an inverse King's Law or polynomial relationship [119][122][98][127][102][128]. Freymouth combined both techniques, using a King's Law lineariser followed by a 10-chord straight-line lineariser to achieve a 250 : 1 dynamic range within 5 percent [129]. Disa Elektronik manufacture a lineariser using a modified King's Law relationship in which the exponent (n of equation 4.16) can be a function of velocity [98]. Making the exponent a simple linear function of velocity can extend linearity substantially [130] although Bruun has shown that this approximation deteriorates at low velocities [123][115]. The Disa lineariser extends its range to very low velocities by including an additional correction term with an exponent of 0.5 for low velocities [98].

Bruun [115] used experimental data from a hot-wire sensor to compare theoretically the accuracy of three different linearisation techniques :

(i) Froebel's [128] polynomial :

$$U = k_1 (V_b - V_o) + k_2 (V_b - V_o)^2 + k_3 (V_b - V_o)^4 \quad \dots \quad 4.17$$

(with k_1, k_2, k_3 constants for fixed ambient conditions);

(ii) an extended power law (similar to King's Law but with an additional term CU with C a constant having a small negative value) :

$$V_b^2 = A + B U^{0.5} + C U \quad \dots \quad \dots \quad 4.18$$

and

(iii) a 10-chord straight-line segment approximation.

The extended-power law was slightly more accurate than the polynomial over a wide range of flow rates, while the straight-line approximation was inferior to both techniques (although the performance was better than a simple King's law lineariser [115]).

From a practical point of view straight-line approximations are simple to implement, but very tedious to adjust and use a large quantity of hardware. Froebel's polynomial requires hardly any more hardware than a simple King's Law lineariser, but, like a King's Law lineariser, it requires two high performance multipliers. The extended-power law requires more hardware for a direct implementation of the inverse relationship of equation 4.18. In addition, the square root followed by the squaring operation required for the direct implementation will result in a limited dynamic range. (Exactly the same problem exists in measuring root-mean-square quantities and has led to the use of implicit circuits for this purpose.) However, using an implicit circuit, it should be possible to implement this technique with an acceptable accuracy and the same level of complexity as Froebel's polynomial. Figure 4.8 shows an implicit implementation of the extended-power law which was initially designed and then discarded in favour of a totally new approach which is simple and has a very wide dynamic range. (See section 4.8.2)

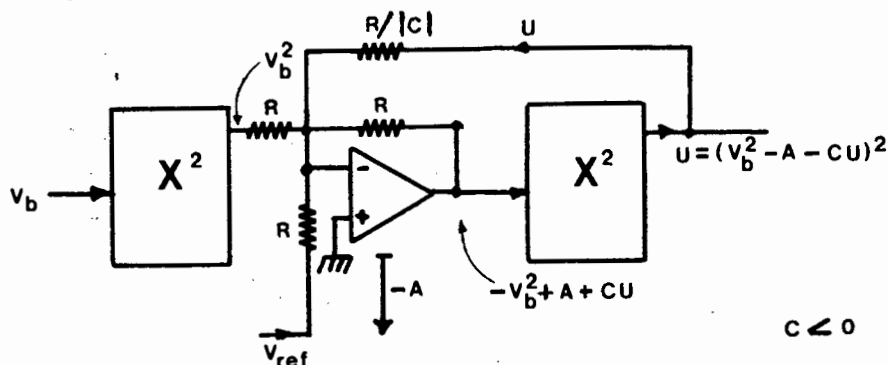


Figure 4.8 Novel implicit implementation of extended-power-law lineariser. This technique was not implemented as a better technique described in section 4.8.2 was developed. C is a small negative quantity which explains the apparently incorrect sign of the feedback from the overall output.

4.5 Thermistors

Thermistors are semiconductors made from sintered mixtures of divalent and trivalent metal oxides. They have a large but non-linear negative temperature coefficient, typically ten or more times greater than the positive temperature coefficient of metals [131]. Resistance at any temperature over a range of at least 100° K can be calculated within one percent using the relationship :

$$R_1 = R_2 e^{\left(\frac{B}{T_1} - \frac{B}{T_2}\right)} \dots \dots \dots 4.19$$

where B is a constant dependent on thermistor material (B typically lies between 2000° and 3500° K) and R_1 and R_2 are the resistances at temperatures T_1 and T_2 [131]. For the thermistor chosen for this work (U23US/D [131]) $B = 2900^\circ \text{K}$ and R is $2\text{k}\Omega$ nominal at 20°C . Using equation 4.19 yields a resistance of 232Ω at a constant operating temperature of 102°C . The long-term stability of thermistors can be extremely high[132][133]but very small beads can have a lower stability (personal correspondence with Yellow Springs Inst. Co., Ohio, U.S.A.). The interchangeability of low-cost commercial thermistors is poor without special selection, which increases cost. Commonly available low-cost thermistors have an initial resistance tolerance of about 20 percent at room temperature, with an additional tolerance on the constant B. A selected thermistor with a tolerance on resistance of \pm one percent might cost eight times more than an unselected device, but still have a tolerance of \pm 20 percent at a temperature 250°C higher, owing to this tolerance on B [133].

4.6 Hot-Thermistor or Hot-Wire Spirometer?

Small commercial bead thermistors suitable for use as flow sensors range in diameter from 130 to $400\mu\text{m}$. This relatively large size, combined with a low thermal

conductivity severely limits the bandwidth of these sensors. Wire sensors are typically 3 to 5 μm in diameter, have a high thermal conductivity and thus achieve bandwidths in air typically two to three orders of magnitude better than thermistors. Nevertheless, it is shown below that an adequate bandwidth for respiratory monitoring can be achieved with commercial bead sensors.

Sensitivity to dirt collection is inversely related to size [94]. Thus thermistors are far less prone to contamination than wire sensors, which suffer from stability problems caused by dust [94][134][123][109][135]. For the relatively low velocities encountered in respiratory monitoring, thermistor sensors are far more robust than the fine wire sensors which are essential to minimise end effects and maximise signal-to-noise ratio. The stability of commercial platinum-plated tungsten sensors is inadequate for long-term use [109] making the even more fragile platinum wires desirable for respiratory monitoring. Unfortunately heated platinum can act as a catalyst [135] and could thus possibly cause anaesthetic agents to decompose and produce harmful by-products.

Wire sensors have a small attitude dependence [109] at velocities where free convection is significant but this effect is insignificant for bead thermistors.

Lumley has compared thermistor sensors with wire sensors in a detailed theoretical investigation [96]. He found that thermistors offer at least an order of magnitude improvement in signal to noise ratio compared with wires, when operated under similar conditions. This improvement results from the thermistor's larger resistance-temperature coefficient. The signal-to-noise ratio improvement will normally be substantially greater than this because thermistors with very much higher resistances than the wire sensor's typical 15 ohm value can be used. We can see this by noting that even special low-noise amplifiers seldom have an equivalent noise voltage resistance below $100\ \Omega$ while most monolithic operational

amplifiers have equivalent noise voltage resistances above $6 \text{ k}\Omega$. Thus, by using a thermistor sensor with a resistance of 100 ohms (or greater), the signal-to-noise ratio will be at least $\sqrt{100/15}$ times better for the same operating conditions (dissipation), because the bridge output voltage will increase with increasing sensor resistance. The higher thermistor resistances also reduce sensor current, thus eliminating lead resistance and contact resistance problems. The larger bridge output from the thermistor sensor also reduces problems from thermocouple effects and amplifier d.c. drift. This high output allows a much more flexible choice of bridge operating conditions, since a high signal-to-noise ratio can still be achieved at low sensor temperatures.

Lumley showed that the thermistor's frequency response is dynamically limited to a relatively low value by the thermistor's low thermal conductivity, which attenuates rapid fluctuations in temperature, caused by flow fluctuations, and prevents them from penetrating to the interior of the bead. The bridge amplifier is thus unable to compensate for this degeneration in frequency response [96].

At high velocities the low thermal conductivity of the thermistor material (and its thin glass coating) can produce substantial temperature gradients in the bead, although the amplifier/bridge still maintains the overall average resistance constant. This acts to reduce the velocity sensitivity and hence reduces the signal-to-noise ratio [96]. However, providing that velocities are not too high, this additional reduction in output can be corrected in the lineariser.

4.7 Frequency Response

Lumley has shown that the conventional test technique, used for optimising the dynamic response of hot-wire anemometers and estimating their bandwidth (by injecting a small sinewave or square wave test signal into one arm of the sensor bridge,) over-estimates the thermistor sensor's bandwidth,

which is dynamically limited [96]. He suggested that it is possible to estimate a limiting frequency f from :

$$f = \frac{4 K_m}{r^2}$$

where K_m is thermal diffusivity of the thermistor material, ($K_m = 0.402 \text{ E} - 6 \text{ m}^2/\text{sec}$ [96]) and r is the bead radius. Calculating this frequency for the sensor used in this work the U23UD bead with a radius of $200 \mu\text{m}$ [131] yields $f = 40.2 \text{ Hz}$. This is probably a conservative estimate as a substantial amount of heat is conducted from the centre of the bead by the wire leads which have a much higher thermal diffusivity than the thermistor material. A 40 Hz bandwidth is more than adequate for normal respiratory monitoring. However, we could achieve a bandwidth up to about 250 Hz using the smallest available commercial beads with $r = 80 \mu\text{m}$ [133].

The frequency response that can be attained also depends slightly on Reynolds' number (especially at low Reynolds' numbers), on system-damping coefficients and ΔT [136][137][138]. For hot-wire anemometers the system-damping coefficient is normally adjusted by having a variable offset voltage included in series with one of the bridge amplifier's inputs. A small square wave (or sinewave) test signal added to one of the bridge arms via a high-value resistance then allows system damping (and frequency response) to be optimised [139][136]. For simplicity and because the dynamic limitation on frequency response is a severe restriction for thermistors, no offset adjustment was used in this work. For completeness a small-signal sinewave test was performed and this is shown in figure 4.9. The 20 dB peak at about 850 Hz would normally indicate that system response begins to decline near this frequency but the dynamic limitation calculated earlier indicates that this is erroneous and sensor response must begin to decrease from about 40 Hz.

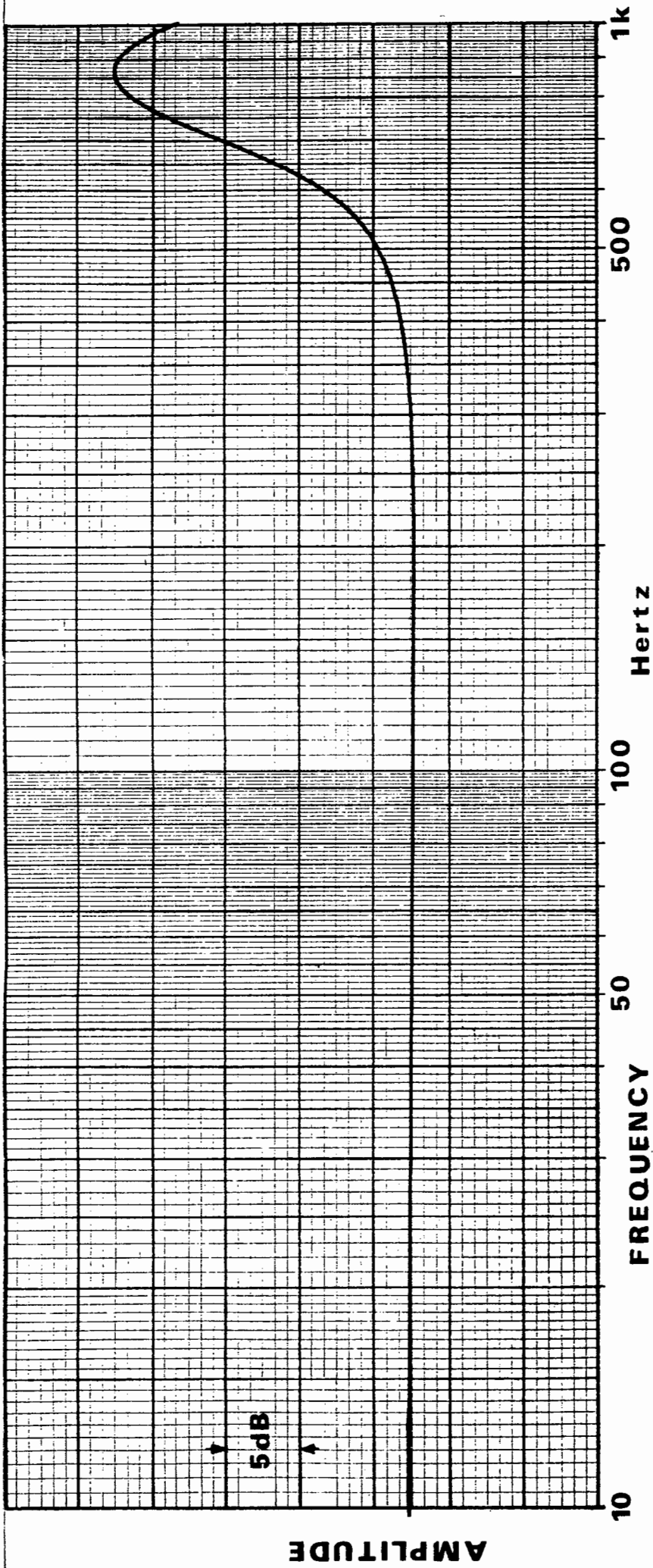


Figure 4.9 Small-signal amplitude-frequency response of thermistor flowmeter obtained by injecting signal into bridge circuit via a 39 K resistance. Frequency response is dynamically limited to a much lower value than is apparent from the above perturbation response.

4.8 Thermistor Spirometry : More Detailed Aspects of This Work.

One of the primary objectives of this work was to develop simple reliable monitoring equipment and techniques. To achieve high reliability it was important to try to minimise the amount of circuitry and simplify the sensor mechanical construction. With this in mind it proved possible to include the temperature compensation as part of the lineariser. The lineariser is no more complex than a simple low-performance King's law lineariser, yet it can achieve a dynamic range of about 200 : 1 while simultaneously providing temperature compensation. The temperature-compensation technique also provides a signal proportional to temperature which is useful for monitoring instantaneous gas temperatures. An integrator was included to allow testing and calibration using a super syringe.

The thermistor operating temperature was chosen at a much lower value than is common for wires to minimise heating power (for safety reasons) and to minimise any temperature-loading factor on heat transfer relationship. Equipment operating at temperatures up to 90°C does not need any additional safety testing for the highest safety rating ("Anaesthetic-proof category G") of IEC 601-1, 1977. [42]. However, a slightly higher temperature of 102°C was chosen as the total heating power to the sensor is extremely small (≤ 8 mW at zero flow).

To estimate the apparent changes in flow rate produced by changes in gas composition we need an approximate value for the constant $A \left(\frac{\mu_1}{\rho_1} \right)^{0.5}$ in equation 4.12. Figure 4.10 summarises data used to determine this constant based on a simple King's law form.

Experimental		Calculated	
\dot{V}	V_{th}	$V_{th}^2 = ?$	$A \left(\frac{\mu}{\rho} \right)^{0.5}$
L/min	Volts	(Volts) ² at 30°C	(See text)
0 (Vo)	1.264	$V_o^2 = 1.6$	-
5	2.15	$1.6 + 1.35(\dot{V})^{0.5}$	$1.6/1.35 = 1.18$
10	2.35	$1.6 + 1.24(\dot{V})^{0.5}$	$1.6/1.24 = 1.29$
15	2.48	$1.6 + 1.18(\dot{V})^{0.5}$	$1.6/1.18 = 1.35$

Figure 4.10 Experimental data used for estimating thermistor sensor heat transfer "constants" in air. A value of $A \left(\frac{\mu_1}{\rho_1} \right)^{0.5} = 1.2$ was subsequently used

for calculating absolute errors arising from gas property changes. The error arising from replacing velocity by volume flow rate adds to the error of the simple King's Law form used here, since the velocity profile will probably vary slightly over the range of flow rates used.

(Note : \dot{V} in the V_{th}^2 equation is expressed in L/min.)

To allow calculation using volume flow rate rather than velocity, this constant was determined in terms of volume flow rate rather than velocity. Thus, replacing velocity and apparent velocity in equation 4.12 by volume flow rate (\dot{V}) and apparent volume flow rate (\dot{V}_{app}) and assuming temperature is constant :

$$\dot{V}_{app} = \left[\left(\frac{k_2}{k_1} \right) \left(\frac{\rho_2}{\rho_1} \right)^{0.5} \left(\frac{\mu_1}{\mu_2} \right)^{0.5} (\dot{V})^{0.5} - A \left(\frac{\mu_1}{\rho_1} \right)^{0.5} \left(1 - \left(\frac{k_2}{k_1} \right) \right) \right]^2 \dots 4.20$$

where subscript 1 refers to the calibration gas (air), subscript 2 refers to the new gas mixture and

$A \left(\frac{\mu_1}{\rho_1} \right)^{0.5}$ has a value of about 1.2 for \dot{V} in L/min.

For respiratory monitoring purposes the lineariser must be adjusted to account for any gradual changes in velocity profile. This tends to compensate for any errors in equation 4.20 which may arise from replacing velocity by volume flow rate.

Equation 4.20 was used to calculate the changes in apparent flow rate produced by oxygen and nitrous oxide mixtures. The results are summarised in figure 4.11. A useful fact which emerges from the equations in figure 4.11 is that a simple correction technique which compensates for the zero shift term will virtually eliminate the errors introduced when using nitrous oxide. This makes the experimental bidirectional flow sensor described earlier (figure 4.7) attractive, as it would automatically compensate for errors from nitrous oxide mixtures. As a less accurate alternative, the original flowmeter developed in this thesis was modified with the addition of a switch to switch in fixed offsets for different nitrous oxide mixtures. This is simple but has the disadvantage that the flowmeter can over-estimate flow if the switch is left in the nitrous oxide position when measuring air or oxygen. From a safety point of view, this is undesirable and, on balance, it might be better to delete this feature.

4.8.1 New Temperature-Compensation Techniques

A direct bridge temperature-compensation technique which tries to maintain ΔT constant was rejected mainly because of the setting-up difficulties.

Instead, the flow sensing thermistor was operated at a fixed temperature ($\approx 102^\circ \text{C}$), while a nominally identical thermistor was operated as temperature-compensation sensor. This eliminates interaction between setting the temperature compensation and setting ΔT . In addition the operating conditions for the temperature sensor can be chosen independently from those for the flow sensor. The temperature sensor was operated at

Errors were Calculated Using :					% Error At		
	(k/k_{air})	(μ/μ_{air})	(ρ/ρ_{air})	\dot{V}_{app}	1 L/min	10 L/min	60 L/min
100 % O ₂	1.021	1.13	1.11	$\dot{V}_{\text{app}} = (1.012 \dot{V}^{0.5} + 0.024)^2$	7.3 %	4.0 % #	3.0 %
67 % N ₂ O 33 % O ₂	0.812	0.917	1.396	$\dot{V}_{\text{app}} = (1.002 \dot{V}^{0.5} - 0.22)^2$	-37 %	-12.4 % #	-4.9 %
50 % N ₂ O 50 % O ₂	0.864	0.971	1.324	$\dot{V}_{\text{app}} = (1.009 \dot{V}^{0.5} - 0.16)^2$	-26 %	-7.6 % #	-2.1 %

Figure 4.11 Theoretical errors produced by flowmeter with changes in gas composition, assuming that the sensor was initially calibrated in air. Note that for nitrous oxide the predominant error is produced by a large zero shift.

These values are close to measured values. (See figure 7.3)

a low voltage (≈ 70 mV) to keep self dissipation, and thus self heating, to a low level ($\approx 2.5 \mu\text{W}$ and 0.035°C). The non-linear temperature-resistance characteristic of the temperature sensor was linearised by including a resistor in series with the thermistor. The series resistance was selected using a trial-and-error technique programmed on a programmable calculator. (Equation 4.19 was used for estimating the thermistor resistance.) The calculated deviation from linearity over a 20° to 40°C range is within 0.1°C for the resistance-thermistor combination chosen (r_{21} figure 4.17 and F.2.) From equation 4.15 it can be seen that the direct (ΔT) temperature sensitivity of the flow sensor can be corrected by dividing the squared output of the bridge by a signal proportional to ΔT and then squaring the resultant output. Since the flow sensor is maintained at a constant temperature, a signal proportional to ΔT is easily generated by subtracting the linearised temperature sensor signal from a constant (designated here T_c with the corresponding compensation signal designated $\Delta T_c = (T_c - T_a)$). The remaining temperature dependence resulting from film property changes mainly affects zero rather than scale factor. This can be seen by rewriting equation 4.15 :

$$U_{\text{app}} = \left[\frac{\Delta T_2}{\Delta T_1} \left(\frac{T_1}{T_2} \right)^{0.09} U^{0.5} - A \left(\frac{\mu_1}{\rho_1} \right)^{0.5} \left\{ 1 - \frac{\Delta T_2}{\Delta T_1} \left(\frac{T_1}{T_2} \right)^{0.09} \left(\frac{T_2}{T_1} \right)^{0.9} \right\} \right]^2 \quad \dots \quad \dots \quad \dots \quad 4.21$$

If we assume that $(\Delta T_2 \cdot (T_2)^{-0.09})$ can be approximated by a linear function of temperature over a limited temperature range, then $(T_2)^{-0.09}$ can be included in the main temperature correction term ΔT_c by changing T_c very slightly. This leaves :

$$U_{\text{app}} = \left[U^{0.5} - A \left(\frac{\mu_1}{\rho_1} \right)^{0.5} \left\{ 1 - \left(\frac{T_2}{T_1} \right)^{0.9} \right\} \right]^2 \quad \dots \quad \dots \quad 4.22$$

If we assume that $(T_2)^{0.9}$ can be approximated by a linear function of T_a for a limited temperature range, then we can correct for this "zero shift" by subtracting a small signal proportional to T_a from the normally fixed zero set signal (V_0^2). The overall proposed new temperature-compensation technique is shown diagrammatically in figure 4.12 using a simple King's Law linearisation.

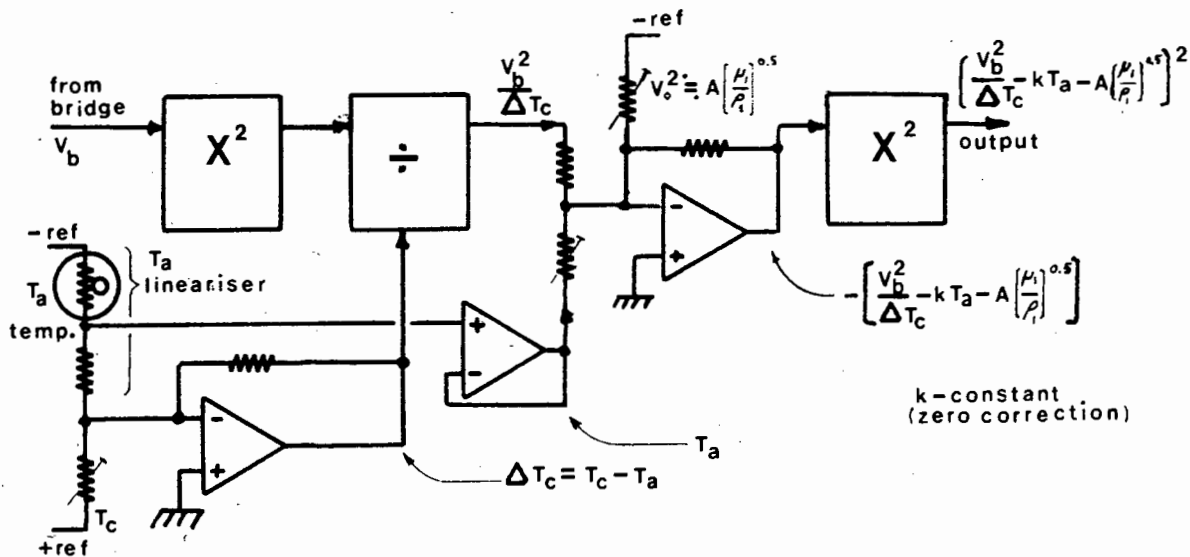


Figure 4.12 Proposed New Temperature-Compensation Technique

Instead of using a separate multiplier followed by a divider (figure 4.12), which would have had errors contributed by both function circuits, a single multiplier-divider based on transistor logarithmic amplifiers was used. These can easily achieve accuracies of 0.05 percent FS over the range of inputs encountered in this application, and have very low temperature drift when implemented with matched monolithic transistor arrays.

Although the circuit shown in fig. 4.12 is relatively simple, and should be capable of completely temperature-compensating the spirometer, the circuit was simplified still further to reduce the number of components. The "zero compensation" circuit was deleted and ΔT_c adjusted to minimise the error over the range of flow rates encountered in respiratory monitoring. In addition both the temperature-compensation signal and the fixed zero set signal (V_0^2) were fed into summing junction inputs

of the multiplier-divider eliminating all three op-amps in figure 4.12. This reduces the component count still further, reducing possible sources of noise, drift and error, and thus increasing stability and reliability.

The proposed simplified temperature correction technique was investigated theoretically by calculating the errors for a variety of values of T_c and volume flow rates. The results shown in figure 4.13 were expressed as a percentage of actual volume flow rate :

$$\text{percent error} = \left(\frac{\dot{V}_{\text{app}} - \dot{V}}{\dot{V}} \right) 100$$

where U_{app} was calculated by rewriting equation 4.21 including the effect of ΔT_c setting

$$A \left(\frac{\mu_1}{\rho_1} \right)^{0.5} = 1.2 \quad (\text{fig. 4.10})$$

and assuming initial calibration at 30°C (303°K) :

$$\dot{V}_{\text{app}} = \left[\frac{(T_c - 303)(375 - T_a)}{(T_c - T_a)(375 - 303)} \left(\frac{303 + 375}{T_a + 375} \right)^{0.09} \left\{ \dot{V}^{0.5} + 1.2 \left(\frac{T_a + 375}{303 + 375} \right)^{0.9} \right\}^{-1.2} \right]^2 \quad 4.23$$

(T_a is in degrees Kelvin.)

T_c (°K)	379			375			- (No compensation)		
	0.3	10	60	0.3	10	60	0.3	10	60
22°C	-0.5%	1.0%	1.3%	-3.9%	-0.49%	-0.06%	78%	32%	27%
26°C	-0.17%	0.5%	0.6%	-2.0%	-0.25%	-0.03%	36%	16%	13%
30°C	0	0	0	0	0	0	0	0	0
34°C	-0.03%	-0.6%	-0.7%	2.0%	0.25%	0.03%	-30%	-15%	-12%
38°C	-0.3%	-1.3%	-1.5%	4.0%	0.49%	0.06%	-56%	-28%	-24%

Figure 4.13 Temperature Compensation of Flowmeter

Theoretical percentage error produced by changes in gas temperature for different temperature-compensation constants, T_c , and various flow rates, \dot{V} .

Calculations are based on a simple King's Law relationship with calibration performed at 30°C. (See text.)

The results of figure 4.13 show that with no temperature compensation large errors from temperature changes will occur. With temperature compensation for direct ΔT dependence alone ($T_c = 375$) errors are only significant (± 4 percent) at low flow rates, while by a suitable choice of compensation constant ($T_c = 379$), temperature induced errors are reduced to within ± 1.5 percent from 22°C to 38°C over a range of flow rates from 0.3 L/min to 60 L/min.

4.8.2 New Linearisation Techniques

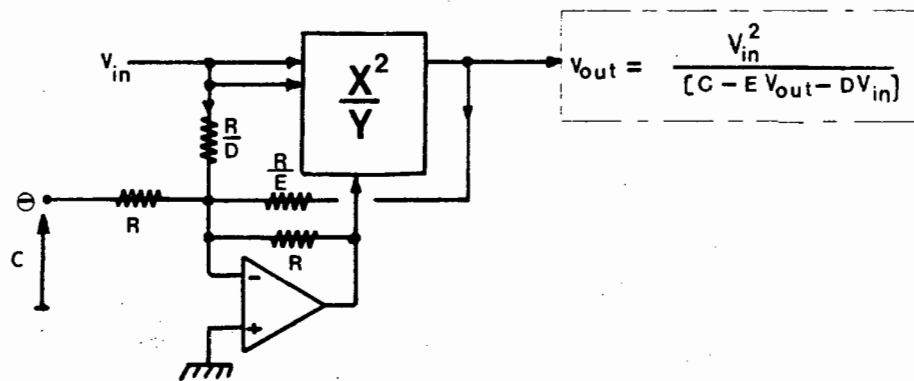
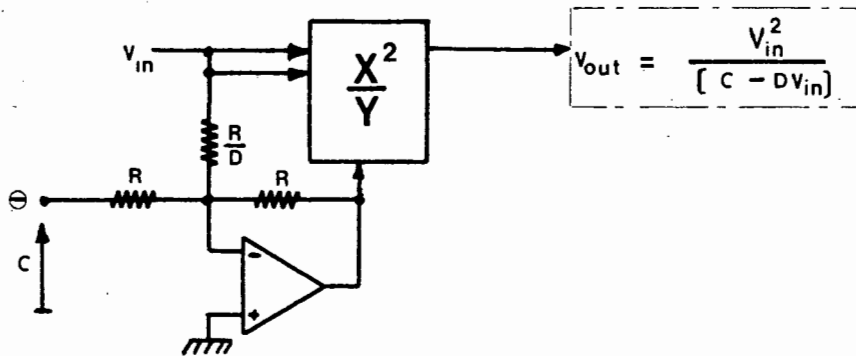
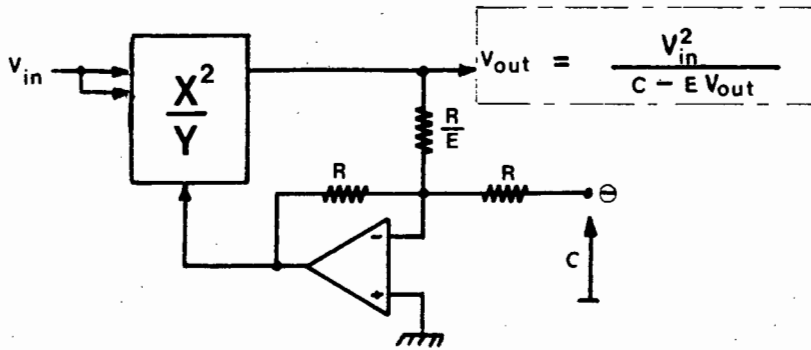
The main problem in developing a lineariser involves finding a simple analytical function which linearises over a wide dynamic range, yet can be implemented with an absolute minimum of hardware and adjustments.

Tests using the simplest King's Law lineariser (figures 4.2;4.12) confirmed that the achievable dynamic range is low (less than 10 : 1). Most popular high accuracy multipliers are multiplier-dividers used with a fixed denominator. This denominator input was used on the first squaring circuit (figure 4.12) for temperature compensation. This input on the second squaring circuit was used to supply a small additional linearisation term to the basic King's Law lineariser to extend the dynamic range in the new linearisation technique.

Figure 4.14 shows three possible implementations which can be used in this manner to extend dynamic range. A practical problem in implementing these techniques involves operating a conventional single quadrant multiplier-divider with inputs at or near zero. One solution would be to place an active clamp at the input of the circuit so that the input would not become zero but would always be kept slightly positive. This proved unnecessary as the addition of a single resistor to a commercial four-quadrant multiplier gave the transfer function :

$$V_{\text{out}} = \frac{V_{\text{in}}^2}{(C - D V_{\text{in}} + E V_{\text{out}})} \quad (\text{See Appendix D})$$

(With C, D, E constants with C D V_{in} E V_{out} for the conditions of usage).



4.14 Modified King's Law linearisers make use of divider function available with most multipliers. C, D, E are constants chosen to maximise dynamic range.

$$v_{in} = (v_b^2 - v_o^2)$$

By adjusting the terms in the denominator this "multiplier" linearised the flowmeter output within ± 5 percent over a 200 : 1 range of flowrates. A wider dynamic range could probably be achieved by one of the forms of figure 4.14 where it is easier to choose the precise form of the denominator terms. These can be adjusted independently, unlike the four quadrant multiplier used, in which the internal biasing results in interaction between adjustments. (See appendix D.) The overall transfer function of the lineariser and temperature-compensation circuitry is shown in figure 4.15 for three different temperatures.

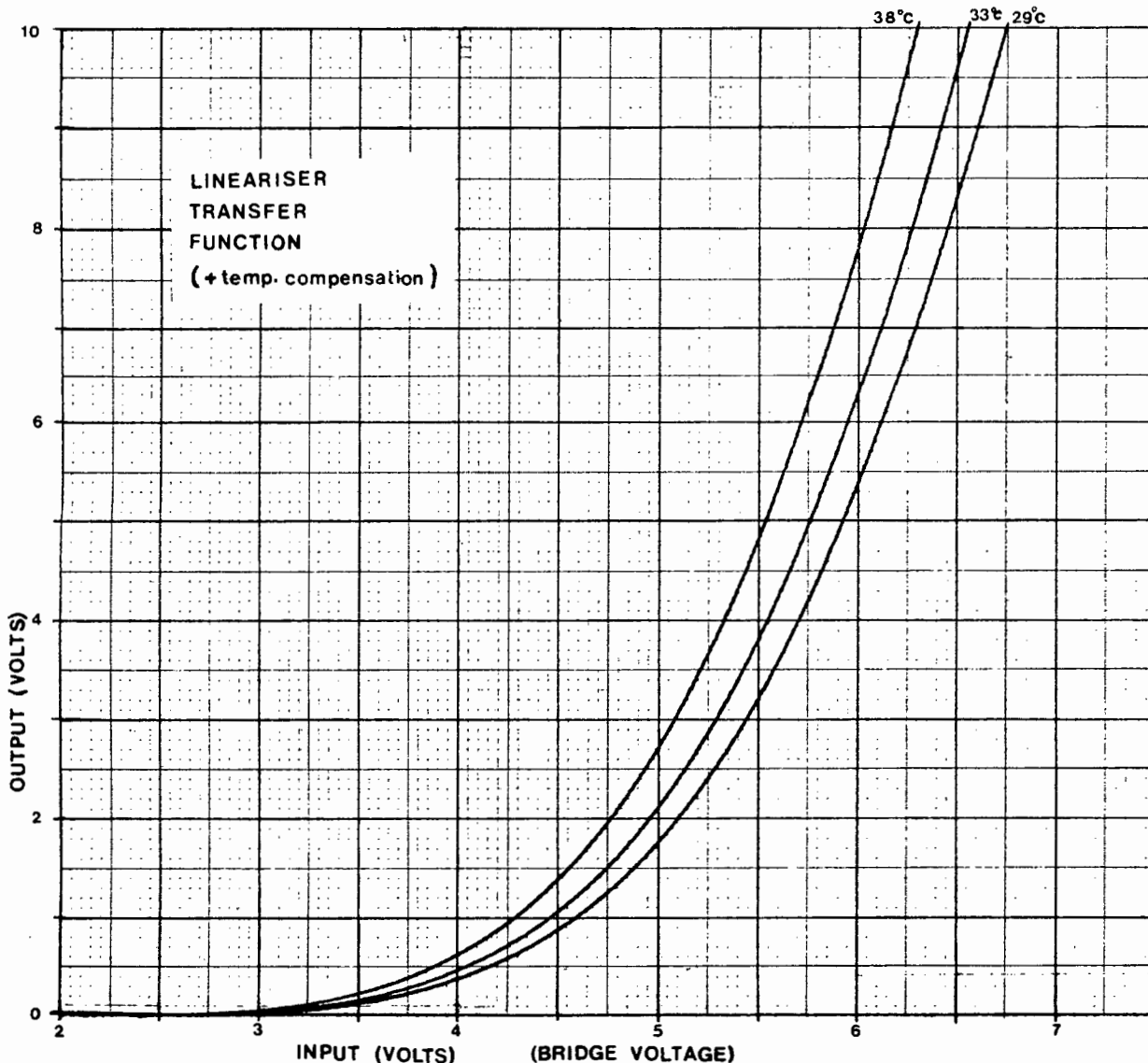


Figure 4.15 Overall transfer function from bridge voltage input to linearised output. Temperature compensation is shown for three different gas temperatures.

4.8.3 Complete Flowmeter System

The complete flowmeter system is shown in block diagram form in fig. 4.16. (The points marked p1 to p3 correspond to the same points on the more detailed diagrams in figure 4.17 and appendix F.) The main display normally displays mean flow rate - minute ventilation. (See figure P 4.8.) The fact that the flowmeter is inherently not direction-sensitive has some advantages. The output is measured using a simple low pass filter which measures both inspiration and expiration. The resultant output must then be scaled by a factor of a half. This effectively reduces output circuitry errors by a factor of two compared with measurements in one direction. A more important advantage of using this technique is that the filtering required is reduced and the response time for changes in flow rate can be correspondingly much more rapid. Figure 4.18 shows the measured step response of the third-order Bessel filter used. A Bessel filter was chosen as the filter's phase characteristic is important for an averaging application such as this.

A simplified circuit diagram of the flowmeter is shown in figure 4.17 with component numbering corresponding with that of the detailed circuit diagrams in appendix F. R9 and the diode at the output of ic1 ensures that the constant-temperature bridge always starts reliably with a positive output which is necessary for the following squarer/divider (consisting of ic5, 6 and 8 and the transistor array). This function circuit is similar to the basic multiplier circuit discussed in appendix D, except that the circuit operates in only one quadrant and transistor 2 is diode-connected, eliminating one op-amp and associated circuitry. This improves accuracy in this application. The diode in the collector of the third transistor helps to maintain its collector base voltage at, or near, zero. r_6 sets temperature display zero, while r_{12} sets temperature output scale

Jan 1979

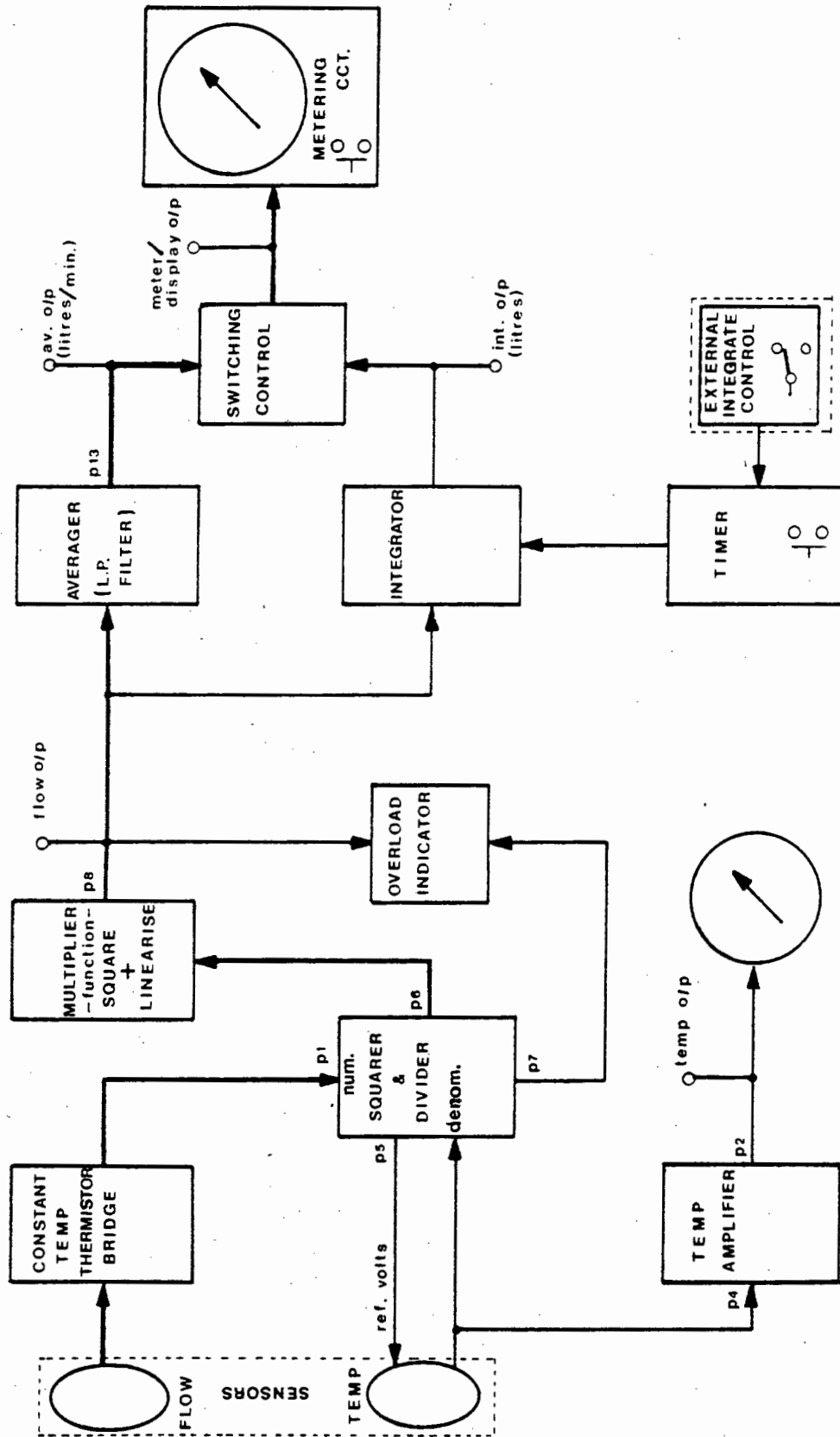
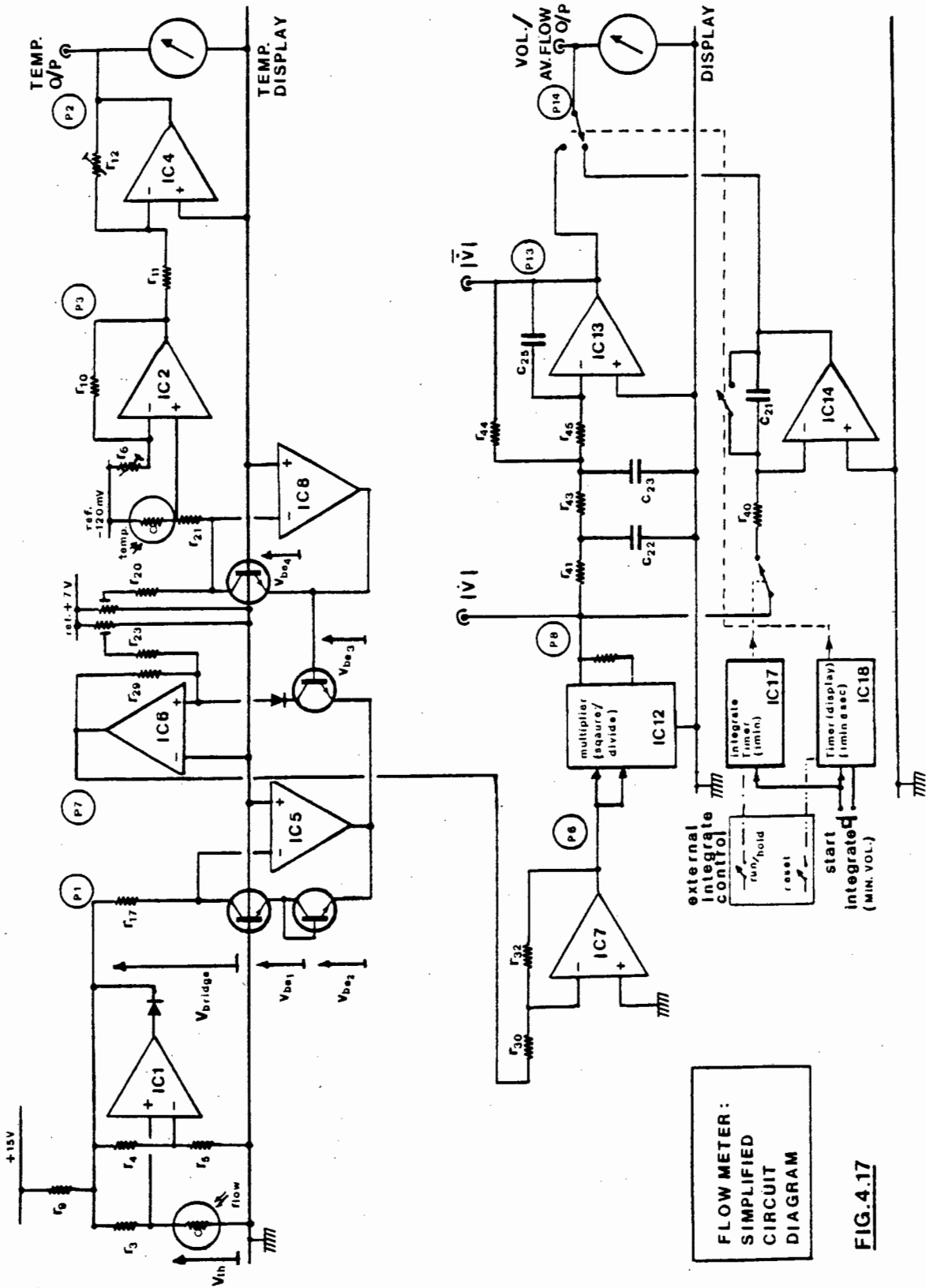


FIG. 4.16 FLOWMETER BLOCK DIAGRAM.



FLOW METER:
SIMPLIFIED
CIRCUIT
DIAGRAM

FIG. 4.17

factor. The temperature sensor signal is measured across r_{21} . r_{20} and its associated potentiometer set the reference compensation temperature, while r_{23} and its potentiometer set the flowmeter zero. icl4 timed by the timers (icl7 and icl8) integrates the flow signal for one minute, displaying "true minute volume" for ten seconds at the end of this period. This integrate cycle is initiated by pressing the integrate button.

The flowmeter includes components to increase electrical safety, using the ideas of "intrinsic safety" [140] used industrially. Passive components (resistors etc) are normally considered intrinsically safe while active protection devices require redundant protection [140]. Safety circuitry in this flowmeter includes separate active and passive devices leading to three levels of protection for the sensor assembly. Transistor tr8 and diode d21 (figure F.1) act as a high-power zenner diode (≈ 10.5 V) and, in combination with d22, limit both the maximum positive and negative voltage which can be supplied to the bridge in the case of amplifier and/or power supply failure. r8 limits the maximum current through tr1 and similarly r2 and r3 limit the current that can be applied to the flow sensor in the case of amplifier failure. Back-to-back diodes and a 330 ohm resistor connected to the output of icl11 limit the voltage and current (figure F.2) that can be applied to the temperature sensor in the case of amplifier failure. The power supply to the circuitry also includes current limiting. The flowmeter output circuitry for driving external monitors or displays includes current-limiting components, as connections from these sockets could conceivably come into contact with the patient by accident.

4.8.4 Flow-Sensing Threshold

We can estimate a limit to reliable flow sensing for the equipment described here by using a result determined for wires [112][121] which shows that

buoyancy effects become significant at :

$$R_e = [G_r]^{1/3}$$

$$\text{or } U = \left[\frac{\mu}{\rho} \cdot g \cdot \frac{\Delta T}{T_a} \right]^{1/3}$$

(where g is the acceleration due to gravity)

Thus the sensing threshold

$$U = \left[(2E-5) (9.8) \left(\frac{72}{303} \right) \right]^{1/3} = 0.036 \text{ m/sec}$$

in air.

This velocity corresponds to a volume flow rate for the sensor described here of ≈34 ml/min.

4.9 Summary and Conclusions

The effects of gas composition and temperature on the calibration of a hot-thermistor anemometer were investigated theoretically. Previous techniques used for temperature compensating hot-wire (thermistor) anemometers were reviewed and new temperature compensation techniques developed. From theoretical considerations it was shown that a proposed new bi-directional flow sensor could reduce errors introduced by high concentrations of nitrous oxide. Practical problems and relatively complex circuitry led to the abandonment of this technique. The temperature-compensation technique adopted is extremely simple because it makes use of part of the anemometer's lineariser circuit. The temperature compensation technique also provides a signal proportional to temperature which is useful clinically for optimising humidification. Previous linearisation techniques were reviewed and found to be either inaccurate or very complex and thus expensive. A new, simple lineariser with a very wide dynamic range (200 : 1) was developed. Hot-thermistor and hot-wire anemometers were compared and hot-thermistor anemometers were found to be superior for respiratory monitoring purposes. A serious limitation of hot-wire anemometers is their high sensitivity to contamination.

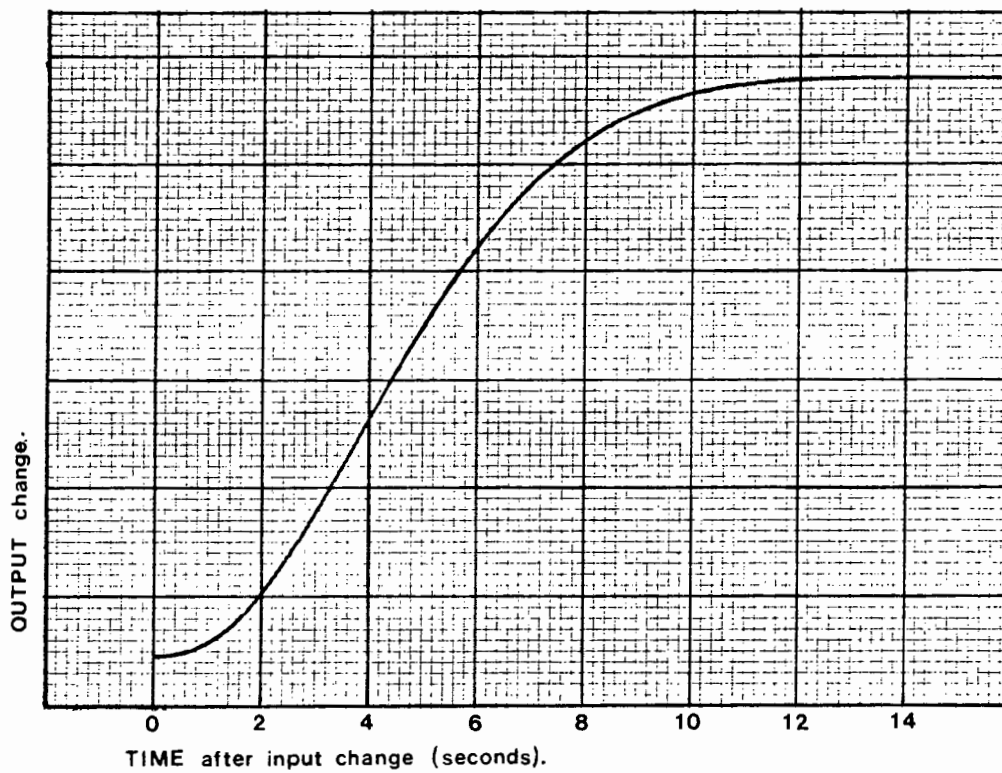


Figure 4.18 Step response of flowmeter filter. Filter allows rapid detection of changes in flowrate (2 to 3 seconds) with final value achieved after about 10 seconds. Yet at the slowest likely respiratory rate (= 10 breaths/min), meter fluctuates only a few percent of reading.

Figure P 4.8 (See overleaf.)

The flowmeter front panel was designed for safe and simple operation. The analogue, rather than digital, display allows "at a glance" reading from a distance. Apart from the power on/off switch, push button switches temporarily select a more sensitive range (0-2 L/min) or a less sensitive range (0-20 L/min) than the primary range (0-7 L/min). When the push buttons are released, the display reverts to the primary 0 to 7 L/min scale. This reduces the likelihood of reading the wrong scale. Pushing the integrate button starts a one-minute timer (causing the "measure" light to come on). At the end of one minute the "read" light comes on for ten seconds, while the meter displays the integrated volume during the previous minute. At the end of the ten-second period the read light is extinguished and the display reverts to an averaged flow-rate reading. This ensures that the display will always return to the averaged 0 to 7 L/min scale to avoid any possibility of misinterpretation. For research purposes an external control can be plugged into the flowmeter which overrides the internal timers and allows the integrator to be started, stopped and reset manually. The integrator can also be electronically controlled to allow cumulative measurements of, for example, expired volumes alone. The overload indicator above the small temperature display meter lights if the flow sensor is disconnected or the flow rate exceeds 60 L/min.



Figure P 4.8 (See previous page for title.)



Figure P 5.0

Flow sensor assembly (second from right) fits within modified Bird ISO infant connector (third from right). Knurled fitting on Bird connector is dummy luer fitting to seal pressure tapping point. Endotracheal tube connector (extreme right) is available in a variety of sizes to fit et. tubes as small as 2 mm diameter.

5.0 Design of Flow-Sensor Assembly

The flow-sensor assembly described here was developed jointly with D. Ijams and J.F. North, whose contributions are gratefully acknowledged. The requirements for the sensor were discussed in section 2.2.1.

The flow sensor fits inside a Bird (ISO) infant connector. This has a number of advantages :

- (i) It enables the sensor to be used with the two ISO fitting sizes for endotracheal tubes or facemasks. (The latter are particularly convenient for measuring spontaneous ventilation.)
- (ii) The sensor can be rapidly plugged into circuit to replace an unmodified fitting.
- (iii) The sensor does not increase patient deadspace but reduces it, in comparison with the unmodified fitting.
- (iv) The sensor does not displace any fittings forward from the patient's face and thus interfere with the surgeon's work space.

Figures 5.1,5.2 show the internal sensor assembly which is a press fit into the modified Bird connector. The overall assembly is shown in figure 5.3 and figure P 5.0.

The internal diameter of the sensor was chosen to be the same as the maximum expected et. tube size (5 mm). The metal end pieces were designed to straighten the flow through the sensor to produce similar velocity profiles for inspiration and expiration, and hence equal forward and reverse sensitivities. This is very difficult to achieve because of the 90° change in direction of flow at the entrance to the sensor. Figure I.2 shows that the forward and reverse sensitivities are slightly different. This is attributed to the differences in entry conditions for inspiration and

expiration. The metal end piece on the patient side of the fitting prevents gas from a small et. tube "jetting" onto the flow-sensing thermistor and causing erroneous readings on expiration. This end piece also helps prevent the flow-sensing thermistor from being contaminated by mucus.



Figure P 5.0.1

Flow-sensor assembly end caps reduce "entrance" effects and act as inertial separators.

Large diameter offset holes in these end pieces ensure that they cannot be easily plugged by mucus. Changes in direction of flow through the end pieces and the narrower inner diameter increase the flow resistance of the Bird fitting. (See figure I.2) At 20 L/min, a higher flow rate than will be encountered during spontaneous ventilation, this resistance produces a pressure drop across the transducer of 4.1 cm H₂O on expiration and 3 cm H₂O on inspiration.

Placement of the temperature-compensating thermistor should, ideally, be as close to the flow sensor as possible,

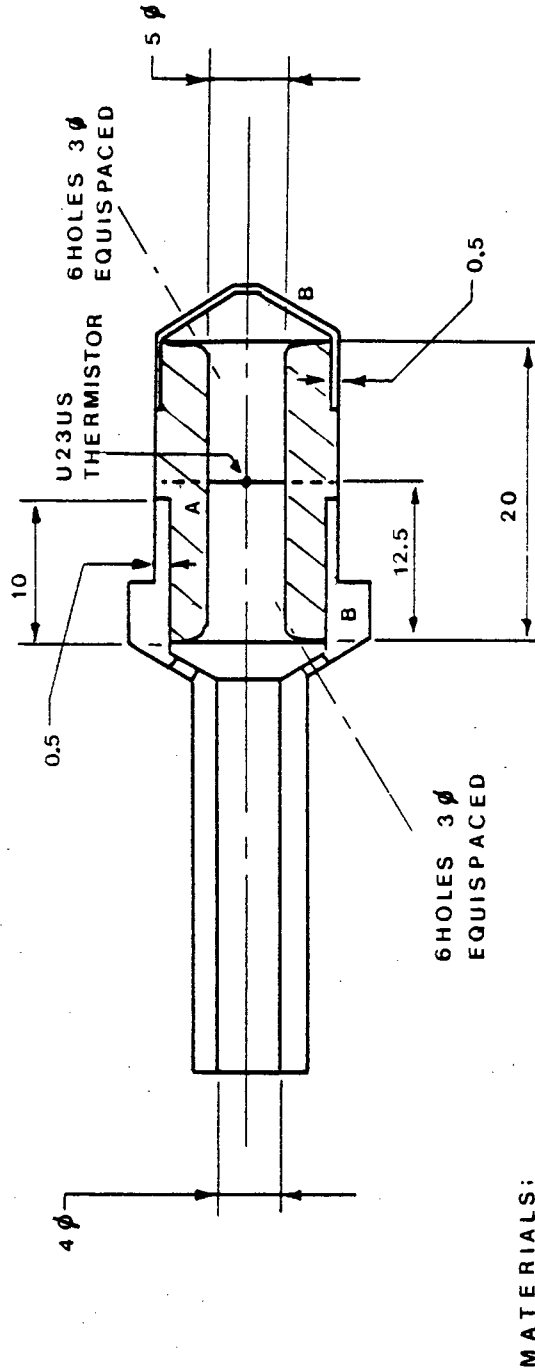
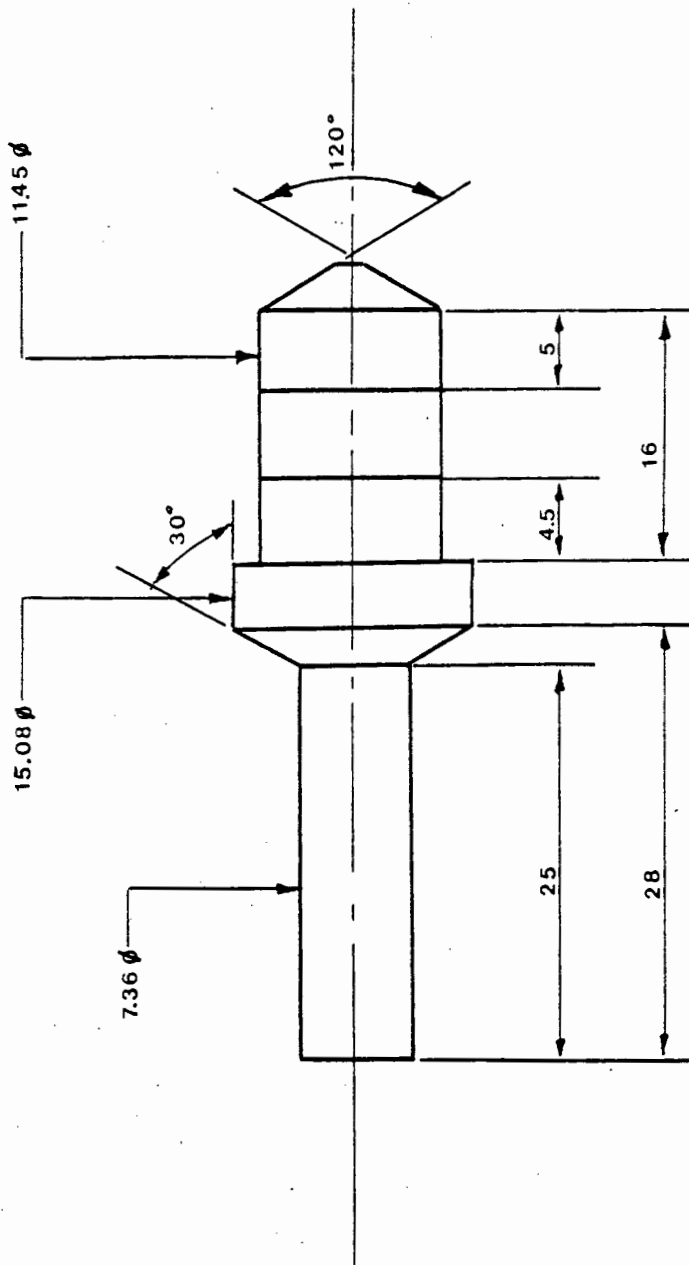
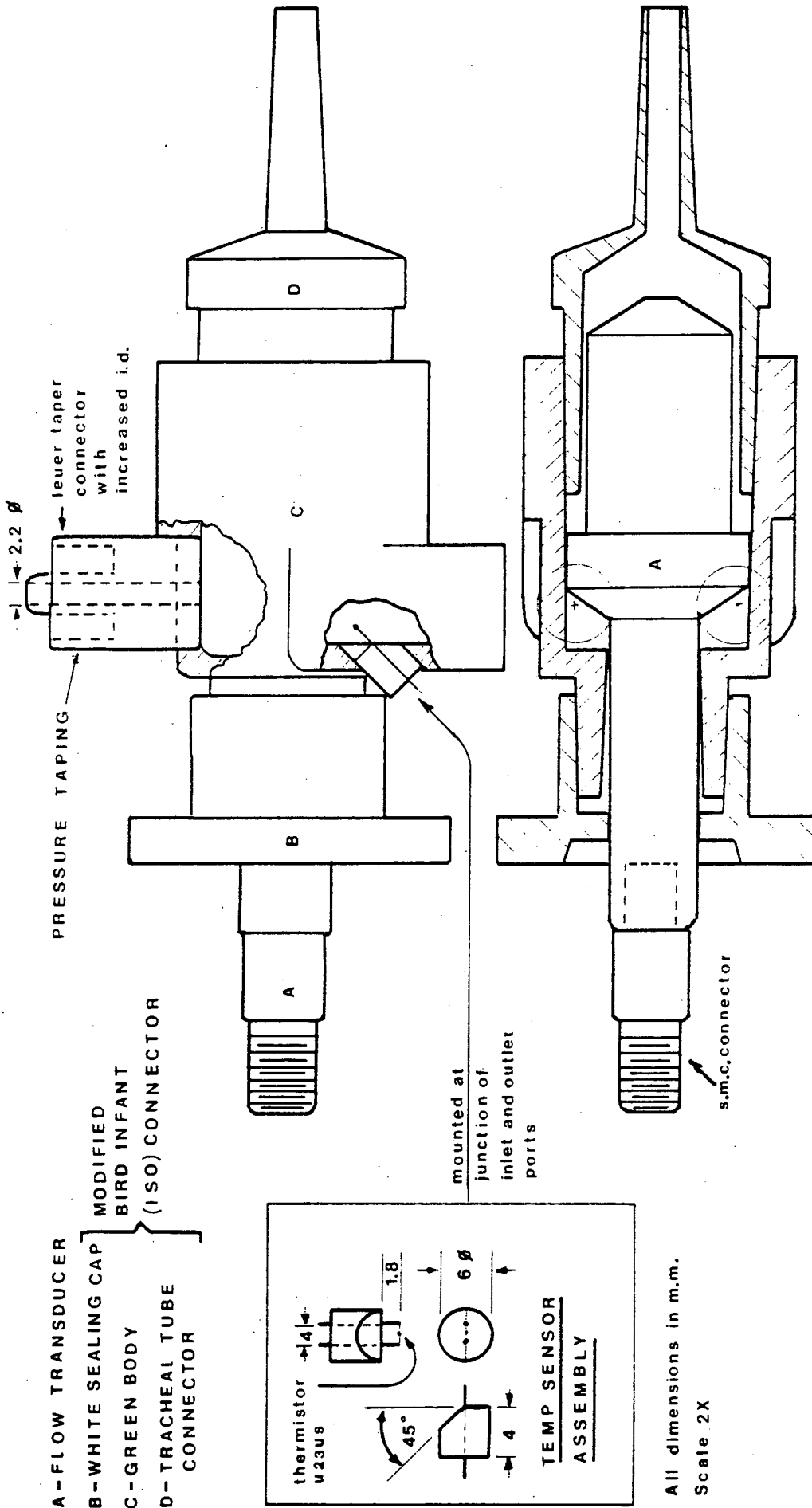


FIG. 5.1 FLOW SENSOR INTERNAL DIMENSIONS



All dimensions in mm
Scale 2X

FIG.5.2 FLOW SENSOR EXTERNAL DIMENSIONS



All dimensions in m.m.
 Scale 2X

FIG. 5.3 COMPLETE FLOW TRANSDUCER ASSEMBLY

to prevent temperature gradients through the probe giving rise to errors. Placing this sensor within the insert would make construction more difficult. The sensor was instead placed in a position between the inlet and outlet part of the Bird connector where flow rates are high and will clear fluid collecting on or near the sensor. Soldering the thermistor leads should be done with silver solder, since corrosion of the lead-tin solder connections to the thermistor's Platinum-Ruthenium leads gave rise to intermittent operation when an acidic water-based disinfectant solution was used accidentally to store the sensor.

The pressure tapping point for measuring et. tube or mouth pressures should, ideally, be at the et. tube exit of the transducer, so that pressure across the flow resistance of the transducer is not measured. Unfortunately, this adds the risk of introducing a leak on the patient side of the transducer. This is highly undesirable from a safety point of view, since the flowmeter could show an erroneously high ventilation level. The pressure tapping was thus placed on the inlet side of the flow transducer. (See figure 5.3) Normally a dummy luer connector seals this tapping point. For patient resistance measurements the sensor flow resistance will be included in any measurements when this tapping point is used.

The body of the sensor insert is made of perspex, so that the sensor can be checked for contamination. Using perspex precludes autoclaving the unit, but allows gas sterilization and liquid dip sterilization.

Figure I.2, appendix I, shows how the flow resistance of the flow sensor was tested and how this resistance varies with flow rate. Figure I.2 also shows the resistance of the unmodified Bird fitting. At the normal peak flow rates encountered during spontaneous breathing, the pressure across the flow sensor is less than 1.5 cm H₂O, while at the highest flow rates encountered during spontaneous ventilation in anaesthesia, the pressure across the flow sensor is less than 4 cm H₂O. These values are acceptable for infant use. See section 2.2.

6. Measuring the Work of Ventilation and the Respiratory System Impedance

6.0 Introduction

This section describes new methods for measuring respiratory-system impedance and reviews previous methods used by other workers. Measurements of the mean respiratory power and the work of ventilation are also discussed. The primary objective in investigating different measurement methods for theatre use was to develop automatic measurement methods which will work reliably under clinical conditions.

Many different techniques have been used for measuring the mechanical properties of the respiratory system. Since the pioneering work of Neergard and Wirz [141][142] in the late 1920's, one of the most common techniques involves determining the constants of a simple first or second-order mechanical or electrical analogue of the respiratory system. (See section 0.5.) The methods of measurement of Neergard and Wirz are still used, with some modifications, today, but a variety of other techniques for measuring the same quantities are also used. Unfortunately, different measurement techniques yield different measured values for the same quantities. Even with a single technique the reproducibility of measurements is often poor [143][144][18(ii)].

Some of the differences arise directly from the measurement technique used. For example, pleural pressure is often estimated from measurements of oesophageal pressure. This is an approximate technique with a variety of possible systematic errors [33][18(ii)]. Other differences and errors arise from fundamental assumptions about the simple lumped models used [18(ii)]. Problems of this type include the assumptions that the respiratory system can be modelled as a linear system, that there are no differences from inspiration to expiration and that there are no path effects (i.e. lung properties do not depend on immediate inflation history).

Ideally, from an artificial ventilation point of view, we would like to characterise the properties of the respiratory system using simple, highly reproducible measurements which can be automated and used continuously for optimising ventilation and detecting changes in the patient's condition. From the ventilator's point of view the mechanical driving point characteristic of the total respiratory system (lungs + airways + chest + abdomen) is more important than the individual subdivisions.

For detecting changes in the patient's status, measurements of changes in the respiratory system subdivisions may be a more sensitive technique, but, since we already wish to measure the overall characteristic, this would tend to swamp the clinician with a plethora of information. One additional piece of information which might be useful to the clinician for optimising ventilation is the respiratory time constant (product of resistance and compliance). There are two reasons for this : (i) it allows a rational choice of inspiratory or expiratory time (to avoid gas trapping etc), and (ii) it provides a possible way of evaluating the significance of any compliance or resistance changes. We can see this by noting that a change in functional residual capacity (FRC) tends to cause changes in compliance and resistance in opposite directions [29(iii),18(ii)] Thus the respiratory time constant will tend to be relatively constant with changes in lung inflation level, although the resistance and compliance change. We may thus be able to differentiate between changes in FRC and some pathological change, or between different pathological changes, using this information.

6.1 Modelling the Ventilator

For some of the calculations in this section we need to examine the effect of the ventilator on the measurements. Figure 6.1 shows a simple lumped-element

equivalent circuit that can be used to represent many common ventilator-tubing combinations.

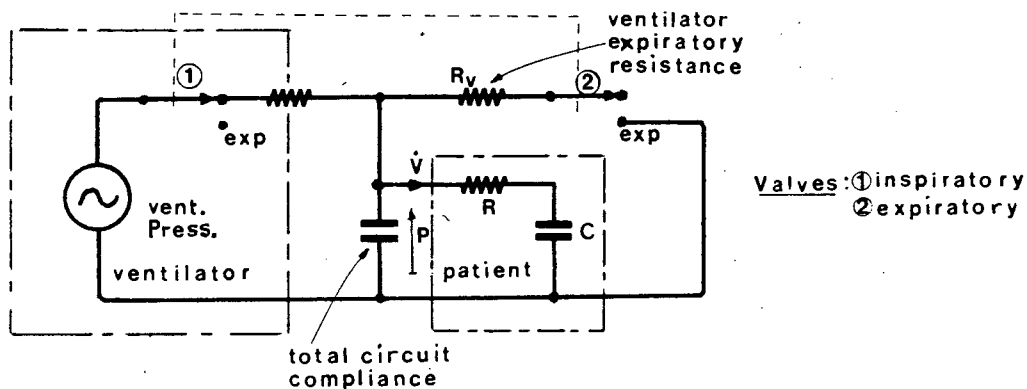


Figure 6.1 Lumped-element equivalent circuit of ventilator and fittings. Gas inertance and valve inertance have been neglected. The total compliance (typically 4 ml/cm H₂O [1]) includes tubing, humidifier, vaporiser, CO₂ absorber and ventilator. The expiratory resistance depends largely on the expiratory valve and size of tubing.

Making Measurements during Controlled Ventilation and Spontaneous Ventilation

It is desirable to be able to measure the mechanical properties of the respiratory system both in apneic, anaesthetised or paralysed patients during controlled ventilation and in spontaneously breathing patients. Few measurement techniques can be directly applied to both situations. Some techniques require patient cooperation and are thus unsuitable for use on anaesthetised patients or infants. Difficulty in applying a technique to both situations arises from the difficulty in measuring driving pressure. In controlled ventilation this corresponds to mouth or et. tube pressure which is easy to measure. In spontaneous ventilation we need to measure the difference between pleural and mouth pressure. Pleural pressure is usually measured approximately by using a catheter and oesophageal balloon coupled to an external pressure transducer. Pressure measurement errors in this technique are greatest when the patient is supine. However, a major problem is the added complication of

inserting and positioning the balloon/catheter.

One of the few techniques which can be applied to both spontaneous and controlled ventilation is the method of forced oscillations. The forced oscillation technique was initially modified (see appendix B) for this work but eventually abandoned because of technical difficulties. (See below.) The other two techniques which were developed in this work are suitable for use only in controlled ventilation, although one of them could be used with an oesophageal balloon during spontaneous ventilation.

6.2 Respiratory Power and the Work of Ventilation

In respiratory and cardiac diseases the work of ventilation may increase to become a substantial proportion of the patient's metabolic requirements, ultimately contributing to respiratory failure. In a similar way the work of ventilation is often substantially increased postoperatively. [150] Measuring the work performed by the ventilator on the patient in controlled ventilation allows a more objective assessment of what ventilatory assistance is required postoperatively. This may also be valuable during assisted ventilation for deciding when to wean from the ventilator and for selecting ventilator settings during weaning. Various workers have measured respiratory power previously using either analogue or digital techniques [145][184][146][147][148][149][150][43]. Other workers have used approximate techniques for estimating the work of ventilation [151][152][153]. Work and power measurement do not seem to have been routinely used for direct patient management by many workers. A useful qualitative technique involves plotting pressure-volume loops. The area enclosed by one axis and the inspiratory loop depends on the energy dissipated in the respiratory system during a respiratory cycle. (See figure 6.2.)

Three basic measurements were used in this work : instantaneous power (product of pressure and flow rate), mean power (real power) and normalised work of ventilation (hereafter termed W_n). W_n was calculated by dividing the mean power by the mean flow rate. The result has the dimensions joules/litre. This normalising process gives an estimate of ventilatory efficiency, the work done in moving one litre of gas, and has previously been shown to give a reliable indication of when ventilatory support is required [15].

Using the equivalent circuit of figure 6.1 we see that, during inspiration, energy is dissipated in the respiratory system resistance (R) and stored in the respiratory compliance (C). During expiration the energy stored in C from inspiration is dissipated in R and the ventilator expiratory resistance (R_v). (This assumes passive expiration and an apneic patient.)

If we call inspiratory work W_{insp} and P is the instantaneous et. tube pressure, with V the corresponding flow rate, then, during inspiration, the work done by the ventilator is :

$$W_{insp} = \int_{insp} P \cdot \dot{V} dt \quad \dots \quad \dots \quad \dots \quad \dots \quad 6.1$$

Ignoring any effects of ventilator compliance :

$$W_{insp} = \int_{insp} \dot{V}^2 \cdot R dt + \int_{exp} \dot{V}^2 \cdot R dt + \int_{exp} \dot{V}^2 \cdot R_v dt \quad \dots \quad 6.2$$

The first term on the R.H.S. of equation 6.2 is the energy dissipated in the respiratory resistance during inspiration, while the two remaining terms represent the energy stored during inspiration which is subsequently dissipated in the respiratory resistance, and the ventilator resistance during expiration.

The energy dissipated in the ventilator resistance is what we measure from mouth pressure and flow rate during expiration :

$$|W_{\text{exp(vent)}}| = \left| \int_{\text{exp}} P \cdot \dot{V} dt \right| = \int_{\text{exp}} \dot{V}^2 R_v dt \dots \dots 6.3$$

The ventilator (expiratory) resistance is usually only a few percent of the infant's respiratory resistance, making the last term of the equation 6.2 small in comparison with the other terms (and errors from ignoring ventilator compliance are thus also small). We are interested in the work of ventilation of the patient (without the influence of the ventilator). Thus we calculate the work of ventilation (W), eliminating the work performed on the ventilator resistance :

$$W = W_{\text{insp}} - |W_{\text{exp(vent)}}| = \int_{\text{insp}} P \cdot |\dot{V}| dt - \int_{\text{exp}} P \cdot |\dot{V}| dt \dots 6.4$$

(The hot-thermistor flowmeter measures $|\dot{V}|$)

(Note that W , the work done on the patient's respiratory system, will generally not be equal to the work done on the respiratory system in the absence of ventilator resistance, since, without R_v , the expiratory flow rate would increase, changing the energy dissipated in the patient.)

Equation 6.4 does not apparently give us a large advantage over a measurement ignoring the effect of ventilator resistance, since we have already pointed out that the energy dissipated in this resistance is normally small. However, the effect of zero drift of the pressure transducer, which may be a significant source of error (see appendix E), is eliminated using this technique.

We can see this by rewriting equation 6.4 after the pressure transducer zero has shifted by Δ_p :

$$\begin{aligned}
 W &= \int_{\text{insp}} (P + \Delta_p) \cdot |\dot{V}| dt - \int_{\text{exp}} (P + \Delta_p) \cdot |\dot{V}| dt \\
 &= \int_{\text{insp}} P \cdot |\dot{V}| dt - \int_{\text{exp}} P \cdot |\dot{V}| dt + \Delta_p \left(\int_{\text{insp}} |\dot{V}| dt - \int_{\text{exp}} |\dot{V}| dt \right) \\
 &= \int_{\text{insp}} P \cdot |\dot{V}| dt - \int_{\text{exp}} P \cdot |\dot{V}| dt
 \end{aligned}$$

i.e. pressure transducer zero drift does not affect the measurement, because in the steady state inspired and expired volumes are equal. The application of continuous positive airways pressure (CPAP) has the same effect as a pressure transducer zero shift. Thus, its application does not cause direct errors with this measurement technique.

We normalise W with respect to tidal volume to obtain the normalised work of ventilation $\underline{W_n}$ and define W_n as :

$$\underline{W_n} = \frac{W}{V_T} \quad \dots \quad \dots \quad \dots \quad \dots \quad \dots \quad 6.5$$

($V_T =$ tidal vol.)

Assuming pressure and flow waveforms do not change substantially over the averaging time T where $T \gg (\text{respiratory rate})^{-1}$, then we replace integration by averaging (using low pass filters). Using equation 6.4 the average power dissipated in the respiratory system is :

$$\overline{P \cdot \dot{V}} = \frac{\int_0^T ([P \cdot |\dot{V}|]_{\text{insp}} - [P \cdot |\dot{V}|]_{\text{exp}}) dt}{T} = \overline{[P \cdot |\dot{V}|]_{\text{insp}}} - \overline{[P \cdot |\dot{V}|]_{\text{exp}}}$$

... .. 6.6

(where bar denotes average in time T)

and from 6.5 $\underline{W_n} = \frac{\overline{P \cdot \dot{V}}}{\overline{\dot{V}}}$ 6.7

This technique was used for measuring the normalised work of ventilation. (See figure G 1) The instantaneous power waveform was displayed and used qualitatively to assess changes in the work of ventilation and the effects of ventilator setting.

6.3 Measuring Respiratory Impedance - A Review

Many different techniques have been applied to measuring respiratory system impedance but relatively few automated systems have been described. This section discusses the measurement principles used by previous workers for measuring respiratory impedance.

6.3.1 Static measurements of respiratory compliance are made by inflating the (relaxed) respiratory system and then allowing it to come to equilibrium. Compliance is then calculated from : (change in volume)/(change in pressure). Super-syringes or weighted bell spirometers have often been used to inflate the respiratory system in a repeatable manner [154][155][33][156][157][158].

6.3.2 Sampling techniques are based on the pioneering work of Neergaard and Wirz [141][142] The quantities measured by these techniques are often termed "dynamic compliance" and "dynamic resistance". In the zero-crossing method compliance is calculated by dividing the change of volume by the corresponding change of pressure between successive zero flow points during the respiratory cycle. (See figure 6.2 and sect.6.4.3)[164][148][25][156][18(ii)] This method assumes that inertance is negligible, so that the pressure at zero flow rate results from compliance alone. Technical problems with this method make measurement reproducibility poor. Zero flow points are sometimes produced artificially using the interrupter method of Neergaard and Wirz [141]. The interrupter method can also be used to calculate resistance by assuming the change in pressure produced by the interrupter results solely from the pressure across the flow resistance at the flow rate immediately preceding flow interruption. The interrupter technique is particularly prone to errors from inertance effects, as the volume acceleration caused by the flow interruption is large, and it is doubtful whether "static" conditions are ever approached using this technique. The iso-volume method calculates resistance from measurements of both pressure

and flow rate made at successive points of equal volume during the respiratory cycle [153][159][18(ii)].

If subscripts i and e refer to measurements at equal volume (V) points during inspiration and expiration, respectively, then,

$$P_i = \dot{V}_i R + V/C$$

$$P_e = \dot{V}_e R + V/C$$

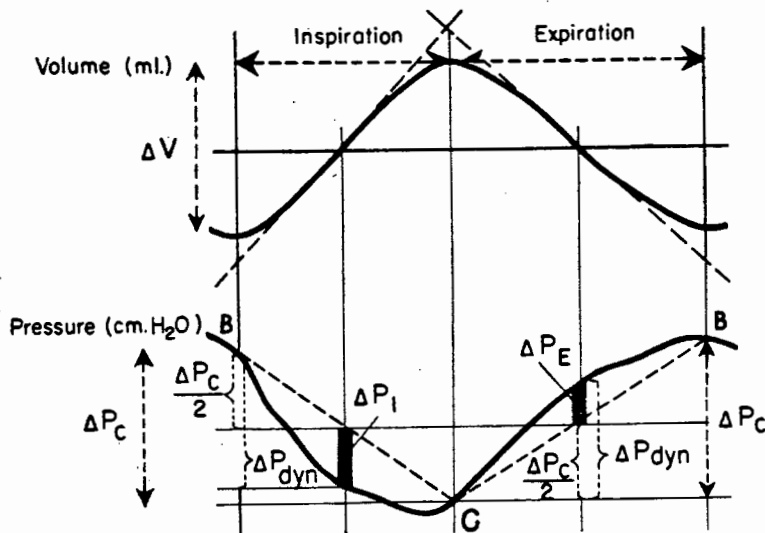
(for a linear first-order system)

and, thus,

$$R = \frac{(P_i - P_e)}{(\dot{V}_i - \dot{V}_e)} \quad (\text{Note: } \dot{V}_i \text{ is of opposite sign to } \dot{V}_e)$$

This method assumes that the effect of inertance is negligible at the time of measurement and that compliance and resistance do not change from inspiration to expiration. Compliance hysteresis may give rise to errors with this technique [59], and resistance calculated in this manner is an average value for inspiration and expiration. To calculate resistance separately for inspiration and expiration, to account for resistance non-linearity and hysteresis, the technique is sometimes modified by estimating compliance pressure. (Figure 6.2.) However, this tends to decrease the reproducibility, because reliable measurements of compliance pressure are difficult to make. The variability of these pressure measurements is the source of difficulty in making reliable compliance measurements using the zero crossing technique [143][18(ii)] [144][160].

A



Diagrammatic representation of simultaneous recordings of pressure and volume.

Method for calculating pulmonary compliance. Compliance is expressed as the ratio of tidal volume to change in intraesophageal pressure, measured between points of no flow (i.e., extremes of tidal volume).

$$Compliance = \frac{\Delta V}{\Delta P_c}$$

Method for calculating inspiratory and expiratory nonelastic resistance. Resistance is measured at points of equal volume, midway between extremes of tidal volume in inspiration and expiration. Resistance is the ratio of

instantaneous flow-resistive pressure (ΔP_i or ΔP_e) to actual airflow (\dot{V}), as measured graphically by drawing a tangent to the volume slope at midpoint. Resistance = $\frac{\Delta P_{dyn} - \frac{\Delta P_c}{2}}{\dot{V}}$

B

Diagrammatic average, normal pressure-volume loop. Pressure and volume measurements used in the calculation of compliance and resistance are indicated. Elastic work is represented by the triangular area ABC. Inspiratory and expiratory nonelastic work is represented by the elliptic area BDCE. When expiration is passive, total respiratory work is represented by the sum of elastic work (ABC) plus inspiratory nonelastic work (BCD).

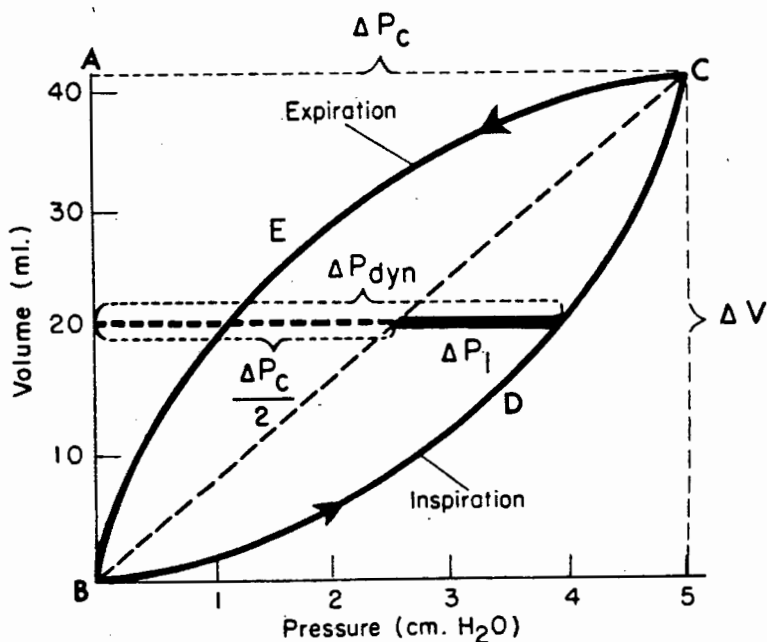


Figure 6.2 Sampling techniques : Zero-crossing method for calculating "dynamic" compliance and a modified iso-volume technique for measuring "dynamic" resistance during both inspiration and expiration. As shown here pressure is measured using an oesophageal balloon. B shows the same data as in A plotted as a flow-volume loop. The work of ventilation can be qualitatively assessed from changes in the loop shape (from [153]).

Respiratory time constant can be determined from the shape of the flow rate versus log time curve during a passive expiration (assuming a first-order system).

From two such time constant measurements, the first without any added flow resistance and the second with a known flow resistance added, it is possible to calculate R and C [161].

All sampling techniques tend to suffer from large variability in the measured quantities, because the measurements are made at only a few points on the respiratory waveform. Various workers have automated these techniques [25][160][162], and commercial measurement systems using analogue [163] or digital [164] computers use methods of this type.

6.3.3 Loop-Flattening and Related Techniques

The loop-flattening method (also called "subtraction method") developed by Mead and Whittenberger [165] makes use of the whole respiratory waveform. This improves the reproducibility compared with sampling methods [166]. In addition, qualitative visual information allows simple detection of abnormalities in disease (figure 6.3.)

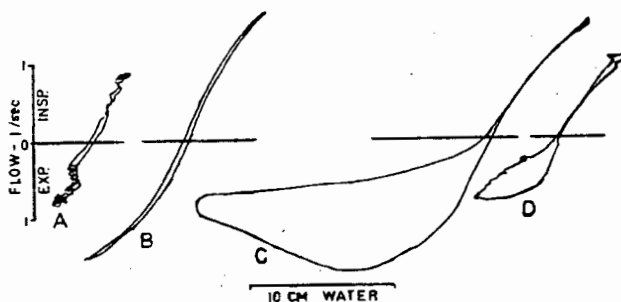


Figure 6.3

Loop-flattening method of Mead [165] can detect respiratory abnormalities (from [18(ii)]).

Tracings obtained by the subtraction method of Mead & Whittenberger A: Normal subject, normal respiration. B: Normal subject panting. C: Patient with emphysema panting. D: Patient with emphysema, normal respiration.

For a single-compartment first-order respiratory model :

$$(P - \frac{V}{C}) = \dot{V} R$$

Thus, if we display a signal proportional to \dot{V} on the y-axis of an oscilloscope versus a signal proportional to $(P - kV)$ on the x-axis, where k is an adjustable factor, then we can adjust k to flatten the loop to a line (figure 6.3). C can then be determined from the value of k , and R from the slope of the resultant \dot{V} versus $(P - kV)$ line. If compliance is a linear function of volume, non-linearity of the resultant line indicates variations of R with flow rate. The pressure and flow signals are sometimes filtered to produce only the fundamental frequency components [167]. This improves measurement reproducibility because complete closure of the resultant ellipse can always be achieved. The method is then equivalent to the phase angle / Fourier analysis techniques described below. Various techniques have been described which are very similar to loop flattening in that they try to minimise the difference between a simple first-order model and an analogue of the respiratory system over the complete respiratory cycle, e.g. by loop leveling [166] or using an "adaptive tracker" [168].

6.3.4 The Method of Forced Oscillations and other Phase Angle Methods

The method of forced oscillations involves measuring the mechanical driving-point impedance of the respiratory system by applying a sinusoidal pressure signal to the respiratory system. The resultant small pressure and flow signals measured at the patient's mouth are separated from the corresponding respiratory waveforms by filtering. Originally [169][170] the driving frequency was varied until the pressure and flow signals were in phase (i.e. resonance for a second-order system). The ratio of pressure amplitude to flow rate amplitude then represents the resistive part of the respiratory impedance. It is now more common to calculate the complex impedance from the amplitude of the filtered pressure and flow rate signals and the phase angle between these signals.

The variation of the imaginary part with frequency can then be used to calculate the constants of a linear first, second or higher order model. The method of forced oscillations has many practical advantages over most other methods : it does not require patient co-operation; (ii) it can be used during spontaneous or controlled respiration; (iii) it can be used without an oesophageal balloon; (iv) it can be used to investigate non-linearity of the respiratory system because it measures the "small signal" response and makes no assumptions about respiratory system linearity; (v) reproducibility is good [171]; (vi) it can be automated relatively simply.

Schmid-Schoenbein [172] analysed the method of forced oscillations theoretically and came to the conclusion that, when testing the total respiratory system, the method predominantly measures the characteristics of the upper (extralobular) airways and that the resistance measured at high frequencies (≥ 5 Hz) depends strongly on the elastic properties of the airway walls as well as the viscous losses and turbulence in the upper airways. (Measurements are usually made in the frequency range of 2 to 7 Hz.) Two sampling techniques have previously been applied to the method of forced oscillations to simplify and speed evaluation of resistance [173][174]. A new sampling technique (appendix B) which allows both resistance and reactance to be simply evaluated was developed in this work, but the forced oscillations method was finally abandoned for various practical reasons. (See section 6.4.1)

Various other phase angle measurement techniques have been used to measure respiratory impedance. Most of these methods use Fourier analysis techniques to extract the required sinusoidal measurement signals from the complex waveforms. This can be quite slow [162], depending on hardware. Noise [175][32], impulses [176][172] and the respiratory waveforms themselves [143][167] have all been used in this way as replace-

ments for the sinusoidal test signal of the method of forced oscillations.

6.3.5 Respiratory Impedance from Work or Power Measurements

A new technique is described in section 6.4.2 for measuring both compliance and resistance from mean power measurements. In section 6.4.2 it is shown that :

$$R = \frac{\overline{P \cdot \dot{V}}}{\overline{\dot{V}^2}}$$

where $\overline{P \cdot \dot{V}}$ is the mean (real) power

and

$\overline{\dot{V}^2}$ is the mean square flow rate

This method has the advantage that resistance is always representative of dissipative losses in the respiratory system, while compliance is always related to energy storage. Varene [177] has derived an essentially similar result for resistance alone, although he used a slightly different derivation and expressed the result in a different form :

$$R = \frac{W}{\int \dot{V}_T \dot{V} dV}$$

where W is the dissipative work per breath.

Measurement repeatability is particularly good using the new method, because the whole respiratory waveform is used and averaging takes place over a number of respiratory cycles. For the same reason precise detection of end inspiratory or expiratory points is not necessary, in contrast to sampling methods where these points must be detected accurately. This is advantageous in our implementation as zero crossing points are more difficult to detect with the inherently direction-insensitive hot-thermistor spirometer.

6.4 Measuring Respiratory Impedance - This Work -

6.4.1 Problems with the Method of Forced Oscillations

As we were already measuring instantaneous respiratory power, a simple sampling technique was developed using this power waveform which eliminates the necessity of evaluating trigonometric functions in the method of forced oscillations. This technique is described in appendix B.

Normally a loudspeaker is used to supply the sinewave pressure signal to the respiratory system. However, this is impractical during controlled ventilation because ventilator pressures will displace the loudspeaker diaphragm and burst it. A motor-driven piston pump could be used in place of the loudspeaker, but this is noisy, requires maintenance and is difficult to lubricate, because of fire hazards, with normal lubricants in enriched oxygen mixtures. Another practical problem involves coupling the signal from the pump to the patient. A relatively fine bore tube (< 5 mm o.d.) is desirable to minimise interference with patient manipulations. However, tests showed that this substantially attenuated the pressure signal. An even more serious limitation involves the hot-thermistor flowmeter which is not direction sensitive, thus rectifying and distorting the small oscillation at flow rates approaching zero. This prevents us from using simple filtering to separate the forced oscillation from the respiratory waveform. For these reasons the method of forced oscillations was not pursued any further.

6.4.2 Measuring Respiratory Resistance and Compliance from Measurements of Respiratory Power

The theory developed here is based on linear electrical network theory. (The reader unfamiliar with these techniques is referred to [178].) Using linear theory is an approximation, particularly in disease.

However, since the derivation is based on power and energy considerations alone, measured values will always retain a physical and physiological significance. That is, they model the energy stored and dissipated in the respiratory system. Measurements are made using the complete respiratory waveform, unlike many other techniques. This eliminates artifacts from noise or incorrect sampling time and provides good reliability and repeatability. In the past many workers estimated respiratory work using approximate relationships based on assumptions such as sinusoidal waveforms and using measured values of respiratory resistance. The technique presented here makes no assumptions about sinusoidal respiratory waveforms but reverses the process by calculating resistance (and compliance) from measurements of work and power. The technique makes use of the approximately stationary properties of the respiratory waveforms averaged over a number of respiratory cycles. This makes no critical demands for detecting the precise end of inspiration or expiration. The latter is more difficult to detect with the hot-thermistor flowmeter used than with true direction-sensing flowmeters.

Resistance

From equations 6.2 and 6.4 the work per breath done on the respiratory system (dissipated in R) is :

$$W = \int_{\text{insp}} P \cdot \dot{V} dt - \int_{\text{exp}} P \cdot \dot{V} dt = R \int_{\text{insp}} \dot{V}^2 + \int_{\text{exp}} \dot{V}^2 = R \int_{\text{insp+exp}} \dot{V}^2 dt \quad \dots \quad \dots 6.8$$

or

$$R = \frac{\int_{\text{insp}} P \cdot |\dot{V}| dt - \int_{\text{exp}} P \cdot |\dot{V}| dt}{\int_{\text{insp+exp}} \dot{V}^2 dt} \quad \dots \quad \dots 6.9$$

and replacing integration by averaging :

$$R = \frac{[\overline{P.V}]_{\text{insp}} - [\overline{P.V}]_{\text{exp}}}{\overline{V^2}} \quad \dots \quad \dots \quad \dots \quad 6.10$$

(where $\overline{V^2}$ is the mean square flow rate during inspiration and expiration)

or rewriting :

$$R = \frac{\overline{P.V}}{\overline{V^2}} \quad \dots \quad \dots \quad \dots \quad \dots \quad 6.11$$

This result is not unexpected. We could have obtained it directly from our knowledge of root mean squared quantities.

Equation 6.11 was implemented for measuring R .
(See figure G.1)

From electrical network theory we can calculate the work done by the respiratory system W_{exp} during passive expiration :

$$W_{\text{exp}} = \frac{1}{2} C (P_{\text{end insp}})^2 - \frac{1}{2} C (P_{\text{end exp}})^2 \quad \dots \quad 6.12$$

where

$P_{\text{end insp}}$ is the pressure across the compliance at the end of inspiration, and

$P_{\text{end exp}}$ the corresponding pressure at the end of expiration at zero flow.

Normally (when "gas trapping" is small)

$P_{\text{end exp}}$ will be zero but, where pressure transducer zero has drifted, or where CPAP is used, the effects of

$P_{\text{end exp}}$ must be considered.

We rewrite 6.12 :

122.

$$W_{\text{exp}} = \frac{1}{2} C \left(\left[P_{\text{end exp}} + \frac{V_T}{C} \right]^2 - P_{\text{end exp}}^2 \right)$$

$$W_{\text{exp}} = P_{\text{end exp}} V_T + \frac{V_T^2}{2C} \quad \dots \quad \dots \quad \dots \quad 6.13$$

This energy is dissipated in the respiratory resistance and ventilator during expiration :

$$P_{\text{end exp}} V_T + \frac{V_T^2}{2C} = \int_{\text{exp}} \dot{V}^2 (R + R_V) dt + \int_{\text{exp}} P_{\text{end exp}} \dot{V} dt$$

$$\frac{V_T^2}{2C} = \int_{\text{exp}} \dot{V}^2 (R + R_V) dt \quad \dots \quad \dots \quad 6.14$$

If f is the respiratory rate, from 6.14, the average power during expiration is :

$$\frac{f V_T^2}{2C} = \overline{\dot{V}^2} (R + R_V) \quad \dots \quad \dots \quad \dots \quad 6.15$$

Using $f \cdot V_T = \bar{V}$

we rewrite 6.15 as $C = \frac{\bar{V} \cdot V_T}{2 \overline{\dot{V}^2} (R + R_V)}$... 6.16

Using our knowledge of root mean square quantities,

we can substitute $R_V = \frac{\overline{P \cdot \dot{V}}_{\text{exp}}}{\overline{\dot{V}^2}_{\text{exp}}}$ and equation 6.10

into 6.16 :

$$C = \frac{\bar{V} \cdot V_T \overline{\dot{V}^2}}{2 \left(\overline{\dot{V}^2}_{\text{exp}} \overline{P \cdot \dot{V}}_{\text{exp}} - \overline{\dot{V}^2} \left[\overline{P \cdot \dot{V}} \right]_{\text{exp}} \right)} \quad \dots \quad 6.17$$

For normal conditions $R \gg R_V$, we can rewrite equation 6.16 as :

$$C = \frac{\bar{V} \cdot V_T}{2 \overline{\dot{V}^2}_{\text{exp}} R} \quad \dots \quad \dots \quad \dots \quad 6.18$$

and from equation 6.11 :

$$C = \frac{\overline{\dot{V}} \cdot \overline{\dot{V}}_T \cdot \overline{\dot{V}}^2}{2 \cdot \overline{\dot{V}}_{\text{exp}}^2 \cdot (\overline{P \cdot \dot{V}})} \quad \dots \quad \dots \quad \dots \quad \dots \quad 6.19$$

Equation 6.16 shows that the total expiratory time constant including the ventilator valves and tubing is :

$\text{expiratory time constant} = \frac{\overline{\dot{V}} \cdot \overline{\dot{V}}_T}{2 \cdot \overline{\dot{V}}_{\text{exp}}^2} \quad \dots \quad \dots \quad 6.20$
--

At the end of inspiration, assuming negligible "gas trapping" (see appendix A.) we can calculate end-inspiratory pressure in the alveoli using :

$$P_{\text{end insp}} = \frac{\overline{\dot{V}}_T}{C} \quad \dots \quad \dots \quad \dots \quad 6.21$$

and, substituting from equation 6.19, we obtain the alveolar pressure at the end of inspiration :

$$P_{\text{end insp}} = \frac{2 \cdot \overline{\dot{V}}_{\text{exp}}^2 \cdot (\overline{P \cdot \dot{V}})}{\overline{\dot{V}} \cdot \overline{\dot{V}}^2} \quad \dots \quad \dots \quad \dots \quad 6.22$$

This is a useful result, as it allows us to estimate peak alveolar pressures without the practical problems of direct measurement. Errors in estimating pressure using this technique depend on the linearity of the respiratory pressure volume relationship.

Of the techniques described in this section only the resistance measurement technique was implemented for practical testing in the impedance analyser which was constructed. (See figure G.1 and chapter 9.)

Most of the results of this section require evaluation of the mean square flow rate. This tends to introduce errors, as the squaring operation limits the dynamic range, especially in an analogue implementation as was used for

test purposes. By suitably configuring the squaring circuit to feed this squared output current into a current summing junction forming the input of the low pass (averaging) filter, this limitation can be overcome.

6.4.3 Sampling for Measuring Respiratory Resistance and Compliance

Sampling techniques, in theory, are simple to implement and have been widely used in non-automated form. An automated technique of this type was developed and implemented to allow clinical comparison with the other method implemented based on mean power measurements. (Section 6.4.2) The technique used here ignores inertial effects.

Respiratory Compliance was measured by using equation 6.21 and assuming that the mouth pressure P_{pause} , at the end of inspiration when inspiratory flow ceases and the expiratory valve is about to open, is equal to alveolar pressure ($P_{\text{end insp}}$). For a long pause period this assumption is correct, as the pressure is measured "statically" after gases and the respiratory system have come to rest. However, many widely used ventilators do not have a pause control, and, in any case, it may not be desirable to use an end inspiratory pause on all patients. We are therefore commonly forced to make this measurement "dynamically" and should thus consider how this influences the measurement. The ventilator compliance (figure 6.1) helps us to make this measurement, because it prevents the mouth pressure from dropping to zero at the instant the expiratory valve opens. The inertance of both the expiratory valve and the gas in the ventilator's expiratory limb also help in this way.

The inertance of the respiratory system may contribute an error, since the volume acceleration of the gas may not be zero near zero flow rate. The importance of "correct" sampling time cannot be overemphasised, since

additional errors from resistance or expiratory valve opening will otherwise result. From experience using the equipment developed it appears that a very short sampling period is necessary (because pressure changes very rapidly at the sample point) and sampling just prior to zero flow rate will generally improve accuracy under most conditions. (See also section 6.3.2 and chapter 9.)

Errors from using CPAP or pressure transducer zero drift were eliminated by measuring the pressure difference $\Delta P = P_{\text{pause}} - P_{\text{end exp}}$ and rewriting equation 6.21 :

$$C = \frac{V_T}{\Delta P} \quad \dots \quad \dots \quad \dots \quad \dots \quad \dots \quad 6.22$$

This form also ensures that, in the presence of "gas trapping," equation 6.22 remains correct.

Respiratory resistance was measured by assuming that, when the expiratory valve opens, the alveolar pressure ($P_{\text{end insp}}$) is suddenly applied across the respiratory resistance and ventilator resistance in series. This causes the flow rate to rise rapidly to a peak value of \hat{V}_{exp} (figure I.3). If we call the corresponding pressure across the ventilator expiratory resistance $P_{\hat{V}_{\text{exp}}}$ and pressure across the respiratory resistance

$$\Delta P_1 = (P_{\text{pause}} - P_{\hat{V}_{\text{exp}}})$$

then we can calculate

R from :

$$R = \frac{\Delta P_1}{\hat{V}_{\text{exp}}} \quad \dots \quad \dots \quad \dots \quad \dots \quad 6.23$$

Note : Using P_1 rather than P_{pause} eliminates errors from pressure transducer zero drift, ventilator resistance and the use of CPAP. An advantage of this measurement technique is that any errors in P_{pause} (e.g. from incorrect sampling time) will tend to cause equal errors of opposite sign in R and C (from equations 6.22 , 6.23 and noting $R \gg R_v$ implies $\Delta P_1 \approx \Delta P$).

Therefore, the product RC , respiratory time constant, will tend to be more constant and reproducible than either R or C individually :

$$RC = \frac{V_T \cdot \Delta P_1}{P \cdot \dot{V}_{exp}} \doteq \frac{V_T}{\dot{V}_{exp}} \quad \text{for } R \gg R_V \quad \dots \quad \dots \quad 6.24$$

(V_T and \dot{V}_{exp} are much easier to measure accurately than P_{pause} .) (See also section 6.3.2)

If an alternative measurement technique had been used for either R or C , RC would have been far less reproducible. A disadvantage of the technique for measuring respiratory resistance is that it measures resistance at peak flow rate where resistance will tend to be greatest from turbulence and where resistance will thus tend to be most affected by changes in tidal volume which determines the peak expiratory flow rate (appendix A).

6.5 Summary and Conclusions

Previous techniques used for measuring the respiratory system driving point impedance were reviewed. Many techniques suffer from systematic errors and poor repeatability. Errors are often related to fundamental assumptions implicit in the simple lumped element linear models used. Measurement techniques which use only a few points on the respiratory waveform are particularly prone to artifacts.

A new theoretical technique for use with the method of forced oscillations was developed but abandoned because of practical difficulties.

A new theoretical technique for calculating respiratory resistance, compliance and end inspiratory alveolar pressure was developed based on energy considerations and utilizing power measurements. The work of ventilation is often important physiologically in respiratory failure and can be related to difficulties in controlling ventilation. Therefore modelling and measuring the mechanical properties of the respiratory system from

measurements of energy stored and dissipated in the respiratory system over the whole respiratory cycle appears to have a sound physical and physiological basis.

A respiratory impedance analyser was constructed to compare a slightly modified classical sampling technique (zero-crossing method) with the new technique for measuring respiratory resistance.

7. Evaluation of the Hot-Thermistor Spirometer/ Flowmeter

The performance of the hot thermistor spirometer/flowmeter was assessed in both laboratory and clinical testing.

The clinical utility of the flowmeter was also assessed. Simple techniques for assessing some mechanical aspects of ventilation are discussed. These techniques are based on theory developed elsewhere in this thesis.

7.1 Test Methods

Two techniques were used to assess basic accuracy under a variety of conditions.

The primary method involved maintaining as constant a flow rate as possible through the flow transducer and collecting the volume of gas passed, in a timed interval, in a 120 litre "Tissot" wet seal spirometer (Warren E. Collins, Inc., Braintree, Mass.). Measured volume was corrected for changes in vapour pressure and temperature which occurred during collection. (See appendix C.) Mean flow rate was then calculated from the measured time and corrected volume. Flow rate was maintained constant by continuously adjusting the blower of a Godart-Statham (type 18987) inclined manometer flow calibrator to maintain indicated flow rate constant. This flow calibrator proved surprisingly inaccurate and could not be used directly, since it was accurate only to ± 4 percent near full scale on each of its ranges.

The second method, which was used where less precise determinations were required, used a "super syringe" (Hamilton, Co., Reno, Nevada) and the internal integrator of the flowmeter. Constant volumes



Figure P 7.1

Calibrating hot-thermistor spirometer (top right)
using inclined manometer flow calibrator (lower right)
and "Tissot" wet-seal spirometer (left).

delivered by the syringe should result in a constant measured volume independent of delivery rate. By observing the flowmeter instantaneous-velocity signal on a fast-response meter, flow rate can be kept constant manually whilst delivering the volume. Linearity and accuracy can then be assessed from any variations in the volume measured at different flow rates. One complication using this technique involves flowmeter and integrator offsets, which result in an error which increases with time and is thus greater at low flow rates where integration must take place over a longer time for a constant delivered volume. (Using different volumes is undesirable as the commercial calibration syringe was found to be inaccurate when tested by filling with water from a measuring cylinder. Using the syringe repeatedly at one setting ensures a more consistent delivered volume.) Integrator zero offset is negligible compared with flowmeter offset which is purposely offset slightly from zero to improve linearity at higher flow rates. Provided the integrator is zeroed just prior to a measurement, zero offsets do not introduce any additional error compared with the normal (averaged) minute volume output or instantaneous flow rate signal.

The Tissot spirometer was used for only one set of measurements in air, as it proved difficult to maintain flow rate constant for the long periods required, and the syringe technique was quicker and simple to use with different gas mixtures and vapours. Volumes could be reproduced to an accuracy of better than $\pm 2\frac{1}{2}\%$ without great difficulty using the syringe technique. Errors using this technique are greatest at high flow rates where gas compression through the syringe's nozzle caused appreciable, rapid temperature fluctuations.

Flowmeter frequency response was measured by mounting two thermistor sensors between three metal prongs protruding well forward from the end of a perspex rod and connecting these to the flowmeter in place of its flowsensor. The rod was made to follow a cam attached to a variable speed motor. (See figure 7.1)

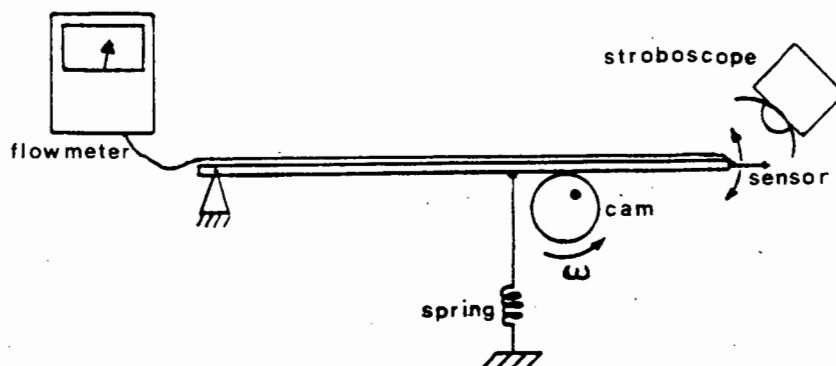


Figure 7.1 Measuring Flowmeter Frequency Response

The cam consisted of an eccentrically mounted disc which produced an approximately sinusoidal movement of the thermistor. A General Electric "Strobotac" stroboscope was used to measure the frequency of rotation of the motor. Minute ventilation indicated on the flowmeter was normalised by dividing the reading obtained by the frequency. For constant displacement amplitude A the sensor velocity increases directly with frequency : If displacement $S = A \sin \omega t$, where ω is the angular velocity and t time, differentiating with respect to time yields velocity = $A\omega \cos \omega t$. Thus, by dividing measured "flow rate" (velocity) by ω , we can measure the flowmeter's frequency-amplitude characteristic. To cover the range of frequencies required without too large a change in mean velocity, and to prevent cam follower bounce, measurements were made in overlapping frequency bands with decreasing displacements at higher frequencies.

Minimum flow sensing threshold was assessed, using a 50 ml syringe and injecting gas at slow (timed) rates until the output dropped to below 50 percent of the expected change in level for that particular flow rate.

Dry gas mixtures were obtained from piped medical gas by using a conventional anaesthetic machine mixing system (using rotometers). For humidification gas was passed through a heated Bennet "cascade II" humidifier. The presence of copious condensation on the outlet tubing was taken as an indication of complete saturation at the (lower) collection temperature. Gas mixtures were withdrawn from a tapping in the outlet tubing at a slow rate to avoid air contamination. Percentage saturation of room air with water vapour was determined using a sling psychrometer and standard tables [108].

The explosion hazard was assessed by soaking a piece of cotton gauze in ether and passing oxygen through the gauze and the flowsensor at a very slow rate until all the ether had evaporated from the gauze. It was assumed that the ether concentrations under these conditions would include the most explosive ether/oxygen mixture.

7.2 Results and Discussion

7.2.1 Accuracy and Linearity

Overall accuracy and linearity for the flowmeter is shown in figure 7.2 for a constant flow rate. The insert in the top left-hand corner shows the error as percentage of reading over the commonly encountered flow rates for inspiration, expiration and inspiration plus expiration. It can be seen that more careful calibration would have given higher accuracy, since the scale factor is too low and offsetting zero slightly

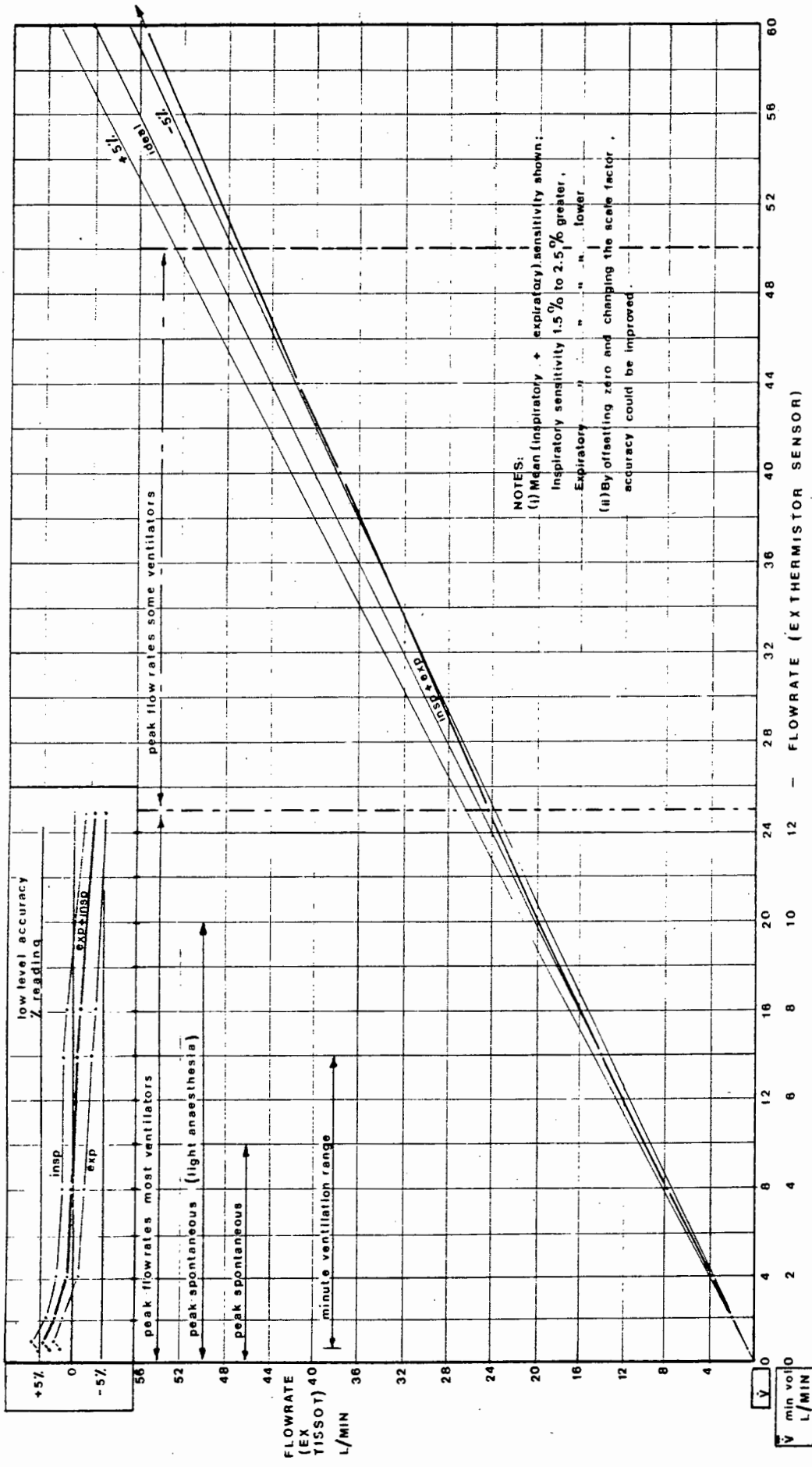


FIG. 7.2 OVERALL ACCURACY/LINEARITY OF FLOWMETER MEASURED AT 27.5 °C IN AIR.

Flowmeter measures minute volume from mean inspiratory and expiratory flowrates.

more would have increased accuracy at low levels. The linearisation technique has worked well and most of the error is from scale factor and zero. Differences between inspiratory and expiratory sensitivity are probably due to "entrance effects" and decrease at high flow rates. This could give rise to subtle errors, since inspiratory and expiratory flow rates will often be different. However, since expired and inspired volumes are approximately equal, and the percentage errors are approximately equal and opposite in sign for the two measurements, these errors tend to cancel out in the measured minute volume. Where other measurements are made directly using the instantaneous-flow rate signal, errors resulting from sensitivity differences are still within five percent of reading for most commonly encountered flow rates. With more careful scale-factor calibration, this would have extended over the full range of flows up to 50 L/min.

7.2.2 Temperature Effects

Measurements corrected to BTPS do not change by more than three percent for temperature changes from 37°C down to 20°C. Part of this error is due to the fact that temperature gradients through the probe cause incorrect temperature correction from the separated temperature and flow sensors. Normally this error should be insignificant as gas temperature is carefully controlled to between 32° and 35° C to minimise heat losses from the patient.

Placing the temperature sensor closer to the flow sensor would reduce this error at the cost of more difficult construction of the sensor assembly. This error tends to be greatest when the flow sensor assembly and gas are at different temperatures.

7.2.3 Humidity and Condensation

Condensation can theoretically affect accuracy in a number of ways. Condensation can cause entrance effects changing the velocity profile, and hence the scale factor, by causing turbulence. Condensation will not occur on the flow sensor (at high temperature) but could cause the temperature sensor to overestimate temperature if contaminated with saline, as the condensed water might then be sufficiently electrically conductive to change the measured temperature. The temperature sensor cannot normally be submerged by condensed water, since it is directly in the gas flow path and in normal use water will drain to the et. tube exit. However, it did prove possible, by inverting the sensor (as might occur if the infant were placed face downwards), to get sufficient water to condense and cover the temperature sensor without actually interrupting gas flow. Even with a poorly conducting condensate this could cause errors, as the fluid will usually not be at the same temperature as the gas. A more subtle error from temperature changes of the temperature sensor might occur due to the latent heat of condensation changing the compensation thermistor's temperature.

It is difficult to separate out the effects of temperature from humidity, since condensation in the flow-sensor assembly may cause temperature gradients between flow and temperature sensor. Where the sensor assembly was at a low temperature $\angle 20^{\circ}\text{C}$, so that copious condensation occurred when gas humidified at 37°C was used, errors up to + 6 percent of reading were recorded with oxygen. (See figure 7.3) Under the same conditions, with the sensor assembly warmed to 35°C , changes of one or two percent (i.e. within the limits of possible experimental error) were recorded. It is very difficult to precisely control and estimate gas volumes under these conditions, owing to continuously

changing temperatures which must be known for accurate correction of volume measurement. With gas humidified to the recommended 80 percent for ventilation [62] and room temperatures above 25°C, errors were less than two percent.

7.2.4 Effects of Gas Mixtures and Vapours

The effects of a variety of anaesthetic gases and vapours on the flowmeter are shown in figure 7.3 relative to measurements made in air at 50 percent RH.

Figure 7.3

MEASURED EFFECTS OF GAS AND VAPOUR MIXTURES ON FLOWMETER †

MIXTURE (at 25°C)	CHANGE OF READING
Air (50 % sat. H ₂ O)	x 1.0
Air (100 % sat. H ₂ O)	x 0.98 to 1.04 (See text)
Oxygen (dry)	x 1.03
Oxygen (100 % sat.) 37°C	x 0.99 to 1.06 (See text)
66 % N ₂ O + 34 % O ₂ (dry)	x 0.86
50 % N ₂ O + 50 % O ₂ (dry)	x 0.91
50 % N ₂ O + 50 % O ₂ (dry)	x 1.01*
10 % CO ₂ + 90 % air (40 % sat.)	x 0.97
10 % CO ₂ + 90 % O ₂ (dry)	x 1.01
	*with switched correction

†(Measured at a flow rate of 8 to 10 L/min.)

(cf. fig. 4.11)

With the exception of nitrous oxide, the effect of most agents is quite small and hardly greater than the potential experimental errors (estimated at ± 2.5 percent max.). With the switchable correction this nitrous oxide error becomes quite small. If no correction were applied the anaesthetist would tend towards the safer error of hyperventilation, since the flowmeter would underestimate flow in the presence of nitrous oxide.

Although expired CO₂ levels are normally only four percent, additional CO₂ up to about ten percent is sometimes added to inspired mixtures to allow hyperventilation of the patient. If very high CO₂ levels

were used in error, the flowmeter would indicate a significant reduction in flow rate, again a safer condition.

7.2.5 Entrance Effects

Changes in the velocity profile across the diameter of the flow sensor arising from fluid accumulations or from tubing bends or connectors can give rise to changes in sensitivity. (See also condensation above.) Almost all flow sensors measuring velocity and calibrated in terms of volume flow rate suffer from this type of error and often require flow straighteners upstream and downstream to prevent instability in the flow profile. Instability is a particular problem here where the flow sensor must be as short as possible to minimise deadspace. The sensor assembly was carefully designed to try to minimise these entrance effects and hence make it equally sensitive to inspiration and expiration but insensitive to nearby tube bends. Figure 7.2 shows that sensitivity forward to reverse is not quite the same. The flow probe is largely insensitive to nearby tube bends, except for the largest size et. tube connector (5 mm), where changes of about two percent occur with a bend simulating conditions in an intubated infant. Larger size et. tubes, which would not be used on infants, can introduce larger errors (6 percent), since entrance conditions with these tubes are no longer properly controlled by the sensor assembly. Tubing bends on the ventilator side of the sensor introduce negligible errors.

Errors from et. tube bends will tend to be constant for any one patient, since great care is taken to immobilise the et. tube assembly for safety reasons.

7.2.6 Long-Term Stability

The flowmeter was used and tested over a three-year period. During this time it was used on approximately thirty-five infants and six dogs. At

end of three years the calibration had changed by three percent.

During this period the probe did once show a large reduction in sensitivity (\approx -15 to 20 percent). Careful examination showed the flow sensor was contaminated with dried dip sterilizing solution. Soaking the sensor in alcohol returned the sensitivity to normal. The sensor should thus always be soaked in alcohol after dip sterilization to prevent contamination.

The one minute integrator timer had drifted by about one second after three years.

The temperature display was still accurate to within 0.3° C from 20° to 40° C after three years.

7.3 Clinical Evaluation

7.3.1 Reliability

In clinical use very few problems were encountered and the equipment proved very reliable. One lead failure occurred from flexure at the connector near the patient.

Erratic sensor operation occurred after an acidic water-based dip sterilizing solution had been used for some time. Resoldering the thermistor leads solved the problem, but for more reliable solder joints it is necessary to use a precious metal based solder. Conventional lead-tin solder, as was used, forms a mechanical joint not a proper bond to the thermistor's platinum-ruthenium leads.

Sensor contamination from mucus did not occur in any of the cases in which the sensor was used. The sensor end caps tend to act as inertial separators. In longer-term use contamination might be a problem. Water accumulations blown through the flow sensor

caused a negligible increase in reading during clinical use, although the flowmeter's overload light would sometimes light momentarily.

Flow sensor disconnection could easily be detected, since the overload indicator would come on and the meter would deflect past full scale.

Temperature sensor disconnection is not quite so obvious, since the temperature meter deflects slightly below display minimum (20°C), while the flowmeter still works but with a very much lower sensitivity. Normally the temperature sensor flicks backwards and forwards between inspired and expired temperature or stays constant at 37°C for an inspired temperature the same as body temperature. It is thus quite easy to detect this fault.

Reproducibility of measurements was very good. Using a rotometer as standard (at its full scale to maximise accuracy), flowmeter output would stay constant, at a constant flow rate and temperature, to within one percent of reading over extended periods of time.

7.3.2 Clinical Utility of the Hot-Thermistor Flowmeter

In its primary role for setting ventilation levels during anaesthesia the flowmeter allowed simple, rapid ventilator adjustment, although anaesthetists usually took a short period to adjust from thinking in terms of tidal volumes.

In some cases the flowmeter allowed the early detection of changes in status of the patient. The following case illustrates this quite well. In this infant ventilation levels fell steadily from shortly after the beginning of controlled ventilation without any obvious reason. Blood gases were approximately normal and the reduction in minute volume could

not be attributed to the ventilator or the surgeon's manipulations. The anaesthetist commented that the flowmeter was "obviously playing up." Blood gases eventually started to show marked changes and chest radiographs showed that the infant had developed pulmonary oedema.

Under constant ventilator settings changes in ventilation level reflect changes in the mechanical properties of the respiratory system.

Viewing instantaneous flow rate waveforms on a multi-channel theatre memory 'scope proved very rewarding. It allowed rapid visual setting of inspiratory/expiratory ratio in non-timed ventilators. It has been suggested that the reason certain clinicians advocate the use of high I/E ratios greater than one, is that ventilator-system compliance effectively reduces inspiratory time markedly from that set [1]. Monitoring I/E ratio visually allows "effective" I/E ratio to be estimated for infants where this reduction of inspiratory time is significant. Figure 7.4 shows a typical flow waveform recorded using a heated stylus recorder in theatre.

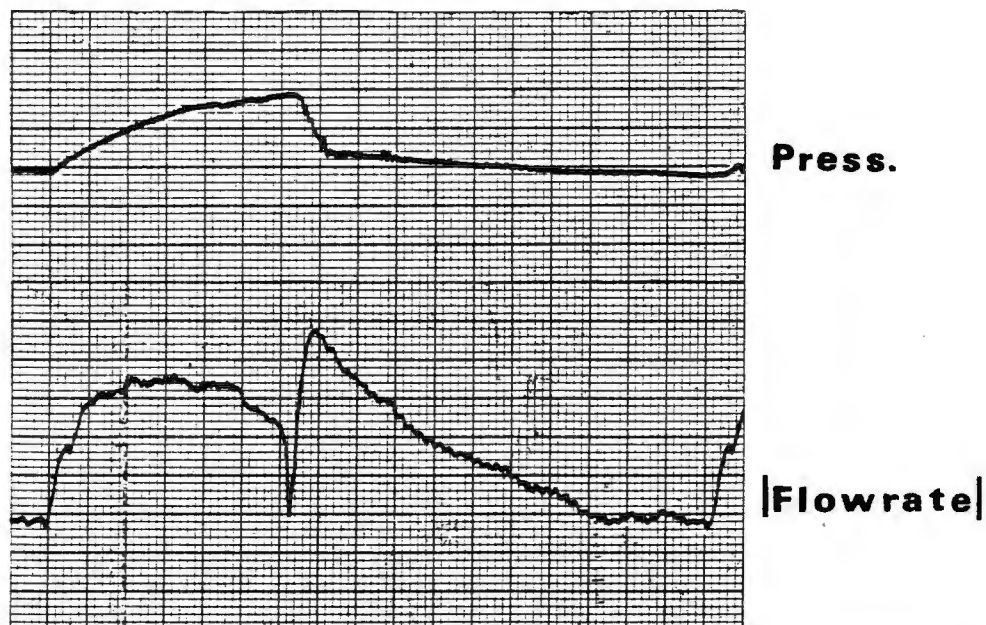


Figure 7.4 Typical Airways Pressure and Flow Waveforms recorded in Theatre while using a Dräger Narkose Spiromat 650 Ventilator.
Horizontal scale 25 mm = 1 sec.
(Pressure and flow waveforms were recorded sequentially and not simultaneously.)

Using a display, made synchronising the patient to the ventilator during assisted ventilation a very simple task, eliminating "out of phase." In thoracic surgery the display was also used to replace the conventional impedance plethysmograph equipment which does not usually work after the chest has been opened. In this role it allows the detection of gross leaks and the estimation of et. tube leaks. In all of the tests the latter appeared small even when appreciable bubbling was audible at the patient's mouth.

From the results of Appendix A peak expiratory flow rate increases with decreasing respiratory time constant for a constant tidal volume. (This would normally be maintained constant by adjusting the ventilator using flowmeter measurements.) Figure 7.5 illustrates how this result may be used qualitatively to assess changes in respiratory time constant.

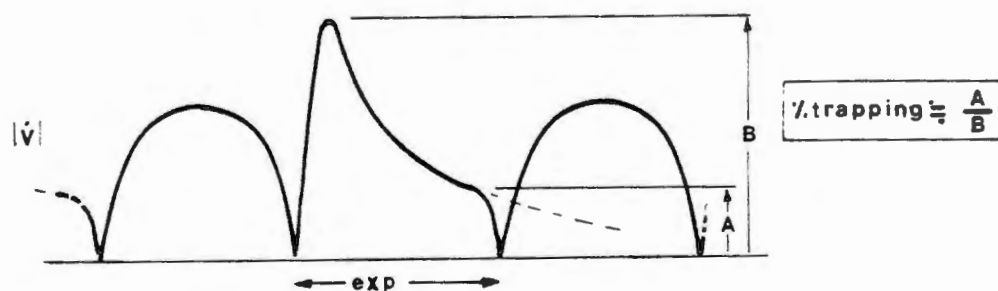


Figure 7.5

Peak expiratory flow rate varies directly with respiratory time constant when tidal volume is maintained constant.

This may be a rational way to rapidly select PEEP pressures. An approximation - to "optimum" PEEP pressure is sometimes made at the pressure which gives maximum compliance [179]. Assuming resistance is relatively independent of pressure, this would correspond to choosing PEEP to maximise respiratory time constant. (Resistance also depends on lung inflation level, so that this may not be a very sensitive method, since R and C will tend to change in opposite directions with an increase in lung inflation level.)

Figure 7.6 illustrates how gas trapping can be detected and assessed qualitatively from the expiratory waveform using the results of Appendix A.

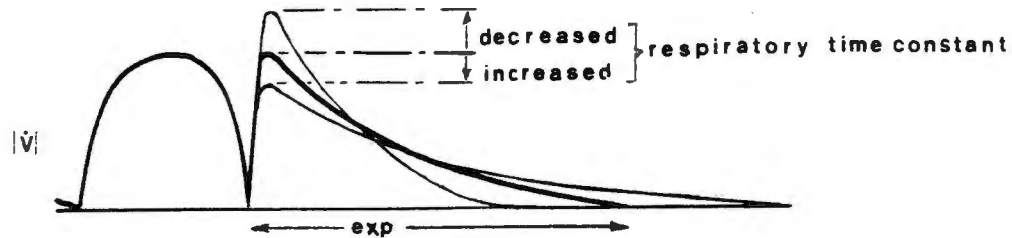


Figure 7.6

Detecting gas trapping : Peak expiratory flow rate is markedly increased and flow rate is still appreciable just prior to the end of expiration.

This may be useful for assessing end expiratory alveolar pressure in infants who are difficult to ventilate and in whom some gas trapping may be unavoidable.

The flowmeter is direction insensitive so that it takes a while to learn to differentiate between inspiratory and expiratory waveforms. This is unfortunate, since it slows acceptance by the user. Including direction sensing in the flowmeter would complicate sensor construction and thus tend to decrease reliability.

The flowmeter showed that large reductions in ventilation of sixty percent or more often occurred during surgical manipulations. This agrees with Okmian who found reduction in ventilation as high as ninety percent under similar conditions [16].

Large water accumulations in the ventilator circuit caused very rapid flowrate fluctuations on the displayed instantaneous flow rate waveform. This serves to remind the anaesthetist to clear the tubing.

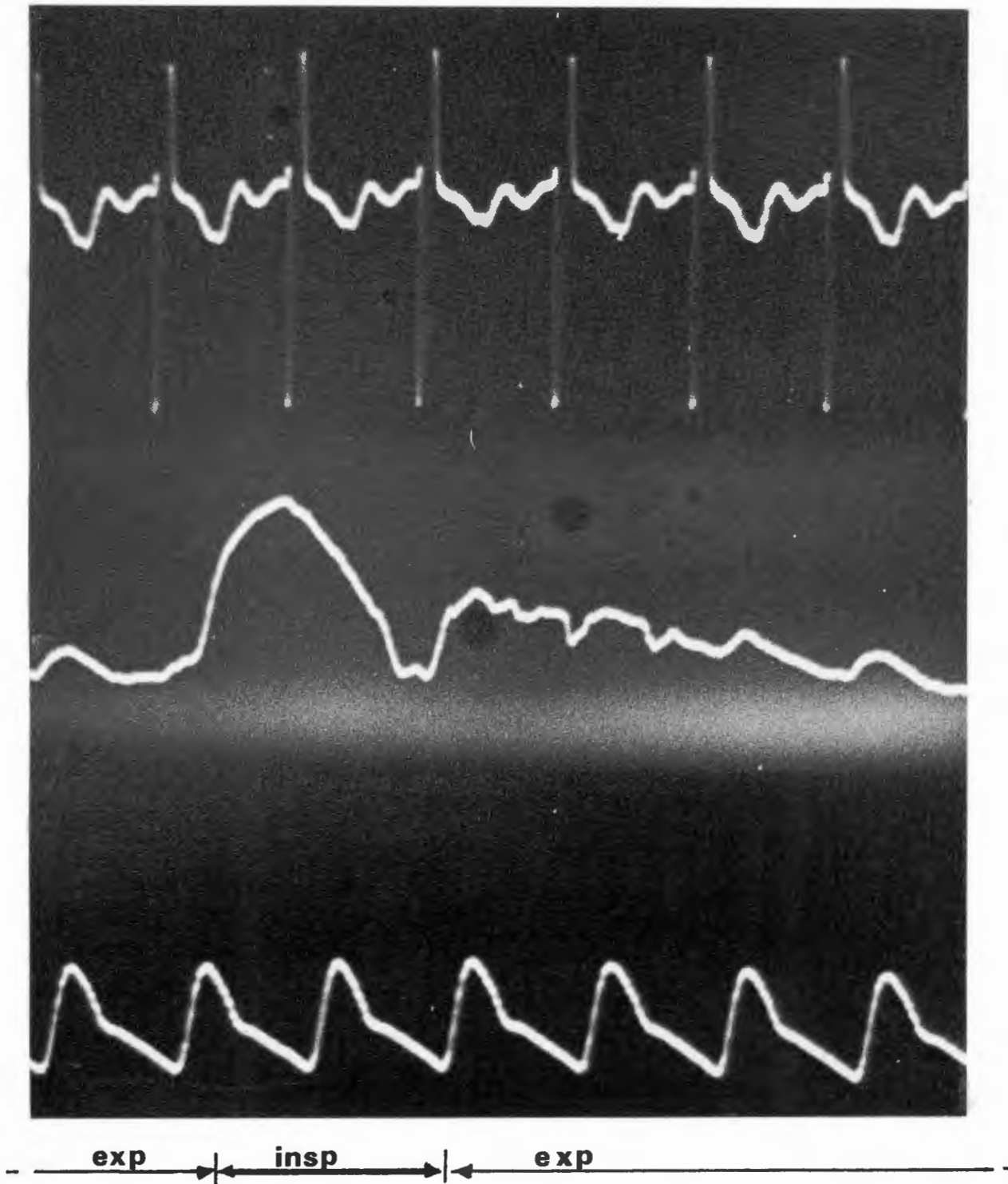


Figure P 7.3 Instantaneous flow rate (centre) displayed on memory oscilloscope with e.c.g. (top) and blood pressure (lower). (Horizontal axis : time) Notice the long expiratory time constant and the large cardiac "artifacts" on the flow waveform near the end of expiration. (cf figure 7.4)

7.4 Suggested Improvements to the Hot-Thermistor
Flowmeter Based on Clinical Experience and Testing

- (i) The flow sensor assembly should include the temperature-compensation thermistor internally as an integral part. This would eliminate possible errors from temperature gradients/condensation and temperature sensor "flooding." At present the later might be possible if the patient is placed face downward.
- (ii) The plug and socket on the flow sensor should be reduced in size, so that it does not protrude forward (at present by 25 mm) and encroach on the surgeon's work space.
- (iii) Adjustable alarms should be incorporated for upper and lower limits on minute volume.
- (iv) A 40°C alarm for upper temperature limit should be incorporated to detect ventilator humidifier failure.
- (v) The flowmeter should be made smaller and arranged so that it is easily "stackable" and can be rack mounted.
- (vi) An analogue rather than a digital display must be retained but a light-emitting diode bar-graph might form a more robust analogue display. An analogue display allows easy "at a glance" reading and early detection of changes.
- (vii) Probes should be made interchangeable by incorporating three pre-set calibration potentiometers in the plug of each sensor. This would allow a single flowmeter to be used in an I.C.U. for testing a variety of patients without any possibility of cross-infection.

(viii) In some applications it may be desirable to make the flow sensor totally earth free. This can be achieved by floating the complete front end of the flowmeter using a suitable commercial isolation amplifier (with isolated power supply brought out). The temperature-corrected flow signal would then be transferred across the isolation barrier after the first multiplier/divider. In its present form mains leakage is low enough for use as a "floating system", if the transformer screen and frame were earthed and the circuit common were allowed to "float."

7.5 Conclusions

Hot-thermistor spirometry is sufficiently reliable and accurate for most applications in controlling and monitoring the ventilation of infants.

Monitoring average ventilation and instantaneous flow rate allows simple qualitative assessment of the mechanical aspects of ventilation.

The performance achievable with the hot-thermistor spirometer described in this thesis is summarised in figure 7.7.

Figure 7.7

PERFORMANCE OF HOT-THERMISTOR SPIROMETER/FLOWMETER

		<u>Comment</u>
Accuracy	<u>Minute ventilation</u> : + 5 % of reading from 0.3 L/min to 25 L/min for any inspiratory/expiratory ratio and peak instantaneous flow rate up to 50 L/min Typical accuracy : + 3 % from 1 to 7 L/min	Zero and scale factor calibrated for 0 % error at 2 L/min and 25 L/min (Instantaneous flow rate)
	<u>Instantaneous flow rate</u> : + 5 % of reading from 0.45 L/min to 50 L/min + 80 ml/min below 0.45 L/min <u>Overload</u> at 65 to 70 L/min	(as above) In terms of FSD : Accuracy + 2 % FSD from 0 to 25 L/min FSD
	Effects of <u>anaesthetic gas mixtures, vapours and humidity</u> normally less than + 5 % change in reading	(See text) N ₂ O requires switched correction factors
	Effects of <u>temperature</u> : No additional error 30 to 38°C within 3 % to 20°C	Reads volume at temperature. Manual correction to BTPS
Resolution	Better than 20 ml/min	Tested at low flow rates
Sensing Threshold	< 50 ml/min	
Repeat-ability	+ 1 %	Constant conditions
Frequency Response	0 to 20 Hz within + 3 %	Measured above 0.3 L/min
Warm-up Time	< 2 min to 5 % final value	
Long-term Stability	+ 1 % per annum	Probe rinsed regularly in alcohol
Safety	No explosion hazard with most explosive ether/O ₂ mixture Leakage current single fault < 35 µA	
Temperature Display	20 to 40°C accuracy ± 0.3°C	Rapid response analogue meter
Display	0 - 7 L/min - primary scale 0 - 2 L/min) Push button selected 0 - 20 L/min) cannot be permanently selected for safety	17 cm mirror scale analogue meter
Integrator	0 to 40 litres (i) With plug in external controls : run/hold and reset (ii) Internal : 60 + 1 second integrate timer 10 seconds display timer	+ ½ % additional error After 70 seconds returns to average mode

CHAPTER 8

8.0 Selection and Evaluation of Pressure Transducer

The "ideal" requirements for a pressure transducer for this application are summarised in figure 8.1 and compared with the results achieved with the chosen transducer.

The requirements for the transducer are very stringent. The transducer should be able to measure pressures up to 60 cm H₂O, withstand pressures of 150 cm H₂O [36] and measure accurately at the end of inspiration, where the pressure could be a low 5 cm H₂O. Zero drift is particularly important, since quite small drift in terms of full scale may give large errors at normal pressure levels during ventilation. Transducers are often specified only in terms of total error as a percentage of full scale. This gives a poor indication of actual performance at typical operating levels, which are well below full scale. For this application, the measurement techniques were carefully designed to minimise errors from zero drift by measuring pressure differences or using other techniques to minimise this source of error. (See chapter 6.) The required zero drift performance (figure 8.1) was estimated by assuming a square wave ventilator pressure waveform of about 20 cm H₂O (a typical level [4]) with an accuracy $\pm 4\%$ over a temperature range of $\pm 4^\circ\text{C}$. Achieved performance, although better than claimed by the transducer manufacturer, is about three times worse than this requirement. Because operating theatres are temperature controlled, the performance is probably just adequate, but the transducer will require periodic re-zeroing in an I.C.U. environment.

Four transducers were initially evaluated. The choice of transducer was limited largely by cost considerations. Fortunately, two transducers were obtained as surplus. Widely used "medical" pressure

transducers, such as the Statham Instruments' model finally selected, would otherwise have proved too costly (R1 000) for the limited available research budget. The other transducers were rejected owing to poor zero stability with temperature, and diaphragm clamping problems. Semiconductor pressure transducers seem generally unsuitable for this application, owing to zero drift.

Static measurements were performed, using a steel "metre" rule, calibrated in millimetres, and a water manometer. Measurement accuracy was within 1 mm. of water pressure.

Frequency response of the Statham P23dB pressure transducer was tested using the National Semiconductor LX3700D transducer. The LX 3700 has a wide bandwidth (≥ 5 K Hz), owing to the very high diaphragm resonant frequency, but has a poor zero stability. A sinusoidal pressure signal was produced by a loudspeaker (Richard Allen HD8T) driven by a function generator (Hewlett Packard 3312A). Changes in output of the P23dB, relative to the LX3700D, were measured by precisely superimposing the waveforms from the two transducers on a dual-trace oscilloscope (Tektronix 912), and recording relative amplitude differences as frequency was varied. Exact coincidence of the two signals at 1 Hz was obtained by carefully adjusting the continuously variable gain control of one channel. Both channels were a.c. coupled to eliminate transducer zero drift. Estimated resolution was 1 % or better. Accurate matching of the oscilloscope's vertical amplifiers over the frequency range of 1 to 100 Hz was first checked using a single input to both channels. The transducers were then compared directly coupled to the loudspeaker. The responses were found to match over the range of interest from 1 to 80 Hz, within the limits of the measurement technique. The test was repeated with the P23dB connected via its tubing and connector (1.15 metres of green "Bird" high-pressure ventilator tubing,

6 mm. o.d., 3 mm. i.d.). The frequency response was found to fall to -3% at 20 Hz, dropping smoothly to - 3 dB at 75 Hz. The use of thick walled tubing in this application is very important, as otherwise movement artefacts are introduced by vibration and patient movements.

8.1 Summary and Conclusions

Manufacturers specifications are a poor indication of pressure transducer performance. Zero stability of many transducers is often the most serious limitation, provided the device has good linearity. Automatic zeroing of both electronics and transducer would give a large improvement in device performance at the cost of added electronic and electromechanical complications. [72]. The Statham P23dB strain gauge pressure transducer used has a barely adequate performance for this application owing to zero drift with temperature. Warm-up time of the transducer is also excessively long, unless the bridge supply is limited to less than 3 V, far below the manufacturer's recommendation. (See appendix E) The bridge output is then very small, requiring an extremely low drift, low-noise instrumentation amplifier. The transducer must also be shielded from vibration and draughts. The higher sensitivity Statham PM6+1 transducer would reduce zero drift problems but would probably compromise the frequency response as it has a larger compressible volume and has other problems: large size, vibration sensitivity and greater cost.

CHAPTER 9

9. Evaluation of Respiratory Impedance Analyser9.0 Introduction

The performance of hardware for measuring respiratory system impedance and work of ventilation was assessed. The performance of the equipment and techniques used are discussed in the light of the tests and clinical experience.

Testing the performance of the impedance analyser posed four problems :

- (i) How to produce a suitable patient simulator with accurately known characteristics;
- (ii) Separating the measurement instrument's errors from errors inherent in the measurement techniques;
- (iii) Assessing this accuracy under representative combinations and permutations of ventilator, ventilator settings, flow rates, valves, tubing, anaesthetic circuits and patient (simulated) characteristics;
- (iv) How to assess clinical problems related to the equipment.

Measuring flow resistance based on mean power measurement measures resistance during both inspiration and expiration. Measurement of flow resistance also includes the resistance of the flow sensor, since pressure sensing is on the inlet (ventilator) side of this fitting. The flow sensor and the simulated flow resistance have a combined non-linear resistance to flow. (The flow resistance increases with flow rate. See fig.I.1 (appendix I))



Figure P 9.0

Front panel of experimental impedance analyser was kept as simple as possible to allow use by busy clinicians. "Simulated" switch position connects electronically generated test waveforms to allow for self testing of circuitry and for setting up waveform monitors or recorders.

This means, excluding other considerations, that the sampling technique (measuring at instant of peak expiratory flow) may yield a different value for resistance from the mean power technique. This will also be true for actual patients since turbulence in the upper airways causes resistance to increase at higher flow rates. [149] [180]

9.1 Laboratory Tests

In assessing the performance of the impedance analyser two questions were addressed :

What is the absolute accuracy under "typical" conditions compared with values measured statically? and

What is the accuracy compared with values which a human observer would measure manually, given the same pressure and flow waveforms?

This latter question is of particular importance for assessing the sampling techniques, since the techniques measure "dynamic" values which are usually different from statically determined values [181]. These errors arise from inertial effects [144] (dependent on volume acceleration at sample time) and unequal lung time constants [181]. These errors are dependent on ventilator timing and settings. Also, since flow resistance of the expiratory tubing and valves is likely to be non-linear (owing to turbulence), this introduces an additional source of error in the sampling technique for resistance which is measured at peak expiratory flow under conditions of high flow rate with the expiratory valve just opening.

Two basic simulations were used :

- (a) A ventilator and mechanical lung-airways simulator.
- (b) An electronic simulator to test the inherent accuracy of the impedance analyser without the errors contributed by the mechanical simulator or flow and pressure transducers.

The simulator (b) was built into the analyser and can be switched on to test correct operation of the analyser at any time. (See appendix G, fig.G.4) The electronic simulator has the advantage that it can test the analyser without inertial effects or non-linearities.

In both sets of tests pressure and flow waveforms were recorded on an S.E. Labs. U.V. recorder and analysed manually for comparison with the instrument-determined values.

The accuracy of the inspiratory/expiratory detector circuit was evaluated using a wide range of ventilator settings and comparing the detection points with manually-determined points.

9.1.1 Lung and Airways Simulator

Simulator A

A mechanical lung simulator was built using a 2.55 litre glass bottle filled with steel wool to ensure isothermal conditions. Hill has described theoretical and practical aspects of such simulators [62][182]. Under isothermal conditions at sea level (press. = 10344 cmH₂O) for a small increment of pressure (as in ventilation) the compliance is calculated [182] :

$$\begin{aligned} \text{compliance} &= 2550/1034 \text{ ml/cmH}_2\text{O} \\ &= 2.47 \text{ ml/cmH}_2\text{O} \end{aligned}$$

The compliance was also tested statically by injecting 50 ml of air from a syringe into the "lung" and measuring the corresponding pressure change (using the Statham pressure transducer described in chapter 8):

$$\begin{aligned} \text{measured compliance} &= 50/20.1 \text{ ml/cmH}_2\text{O} \\ &= 2.49 \text{ ml/cmH}_2\text{O} \end{aligned}$$

The construction of linear flow resistances that are linear within 20 percent over a wide range of flow

rates has been described [183]but these are relatively complex. A simpler, although more non-linear, flow resistance consisting of 0.95 m. of 3 mm i.d. bubble tubing was used. The variation of resistance with flow rate (including the thermistor flow sensor) was measured by passing air through the resistance and flowmeter at different flow rates and measuring the pressure developed across the assembly. Figure I.1 shows the variation of resistance with flow rate. Using the thermistor spirometer for calibrating the flow resistance in this manner means that the flowmeter error cancels out when it is used with the impedance analyser. This makes the overall system seem more accurate than it really is. Accuracy could be worse than assessed below by as much as the maximum error of the flowmeter. (See chapter 7.)

In calibrating the flow resistance the final conditions of use were approximated as nearly as possible, i.e. pressure tapping point and input and output conditions. (See figure I.1) Workers have stressed the importance of these precautions, if anomalous results are to be avoided. [184,pp 84-85][185]

Simulator B.

A calibrated "super syringe" (Hamilton Co., Reno, Nevada) was used to provide an adjustable low compliance. This compliance has characteristics which are not precisely known since compression may vary from isothermal to adiabatic depending on ventilation rate. However, using Hill's results [184, p 250] at realistic ventilation rates (> 10 BPM) compression is probably close to adiabatic, so compliance will be 71 percent of the value under isothermal conditions [184].

Syringe Volume	1500	750	350	ml
Approx.C	1.03	0.51	0.24	ml/cm H ₂ O

If anything, these values will underestimate compliance slightly, owing to heat exchange with the walls of the syringe.

Simulator C

The Blease "Pulmo-Sim", which provides adjustable resistance and compliance, was also used in tests. The Pulmo-Sim has higher values of compliance (nominal 12 ml/cmH₂O minimum, measured 9.2 ml/cmH₂O). Unfortunately, the weighted bellows and counterweight used to construct the variable compliance adds substantial inertia to the "lung". This can give large errors in measuring resistance and compliance using sampling. The flow resistance on the Pulmo-Sim is calibrated at only one high value of flow rate (30 LPM) and is non-linear.

Both these lower accuracy simulators (B and C) proved useful in assessing the operation of the inspiratory/expiratory detector circuit and the overall impedance analyser in a more qualitative fashion.

Simulator D

Electrical simulator accuracy is determined largely by the accuracy of the capacitance and resistance and by op-amp offsets. The capacitance was measured using a Radiometer RLC meter (accuracy $\pm 2\%$) and found to be 0.81 μ F. The simulator resistances were within 1 percent of design values measured on a Fluke 8022A (3½ digit) multimeter :

calculated compliance	20.0 ml/cm H ₂ O
calculated resistance	40.5 cm H ₂ O/L/sec

Op-amp offsets (< 10 mV) should contribute < 3 percent error for the more critical low level simulation, since signal levels are ≥ 0.3 V.

9.1.2 Mechanical Simulation

Method: A Bird mk 10 ventilator with infant Q circuit was attached to the mechanical lung simulator (A, B or C). An S.E.Labs.model 1203 U.V. oscillographic recorder, with associated galvo' driver amplifiers (S.E.Labs."Emma"), was used for recording waveforms from the impedance analyser. A $3\frac{1}{2}$ digit (Fluke 8020A) digital voltmeter was used to measure voltages from the analyser. A precision voltage reference source (modified $5\frac{1}{2}$ digit Fluke differential voltmeter) with switchable output was used to calibrate the U.V. recordings after each test. Scaled outputs from the impedance analyser showing the instantaneous flow rate, pressure and inspiratory/expiratory detector waveforms were recorded. In some cases the instantaneous power waveforms were also recorded. U.V. recordings were retouched with a fine draughting pen to improve reproduction by photostating and to show sampling points. Meter readings of the impedance analyser were recorded and compared with the values obtained by manually analysing the recorded waveforms. In each case the sampling points were assessed manually, ignoring the automatically detected points. In a few cases internal analyser voltages were measured to allow comparison with values determined manually.

9.1.3 Electrical Simulation

Internally generated simulator (D) waveforms were recorded and analysed in the same manner as the mechanical simulation above. The simulator was also modified to increase the amplitude of the waveforms produced (by reducing the value of the collector load resistor connected to the positive supply in the simulator).

9.1.4 Calculations

Figure I.3 shows how the resistance and compliance were calculated manually using the sampling technique. Tidal volume was determined by dividing the expiratory flow-signal waveform into narrow strips and determining the area. The time-constant of the system was calculated in each case by taking the product of resistance and compliance. In the case of resistance determined by power measurement (R') no time-constant was calculated. However, a new value of compliance - C' - was calculated by dividing the value of the time-constant determined by sampling by R' . The time-constant (determined by sampling) should be less sensitive than R and C to sampling-point errors, thus, recalculating compliance in this way using R' , which is also not sensitive to precise inspiratory/expiratory detection, should give a better estimate of static compliance.

The "static" values of flow resistance were obtained from the graph (figure I.1) at peak expiratory flow rate corresponding to the point at which the impedance analyser measures it in sampling. An estimated value for R' was obtained by splitting the flowrate waveform into a number of equal time-periods during which the flow rate was greater than 50 percent of the peak value. R for each time-period was obtained from figure I.1, and the mean value for the selected number of time intervals determined. (The 50 percent level was chosen as power is proportional to \dot{V}^2 , so resistance measured by this technique will tend to be the value measured at high flow rates.)

Values recorded from the impedance analyser were as displayed on the meters (i.e. including meter error), except where the values were over scale on the meters in which case a digital volt-meter was used.

Absolute accuracy of manual determinations was estimated at better than 5 percent for most single values obtained from a tracing. Most calculations involve two values giving a potential worst case error of about 10 percent.

9.2 Results

A representative sample of recordings is shown in figures I.3 through I.8. These recordings were chosen to illustrate problems related to the different techniques. The processed results from these recordings and the impedance analyser are shown in figure 9.1. Values can be compared along any one line of the table to compare the different techniques. Figure 9.2 compares the analyser's internally-measured intermediate quantities (used to calculate R and C), with the same values determined manually for two recordings. The recordings were chosen for their good quality to enhance manual accuracy.

9.3 Discussion

9.3.1 Sampling Point

"Dynamic" values of R and C are critically dependent on accurate detection of end inspiratory point. Figure I.5 illustrates the performance of the inspiratory/expiratory detector in the presence of a highly variable waveform produced by continuously adjusting the ventilator to produce very large increases in tidal volume followed by a decrease in tidal volume. In the face of the wide and rapid variations of waveform,

Simulator	Quantity	Units	STATIC		"DYNAMIC"		from POWER		Estimate	COMMENTS
			Calc.	Meas.	Manual	Analyser	R ^c	C ^a =RC/R ^c		
A (bottle + tube)	R	cmH ₂ O/L/sec.	-	175	122	132	155	-	148	C ^a and est. R ^c . See text.
	C	ml/cmH ₂ O	2.47	2.49	3.71	3.20	-	2.72	-	(See fig. I.8)
	RC	seconds	-	0.436	0.453	0.422	-	-	-	Note valve bounce.
D (elect.)	R	cmH ₂ O/L/sec.	40.5	-	37.2	37	38	-	40.5	(See Fig. I.4)
	C	ml/cmH ₂ O	20.0	-	24.3	23	-	22.4	-	Slight "gas" trapping.
	RC	seconds	0.81	-	0.904	0.851	-	-	-	(See fig. I.3)
D (elect.)	R	cmH ₂ O/L/sec.	40.5	-	42.9	36.5	38	-	40.5	Manual analysis difficult
	C	ml/cmH ₂ O	20.0	-	20.3	21.8	-	20.9	-	Values for R, C from
	RC	seconds	0.81	-	0.871	0.795	-	-	-	d.v.m. not meters.
B (syringe)	C	ml/cmH ₂ O	1.03	-	-	1.5	-	-	-	R not recorded - highly
	C	ml/cmH ₂ O	0.51	-	-	0.75	-	-	-	non-linear resistance
	C	ml/cmH ₂ O	0.24	-	-	0.35	-	-	-	of syringe connector.
C (*Pulmo-sim* + tube)	R	cmH ₂ O/L/sec.	-	178	176	179	152	-	158	(See fig. I.6)
	C	ml/cmH ₂ O	-	9.2	3.82	4.0	-	4.71	-	Differences static vs dynamic
	RC	seconds	-	1.64	0.672	0.716	-	-	-	due to inertia of bellows.
C (*Pulmo-sim*)	R	cmH ₂ O/L/sec.	-	6.5	49	32	13	-	11.5	(See fig. I.7)
	C	ml/cmH ₂ O	-	9.2	5	6	-	14.7	-	Valve bounce
	RC	seconds	-	0.06	0.245	0.192	-	-	-	R = Probe R

Fig. 9.1 Accuracy of Impedance Analyser and Comparison of Different Analysis Techniques.

shape and amplitude, the detector point is only inaccurate (late) at A, correcting itself one "breath" later at B. Generally the accuracy of the detector is dependent on the variability of the slope of the signals near the end of inspiration. In the case of the Bird ventilator valve bounce usually occurs at the end of inspiration; often providing two end inspiratory points for the detector to choose from. (See point A on figure I.8) It normally chooses the first point, since it detects in real time, and looks for the first point of near zero flow. However, because of the feature extraction technique used, under certain conditions it may choose the second point. In some cases, although valve bounce occurs, expiratory flow is already established at the second point (e.g. figure I.6 point B). Gross valve bounce does not appear to occur with ventilators with well controlled characteristics such as the Dräger Narkose Spiromat. (See figure 7.4.) The valve bounce may sometimes increase accuracy if it approximates an end inspiratory pause!

The sample width may also contribute a small error by effectively delaying the sample time slightly. (See figure I.6.) Valve bounce may sometimes add other distortions to the inspiratory and/or expiratory waveform. (See figure I.7 at A, B, and the distorted leading edge of the expiratory waveform.)

The electrical simulation is a very stringent test for the detector, since the expiratory "valve" (switch) causes the waveforms to change extremely rapidly. (See figures I.4, I.3) A delay of only 10 ms (shown to illustrate at B, figure I.3) will cause an error of -20 percent in sampled pressure. This explains why, in this case (see figure 9.1), the analyser-determined values for R and C are about 10 percent low and high, respectively. (Sample/averaging period = 10 ms. therefore average value (figure I.3) is value at 5 ms delay, i.e. approximately -10 percent.) This tends to be confirmed by the fact that the product RC is in error only by about 6 percent and one percent for the two tests.

The manually-determined values for these two tests are less accurate.

In the original version of the detector circuitry sample width was taken into account by making the sample occur just prior to the zero-flow inspiration point. This original detector had a slightly higher rate of false detection points and was modified to the present design with a consequent slightly delayed sampling point. (Subsequent to this testing sample width has been reduced to 3 ms to improve accuracy.)

The detector worked reliably with a wide variety of waveforms (compare figures I.3 to I.8) but could be caused to operate unreliably with some ventilator settings. Mains-borne noise spikes occasionally proved a problem. (See figure I.7 point Z.) At very high respiratory rates the detector was generally less reliable.

9.3.2 Accuracy

Pressure measurement accuracy is probably within 3 percent for these tests, since zero drift is eliminated in calculation. The flowmeter has an accuracy of better than 5 percent under the conditions of test. These transducers were used for calibrating the simulators. This will tend to enhance the apparent absolute accuracy of the overall system (analyser and transducers), because errors will tend to cancel. Thus absolute accuracy of the overall system could be worse by approximately 7 percent than is apparent in these tests. However, because simulator compliance was calculated theoretically these values give an independent assessment of system accuracy. The results of simulator C are of no use in comparing static with dynamic values, because the weighted bellows has a large inertia which markedly reduces dynamic compliance. It was noticed, when using a syringe for static tests that the simulator took a long time to stabilise after rapid volume injection.

To emulate actual conditions of use the analogue meter displays of the analyser were read to record results. This decreases accuracy slightly, even though the units are good quality class 1.5 units (i.e. + 1.5% F.S.D.), owing to reading error.

Manually-determined dynamic values of R, C generally agreed with analyser-determined values within the 10 percent estimated manual accuracy (figure 9.1). Where internal analyser voltages were measured (figure 9.2), the agreement was usually within 5 percent. Analyser-determined values were generally closer to static values than the manually-determined values. This is probably due to the slightly later sampling of the analyser, which usually occurred at the start of the valve-bounce period. Normally this slightly later sampling would decrease accuracy where no end inspiratory hold (pause) is used, but, because of valve bounce, this tends to provide a hold. From the flow-rate tracing it can be seen that the volume acceleration (slope of the flow rate curve) is large at the end of inspiration when the expiratory valve opens. This may give rise to substantial systematic errors, since it has been suggested [144] for spontaneously breathing adult patients inertial effects start to give errors between 30 and 60 B.P.M. when determining dynamic compliance. These errors occurred in patients breathing to produce approximately sinusoidal waveforms. In controlled ventilation the transients at valve opening are likely to give rise to much larger accelerations, and hence larger errors, even at very low breathing rates.

With the exception of simulator C (see comment above), these measurements showed that the dynamic compliance was consistently higher (typ. 30 percent) and the resistance consistently lower (typ. 30 percent) than static values, with the product (time constant) approximately correct (within 10 percent of static value). This is consistent with too low a value of end expiratory pause pressure. A part of this error is due

		ΔP_1	\hat{V}	$R = \frac{\Delta P_1}{\hat{V}}$	ΔP	V_T	$C = \frac{V_T}{\Delta P}$
Sim. D (fig. I.4)	Manual	5.81	0.156	37.2	7.74	188	24.3
	Analyser	5.98	0.158	37.8	7.74	181	23.4
Sim. C (fig. I.6)	Manual	19.4	0.110	176	22.3	85.4	3.82
	Analyser	20	0.110	182	21	84.8	4.03

Fig. 9.2 Accuracy of internal sampled values of analyser compared with manually determined values. (R and C calculated manually from adjacent values in all cases.) (Units deleted for clarity.)

to neglecting inertial effects. Since performing these tests the sampling width has been decreased to 3 ms to eliminate this source of error. Mismatching in phase response of the pressure and flow transducers could also give a similar error. This seems unlikely since the transducers have a flat amplitude response to 20 Hz. Respiratory time constant calculated from dynamic values of R and C was generally far more consistent and accurate (within 10 percent) than individual values for R and C. Resistance R' calculated from power measurements was similarly more consistent and closer to static values (typically within 5 percent). Combining these results also produced a more accurate estimate C' for compliance. In the face of a highly non-linear resistance and an unusual flow waveform, C' could conceivably be a worse estimate.

Figure I.6 illustrates that too short an expiratory time causes "gas trapping". Expiratory flow has not yet ceased (at point A) when the ventilator starts to increase pressure for inspiration. Under these conditions minimum mouth pressure at the end of expiration is not the same as the still elevated alveolar pressure. This gas trapping causes an apparent decrease in compliance due to overestimating ΔP for a given tidal volume. This is consistent with the higher value of compliance measured in figure I.7 where no gas trapping occurs, although both these simulations are imprecise owing to simulator construction. Gas trapping should not normally cause errors, since expiratory time is usually chosen to avoid it, as it might lead to a hazardous rise in alveolar pressure. (See Keuskamp in [4])

The results from simulator B (figure 9.1) show that the analyser, although overestimating the compliance, works qualitatively correctly at very low levels of compliance in detecting changes. This is important since there are a number of diseases (e.g. hyaline membrane disease) in which the compliance is reduced to very low levels $< 1 \text{ ml/cmH}_2\text{O}$ making ventilation difficult.

9.3.3 Clinical Evaluation

The impedance analyser was used on a variety of infants undergoing surgery for congenital heart defects. In using the analyser a medical four-channel digital memory scope proved essential for checking correct inspiration/expiration detection and viewing waveforms. No accurate recordings were made as the available multi-channel recording equipment was electrically hazardous for theatre use. However, figure 7.4 does show a recording made in theatre using a heated stylus pen recorder normally used for E.C.G. records.

During anaesthesia, when nitrous oxide is used, the flowmeter underestimates flow (see section 4.8) giving rise to an error in impedance analyser output. In more recent usage the flowmeter was modified (see section 4.8) to eliminate this error. The correction technique employed requires a knowledge of the nitrous oxide concentration, which is then dialed into the flowmeter. In certain anaesthetic applications (e.g. with a circle-absorber circuit), there might still be some error because the nitrous oxide concentration may not be accurately known. This additional error is unlikely to be more than 5 percent, except at very low flow rates. (See figure 4.11.)

The inspiratory/expiratory detector worked erratically under certain clinical conditions. Problems with the detector related to :

- (a) diathermy-induced noise;
- (b) occasional mains transients;
- (c) water P.E.E.P.;
- (d) water condensation accumulating in ventilator tubing;
- (e) highly variable waveforms during assisted ventilation, especially when the patient and machine were out of phase.

Of these only (c) and (d) are significant.

Surgical diathermy is of short-lived duration. Mains transients will cause only a brief shift in reading. Gas bubbling through a P.E.E.P. bottle sometimes caused such fluctuations in flow that the detector became totally unreliable. This was a particular problem with Bird ventilators, which seem to produce a far more variable waveform, with valve bounce and mechanical oscillations. The Dräger "Narkosa Spiromat 650" ventilator produced far smaller fluctuations when used with a P.E.E.P. bottle, probably owing to the larger compressible volume of the ventilator and circuit which would tend to filter these transients. With the use of water P.E.E.P. substantial inertial effects may be present since, on expiration, the mass of water in the immersed tube section of the bottle must be accelerated and forced out of the tube by the expiratory gas. It is thus not surprising that this produces rapid fluctuations and oscillations.

Water-filled P.E.E.P. bottles are widely used to provide C.P.A.P. This is a serious limitation of the analyser, if it will not operate reliably with different ventilators when providing C.P.A.P. It is true that the P.E.E.P. bottle can be briefly adjusted to zero for a measurement but this means continuous monitoring is not possible and P.E.E.P.-compliance curves cannot be plotted. Some newer infant ventilators [31] have P.E.E.P. controls that do not rely on water and hence do not produce flow fluctuations but it is unlikely that these ventilators will come into widespread use for quite some time. When sufficiently large condensations had accumulated in the ventilator tubing, this could momentarily interrupt flow and produce rapid fluctuations. This should not normally occur, as it is one of the anaesthetist's tasks to keep the tubing clear of water. Erratic operation of the analyser could even alert him to clear condensation.

Qualitatively the analyser often showed a slow reduction in compliance during the course of the operation. The compliance then usually increased markedly after the anaesthetist had hyperinflated the lungs, especially when the patient had been on bypass. This is consistent with a gradual increase in atelectasis which is reversed by hyperinflation increasing functional residual capacity and compliance. During surgical manipulations large reductions in compliance were often noted simultaneously with marked reductions in minute volume. Reductions of over 50 percent were not uncommon in these circumstances. In a number of cases the resistance exceeded the range of the display (160 cm H₂O/L/sec.). Internally the analyser is limited to 240 cm H₂O/L/sec. absolute maximum. It appears that a high range switch to cover values of resistance to above 500 cm H₂O/L/sec. is probably necessary. Keuskamp has claimed that very high values of over 500 H₂O/L/sec. are encountered in small patients with narrow endotracheal tubes and infant fittings [4]. R' was generally more constant than dynamically-measured resistance, especially with variable flow waveforms and where cardiac fluctuations on the flow waveform were large.

The measurement accuracy of the work cost of ventilation was not assessed quantitatively. This parameter is derived from parameters used to measure respiratory impedance (i.e. tidal volume and mean power, neither of which is critically dependent on inspiratory/expiratory detection point). Qualitatively, as expected, it increased rapidly with increased flow rate and increased with increases in resistance.

Monitoring "dynamic" compliance and resistance during controlled ventilation poses a number of technical problems which are dependent on the ventilator's characteristics and the ventilator circuit. Problems are related to the use of water P.E.E.P. bottles and the characteristics of the expiratory valves. Valve opening and closing produces large volume accelerations which, it is suggested, may lead to substantial errors in calculating dynamic values, as respiratory inertance can then not be ignored, even at low breathing rates. Respiratory time constant calculated from the product of the dynamic resistance and compliance, however, is far more accurate as errors in measuring dynamic values are opposite in sign and tend to cancel in the product. The new technique of calculating resistance based on mean-power measurement produces a more accurate estimate for resistance and is not critically dependent on accurate inspiratory/expiratory detection. Using this value of resistance to recalculate compliance from dynamically measured respiratory time constant also yields a more reliable estimate of compliance. Water-filled P.E.E.P. bottles add inertance to the expiratory circuit making reliable measurements of dynamic compliance and resistance difficult. Very high values of resistance, partly contributed by the endotracheal tubes, are not uncommon in intubated infants. Further development is needed to improve the inspiratory/expiratory detector circuitry for the very wide range of flow and pressure waveforms produced by the many possible combinations of ventilators, ventilator circuits, patients and ventilator settings. An alternative would be to rely on a simple detection technique and then measure C' and R' . The difficulty in detecting the correct end inspiratory sampling point arises partly from the non-direction sensing characteristic of the hot-thermistor flowmeter. Much more clinical experience is required to assess the place of clinical monitoring of this sort in anaesthesia and the intensive care unit.

Appendix ACalculating Peak Expiratory Flow Rate (\dot{V}_{exp})
and Gas Trapping in Controlled Ventilation

In this section it is shown that for controlled ventilation, when expiration is passive, the peak expiratory flow rate can be calculated from two parameters : the total respiratory system time constant (RC), and the tidal volume (V_T). Where significant gas trapping occurs, so that the alveolar pressure does not drop to near zero at the end of expiration, the expiratory time must also be included in the calculations.

In neonates expiration is active rather than passive, even during sleep [14]. This influences expiratory flow rates. However, patients are usually curarized during major surgery, and sometimes during controlled ventilation in the intensive care unit [4]. Under these conditions and in older patients, expiration is passive as assumed here. In calculating the peak flow rate the respiratory time constant must include the added resistance of the expiratory limb of the ventilator circuit and endotracheal tube, which act to reduce the peak flow rate.

At the end of inspiration, as the ventilator's expiratory valve opens, the pressure (P_{pause}) across the compliance of the patient is applied to the total expiratory resistance. Neglecting inertial effects of expiratory valve and gas :

$$\text{Pressure } P(t) = P_{\text{pause}} e^{-(t/RC)} \quad \dots \quad \dots \text{ A.1}$$

$$\text{Flowrate } V(t) = \left(\frac{P_{\text{pause}}}{R}\right) e^{-(t/RC)} = \hat{V}_{\text{exp}} e^{-(t/RC)} \dots \text{A.2} \quad 168.$$

Taking end inspiration time as $t = 0$
and end expiration time as $t = t_1$,

$$\begin{aligned} V_T &= \int_0^{t_1} \hat{V}_{\text{exp}} e^{-(t/RC)} dt \\ &= RC \hat{V}_{\text{exp}} (1 - e^{-(t_1/RC)}) \end{aligned}$$

$$\text{Therefore, } \hat{V}_{\text{exp}} = \frac{V_T}{RC(1 - e^{-(t_1/RC)})} \dots \text{A.3}$$

For expiratory time much greater than respiratory time constant (i.e. $t_1 \gg RC$),
this reduces to :

$$\hat{V}_{\text{exp}} = \frac{V_T}{RC} \dots \dots \text{A.4}$$

For expiratory times less than about 3 respiratory time constants, significant gas trapping occurs, increasing the peak expiratory flowrate, requiring the use of the full equation A.3

We can calculate the end expiratory alveolar pressure ($P_{A(\text{end exp})}$) during gas trapping from equation A.1 :

$$P_{A(\text{end exp})} = P_{\text{pause}} e^{-(t_1/RC)} \dots \dots \text{A.5}$$

A more practical form, from a conceptual point of view, involves normalising this in terms of end inspiratory pressure (P_{pause}). We define a new quantity :

$$\% \text{ trapping} = \frac{P_{A \text{ end exp}}}{P_{\text{pause}}} \times 100$$

Thus, from A.5

$$\% \text{ trapping} = e^{-(t/RC)} \times 100 \dots \dots \text{A.6}$$

Percentage trapping indicates what proportion of the end inspiratory pressure is due to trapped gas. Alternatively, it can be thought of as indicating the percentage of the volume distending the lungs at end inspiration which is "still trapped" at the end of expiration; this is shown by rewriting equation A.6 using the definition of compliance :

$$\% \text{ trapping} = \frac{\text{Vol.trapped}}{(\text{Vol.trapped} + V_T)} \times 100 \dots \text{ A.7}$$

The following table illustrates how the relative magnitude of expiratory time and respiratory time constant influence gas trapping and expiratory flow rate:

(exp.time/RC)	0.5	1	2	3
Increase in \hat{V}_{exp} over value without gas trapping	x 2.54	x 1.58	x 1.15	x 1.05
% trapping	60	37	13.5	4.9

A short program was written in BASIC for a SHARP PC 1211 pocket calculator which estimates peak expiratory flow rate based on equation A3 . It also calculates a number of other ventilator parameters. The user inputs clinical data : inspiratory/expiratory ratio, tidal volume, respiratory time constant, estimated deadspace and respiratory rate. It calculates mean inspiratory flow rate, peak expiratory flowrate, percentage trapping, minute ventilation, expiratory time, inspiratory time and alveolar ventilation. The program proved useful clinically and is listed overleaf.

```

100 "Z" : INPUT "TIDAL VOL ? ML" ; L
        V = L/1000
110     INPUT "I/E ? " ; X
120     INPUT "RC ? SEC " ; Z
125     INPUT "BPM ? " ; Q
127     T = 60/(Q + Q*X)
128     S = 100*2.7183 ^ (-T/Z)
        : PRINT USING "###.#"
        ; "TRAPPING " ; S ; "% "
130     A = V 60/(Z*(1 - 2.7183 ^ -(T*60/Q)))
        : PRINT USING "###.##"
        ; "PK EXP " ; A ; "L/MIN"
135     G = 60*V/(X T)
        : PRINT "MEAN INSP" ; G ; "L/MIN"
140     D = V*Q
        : PRINT "MIN VOL " ; D ; "L/MIN"
160     PRINT "EXP TIME " ; T ; "SEC "
170     J = X*T
        : PRINT "INSP TIME " ; J ; "SEC"
180 "X" : INPUT "DEAD SPACE ML ? " ; M
190     H = (L - M)*Q/1000
        : PRINT "ALV VENT " ; H ; "L/MIN"
200     BEEP 1 : GO TO 100

```

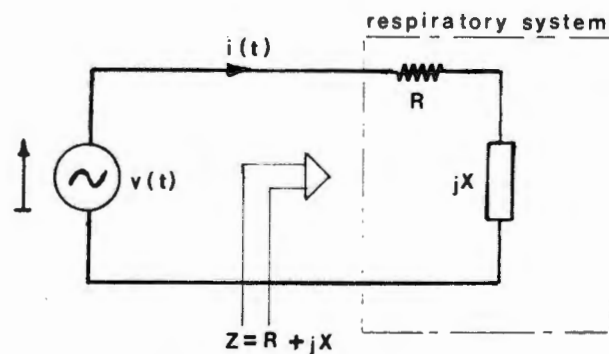
Program example :

Calculator Display	User Input	Comment
	SHIFT Z	Start
TIDAL VOL ? ML	20 ENTER	} data input
I/E ?	0.5 ENTER	
RC ? SECS	0.6 ENTER	
BPM ?	20 ENTER	
TRAPPING	3 %	} results
PK EXP	2.00 L/MIN ENTER	
MEAN INSP	1.20 L/MIN ENTER	
MIN VOL	0.40 L/MIN ENTER	
TIDAL VOL	20.00 ML ENTER	
EXP TIME	2.00 SEC ENTER	
INSP TIME	1.00 SEC ENTER	
DEADSPACE ML ?	10 ENTER	} data input
ALV VENT	0.20 L/MIN ENTER	} result
TIDAL VOL ?		} return for new data

Appendix B : A New Technique for Use with the
Method of Forced Oscillations : Measuring Resistance
and Reactance from Power Measurements

A simple technique for the rapid measurement of active and reactive power is described and applied to determining the driving point impedance of the respiratory system.

Conventional techniques for measuring the driving point impedance involve the use of trigonometric functions. The technique described here is simple to implement in an analogue or digital form, since it does not require the evaluation of trigonometric functions. The reader is referred to references [6][7] where I have discussed a variety of possible implementations of this technique and some related techniques.



Z - complex impedance ($= R + jX$)

R - resistance (real part of Z)

X - reactance (imaginary part of Z)

$i(t)$ - instantaneous current

$v(t)$ - instantaneous voltage

$p(t)$ - instantaneous power ($= i(t) \cdot v(t)$)

I_{RMS} - root mean square value of $i(t)$ ($= \sqrt{(i(t))^2}$)

$$\text{voltage } v(t) = V_p \sin \omega t \quad (V_p - \text{peak voltage})$$

$$\text{current } i(t) = I_p \sin (\omega t + \phi) \quad (I_p - \text{peak current})$$

phase angle ϕ

$$\begin{aligned} \text{power } p(t) &= V_p \sin \omega t \cdot I_p \sin (\omega t + \phi) \\ &= \frac{V_p I_p}{2} \cos \phi (1 - \cos 2\omega t) - \frac{V_p I_p}{2} \sin \phi \sin 2\omega t \end{aligned}$$

$$= A(1 - \cos 2\omega t) - B \sin 2\omega t \quad \dots \quad \text{B.1}$$

average active power = A

peak reactive power = B

If we measure $p(t)$ at $\omega t = \frac{\pi}{4}$ and $\omega t = \frac{3\pi}{4}$

or at corresponding multiples of 2π

then

$$p\left(\frac{\pi}{4}\right) = A - B \quad \dots \quad \dots \quad \dots \quad \text{B.2}$$

$$p\left(\frac{3\pi}{4}\right) = A + B \quad \dots \quad \dots \quad \dots \quad \text{B.3}$$

Taking the sum and difference of B.2 and B.3 ,

$$\text{average active power} = I_{\text{RMS}}^2 R = A = \frac{p\left(\frac{3\pi}{4}\right) + p\left(\frac{\pi}{4}\right)}{2} \quad \dots \text{B.4}$$

$$\text{peak reactive power} = I_{\text{RMS}}^2 X = B = \frac{p\left(\frac{3\pi}{4}\right) - p\left(\frac{\pi}{4}\right)}{2} \quad \dots \text{B.5}$$

$$\text{From B.4} \quad R = \frac{p\left(\frac{3\pi}{4\omega}\right) + p\left(\frac{\pi}{4\omega}\right)}{2 I_{\text{RMS}}^2} \quad \dots \quad \dots \quad 173. \quad \text{B.6}$$

$$\text{From B.5} \quad X = \frac{p\left(\frac{3\pi}{4\omega}\right) - p\left(\frac{\pi}{4\omega}\right)}{2 I_{\text{RMS}}^2} \quad \dots \quad \dots \quad \text{B.7}$$

(Note : $I_{\text{RMS}}^2 = \overline{(i(t))^2}$)

Equations B.6 and B.7 show that by making two power measurements and measuring the mean square value of current, we can calculate the resistance and reactance without the direct use of trigonometric functions.

A technique which is fundamentally similar to this work (see also my general discussion of related techniques in [6]), has been used by other workers to measure respiratory resistance. [173]

Correcting Volumes for Temperature and Vapour
Pressure Changes

Volume measurements made under different conditions were corrected for changes in temperature and water vapour content by using the following equations programmed on a programmable pocket calculator :

Water vapour pressure was approximated to within one percent over the temperature range of 20° to 37° C by fitting known saturated vapour pressures [12] to a simple power law (rather than using the more complex Antoine -equation which would require more calculations):

$$P_{H_2O} = \left(\frac{A}{100}\right) 5.54 (1.0598)^T$$

where

T is the gas temperature expressed in degrees Celsius,
 P_{H_2O} is the vapour pressure in mm Hg , and
 A is the percentage saturation.

Volumes were then calculated assuming "ideal" gas behaviour at sea level :

$$V_1 = \frac{V_2 T_1 (760 - (P_{H_2O})_2)}{T_2 (760 - (P_{H_2O})_1)}$$

where

subscripts refer to the two conditions of measurement,
 V = volume,
 T = temperature in degrees Kelvin, and
 P_{H_2O} = water vapour pressure in mm Hg.

Appendix D : Multipliers and Linearisation

For high accuracy multiplication (accuracy $\leq 0.2\%$ FS, linearity 0.05% FS), two basic circuit configurations are now most commonly used. Both techniques use logarithmic and antilogarithmic amplifiers constructed using four well-matched monolithic transistors on a single substrate to eliminate temperature dependence. The theory of these multipliers is now included in standard texts [186]. The multipliers used in this work are slightly modified versions of one of these standard log-antilog circuits. In the case of one of the multipliers "feedback" was applied around the multiplier substantially modifying its transfer function. This section develops the theory for this configuration. Figure D.1 shows the manufacturer's circuit diagram for the multiplier used. (Burr Brown model 4206 [187])

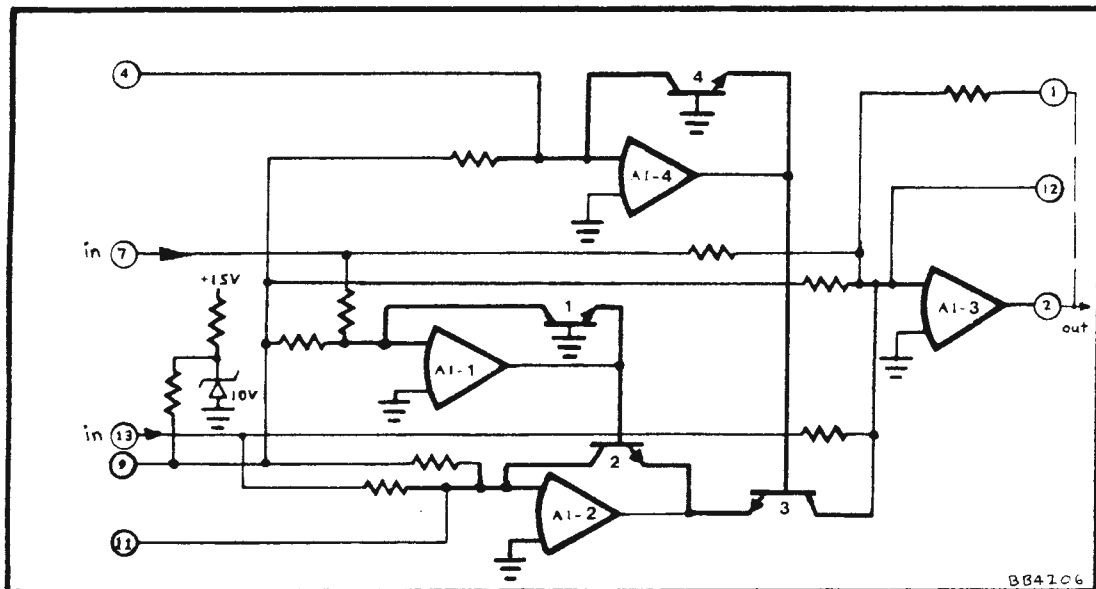


Figure D.1 Manufacturer's simplified diagram of four-quadrant multiplier (Burr Brown model 4206).

This multiplier is not normally used simultaneously for multiplication and division as the biasing required for four-quadrant operation then introduces unwanted additional product terms into the transfer function. In the present application the denominator varies over a limited

range and acts as a correction term to the basic squaring operation. The additional product terms are thus less significant than they would be in other applications.

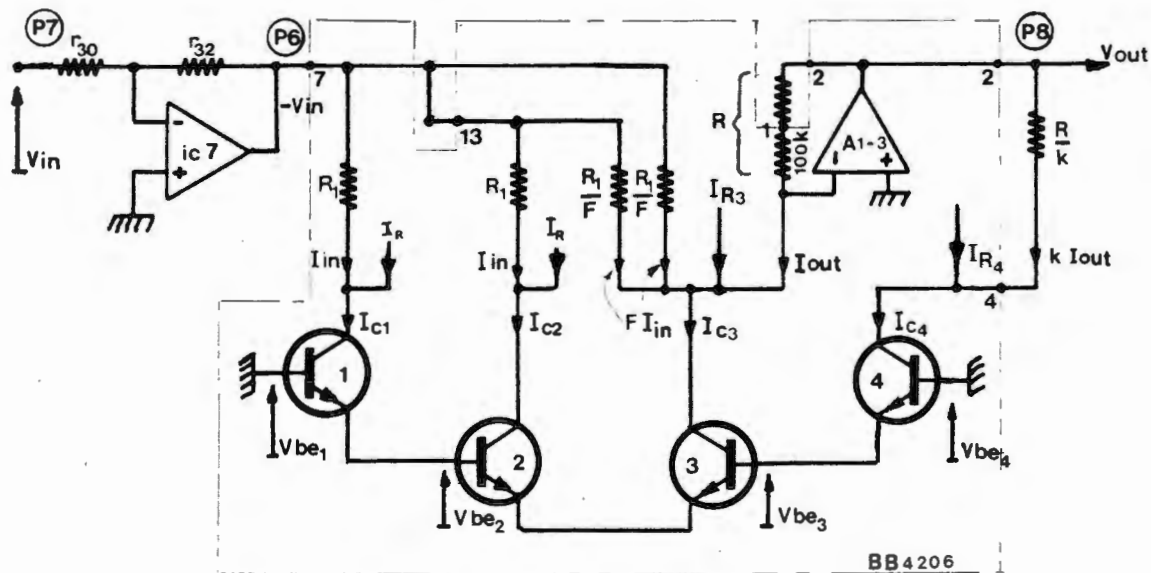


Figure D.2 Simplified diagram of lineariser which uses a modified commercial multiplier. The positive input signal V_{in} is inverted by ic7 to provide a negative input to the "multiplier". Feedback from pin 2 to pin 4 of the multiplier changes both the transfer function and scale factor of the multiplier. (F , I_R , I_{R3} , I_{R4} are constants determined by the multiplier manufacturer. k can be adjusted to adjust linearisation function.)

By using a commercial multiplier we substantially reduce the construction work required but then do not have control over the biasing constant chosen internally.

The following derivation is in terms of current rather than voltage, since this makes the equations slightly less unwieldy than using voltage and resistance values.

We start by deriving the normal multiplier relationship by making use of the logarithmic relationship between base emitter voltage (V_{be}) and collector current (I_c) of a transistor. For $I_c \gg I_s$

$$V_{be} = \frac{KT}{q} \ln \frac{I_c}{I_s} \quad \dots \quad \dots \quad \dots \quad \dots \quad \text{D.1}$$

where q - electronic charge
 K - Boltzman's constant
 T - absolute temperature
 I_s - saturation current of transistors

For figure D.2

$$(V_{be1} + V_{be2}) = (V_{be3} + V_{be4}) \quad \dots \quad \dots \quad \dots \quad D.2$$

If we assume perfectly matched isothermal transistors, substituting equation D.1 into D.2 yields the fundamental relationship :

$$I_1 \cdot I_2 = I_3 \cdot I_4 \quad \dots \quad \dots \quad \dots \quad D.3$$

Substituting the input currents (I_{in}), reference or bias currents (I_R) and output currents (I_o), shown in figure into equation D.3, we have :

$$(I_{in} + I_R)(I_{in} + I_R) = (I_o + I_{R3} + FI_{in} + FI_{in})(I_{R4} + KI_o) \quad \dots \quad D.4$$

where I_{R3} and F are constants chosen by the multiplier manufacturer such that, if our added "feedback" term (KI_o) did not exist, then

$$I_o = \frac{I_{in}^2}{I_{R4}} \quad (\text{The factor } I_{R4} \text{ sets the overall output current scaling factor.})$$

By setting KI_o to zero in equation D.4, we see that this requirement is met if :

$$I_R^2 + I_{in}I_R + I_{in}I_R = (I_{R3} + FI_{in} + FI_{in})I_{R4} \quad \dots \quad \dots \quad D.5$$

that is

$$F = \frac{I_R}{I_{R4}} \quad \text{and} \quad I_{R3} = \frac{I_R^2}{I_{R4}} \quad \dots \quad \dots \quad D.6$$

We expand equation D.4 using equations D.5 and D.6 :

$$I_{in}^2 = I_O I_{R4} + K(I_O + \frac{I_R^2}{I_{R4}} + \frac{2 I_R I_{in}}{I_{R4}}) \quad \dots \quad \dots \quad D.7$$

or

$$I_O = \frac{I_{in}^2}{I_{R4} + K(I_O + \frac{I_R^2}{I_{R4}} + \frac{2 I_R I_{in}}{I_{R4}})} \quad \dots \quad \dots \quad D.8$$

We can rewrite this as :

$$I_O = \frac{I_{in}^2}{C + D I_{in} + E I_O} \quad \dots \quad \dots \quad \dots \quad D.9$$

(where C,D,E are constants)

Notice that this gives the form we are seeking, since the inverting amplifier (ic7) delivers a negative value for I_{in} .

We could rewrite D.9 in terms of voltage :

$$V_{out} = \frac{V_{in}^2}{(C - D V_{in} + E V_{out})} \quad \dots \quad \dots \quad D.10$$

(where C,D,E are new constants)

Equation D.8 shows that we do not have complete control of the constants, since we can vary only K. The other constants are fixed by the multiplier manufacturer. We have slightly more control than equation D.8 shows, since we can also vary the scale factor independently by varying R in figure D.2.

Appendix EPressure Transducer Amplifier

A new, low-cost, high-performance, instrumentation amplifier is described. The amplifier compares favourably with expensive modular designs, and recent monolithic designs. Exceptional features are : extremely low noise $2.8 \text{ nV}/\sqrt{\text{Hz}}$, wide gain bandwidth product $\geq 60 \text{ MHz}$, very high common mode rejection $\geq 140 \text{ dB}$, very low drift $< 1 \mu\text{V}/\text{C}$, low (unadjusted) offset $< 100 \mu\text{V}$, high slew rate $\approx 7.5 \text{ V}/\mu\text{S}$, power supply rejection $\geq 120 \text{ dB}$.

E.1 Statham Instruments Model P 23 db Pressure Transducer

[188]

Sensitivity - $50 \mu\text{V}/\text{V}/\text{cmHg}$

Bridge resistance - 350 Ohm

Excitation voltage = 10 V

i.e. sensitivity $50/13.6 = 3.676 \mu\text{V}/\text{V}/\text{cmH}_2\text{O}$.

Tests at 6 V excitation showed warm-up time to 1 cm H_2O of 10 min. or longer, with a high sensitivity to draughts. Excitation voltage was reduced to 2.117 volts to achieve a warm-up time of less than 2 min., with a lower sensitivity to draughts.

At this voltage

1 cm $\text{H}_2\text{O} = 3.676 \times 2.117 = 7.78 \mu\text{V}$ at bridge output;
therefore

for 0.1 cm $\text{H}_2\text{O}/^\circ\text{C}$ drift,required amplifier drift $< 0.78 \mu\text{V}/^\circ\text{C}$.

Ideally, the noise should also be of this order,
say

 $1 \mu\text{V}$ pK - pK in a 20 Hz bandwidth.Required amplifier output = 10 V at 100 cm H_2O .

Required amplifier gain = $10/(3.676 \times 10^{-6} \times 2.117)$
= 12850 .

Other requirements are modest since the transducer will tend to limit performance.

Therefore, gain, linearity and accuracy - 0.5%

E.2 Instrumentation Amplifier

Conventional three op-amp instrumentation amplifiers [189] are capable of very low drift and excellent linearity [187,190] when (expensive) "instrumentation grade" amplifiers, such as the Precision Monolithics OP07 amplifier [191] are used in their construction. Unfortunately, a number of other factors, especially the AC performance, often limits their accuracy. Common mode rejection, power supply rejection and internal noise can be as serious a limitation as drift [192]. Slew rate and power bandwidth are low in instrument-grade operational amplifiers, resulting in spurious offsets from high frequency noise and transients [193]. Common-mode rejection and power-supply rejection, often limiting factors at D.C., drop rapidly with increasing frequency, so that power-line frequencies can be a particular problem [194]. Chopper amplifiers are also usually limited by internal switching noise and the generation of intermodulation products in the electrically noisy medical environment.

Figure E.1 shows the new instrumentation amplifier with a strain gauge excitation source. The circuit is similar to an old circuit that was previously dismissed as being inaccurate and difficult to use [195]. The use of a modern pair of monolithic "ultra matched" transistors overcomes limitations from transistor matching, while circuit changes overcome other problems. IC2, chosen because its input can operate with common-mode voltages up to the positive supply, senses current through R13, and thus maintains the current through the input pair constant, independent of common-mode input to the transistor pair. This improves C.M.R.R. and common-mode impedance over the old circuit. IC1 provides current feedback to the input pair and maintains the difference between collector voltages close to zero. The inclusion of R8, in parallel with the combination R6 and R5, provides a single resistor gain adjustment - R8. This configuration limits the minimum gain to

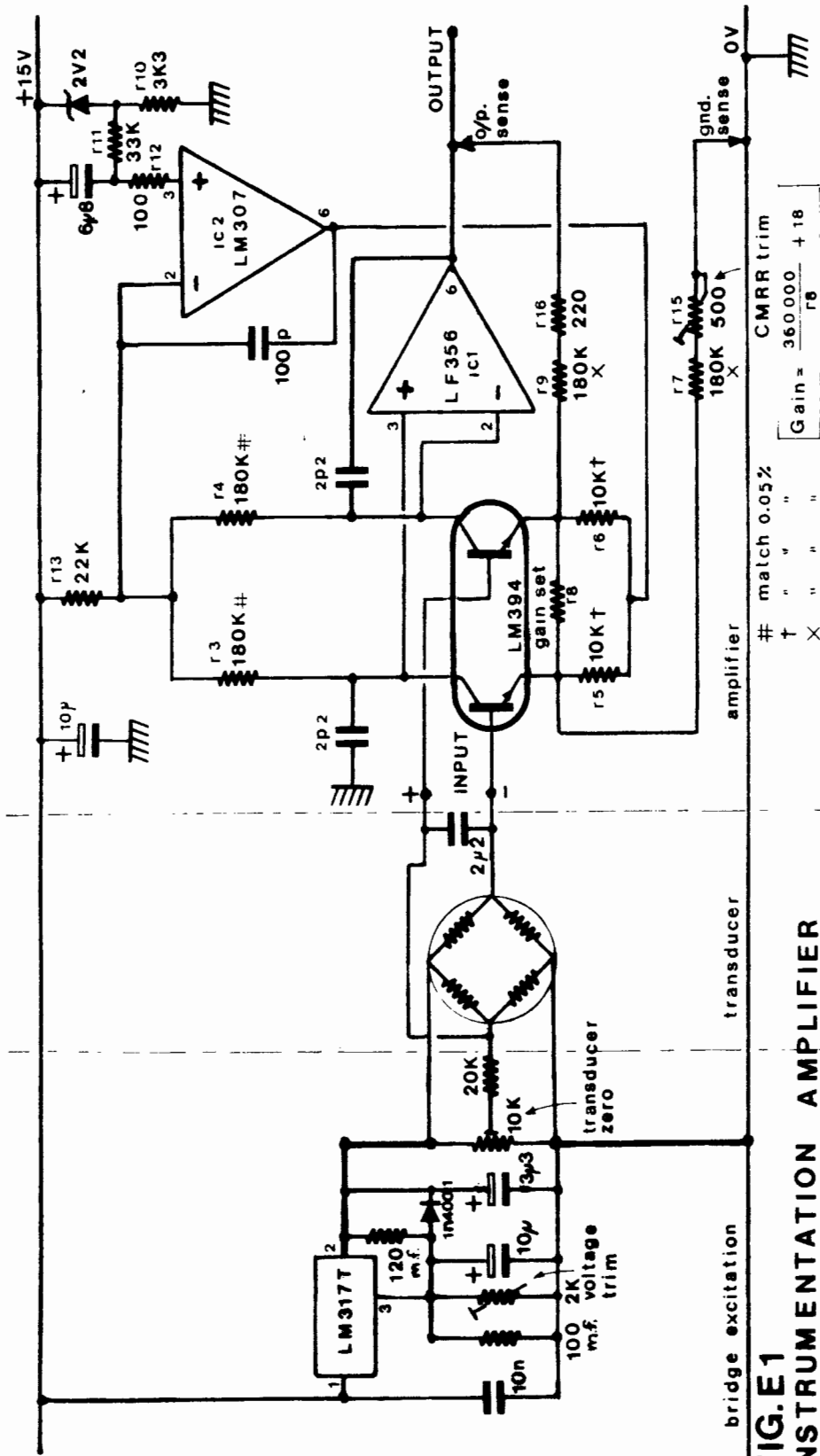


FIG.E1
INSTRUMENTATION AMPLIFIER
FOR PRESSURE TRANSDUCER

greater than one (to 18 for the values shown). Noise introduced by IC2 appears as a common-mode signal, and thus tends to be reduced by the amplifier's good C.M.R.R. For the low source resistance (350Ω) application here, voltage noise predominates. To achieve the lowest possible noise, it is important that the input stage operates without active loads or current sources, which will normally each contribute as much noise as the input transistors. This is the reason why this design offers noise 2.5 times lower than "low noise state of the art" designs such as National Semiconductor's new LM363 [192].

The only disadvantage of this design is slight interaction between correct common-mode rejection adjustment and gain set. This is a problem only if large gain changes are selected by switching R8. If a slightly lower C.M.R.R. (120 dB) is acceptable, the C.M.R.R. trim can be eliminated (delete R15, R16), provided each of the three critical pairs of resistors is matched to 0.05%. The performance of the amplifier depends on close tracking with temperature of each pair of these resistors. High stability metal film resistors with 5 ppm/ $^{\circ}\text{C}$ tracking are thus required to maintain performance. The low frequency noise performance of the amplifier ($\approx 0.8\mu\text{VpKpK}$, BW=20 Hz) can be substantially improved by carefully protecting the input stage leads from any air movement or temperature gradients. The low frequency noise results partly from these minute temperature fluctuations, which generate thermoelectric voltages on the kovar leads of the transistor package. ($10\text{ m}^{\circ}\text{C} = 0.3\mu\text{V}$) [192].

Since the time when this amplifier was first built for this application three years ago, a number of units have been built by other departments at the University of Cape Town, confirming the reproducibility of the design.

Typical performance at gain ≥ 1000 is summarised below. This is a conservative specification, since low cost metal film resistors were used in tests, as well as the loosest specification LM394, both of which contribute to drift.

Typical performance :

Offset voltage (no adjustment)	... $60\mu\text{V}$	R.T.I.
Offset voltage drift	... $0.7\mu\text{V}/^\circ\text{C}$	
C.M.R.R. (untrimmed)	... 120 dB	
C.M.R.R. (d.c., trimmed)	... 145 dB	
C.M.R.R. (1K source unbalance)	140 dB	
C.M.R.R. (1K source unbalance 50 Hz)	130 dB	
Noise (1 - 20 Hz)	... $< 0.8\mu\text{V pK-pK}$	R.T.I.
Noise (1 Hz - 10 Hz)	... $2.8\text{ nV}/\sqrt{\text{Hz}}$	R.T.I.
Warm-up time to of final value	$10\mu\text{V (R.T.I.)}^\dagger < 1\text{ min.}$	
Supply rejection ratio (positive and negative)	... 125 dB	
Slew rate	... $> 7.5\text{ V}/\mu\text{S}$	
Gain non-linearity (D.C.)	... $< 0.1\%$	(Not tested to greater accuracy.)
Gain bandwidth product (gain = 4000)	... 65 M Hz	
Bias current	... 80 nA	
Offset current (ex data not measured)	... 2 nA	

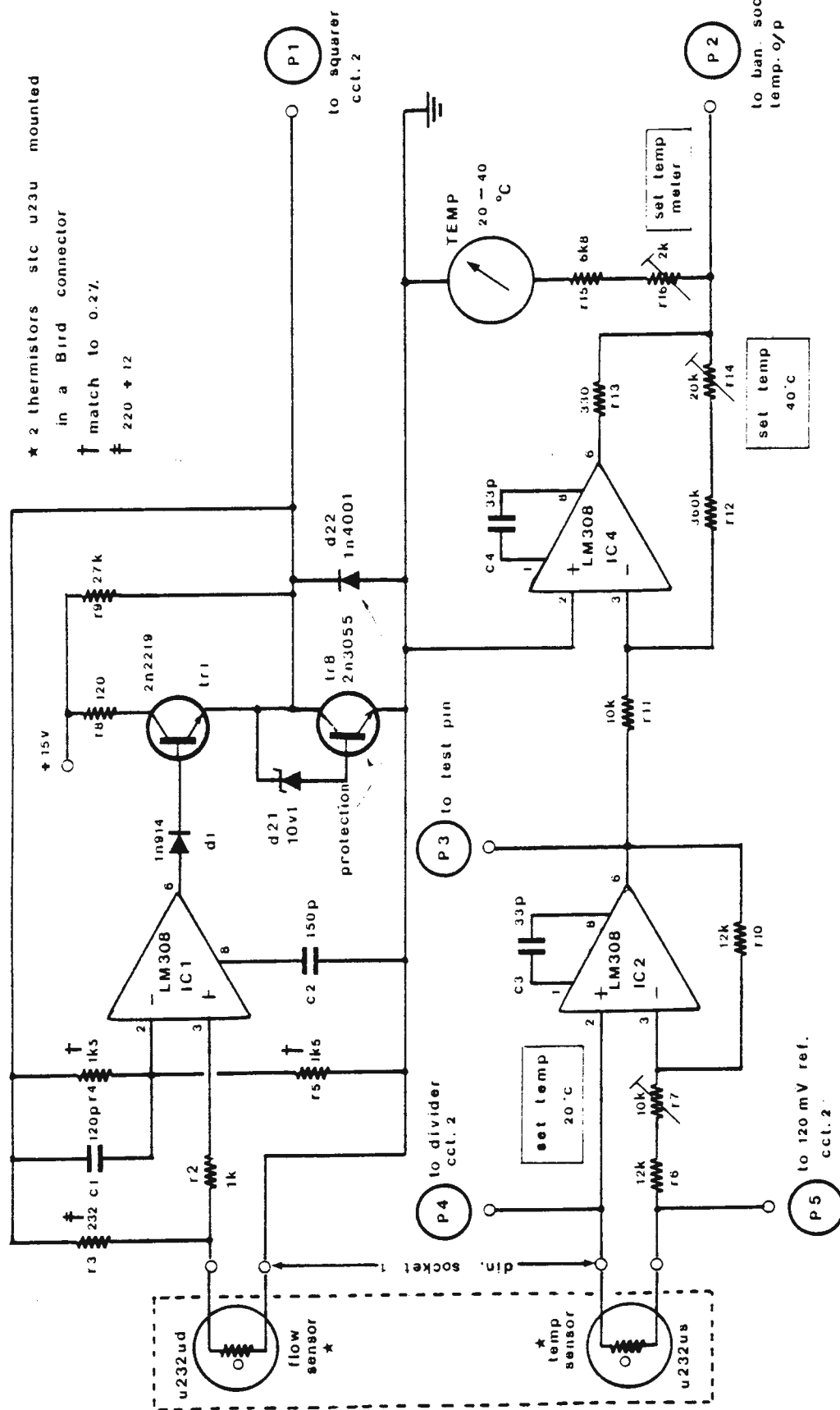
Noise can be reduced still further to about $1.4\text{ nV}/\sqrt{\text{Hz}}$ by increasing the collector currents of the input stage to about 1 mA but this degrades C.M.R.R.

[†] R.T.I. - Referred to input.

Appendix F - Spirometer/Flowmeter Circuits

- Figure F.1 - cct.1 Constant-Temperature Thermistor
Bridge and Temperature Amplifier
- Figure F.2 - cct.2 Squarer and Divider Circuit
(Flow Probe)
- Figure F.3 - cct.3 Multiplier, Averager, Integrator
and Metering Circuit (Flow Probe)
- Figure F.4 - cct.4 Timer and Switching Controls
(Flow Probe)
- Figure F.5 - cct.5 Power Supply and Overload Indicator
(Flow Probe)

FIG.F.1 cct.1 Constant Temperature Thermistor Bridge & Temperature Amplifier
(FLOW PROBE)



★ 2 thermistors stc u23u mounted
in a Bird connector
† match to 0.2%
‡ 220 ± 12

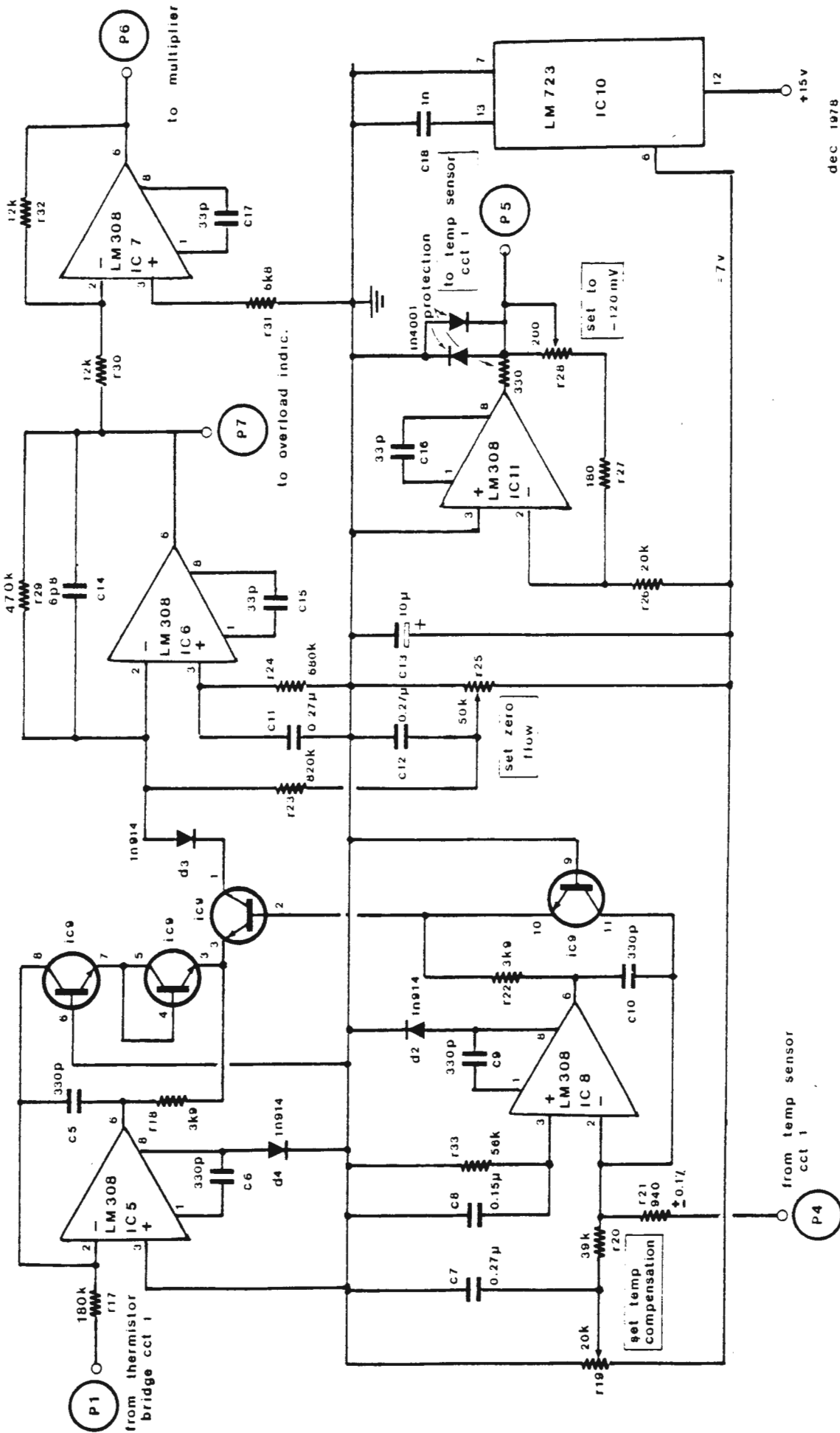
to ban. socket
temp. o/p

set temp
40 °C

set temp
20 °C

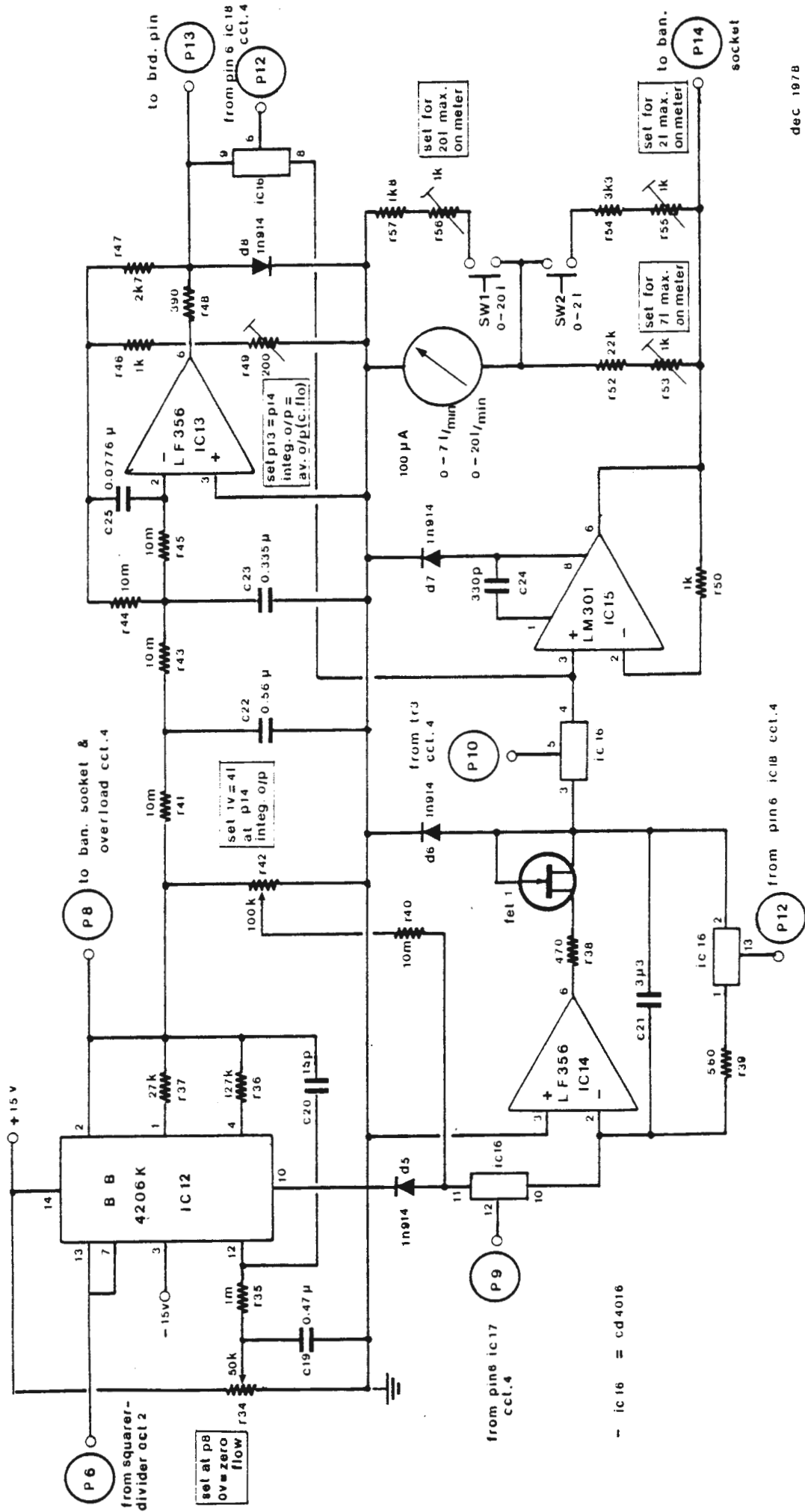
to 120 mV ref.
cct.2.

FIG.F.2 cct. 2 **Squarer & Divider Circuit**
(FLOW PROBE)



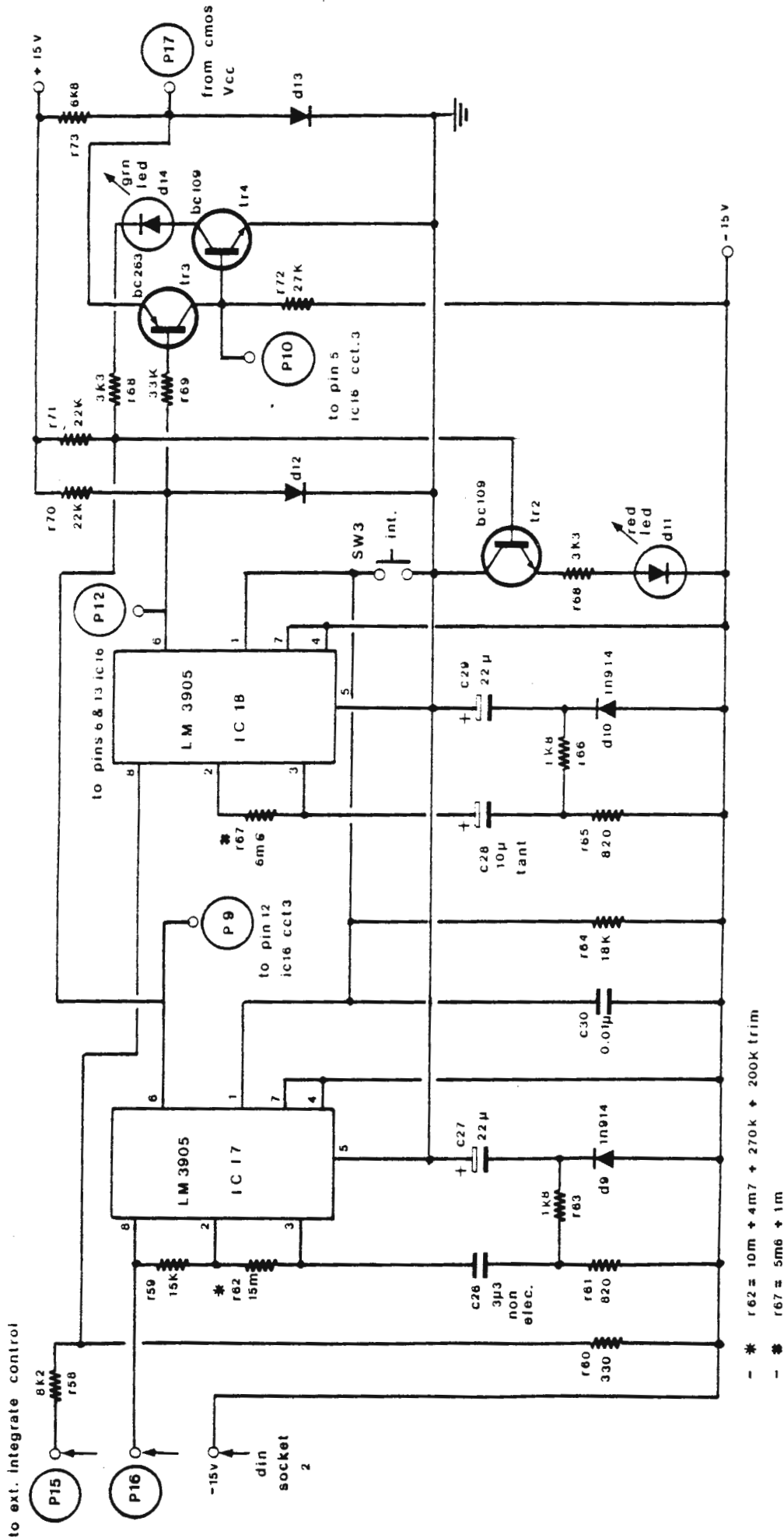
dec 1978

FIG. F3 cct. 3 Multiplier, Averager, Integrator & Metering circuit (FLOW PROBE)



- ic 16 = cd4016

FIG.F4 Timer & Switching Controls
(FLOW PROBE) cct. 4

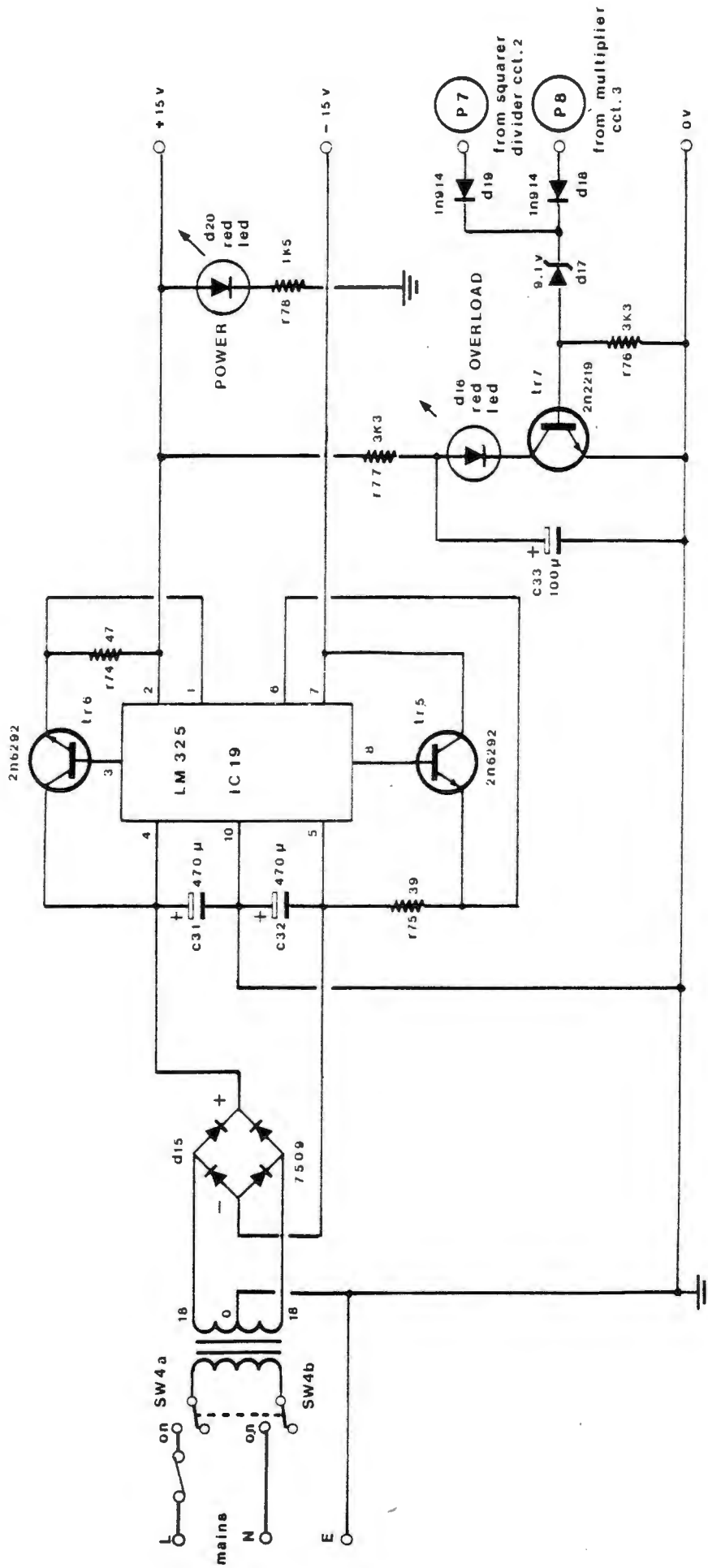


dec 1978

FIG.F.5

cct. 5

Power Supply & Overload Indicator
(FLOW PROBE)



Appendix G - Impedance Analyser Circuits

Figure G.1 Impedance/Work Analyser Block Diagram

Figure G.2 Inspiratory/Expiratory/Pause Detectors

Figure G.3 Dividers (3 off)
Differential Amplifiers (2 off)
Averaging Filters (3 off)

Figure G.4 Flow/Pressure Simulator

Figure G.5 End Expiratory Pressure Detector
Peak Expiratory Flow Detector

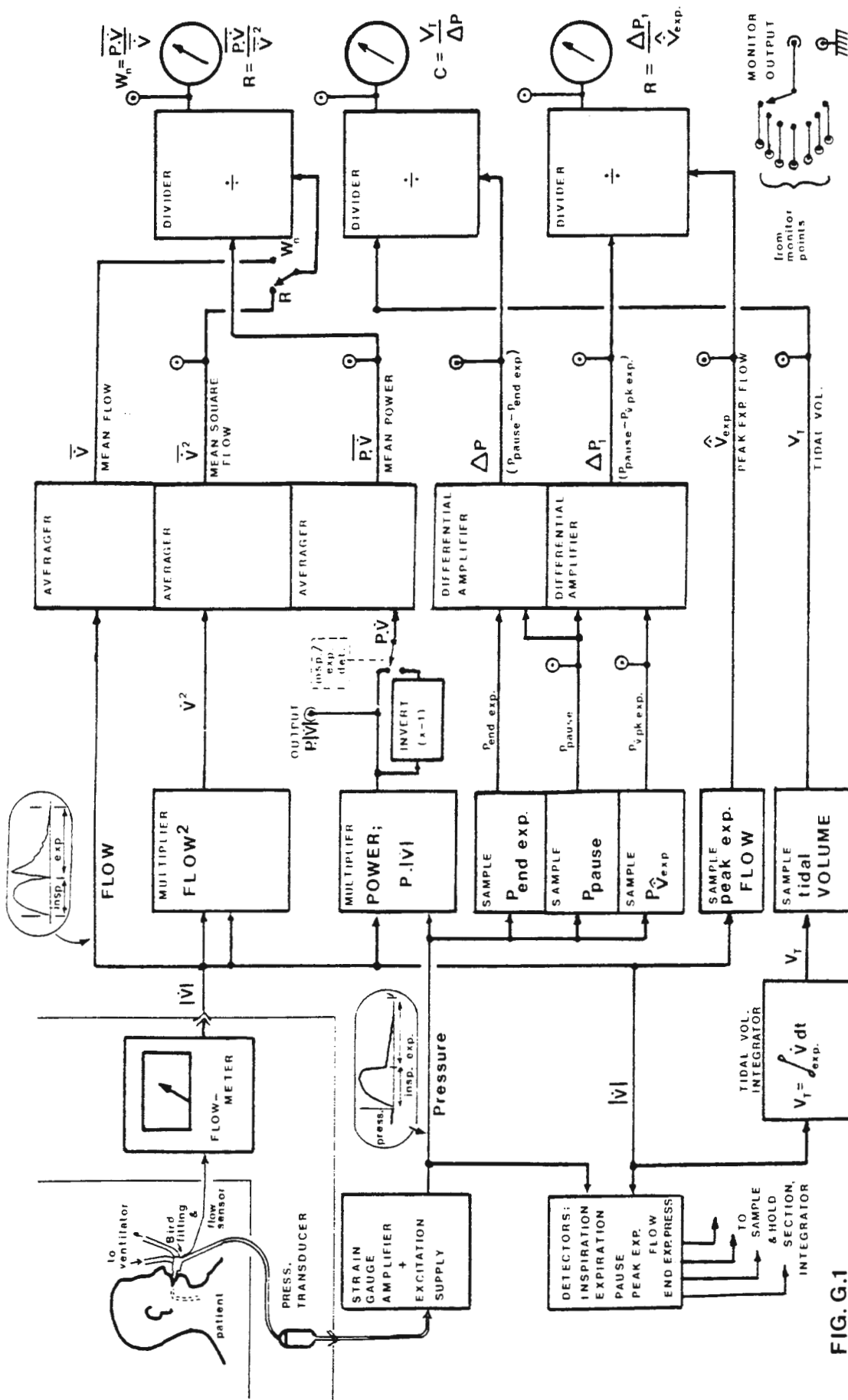


FIG. G.1
IMPEDANCE/WORK ANALYSER
BLOCK DIAGRAM

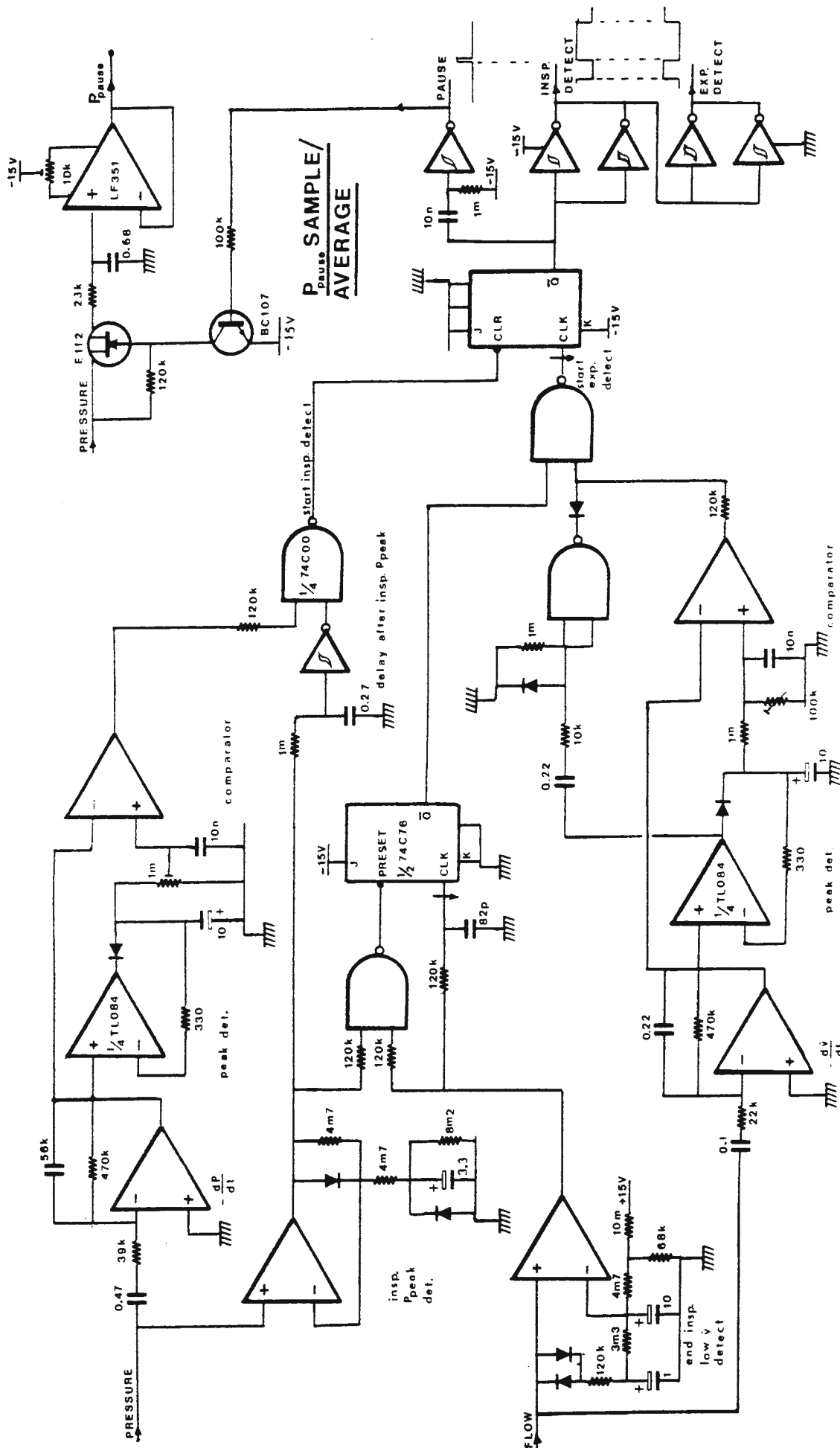


FIG. G.2
INSPIRATORY/EXPIRATORY/PAUSE DETECTORS

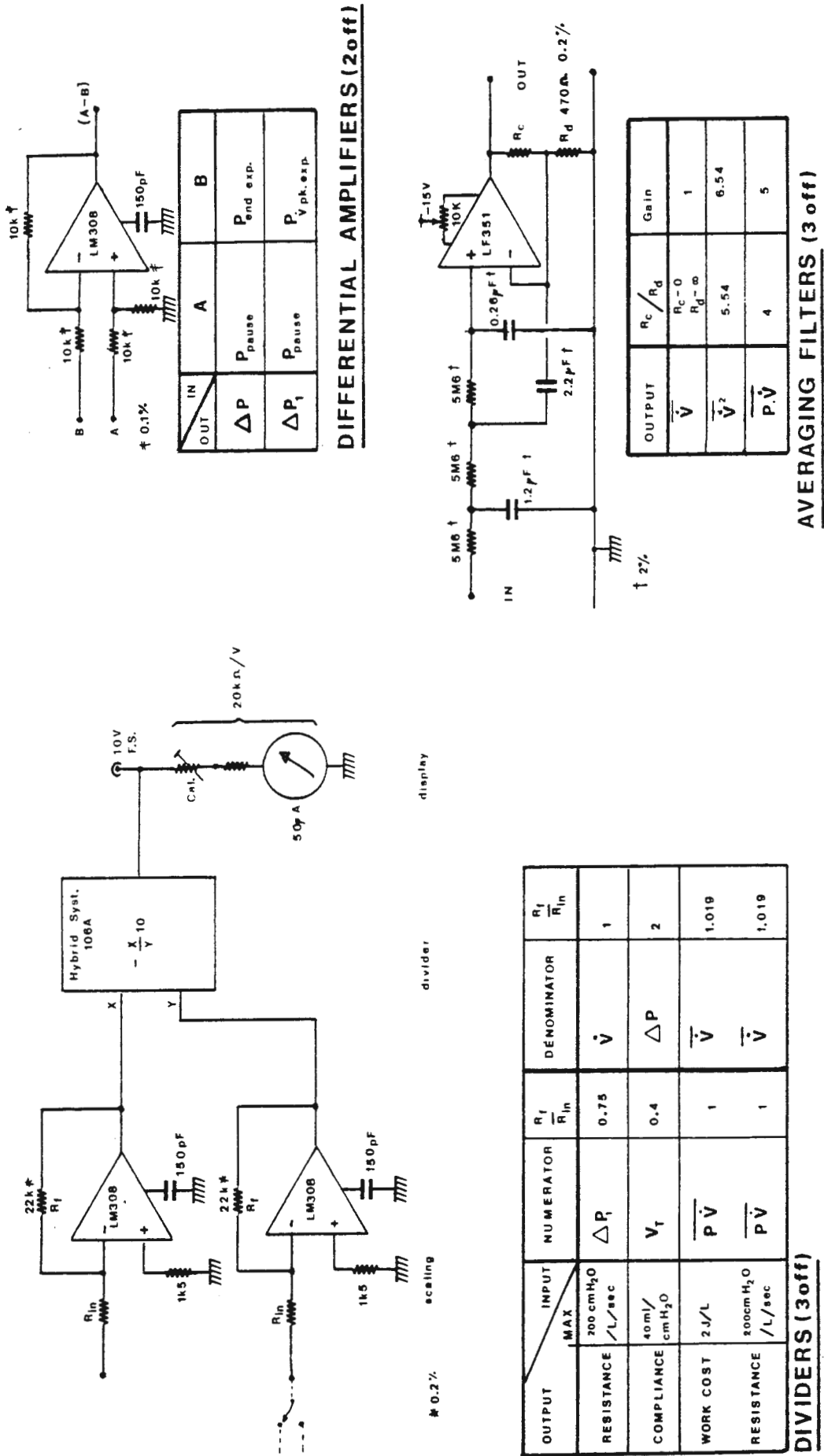


FIG. G.3

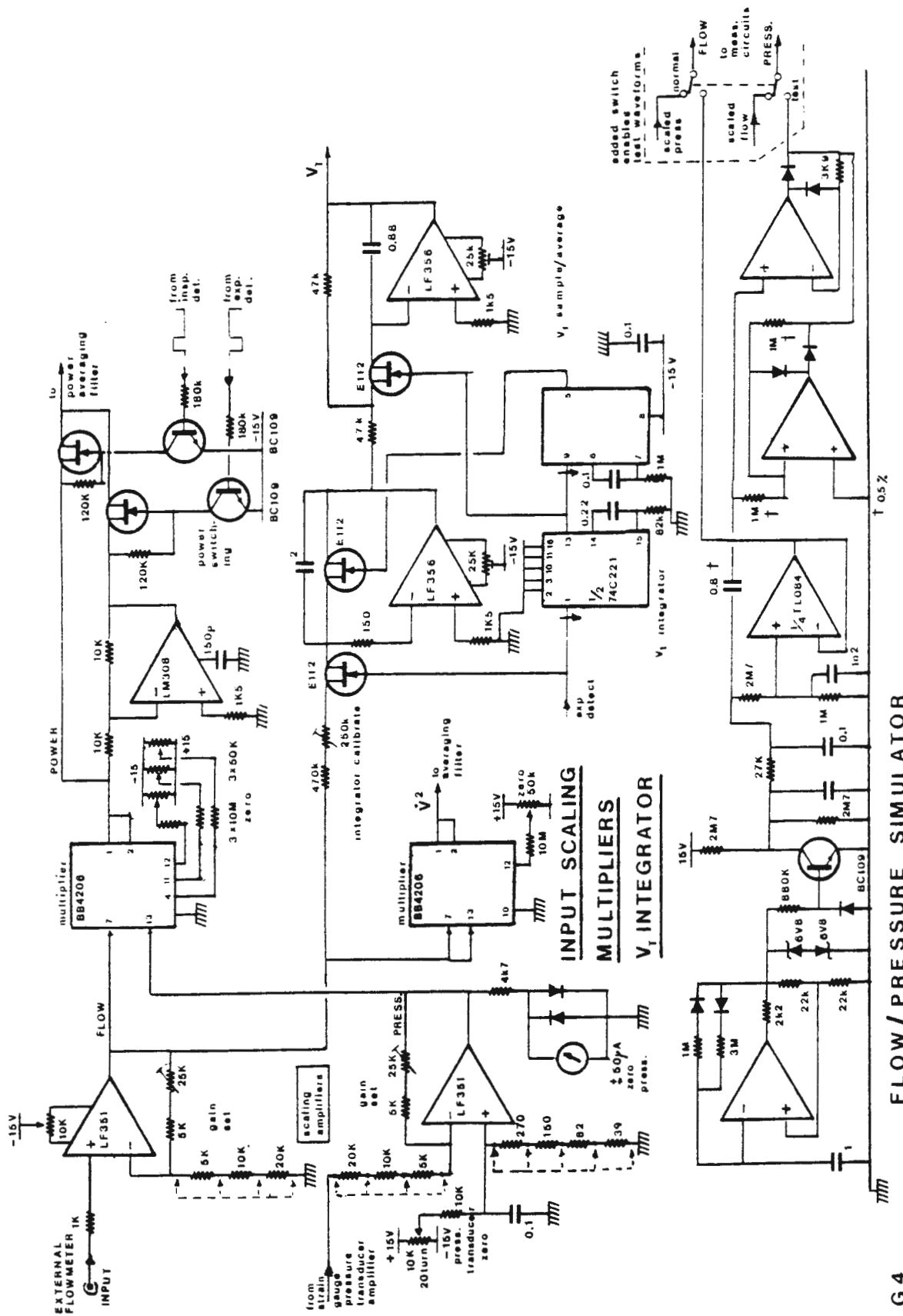


FIG. G.4

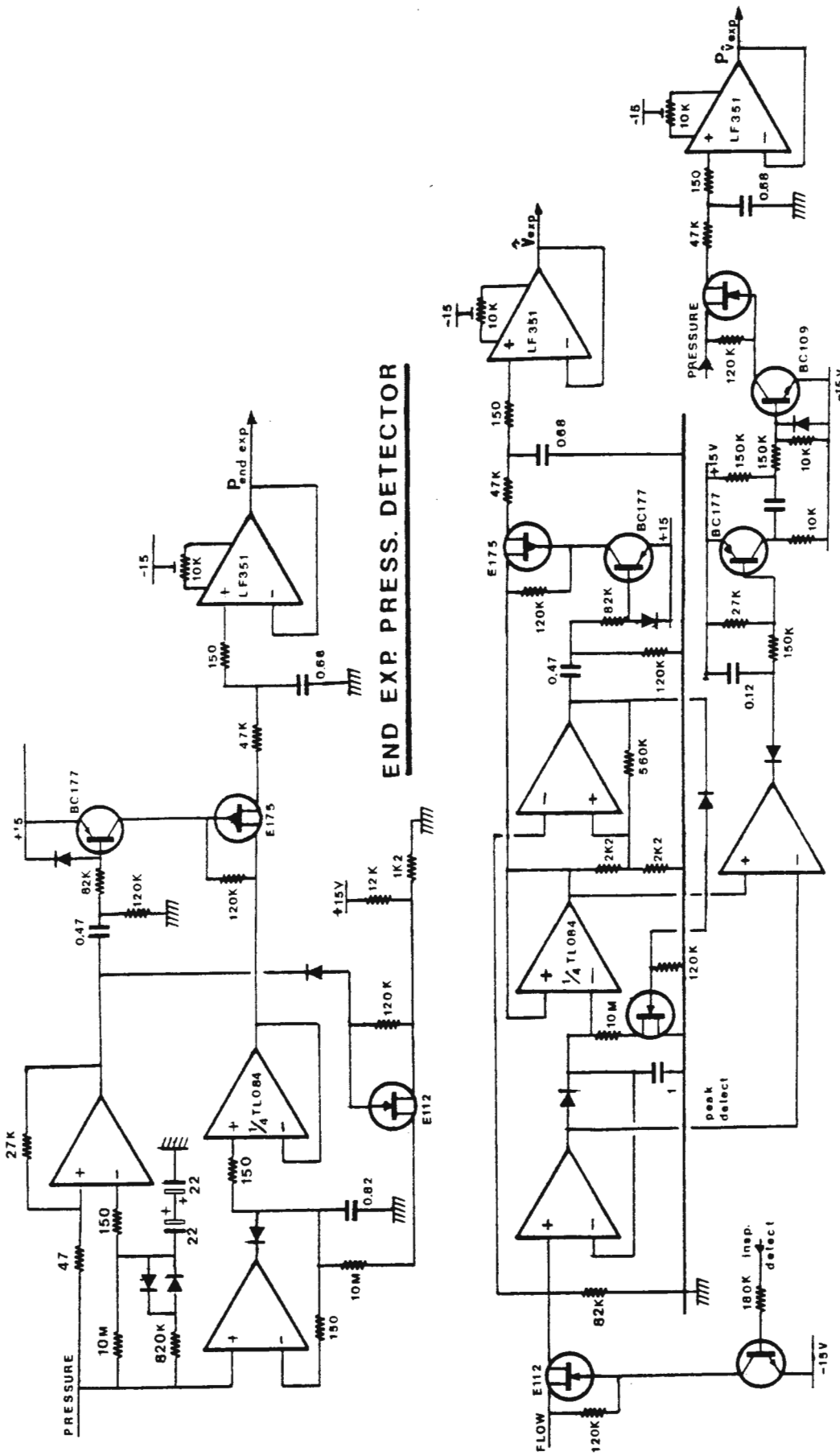


FIG. G.5

Figure H.1 Problems of Infant Ventilation - a Popular View

Machine**that****dooms****babies****to****live**

PHILADELPHIA. — The same machine that keeps seven babies alive at Philadelphia's Children's Hospital by breathing in place of their damaged lungs dooms them to perpetual dependence on its tubes.

The paradox points up the remarkable advances made in pediatric intensive care and the nightmarish problem of science's limitations.

The babies cannot be weaned from the ventilator because the machine damages their weak lungs and retards the growth of new lung tissue.

The children have spent most of their short lives in the hospital's intermediate intensive care unit, dependent on the soft tubes leading from their cribs to the machine.

It costs about R13 760 a week to keep the babies alive.

The total bill at Children's already has surpassed about R1-million.

SUFFOCATING

The babies require round-the-clock care, with nurses pounding their chests and suctioning their lungs every two to four hours to keep them from suffocating on secretions their weak lungs cannot clear.

For 20-month-old Justin Lowe, it is a game.

Justin, who cannot make sounds because of the hole in his throat for the ventilator cord, likes to get attention by pulling out the tube and waving it.

An alarm goes off and a nurse rushes over to scold him and give him the attention he wants.

Parents have visited the children practically every day for months, in some cases years, trying to develop some kind of parent-child relationship, knowing pneumonia or another lung infection could suddenly kill their vulnerable offspring.

Only five percent of the approximately 400 infants served by the ventilator each year at Children's Hospital require long-term support of a month or more.

Of the long-term babies, only 10 percent to 15 percent, two or three, end up permanently chained to the machine.

WEANED

Once a baby has been on the machine more than three months, there is only a 10 percent chance the child can be weaned, said Dr John Downes, director of the anaesthesia department, which runs the unit.

Normally children grow new lung tissue until their eighth year, but the ventilator machine damages the lungs.

The new technology creates ethical problems as well as economic and parental problems.

'I can't imagine what kind of life a kid can have living on a ventilator his entire life,' said Dr Mildred Stahlman of Vanderbilt University School of Medicine in Nashville, Tennessee.

Children's have developed a new programme that gives the children a semblance of normality.

The programme sends the babies home, where parents operate the vital ventilator.

COSTLY

The programme is risky and costly, but Laurelle and Corky Lowe of Tabernacle, New Jersey, were eager for the chance.

Justin, born without an oesophagus, was the first baby sent home under the home-care programme.

His parents needed six months to arrange financing for the tremendous costs, including about R25 800 a year for nursing, about R5 a day for oxygen, about R511 for a portable suction device and about R2 150 for the ventilator.—Sapa-AP.

Appendix I - Respiratory Analyser Test Waveforms and Results

Figure I.1 - Simulator Flow Resistance Calibration

Figure I.2 - Flow Probe Resistance

Figure I.3 - Low Level Electrical Simulation

Figure I.4 - High Level Electrical Simulation
(Sim. D)

Figure 1.5 - Mechanical Simulation..
Illustrates detector accuracy with
Variable Waveforms

Figure 1.6 - Mechanical Simulation (Sim.C)

Figure 1.7 - Mechanical Simulation (Sim.C)

Figure 1.8 - Mechanical Simulation (Sim A)

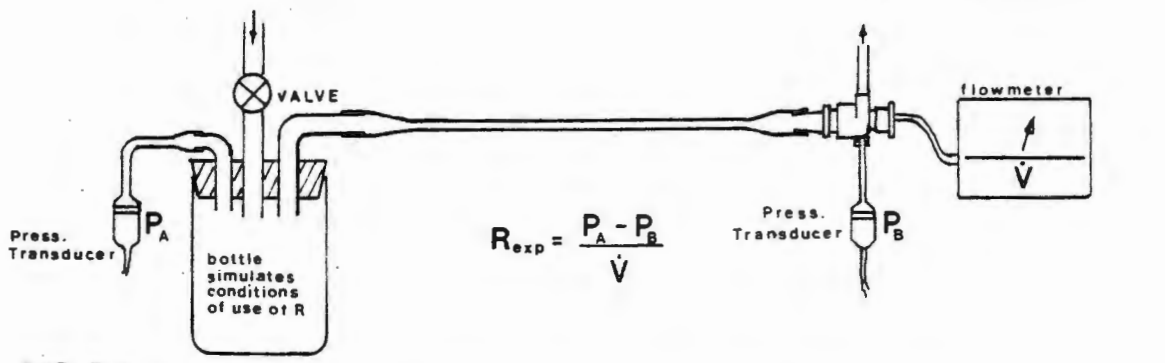
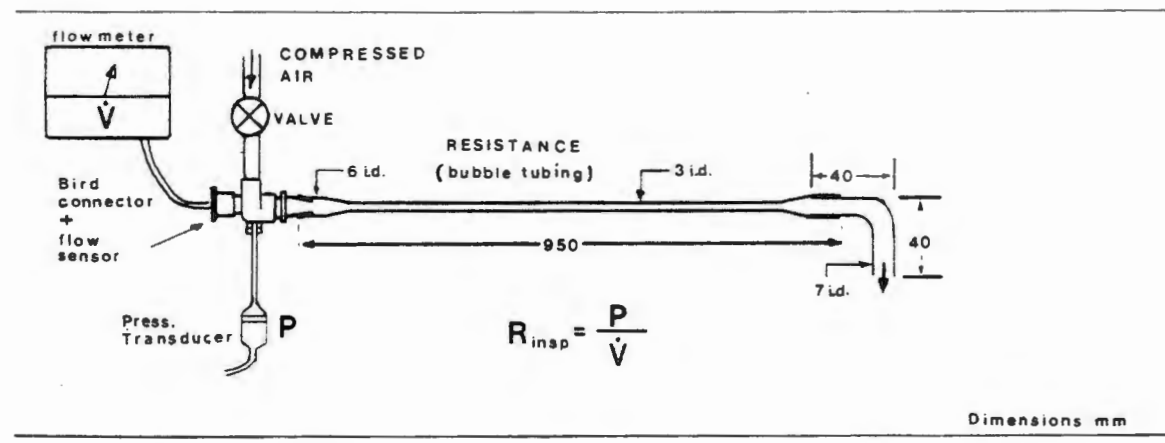
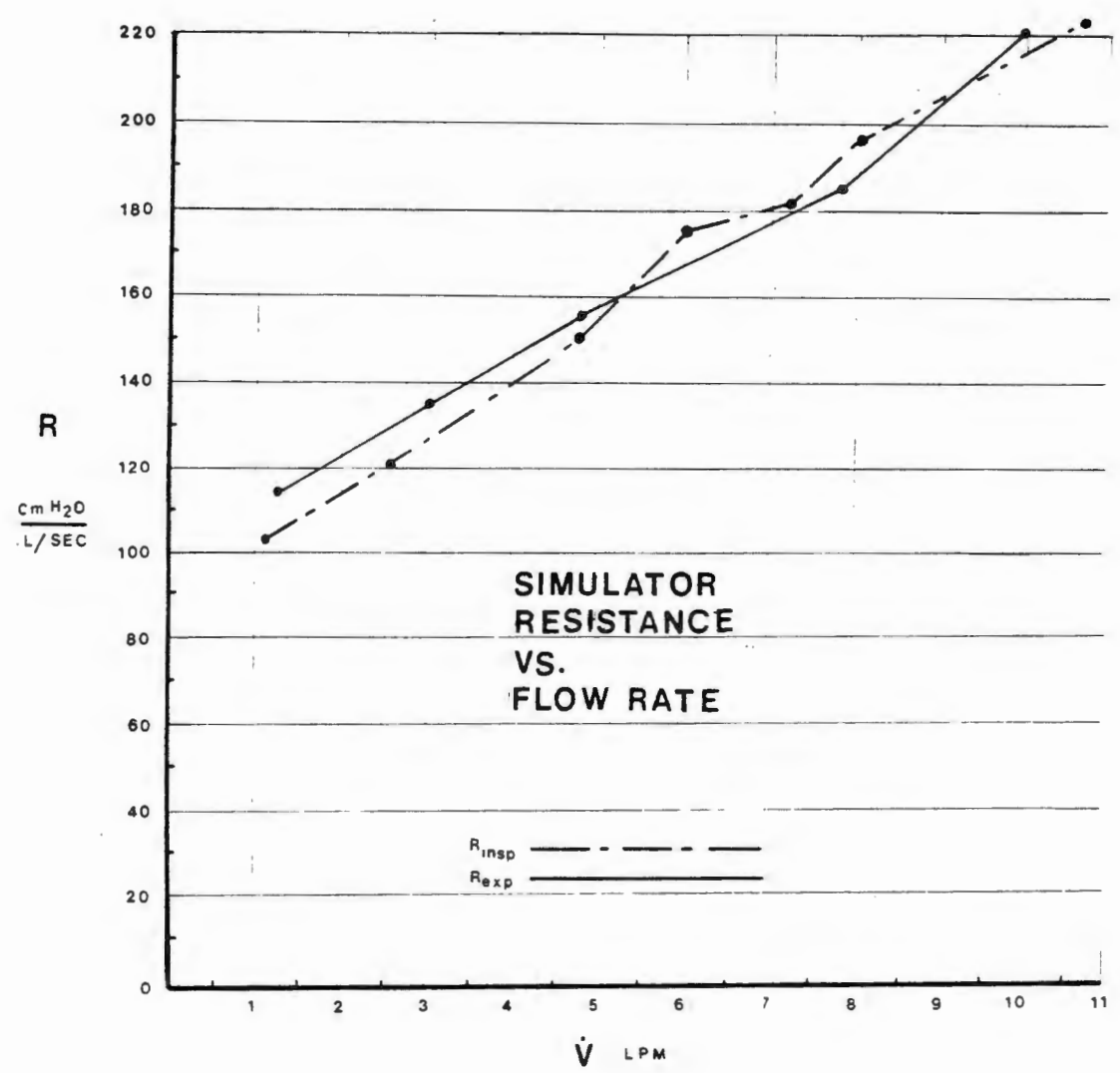


FIG. I.1
SIMULATOR FLOW RESISTANCE CALIBRATION

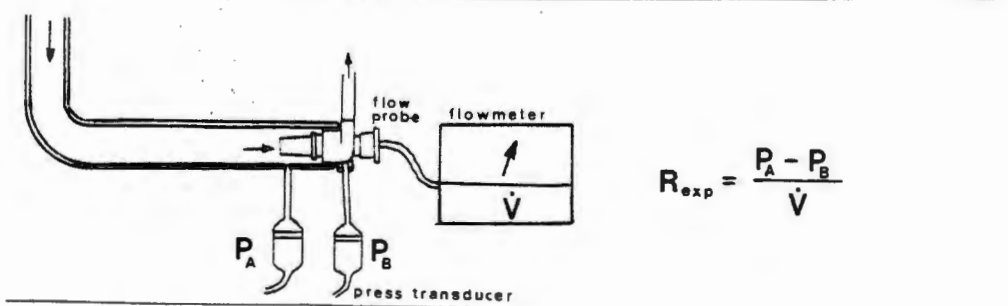
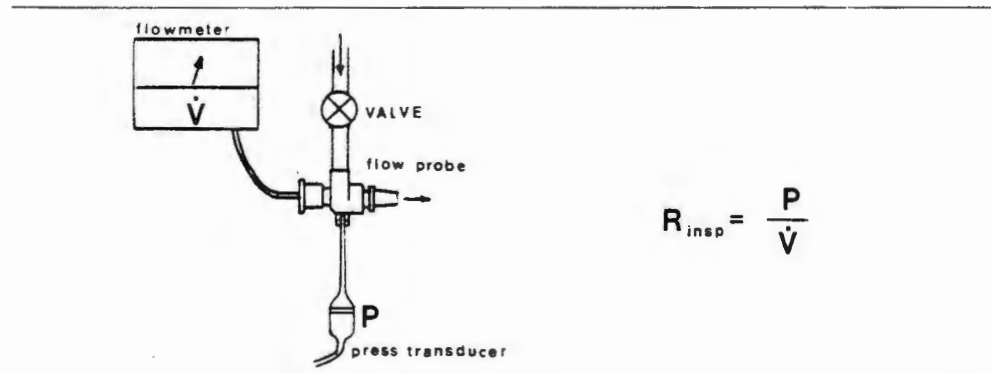
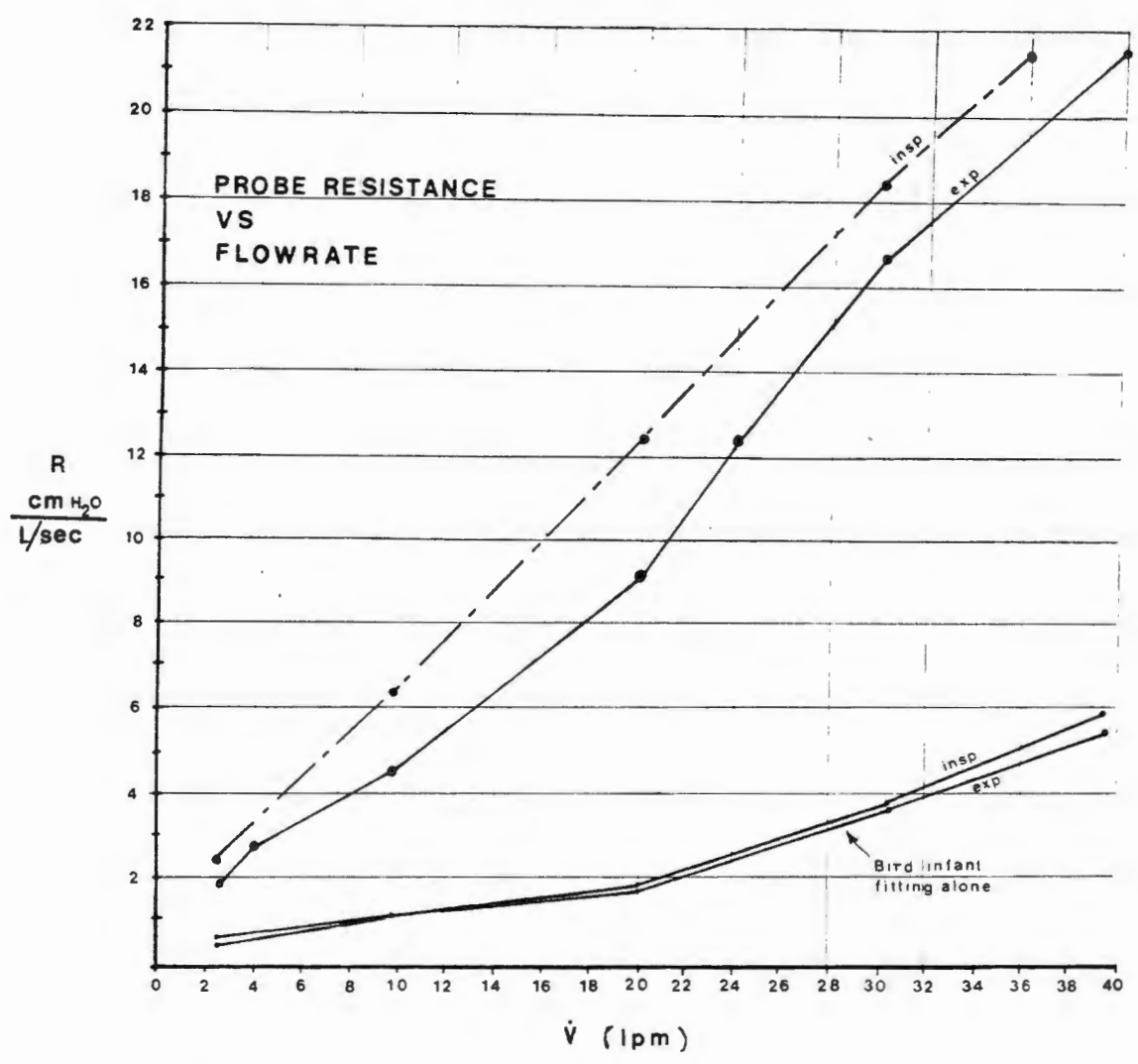


FIG.I.2 FLOW PROBE RESISTANCE

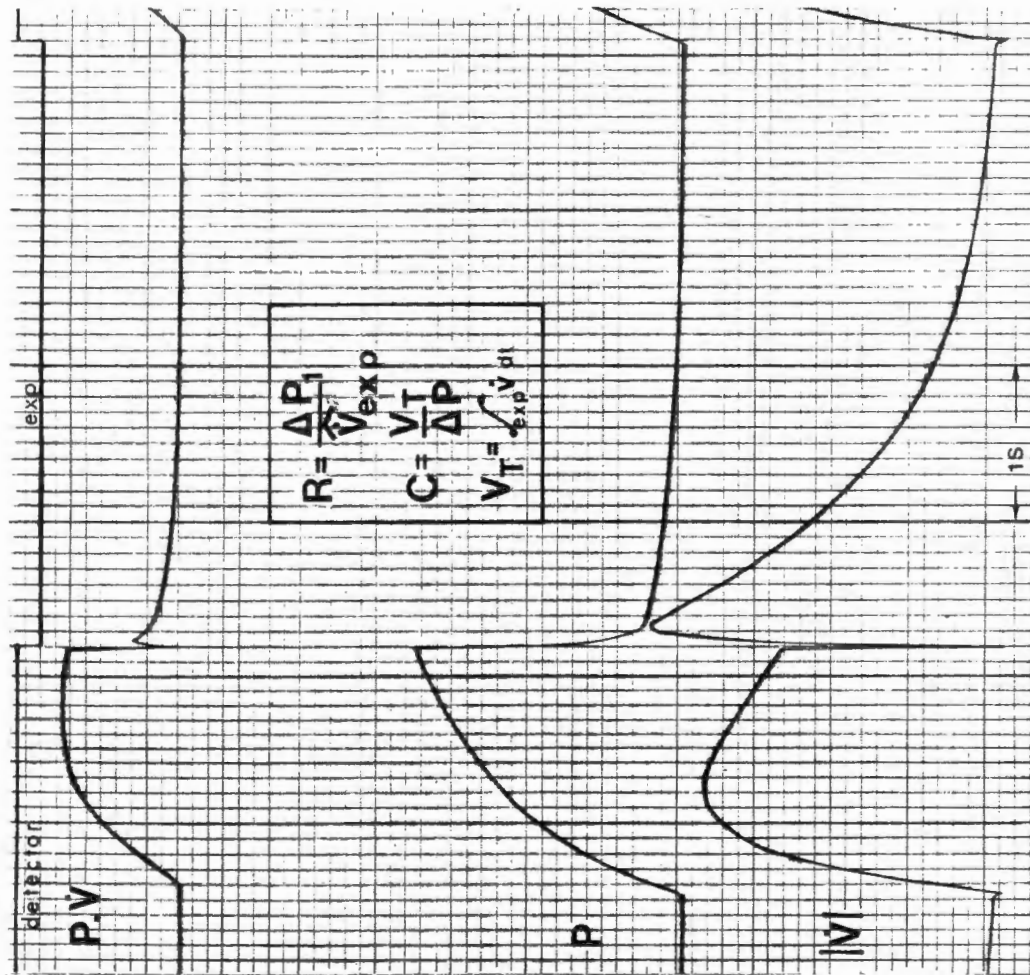
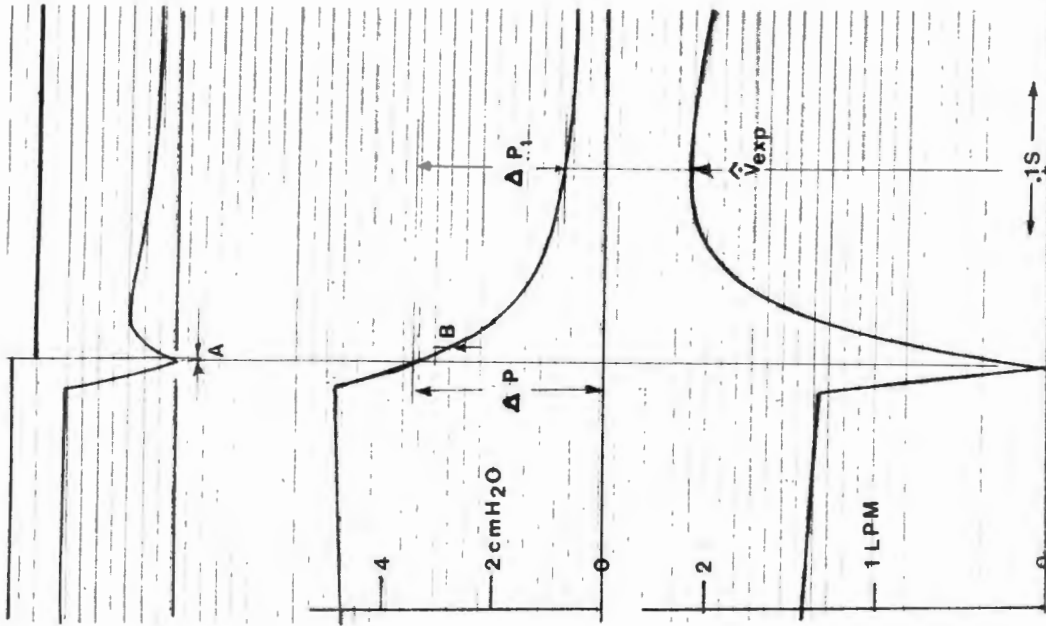


FIG.I.3 Low level electrical simulation

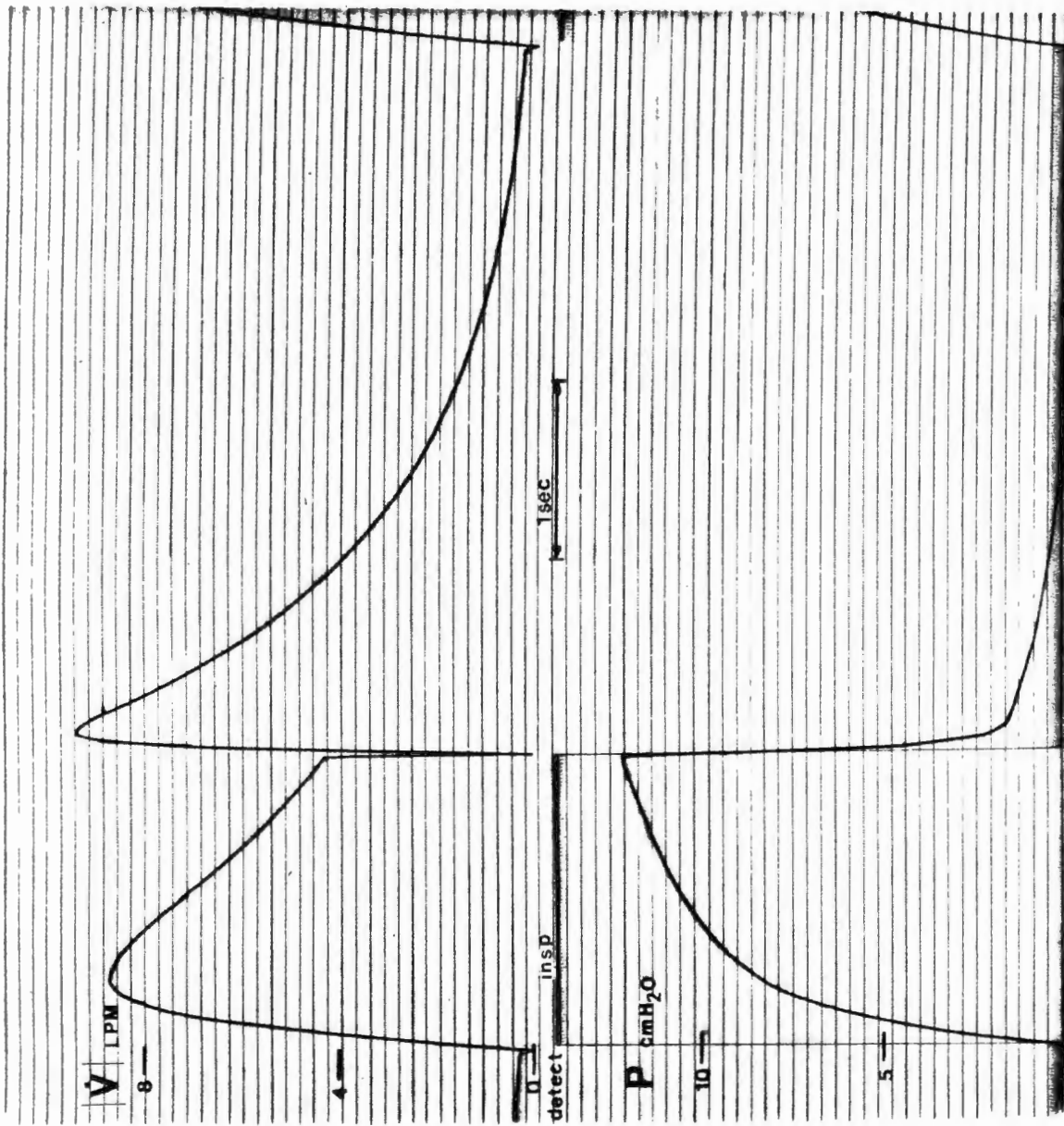


FIG. I.4
High Level Electrical
Simulation (Sim.D).
 Note very slight "gas"
 trapping at the end of
 expiration.

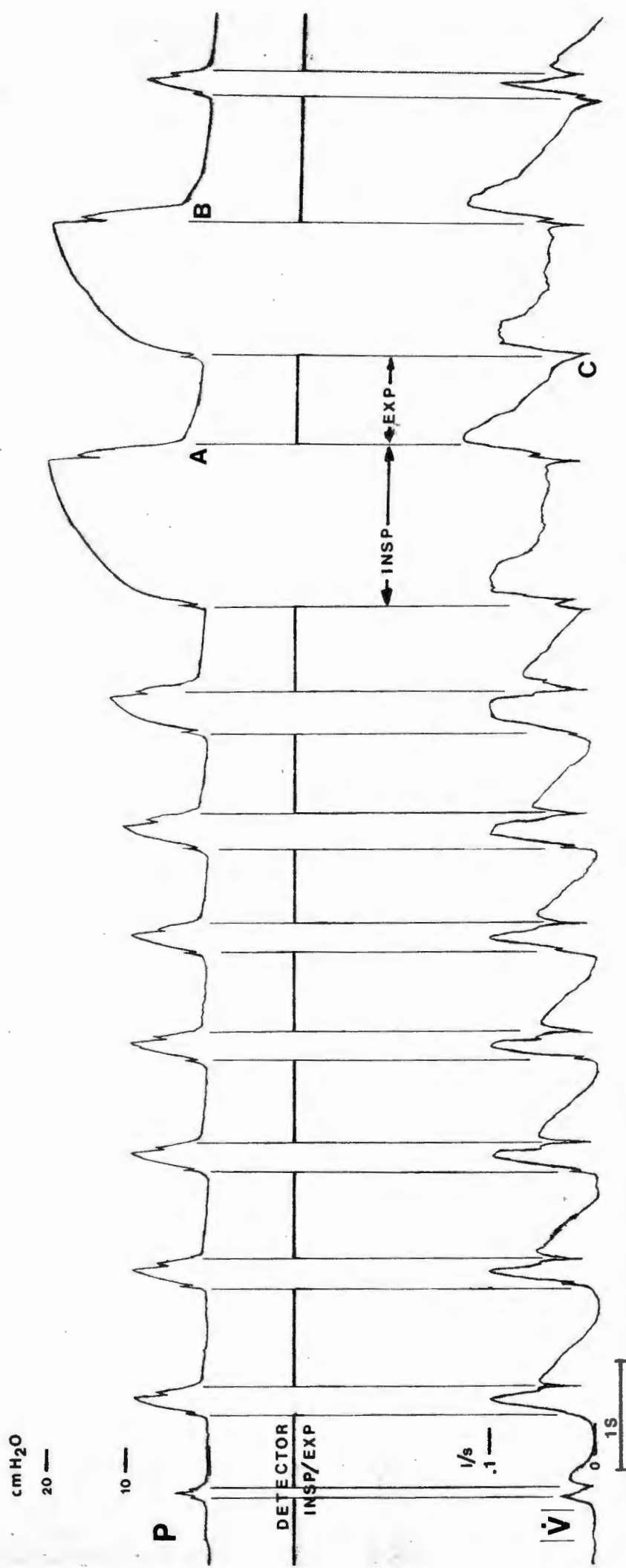


FIG.I. 5 Mechanical Simulation. Illustrates detector accuracy with variable waveforms.

Note the sampling error at A corrected one breath later at B.

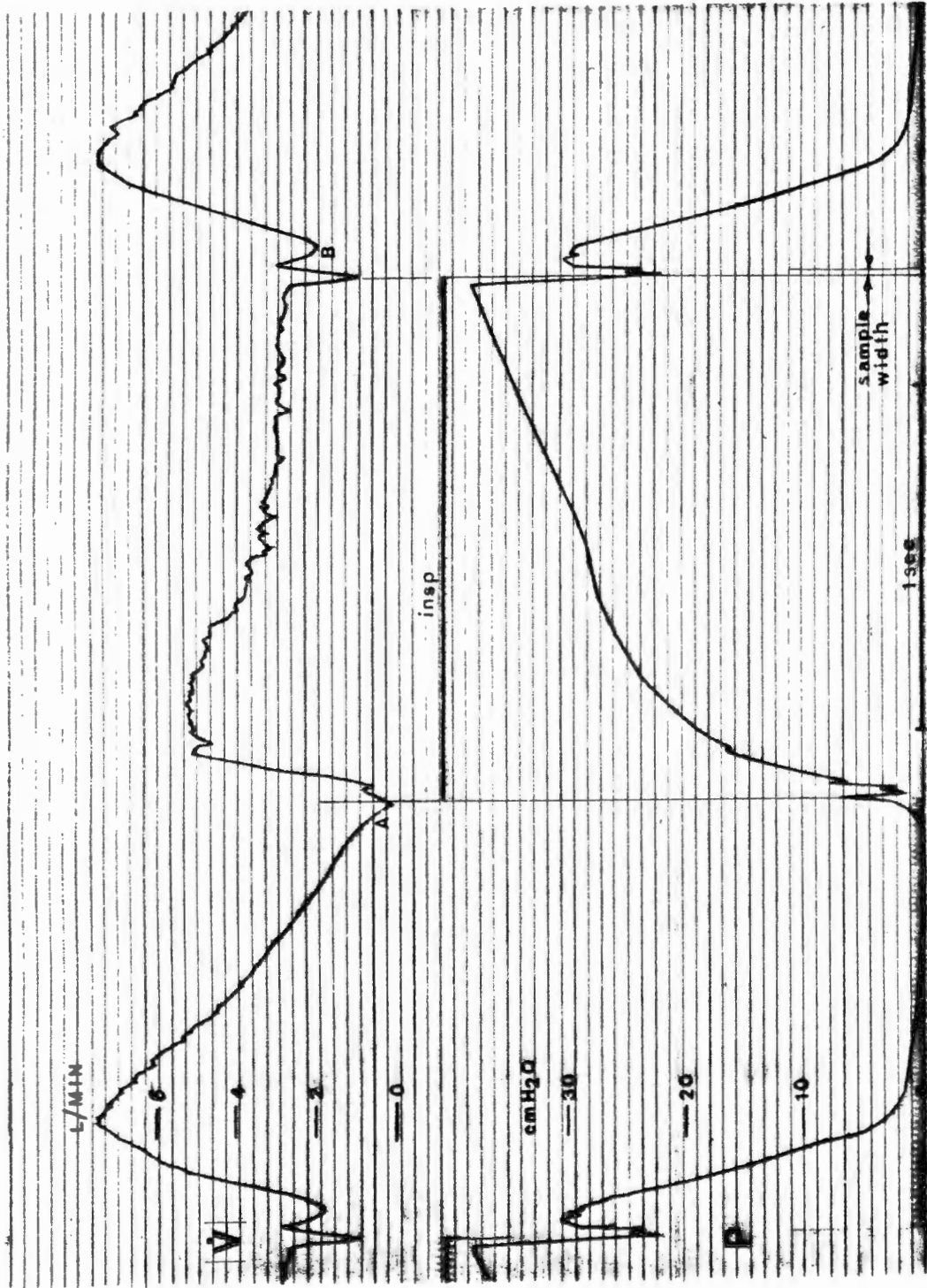


FIG. I.6 Mechanical Simulation (Sim.C). Note gas trapping - A, and valve bounce - A and B.

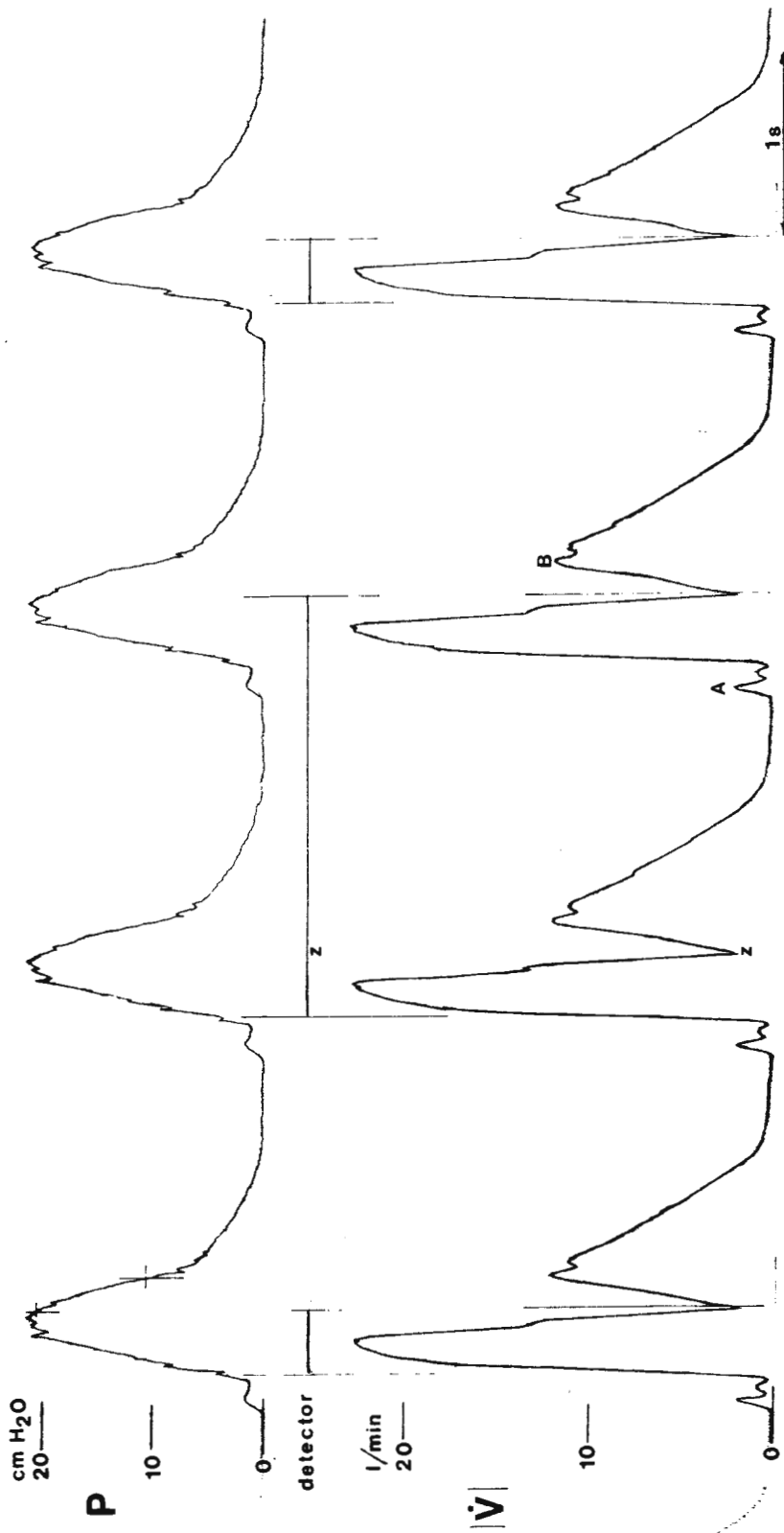


FIG. I.7 Mechanical Simulation (SimC).

Note detector error at Z caused by noise, and valve oscillation at A and B.

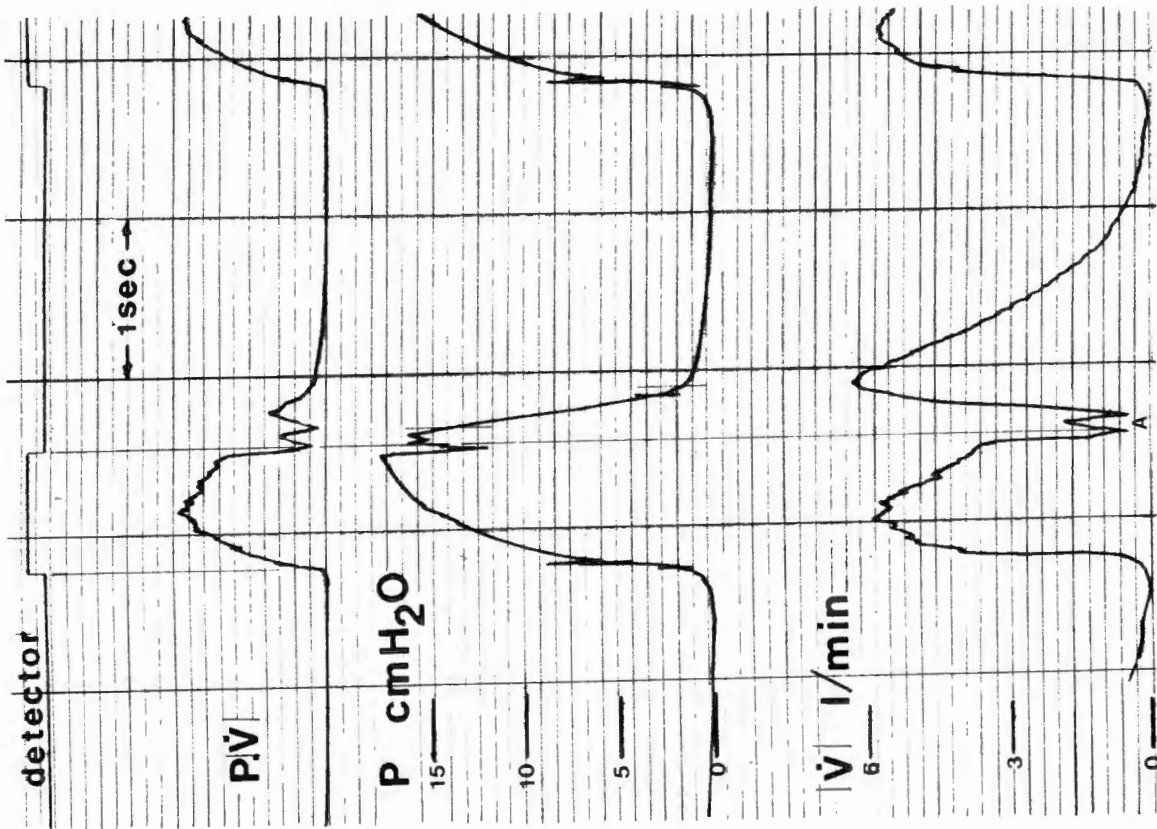


FIG. I.8
Mechanical Simulation (Sim.A).
 Note valve bounce at A and the
 consequent problem of
 detecting the end inspiration point.

References

- [1] Epstein,M.A.F. and Epstein,R.A., "Airway Flow Patterns during Mechanical Ventilation of Infants : A Mathematical Model," IEEE Trans. on Biomed.Eng., Vol.BME 26(5), pp 299-306, 1979.
- [2] Mushin,W.W., Mapleson,W.W. and Lunn,J.N., "Problems of Automatic Ventilation in Infants and Children," Brit.J.Anaesth., Vol.34, pp 514-522, 1962.
- [3] Okmian,L., "Artificial Ventilation by Respirator for Newborn and Small Infants during Anaesthesia," Acta anaesth.Scand., Suppl.20, Vol.10, 1966.
- [4] Keuskamp,D.H.G., (Ed.), Neonatal and Pediatric Ventilation, International Anesthesiology Clinics, Vol.12(4), Little Brown, Co., Boston, 1974.
- [5] Lindahl,S., Okmian,L. and Thomson,D., "Artificial Ventilation in Children during Anaesthesia using Tidal Volume Ventilator," Acta anaesth.Scand., Vol.23, pp 587-595, 1979.
- [6] Hughes,T.J., "Measuring 'Instantaneous' Active and Reactive Power - Part I : Active Power" University of Cape Town, Dept.Elec.Eng.Research Review, Vol.1, No.3, pp 22-24, 1 June,1977.
- [7] Hughes,T.J., "Measuring 'Instantaneous' Active and Reactive Power - Part II : Reactive Power" University of Cape Town, Dept.Elec.Eng.Research Review, Vol.2, No.1, pp 25-27, February,1978.
- [8] Wilson,F.J. and Bone,R.C., "Monitoring Respiratory Function in Acute Respiratory Failure," Pulmonary Disease Reviews, Ed.R.C. Bone, Vol.1, pp 431-447, John Wiley,1980.

- [9] Wilson,R.S., "Monitoring the Lung : Mechanics and Volume," Anesthesiology, Vol.45(2), August, 1976.
- [10] Osborn,J.J., "Cardiopulmonary Monitoring in the Respiratory Intensive Care Unit," Med.Instrum., Vol.11(5), pp 278-282, 1977.
- [11] Hilberman,M., "Monitoring in the Operating Room : Current Techniques and Future Requirements," Med.Instrum., Vol.11(5), pp 283-287, 1977.
- [12] Polgor,G.and Promadhat,V., Pulmonary Function Testing in Children : Techniques and Standards, W.Saunders Co., 1972.
- [13] Brown,T. and Fisk,G., Anaesthesia for Children, Blackwell, Oxford, 1979.
- [14] Smith,R.M., Anaesthesia for Infants and Children, 2nd edit., C.V. Mosby pub. co., 1963.
3rd edit., C.V. Mosby pub. co., 1968.
- [15] Peters,R.M., Hilberman,M., Hogan,J.S. and Cranford,D.A., "Objective Indications for Respirator Therapy in Post-Trauma and Post-Operative Patients," Am.J.Surg., Vol.124, pp 262-269, 1972.
- [16] Okmian,L., Wallgren,G.and Wahlin, A., "Artificial Ventilation by Respirator for Newborn and Small Infants during Anaesthesia III Mechanics of Ventilation," Acta anaesth.Scand., Vol.10, pp 181-202, 1966.
- [17] Mattila, M.A.K., "The Role of the Physical Characteristics of the Respirator in Artificial Ventilation of the Newborn," Acta anaesth.Scand., Suppl.56, pp 1-107, 1974.

- [18] Fenn, W.O. and Rahn, H. (Eds), Handbook of Physiol. : Respiration, Vol. II, American Physiol. Soc., Washington, 1965:
- (i) Cross, K.W. "Respiration and Oxygen Supplies in the Newborn," pp 1329-1343, Chapter 52.
 - (ii) Marshall, R., "Objective Tests of Respiratory Mechanics," pp 1399-1411.
- [19] Frost and Sullivan, Inc., Report 625, Frost and Sullivan Inc., 106 Fulton Street, New York, NY 10038, as quoted in Medical and Biological Engineering and Computing, March, 1980.
- [20] Taylor, G., Larson, P. and Prestwich, R., "Unexpected Cardiac Arrest during Anesthesia and Surgery," JAMA, Vol. 236(24), pp 2758-2760, December, 1976.
- [21] Mushin, W.W., Rendall-Baker, L.K., Thompson, P.W. and Mapelson, W.W., Automatic Ventilation of the Lungs, 2nd edit., London : Blackwell Scientific Publications, 1969.
- [22] Lindahl, S., Kugelberg, J. and Okmian, L., "The Circulatory Response to Specific Ventilatory Patterns using a Tidal Volume Ventilator," Acta anaesth. Scand., Vol. 23, pp 370-378, 1979.
- [23] Lindahl, S. and Okmian, L., "Experimental Studies on Artificial Ventilation using a Tidal Volume Ventilator," Acta anaesth. Scand., Vol. 23, pp 359-369, 1979.
- [24] Norlander, O., Herzog, P., Nordén, I., Hossli, G., Schaer, H. and Gattiker, R., "Compliance and Airway Resistance during Anaesthesia with Controlled Ventilation," Acta anaesth. Scand., Vol. 12, pp 135-152, 1968.

- [25] Johansson,H., "Effects of Different Inspiratory Gas Flow Patterns on Thoracic Compliance during Respirator Treatment," Acta anaesth.Scand., Vol.19, pp 89-95, 1975.
- [26] Bergman,N.A., "Effects of Varying Respiratory Waveforms on Gas Exchange," Anesthesiology, Vol.28, pp 390-395, 1967.
- [27] Lindahl,S., Arborelius,M. and Okmian,L., "Influence of Ventilatory Frequencies and Ventilator Volume/Pressure Quotients on Pulmonary Ventilation using a Tidal Volume Ventilator," Acta anaesth.Scand., Vol.23, pp 379-394, 1979.
- [28] Jain,N.K., "Optimal Respirator Settings in Assisted Respiration," Med.Biol.Eng., Vol.12, pp 425-430, 1974.
- [29] Fenn,W.O. and Rahn,H. (Eds), Handbook of Physiol. : Respiration, Vol.I, American Physiol.Soc., Washington, 1964 :
- (i) Agostini,E. and Mead,J., "Statics of the Respiratory System," pp 387-409.
 - (ii) Defares,J.D., "Principles of Feedback Control and their Application to the Respiratory Control System," Chapter 26.
 - (iii) Dubois,A.B., "Resistance to Breathing," pp 451-461.
 - (iv) Mead,J. and Agostini,E., "Dynamics of Breathing," pp 411-427.
 - (v) Mead,J. and Milic-Emili, "Theory and Methodology in Respiratory Mechanics with Glossary of Symbols," pp 363-376.
 - (vi) Otis,A.B., "The Work of Breathing," pp 463-476.
 - (vii) Radford,E.P.(Jr), "Static Mechanical Properties of Mammalian Lungs," pp 429-449.
- [30] van de Woestijne,K.P., "The Human Respiratory System," CRC Handbook of Engineering in Medicine and Biology, Chemical Rubber Co., 1978.

- [31] Campbell,D. and Brown,J., "The Electrical Analogue of Lung," Brit.J.Anaesth., Vol.35, pp 684-693, 1963.
- [32] Eyles,J.G. and Pimmel,R.L., "Estimating Respiratory Mechanical Parameters in Parallel Compartment Models," IEEE Trans. on Biomed.Eng., BME-28(4), pp 313-317, 1981.
- [33] Deal,C., Osborn,J.J., Ellis,E. and Gerbode,F., "Chest Wall Compliance," Annals of Surgery, Vol.167, pp 73-77, 1967.
- [34] Peslin,R., Papon,J., Duvivier,C. and Richalet,J., "Frequency Response of the Chest : Modeling and Parameter Estimation," J.Ap.Physiol., Vol.39(4), pp 523-534, October,1975.
- [35] Cross,K.W. and Oppe,T.E., "The Respiratory Rate and Volume in the Premature Infant," J.Physiol., Vol.116, pp 168-174, 1952.
- [36] Plaut,D.I. and Webster,J.G., "Ultrasonic Measurement of Respiratory Flow," IEEE Trans.on Biomed. Eng., Vol.BME-27(10), pp 549-558, October,1980.
- [37] American College of Chest Physicians, "The Assessment of Ventilatory Capacity," Chest, Vol.67(1), pp 95-97, January,1975.
- [38] Wever,A.M.J., Britton,M.G. and Hughes,D.D.T., "Evaluation of Two Spirometers," Chest, Vol.70(2), pp 244-250, August,1976.
- [39] American National Standards Institute, American National Standard for Breathing Machines in Medical Use, ANSI Z79.7 - 1976, New York, 1976.

- [40] Munson, E.S., Farnham, M. and Hamilton, W.K., "Studies of Respiratory Gas Flows : A Comparison using Different Anaesthetic Agents," Anaesthesiol., Vol.24(1), pp 61-67, 1963.
- [41] Dekker, E., "Transition between Laminar and Turbulent Flow in Human Trachea," J.Ap.Physiol., Vol.16(6), pp 1060-1064, 1961.
- [42] International Electrotechnical Commission Publication 601-1, Safety of Medical Electrical Equipment, Geneva, 1977.
- [43] Barth, J., Fraser, R., Harvey, R. and Larson, D., "Measurement of Pulmonary Function in Infants and Children," U.S.Dept.of Commerce National Technical Information Service : PB 262 942, December, 1976.
- [44] Plaut, D.I. and Webster, J.G., "Design and Construction of an Ultrasonic Pneumotachometer," IEEE Trans. on Biomed.Eng., BME-27(10), pp 590-597, October, 1980.
- [45] Fleisch, Dr A., "The Pneumotachograph," Data Sheet from Instrumentation Associates, New York.
- [46] Fry, D.L., Hyatt, R.E., McCall, C.B. and Mallos, A.J., "Evaluation of Three Types of Respiratory Flowmeters," J.Ap.Physiol., Vol.10(2), pp 210-214, 1957.
- [47] Minato As-700 Autospirometer Manual, Minato Med.Sc. Co, Osaka, Japan.
- [48] MM10 Digital Thermistor Spirometer Operator's Manual, Micro Medical, U.S.A.
- [49] Aga Spirometer US 800, Data Sheet, Aga Medical AB, Sweden.

- [50] Bidani,A.and Flumerfelt,W., "Models of Respiratory Control," Chemical Engineering in Medicine, D.D.Rencan,(ed.); Ch.13, pp 268-289, Am.Chem.Soc., 1973.
- [51] Hall,K.D. and Reeser,F.H.(Jr), "Calibration of Wright Spirometer," Anaesthesiol., Vol.23(1), pp 126-129, 1962.
- [52] McCall,C.B., Hyatt,R.E., Noble,F.W. and Fry,D.L., "Harmonic Content of Certain Respiratory Flow Phenomena of Normal Individuals," J.Ap.Physiol., Vol.10, pp 215-218, 1957.
- [53] Fitzgerald,M.X., Smith,A.A. and Goensler,E.A., "Evaluation of Electronic Spirometers," New Eng. J.Med., Vol.289, pp 1283-1388, 1973.
- [54] Cross,K.W., "The Respiratory Rate and Ventilation in the Newborn Baby," J.Physiol., Vol.109, pp 459-474, 1949.
- [55] Swyer,P.R., Reiman,R.C. and Wright,J.J., "Ventilation and Ventilatory Mechanics in the Newborn," J.Ped., Vol.56(5), pp 612-622, May, 1960.
- [56] Primiano,F.P.(Jr), "Measurements of the Respiratory System," in Medical Instrumentation, Application and Design, Webster,J.G.(Ed), pp 434-510, Houghton Mifflin, Co., Boston, 1978.
- [57] Clement,J. and van de Woestijne,K.P., "Pressure Correction in Volume and Flow-Displacement Body Plethysmography," J.Ap.Physiol., Vol.27(6), pp 895-897, 1969.
- [58] Milner,A.D., "Assessment of Respiratory Function in Childhood and Infancy," Recent Advances in Paediatrics, 4th edit., Gairdner,D., Hull,D. (Eds), pp 217-244, Churchill, London, 1971.

- [59] Karlberg, P. and Koch, G., "Respiratory Studies in Newborn Infants : III Development of Mechanics of Breathing during the First Week of Life. A Longitudinal Study," Acta Paediatrica, Suppl.135, pp 121-129, 1962.
- [60] Okmian, L., "Artificial Ventilation by Respirator for Newborn Infants during Anaesthesia : A Method using a New Formula and a New Nomogram," Acta anaesth.Scand., Vol.7, pp 31-57, 1963.
- [61] Rolfe, P., "Instruments for the Care of Ill Newborn Babies," Electronics and Power, Vol.23, pp 32-39, January, 1977.
- [62] Hill, D.W., Electronic Techniques in Anaesthesia and Surgery, 2nd edit., London, Butterworth, 421 pp, 1973.
- [63] Walker, C.H.M., "Impedance Respiratory Monitoring in the Newborn Infant," Biomed. Eng., pp 454-459, October, 1968.
- [64] Nunn, J.F., "A New Method of Spirometry Applicable to Routine Anaesthesia," Br.J.Anaes., Vol.28, pp 440-449, 1956.
- [65] Wright, B.M., "A Respiratory Anemometer," J.Physiol., Vol.127, (25 p from Proc.Physiol.Soc. 12-13 Nov.1954) 1955.
- [66] Crane, R.A. and Stuttard, B., "A Digital Technique for Linearising the Output of a Turbine Anemometer," Biomed.Eng., January, 1976.
- [67] Cox, L.A., Almeida, A.P., Robinson, J.S. and Horsely, J.K., "An Electronic Respirometer," B.J.Anaesth., Vol.46, pp 302-310, 1974.

- [68] Bushman, J.A., "Effect of Different Flow Patterns on the Wright Respirometer," Br.J.Anaesth., Vol.51, pp 895-898, 1979.
- [69] Dornette, W., "Monitoring in Anesthesia," Clinical Anesthesia, Vol.9(2 and 3), F.Davis, Co, 1973.
- [70] Elliott, S.E., Shore, J.H., Barnes, C.W., Lindauer, J. and Osborn, J.J., "Turbulent Airflow Meter for Long-Term Monitoring in Patient-Ventilator Circuits," J.Ap.Physiol. : Respirat. Environ. Exercise Physiol., Vol.42(3), pp 456-460, 1977.
- [71] Saklad, M.D., Sullivan, M., Paliotta, J. and Lipsky, M., "Pneumotachography : A New, Low-Dead-Space, Humidity-Independent Device," J. Phys.E. : Sci.Instrum., Vol.14, pp 149-163, 1981.
- [72] National Semiconductor Pressure Transducer Handbook, National Semiconductor, Santa Clara, California, 1977.
- [73] Hewlett-Packard, Medical Products Group, Catalogue, Respiratory Care Products, printed in U.S.A. 5/75.
- [74] Finucane, K.E., Egan, B.A. and Dawson, S.V., "Linearity and Frequency Response of Pneumotachographs," J.Ap.Physiol., Vol.32(1), pp 121-126, 1972.
- [75] Fleisch, A., "Der Pneumotachograph : die Apparatur zur Geschwindigkeitsregistrierung der Atemluft" Plügers Arch. ges. Physiol., Vol.209, pp 713-722, 1925.
- [76] Lilly, J.C., "Flowmeter for Recording Respiratory Flow in Human Subjects," in Methods in Medical Research, Silverman, L. and Whittenberger, J.L. (Eds), Year Book Publishing Co., Chicago, 1950.

- [77] Meriam Laminar Flow Elements, Bulletin File, No.501,215,3 from Meriam Instrument, Cleveland, Ohio.
- [78] Herzog,P. and Norlander,O.P., "A Precision Method for the Dynamic Volume-Flow Calibration During Pneumotachography," Acta anaest.Scand., Supp.24, pp 119-126, 1966.
- [79] Lunn,J.N.,Molyneux,L.and Pask,E.A., "A Device for the Measurement of Ventilation in Young Children under General Anaesthesia," Anaesthesia,Vol.20,pp 135-144,1965.
- [80] Grenvik,A., Hedstrand,U. and Sjögren,H., "Problems in Pneumotachography," Acta anaesth. Scand.,Vol.10, pp 147-155, 1966.
- [81] Hill,D.W., "The Rapid Measurement of Respiratory Pressures and Volumes," Brit.J.Anaesth., Vol.31, pp 352-358, 1959.
- [82] Grenvik,A. and Hedstrand,U., "The Reliability of Pneumotachography in Respirator Ventilation," Acta anaesth.Scand., Vol.10, pp 157-167, 1966.
- [83] Osborn,J.J., Elliot,S.E., Seqyer,F.J. and Gerbode,F., "Continuous Measurement of Lung Mechanics and Gas Exchange in the Critically Ill," Medical Research Engineering, pp 19-23 and p 32, May-June, 1969.
- [84] Flora,C.M. "Process Measurement for Energy Management," Pulse, pp 25-29, March,1979.
- [85] Taylor,A., "Flow Measurement as an Afterthought," Measurement and Control, Vol.9. pp 207-208, June,1976.

- [86] Parker, G.A. and Hay, A.E., "A Planar Fluidic Flowmeter Applicable to Respiratory Flows," Trans. of ASME : J. Dynamic Systems, Measurement and Control, pp 293-299, December, 1977.
- [87] Cops, M.H. and Moore, J.H., "Electronic Petrol Systems Utilizing Corona Discharge Air Mass Flow Transducers," Lucas Engineering Review, paper first read to the S.A.E. International Automotive Engineering Congress, Detroit, in February, 1977.
- [88] Gerrard, J.H., "The Mechanics of the Formation Region of Vortices behind Bluff Bodies," J. Fluid Mech., Vol. 25(2), pp 401-413, 1966.
- [89] Burgess, T.H. "Flow Measurement using Vortex Principles," 'The Application of Flow Measuring Techniques,' Conference Proc., Inst. of Measurement and Control, Brighton, Sussex, U.K., 26-28 April, 1977.
- [90] White, D.F., Rodely, A.E. and McMurtrie, C.L., "The Vortex Shedding Flowmeter," pp 967-974, Symposium on Flow, 2-16-187, Pittsburgh, Pa., 1971.
- [91] Fischer and Porter Liquid Vortex Meter, type IOLV, Data Sheet, Fischer and Porter, Co, Pennsylvania, U.S.A., May, 1976.
- [92] Bourns Ventilation Monitor Model LS75 Instruction Manual, Bourns (Life Systems Division), California.
- [93] Ruiz, J.G. and Hernandez, M.J.G., "Problems and Solutions with Ultrasonic Pneumotachographs," XII International Conf. on Med. and Biol. Eng., Jerusalem, Israel, August, 19-24, 1979.

- [94] Bruun, H.H., "Interpretation of Hot-Wire Probe Signals in Subsonic Airflows," J.Phys.E : Sci.Instrum., Vol.12, p 1116-1128, 1979.
- [95] King, L.V., "On the Convection of Heat from Small Cylinders in a Stream of Fluid : Determination of the Convection Constants of Small Platinum Wires with Application to Hot-Wire Anemometry," Phil.Trans.R.Soc., A.214, pp 563-570, 1914.
- [96] Lumley, J.L., "The Constant Temperature Hot-Thermistor Anemometer," ASME Symposium on Measurement in Unsteady Flow, Worc., Mass., 1962.
- [97] Thermo-Systems Incorporated Technical Information Brochure, Minneapolis-St Paul, Minnesota.
- [98] Type 55M25 Lineariser, Technical Publication No. 5201E, Disa Elektronik, Skovlunde, Denmark, 1975.
- [99] Sakao, F., "Two Point Calibration of the Lineariser for a Hot-Wire Anemometer," J.Phys.E : Sci.Instrum., Vol.13, pp 1278-1279, 1980.
- [100] Kann, T., Hald, A. and Jørgensen, F.E., "A New Transducer for Respiratory Monitoring," Acta anaesth.Scand., Vol.23, pp 349-358, 1979.
- [101] Cox, P., Miller, L. and Petty, T.L., "Clinical Evaluation of a New Electronic Spirometer," Chest, Vol.63(4), pp 517-519, 1973.
- [102] Visick, W.D., Fairley, H.B. and Hickey, R.F., "Evaluation of a New Electronic Spirometer," Anaesthesiol., Vol.34, pp 475-478, 1971.

- [103] Appel, E., "Ein Thermistoranemometer zur Widerstandsformen Ventilationsmessung," Biomed. Techn., Vol.19; pp 112-117, 1974.
- [104] Catalogue MGP681 REV 6-78 Condensed Catalogue : Thermistors/Varistors Victory Engineering, Springfield, New Jersey, U.S.A.1978
- [105] Kramers, H., "Heat Transfer from Spheres to Flowing Media," Physica, Vol.12(2-3), pp 61-80, 1946.
- [106] Schultz, D.L., Tunstall-Pedoe, D.S., Der J. Lee, G., Gunning, A.J. and Bellhouse, B.J., "Velocity Distribution and Transition in the Arterial System," pp 172-202 in Circulatory and Respiratory Mass Transport, (Eds) Wolstenholme, G.E.W. and Knight, J., J.A.Churchill, Ltd, Pub., London, 1969.
- [107] Bellhouse, B.J. and Schultz, D.L., "The Measurement of Skin Friction in Supersonic Flow by means of Heated Thin-Film Gauges," Report No.1002, University of Oxford Engineering Laboratory, 1965.
- [108] CRC Handbook of Chemistry and Physics, 58th Edit., Chemical Rubber Pub.Co., Cleveland, Ohio, 1977.
- [109] Christman, P.J. and Podzimek, J., "Hot-Wire Anemometer Behaviour in Low Velocity Air Flow," J. Phys. E : Sci. Instrum., Vol.14, pp 46-51, 1981.
- [110] Mahajan, R.L. and Gebhart, B., "Hot-Wire Anemometer Calibration in Pressurised Nitrogen at Low Velocities," J. Phys. E : Sci. Instrum., Vol.13, pp 1110-1118, 1980.
- [111] Laurence, J.C. and Sandborn, V.A., "Heat Transfer from Cylinders," Trans. ASME Symposium on Measurements in Unsteady Flow, Worc. Mass, 1962.

- [112] Collis,D.C. and Williams,M.J., "Two-Dimensional Convection from Heated Wires at Low Reynolds' Number," J.Fluid Mech., Vol.6, pp 357-384, 1959.
- [113] Grant,W., Medical Gasses, their Properties and Use, H.M. and M. Publishers.
- [114] Bruun,H.H., "On the Temperature Dependence of Constant-Temperature Hot-Wire Probes with Small Wire Aspect Ratio," J.Phys.E.Sci.Instrum., Vol.8, pp 942-951, 1975.
- [115] Bruun,H.H., "Linearisation and Hot-Wire Anemometry," J.Phys.E.Sci.Instrum., Vol.4, pp 815-820, 1971.
- [116] Morrison,G.L., "Effects of Fluid Property Variations on the Response of Hot-Wire Anemometers," J.Phys.E.Sci.Instrum., pp 434-436, 1974.
- [117] De Villiers,J.F. and Diep,G.B., "Hot-Wire Measurements of Gas Mixture Concentrations in a Supersonic Flow," Disa Inf. No.14, pp 29-36, March, 1973.
- [118] Chevray,R. and Tutu,N.K., "Simultaneous Measurements of Temperature and Velocity in Heated Flows," Rev.Sci.Instrum., Vol.43, pp 1417-1421, 1972.
- [119] Grahn,A.R., Paul,M.H. and Wessel,H.U., "Design and Evaluation of a New Linear Thermistor Velocity Probe," J.Ap.Physiol., Vol.24(2), pp 236-246, 1968.
- [120] Sakao,F., "Constant-Temperature Hot Wires for Determining Velocity Fluctuations in an Air Flow accompanied by Temperature Fluctuations," J.Phys.E.Sci.Instrum., Vol.6, pp 913-916, 1973.

- [121] Zanker, K.J., "Flare Gas Flow Measurement," - the Agar FM 700 series flowmeters, Pulse, pp 26-28, August, 1979.
- [122] Grahn, A.R., Paul, M.H. and Wessel, H.U., "A New Direction-Sensitive Probe for Catheter-tip Thermal Velocity Measurements," J.Ap.Physiol., Vol. 27(3), pp 407-412, 1969.
- [123] Bruun, H.H., "Interpretation of a Hot-Wire Signal using a Universal Calibration Law," J.Phys.E.Sci. Instrum., Vol.4, pp 225-231, 1971.
- [124] Bruun, H.H., "A Digital Comparison of Linear and Non-Linear Hot-Wire Data Evaluation," J.Phys.E.Sci.Instrum., Vol.9, pp 53-57, 1976.
- [125] Kovasznay, L.S.G. and Chevray, R., "Temperature Compensated Linearizer for Hot-Wire Anemometer," Rev.Sci.Instrum., Vol.40(1), pp 91-94, 1969.
- [126] Champagne, F.H. and Lundberg, J.L., "Lineariser for Constant-Temperature Hot-Wire Anemometer," Rev.Sci.Instrum., Vol.37(7), pp 838-863, 1966.
- [127] Appel, E., "Ein Thermistor-Atemstromsensor mit Strömungsmessung im Nebenschluß", Biomed.Techn., Vol.22, pp 228-231, 1977.
- [128] Froebel, E., "A New Lineariser Unit for Hot-Wire Anemometry," DFVLR-Institut für Turbulenz Forschung, Berlin, Reports (as quoted by Bruun, [115]), 1969.
- [129] Freymouth, P. "Improved Linearisation for Hot-Wire Anemometers," J.Phys.E.Sci.Instrum., Vol.5, pp 533-534, 1972.

- [130] Elsner, J. and Gundlach, W.R., "Some Remarks on the Thermal Equilibrium Equation of Hot-Wire Probes," Disa Inf. 14, pp 21-24, March, 1973.
- [131] "Thermistor Data 1978/9", International Telephone and Telegraph Corporation Catalogue 6513/2066E, Ed. III, 1978.
- [132] de Oliveira, W.A., "Uncertainty in the Sensitivity of Thermistor Ebullioscopes," Rev. Sci. Instrum., Vol. 43(7), pp 1273-1280, 1977.
- [133] Thermistor Product Data, Thermometrics Inc., Edison, New Jersey.
- [134] Koch, F.A. and Gartshore, I.S., "Temperature Effects on Hot-Wire Anemometer Calibrations," J. Phys. E. Sci. Instrum., Vol. 5, pp 58-61, 1972.
- [135] Grant, H.P. and Kronaver, R.E., "Fundamentals of Hot-Wire Anemometry," Trans. ASME Symposium on Measurements in Unsteady Flow, pp 44-53, Worc. Mass., 1962.
- [136] Weidman, P.D. and Browand, F.K., "Analysis of a Simple Circuit for Constant Temperature Anemometry," J. Phys. E : Sci. Instrum., Vol. 8, pp 553-560, 1975.
- [137] Smits, A.J. and Perry, A.E., "The Effect of Varying Resistance Ratio on the Behaviour of Constant-Temperature Hot-Wire Anemometers," J. Phys. E : Sci. Instrum., Vol. 13, pp 451-456, 1980.
- [138] Freymouth, P., "Nonlinear Control Theory for Constant-Temperature Hot-Wire Anemometers," Rev. Sci. Instrum., Vol. 40(2), pp 258-262, 1969.

- [139] Freymouth, P., "Feedback Control Theory for Constant-Temperature Hot-Wire Anemometers," Rev.Sci.Instrum. Vol.38(5), pp 677-681, 1967.
- [140] Meijer, H., "Intrinsic Safety," Pulse, July, 1979.
- [141] Neergaard, K. and Wirz, K., "Über eine Methode zur Messung der Lungenlastizität am lebenden Menschen insbesondere beim Emphysem," Z.Klin.Med., 105, pp 51-82, 1927.
- [142] Neergaard, K., "Neue Auffassungen über einen Grundbegriff der Atemmechanik. Die Retraktionskraft der Lunge abhängig von der Oberflächenspannung in den Alveolen," Z.Ges.Exotl.Med. 66, pp 373-394, 1929.
- [143] Bobbaers, H., Clément, J. and van de Woestijne, K.P., "Impedance of the Lungs-Airways System during Breathing in Healthy Man," J.Biomechanics, Vol.10, pp 289-298, 1977.
- [144] Dosman, J., Bode, F., Urbanetti, J., Antic, R., Martin, R.R., Macklem, P.T., "Role of Inertia in Measurement of Dynamic Compliance," J.Ap.Physiol., Vol.38, pp 64-69, 1975.
- [145] Norlander, O.P., "Functional Analysis of Force and Power of Mechanical Ventilators," Acta anaesth.Scand., Vol.8, pp 57-77, 1964.
- [146] Behr, K., Engström, C. G. and Norlander, O.P., "Respiration Analyser for Assessment of Respiratory Power and Work," Acta anaesth.Scand. Suppl. 23, pp 175-179, 1966.

- [147] Engström, C.-G. and Norlander, O.P., "A New Method for Analysis of Respiratory Work by Measurements of the Actual Power as a Function of Gas Flow, Pressure and Time," Acta anaesth. Scand., Vol.6, pp 49-51, 1962.
- [148] Fletcher, G. and Bellville, J.W., "On-Line Computation of Pulmonary Compliance and Work of Breathing," J.Ap.Physiol., Vol.21, pp 1321-1327, 1965.
- [149] McIlroy, M.B., Marshall, R. and Christie, R.V., "The Work of Breathing in Normal Subjects," Clin.Sci., Vol.13, pp 127-136, 1954.
- [150] Thung, N., Herzog, P., Christlieb, I.I., Thompson, W.M., Jr, and Dammann, J.F., "The Cost of Respiratory Effort in Postoperative Cardiac Patients," Circulation, Vol. XXVIII, pp 552-559, October, 1963.
- [151] Cook, C.D., Sutherland, J.M., Segal, S., Cherry, R.B., Mead, J., McIlroy, M.B. and Smith, C.A., "Studies of Respiratory Physiology in the Newborn Infant. III Measurements of Mechanics of Respiration." J.Clin.Invest., Vol.36, pp 440-448, 1957.
- [152] Otis, A.B., Fenn, W.O. and Rahn, H., "Mechanics of Breathing in Man," J.Ap.Physiol., Vol.2, pp 592-607, 1950.
- [153] Krieger, I., "Studies on Mechanics of Respiration in Infants," Am.J. Diseases of Children, Vol.105, pp 439-449, 1963.
- [154] Richards, C.C. and Bachman, L., "Lung and Chest Wall Compliance of Apnoeic Paralyzed Infants," J.Clin.Invest., Vol.40, pp 273-278, 1961.

- [155] Egbert, L.D., Laver, M.B. and Bendixen, H.H., "Intermittent Deep Breaths and Compliance during Anaesthesia in Man," Anaesthesiol., Vol.24(1), pp 57-60, 1963.
- [156] Bodman, R.I., "Clinical Applications of Pulmonary Function Tests," Anaesthesia, Vol.18(5), pp 355-362, 1963.
- [157] Campbell, E.J.M. and Dinnick, O.P., "A Simple Method of Measuring the Compliance and Nonelastic Resistance of the Chest during Anaesthesia," Brit.J.Anaesth., Vol 31, pp 282-289, 1959.
- [158] Janney, C.D., "Super Syringe," Anesthesiol., Vol.20(5), pp 709-711, Sept./Oct., 1959.
- [159] Frank, N.R., Mead, J., Ferris, B.G., Jr, "The Behaviour of the Lungs in Healthy Elderly Persons," J.Clin.Invest., Vol.36, pp 1680-1687, 1957.
- [160] Murphy, B.G., Dosman, J., Bode, F. and Macklem, P.T., "A Dynamic Compliance Computer : Comparison of On-Line Results with Manual Calculations in Man," J.Ap.Physiol., Vol.36(5), pp 629-633, 1974.
- [161] McIlroy, M.B, Tierney, D.F. and Nadel, J.A., "A New Method for Measurement of Compliance and Resistance of Lungs and Thorax," J.Ap.Physiol., Vol.17, pp 424-427, 1963.
- [162] Yoo, J.H.K., Hander, E.W. and Petroff, P.A., "Implementation of Computation Algorithms for Pulmonary Mechanics on a Programmable Calculator," Med.and Biol.Eng. and Computing, pp 528-533, September, 1977.

- [163] Hewlett Packard Model 8816A Respiratory Analyser Data Sheet. Printed in U.S.A.2/75.
- [164] Mennen Greatback Respiratory Mechanics Monitoring System Data Sheet : "Concepts and Techniques - Respiratory Mechanics Monitoring," Mennen Greatback, Israel.
- [165] Mead, J. and Whittenberger, J.L., "Physical Properties of Human Lungs Measured During Spontaneous Respiration," J.Ap.Physiol., Vol.5, pp 779-796, 1953.
- [166] Miller, J.H. and Simmons, D.H., "Rapid Determination of Dynamic Pulmonary Compliance and Resistance," J.Ap.Physiol., Vol.15, pp 967-974, 1960.
- [167] Ostrander, L.E., Chester, E.H. and Franck, J.-B., "Fundamental Frequency Analysis of Pulmonary Mechanical Resistance and Compliance," J.Ap.Physiol., Vol.35(4), pp 526-537, October, 1973.
- [168] Nada, M.D. and Linkens, D.A., "An Adaptive Analogue Tracker for Automatic Measurement of Lung Parameters," Med.and Biol.Eng., pp 609-615, November, 1976.
- [169] Du Bois, A.B., Brody, A.W., Lewis, D.H. and Burgess, B.F., "Oscillation Mechanics of Lungs and Chest in Man," J.Ap.Physiol., Vol.8, pp 587-594, 1956.
- [170] Fisher, A.B., Du Bois, A.B. and Hyde, R.W., "Evaluation of the Forced Oscillation Technique for the Determination of Resistance to Breathing," J.Clin.Invest., Vol.47, pp 2045-2057, 1968.

- [171] Pimmel,R.L., Sunderland,R.A., Robinson,D.J., Williams,H.B., Hamlin,R.L. and Bromberg,P.A., "Instrumentation for Measuring Respiratory Impedance by Forced Oscillations," IEEE Trans. on Biomed. Eng., Vol.BME-24(2), pp 89-93, March,1977.
- [172] Schmid-Schoenbein,G.W. and Fung,Y.C., "Forced Perturbation of Respiratory System, B. A Continuum Mechanics Analysis," Annals of Biomed.Eng.,Vol.6, pp 367-398, 1978.
- [173] Ross,A.J., Raber,M.B., Kirk,B.W., and Goldstein,D.H., "Direct Readout of Respiratory Impedance,"Med.and Biol.Eng., pp 558-564, September,1976.
- [174] Hyatt,R.E., Zimmerman,I.R., Peters,G.M. and Sullivan,W.J., "Direct Writeout of Total Respiratory Resistance," J.Ap.Physiol., Vol.28(5), pp 675-678, May, 1970.
- [175] Pimmel,R.L., Williams,S.P., Fullton,J.M., Tsai,M.J., Winter,D.C. and Collier,A.M., "Respiratory Impedance and Derived Parameters in Small Children," University of North Carolina, An. Conf. for Eng. in Med. and Biol., pp 97-99. 1978.
- [176] Landser,F.J., Nagels,J., Demedts,M., Billiet,L. and van de Woestijne,K.P., "A New Method to Determine Frequency Characteristics of the Respiratory System," J.Ap.Physiol., Vol.41(1), pp 101-106, July,1976.
- [177] Varene,P. and Jacquemin,Ch., "Airways Resistance : A New Method of Computation," in Airway Dynamics : Physiology and Pharmacology, Bouhuys,A., (Ed), Charles C. Thomas, Springfield, Illinois, 1970, p 99. (Not seen, as quoted in reference [30])
- [178] Cassell,W.L., Linear Electric Circuits, J.Wiley and Sons, New York, 1966.

- [179] Freitag, J.J. and Miller, L.W., "Acute Respiratory Failure," Manual of Medical Therapeutics, (23 ed.), pp 143-158, Dept. of Medicine, Washington School of Medicine, Little Brown Pub.Co., 1980.
- [180] Macklem, P.T., "Physiology of the Peripheral Airways," Euromech.lecture, 1977. Draft obtained from author.
- [181] Comroe, J.H. (Jr), Foster (II), R.E., Dubois, A.B., Briscoe, W.H. and Carlson, E., The Lung : Clinical Physiology and Pulmonary Function Tests, (2nd edit.), Year Book Pub. Co., Chicago, 1962.
- [182] Hill, D.W. and Moore, V., "The Action of Adiabatic Effects on the Compliance of an Artificial Thorax," Br.J.Anaesth., Vol.37, pp 19-22, 1965.
- [183] Saklad, M. and Weyerhaeuser, R., "The Construction of Linear Resistances for the Testing of Ventilators," Lab. Report, Anesthesiol., Vol.52, pp 71-73, 1980.
- [184] Hill, D.W., Physics Applied to Anaesthesia, 3rd edit., London Butterworth, 411 pp, 1976.
- [185] Smith, W.D.A., "The Effects of External Resistance to Respiration, Part II : Resistance to Respiration due to Anaesthetic Apparatus," Brit.J.Anaesth., Vol.33, pp 610-627, 1961.
- [186] Non-Linear Circuits Handbook, (Ed) Sheingold, D.H., Analogue Devices, Norwood, Mass., 1976.
- [187] Burr Brown General Catalogue, 1979, Burr Brown, Tucson, Arizona, 1979.

- [188] Statham Pressure Transducers, Model P23 series, Data Sheet, Statham Instruments, California, February, 1967.
- [189] Graeme, G., Tobey, G. and Huelsman, L., Operational Amplifiers : Design and Applications, McGraw Hill, Kogakusha, Tokyo, 1971.
- [190] Analogue Devices Data Acquisition Catalogue (1978) and Supplement (1979), Analogue Devices, Norwood, Massachusetts.
- [191] Precision Monolithics Full Line Catalogue, 1979, Precision Monolithics, Santa Clara, California.
- [192] Nelson, C., "Monolithic Amp Delivers Instrument Precision," Electronic Design, pp 95-102, 9th July, 1981.
- [193] Duffy, W.T., McCormick, J.B., Hamilton, D.J. and Kerwin, W.J., "Distortion and Noise-Induced D.C. Offsets in Operational Amplifiers," IEEE Journal of Solid State Circuits, Vol.S.C.10(3), pp 161-167, June, 1967.
- [194] Sonderquist, D., "Minimisation of Noise in Operational Amplifier Applications," Precision Monolithics Application Note 15, 1979. Precision Monolithics, Santa Clara, California.
- [195] Graeme, J.G., Applications of Operational Amplifiers : Third Generation Techniques, McGraw Hill, New York, 1973.
- [196] Hedley-Whyte, J., Laver, M.B. and Bendixen, H.H., "Effect of Changes in Tidal Ventilation on Physiologic Shunting," Am.J.Physiol., Vol.206, pp 891-897, 1964.

- [197] Radford, E.P., Jr, "Theory of Mechanical Artificial Respiration," in Artificial Respiration Theory and Applications, Wittenberger, J.L., (ed.), pp 156-172, Hoeber, New York, 1962.
- [198] Avery, M.E. and Normand, C., "Respiratory Physiology in the Newborn Infant," Anesthesiol., Vol.26(4), pp 510-521, July-August, 1965.
- [199] Glauser, E.M., Cook, C.D. and Bougas, T.P., "Pressure Flow Characteristics and Dead Spaces of Endotracheal Tubes Used in Infants," Anesthesiol., Vol.22(3), pp 339-341, 1961.
- [200] Brown, E.S., "Resistance Factors in Pediatric Endotracheal Tubes and Connectors," Anaesthesia, Vol.50(3), pp 355-360, 1971.

BIBLIOGRAPHY

- Aalborg Data Sheet, Interchangeable Flowmeters for Liquids and Gases, from Aalborg Instruments and Controls, New York.
- Aga Data Sheet, Spirometer US 800, from Aga Medical AB, Sweden.
- Agostini, E. and Mead, J., "Statics of the Respiratory System," Handbook of Physiol.: Respiration, Vol. I, Fenn, W.O. and Rahn, H. (Eds), pp 387-409, American Physiol. Soc., Washington, 1964.
- American College of Chest Physicians, "The Assessment of Ventilatory Capacity," Chest, Vol. 67(1), pp 95-97, January, 1975.
- American National Standards Institute, American National Standard for Breathing Machines in Medical Use, ANSI Z.79.7 -1976, New York, 1976.
- Ammann, Elizabeth C.B. and Galvin, R.D., "Problems associated with the Determination of Carbon Dioxide by Infrared Absorption," J. Ap. Physiol., Vol. 25(3), pp 333-335, September, 1968.
- Analogue Devices Data Acquisition Catalogue (1978) and Supplement (1979), Analogue Devices, Norwood, Massachusetts.
- Analogue Devices Non-Linear Circuits Handbook, (Ed) Sheingold, D.H., Analogue Devices, Norwood, Mass., 1976.
- Appel, E., "Ein Thermistor-Atemstromsensor mit Strömungsmessung im Nebenschluss," Biomed. Techn., Vol. 22, pp 228-231, 1977.
- Appel, E., "Ein Thermistoranemometer zur Widerstandformen Ventilationsmessung," Biomed. Techn., Vol. 19, pp 112-117, 1974.
- Apter, Julia T. "Dynamic Compliance of Living Lungs before and after Perfusion," J. Biomech., Vol. 3, pp 77-85, 1970.
- Auld, P.A.M., Nelson, N.M., Cherry, Ruth B., Kudolph, A.J. and Smith, C.A., "Measurement of Thoracic Gas Volume in the Newborn Infant," J. Clin. Invest., Vol. 42, pp 476-483, 1963.
- Avery, M.E. and Normand, C., "Respiratory Physiology in the Newborn Infant," Anesthesiology, Vol. 26(4), pp 510-521, July-August, 1965.
- Barth, J., Fraser, R., Harvey, R. and Larson, D., "Measurement of Pulmonary Function in Infants and Children," U.S. Dept. of Commerce National Technical Information Service : PB 262 942, December, 1976.
- Behr, K., Engström, C. G and Norlander, O.P., "Respiration Analyser for Assessment of Respiratory Power and Work," Acta anaesth. Scand. Suppl. 23, pp 175-179, 1966.
- Bellhouse, B.J. and Schultz, D.L., "The Measurement of Skin Friction in Supersonic Flow by means of Heated Thin-Film Gauges," Report No. 1002, University of Oxford Engineering Laboratory, 1965.
- Bergman, N.A., "Effects of Varying Respiratory Waveforms on Gas Exchange," Anesthesiology, Vol. 28, pp 390-395, 1967.
- Bidani, A. and Flumerfelt, W., "Models of Respiratory Control," Chemical Engineering in Medicine, D.D. Rencan, Ed., Ch. 13, pp 268-289, Amer. Chem. Society, 1973.
- Bobbaers, H., Clément, J. and van de Woestijne, K.P., "Impedance of the Lungs-Airways System during Breathing in Healthy Man," J. Biomechanics, Vol. 10, pp 289-298, 1977.

- Bodman, R.I., "Clinical Applications of Pulmonary Function Tests," Anaesthesia, Vol.18(5), pp 355-362, 1963.
- Bourns LS104-150 Infant Ventilator and Accessories, Bourns (Life Systems Div.) data sheet, Aug., 1976, California.
- Bourns Ventilation Monitor Model LS75 Instruction Manual, Bourns (Life Systems Division), California.
- Brown, E.S., "Resistance Factors in Pediatric Endotracheal Tubes and Connectors," Anaesthesia and Analgesia, Vol.50(3), pp 355-360, 1971.
- Brown, T. and Fisk, G., Anaesthesia for Children, Blackwell, Oxford, 1979.
- Bruun, H.H., "Interpretation of a Hot-Wire Signal using a Universal Calibration Law," J.Phys.E.Sci.Instrum., Vol.4, pp 225-231, 1971.
- Bruun, H.H., "Linearisation and Hot-Wire Anemometry," J.Phys.E.Sci.Instrum., Vol.4, pp 815-820, 1971.
- Bruun, H.H., "On the Temperature Dependence of Constant-Temperature Hot-Wire Probes with Small Wire Aspect Ratio," J.Phys.E.Sci.Instrum., Vol.8, pp 942-951, 1975.
- Bruun, H.H., "A Digital Comparison of Linear and Non-Linear Hot-Wire Data Evaluation," J.Phys.E.Sci.Instrum., Vol.9, pp 53-57, 1976.
- Bruun, H.H. "Interpretation of Hot-Wire Probe Signals in Subsonic Airflows," J.Phys.E : Sci.Instrum., Vol.12, p 1116-1128, 1979.
- Burgess, T.H., "Flow Measurement using Vortex Principles," "The Application of Flow Measuring Techniques," Conference Proc., Inst. of Measurement and Control, Brighton, Sussex, U.K., 26-28 April, 1977.
- Burr Brown General Catalogue, 1979, Burr Brown, Tucson, Arizona, 1979.
- Bushman, J.A., "Effect of Different Flow Patterns on the Wright Respirometer," Br.J.Anaesth., Vol.51, pp 895-898, 1979.
- Campbell, D. and Brown, J., "The Electrical Analogue of Lung," Brit.J.Anaesth., Vol.35, pp 684-693, 1963.
- Campbell, E.J.M. and Dimnick, O.P., "A Simple Method of Measuring the Compliance and Nonelastic Resistance of the Chest during Anaesthesia," Brit.J.Anaesth., Vol.31, pp 282-289, 1959.
- Cassell, W.L., Linear Electric Circuits, J.Wiley and Sons, New York, 1966.
- Chakrabarti, M.K., Selman, B.J. and Whitwam, J.G., "A Spirometer for the Continuous Measurement of Tidal Volume," Br.J.Anaesth., Vol.49, pp 83-85, 1977.
- Champagne, F.H. and Lundberg, J.L., "Lineariser for Constant-Temperature Hot-Wire Anemometer," Rev.Sci.Instrum., Vol.37(7), pp 838-863, 1966.
- Chevray, R. and Tutu, N.K., "Simultaneous Measurements of Temperature and Velocity in Heated Flows," Rev.Sci.Instrum., Vol.43, pp 1417-1421, 1972.
- Christman, P.J. and Podzimek, J., "Hot-Wire Anemometer Behaviour in Low Velocity Air Flow," J.Phys.E : Sci.Instrum., Vol.14, pp 46-51, 1981.
- Chu, Josephine, S., Dawson, P., Klaus, M. and Sweet, A.Y., "Lung Compliance and Lung Volume Measured Concurrently in Normal Full-Term and Premature Infants," Paediatrics, Vol.34, pp 525-532, 1964.

- Clement, J. and van de Woestijne, K.P., "Pressure Correction in Volume and Flow-Displacement Body Plethysmography," J.Ap.Physiol., Vol.27(6), pp 895-897, 1969.
- Cogswell, J.J. "Forced Oscillation Technique for Determination of Resistance to Breathing in Children," Archives of Disease in Childhood, Vol.48, pp 259-266, 1973.
- Collis, D.C. and Williams, M.J., "Two-Dimensional Convection from Heated Wires at Low Reynolds Number," J.Fluid Mech., Vol.6, pp 357-384, 1959.
- Comroe, J.H., Nisell, O.I. and Nims, R.G., "A Simple Method for Concurrent Measurement of Compliance and Resistance to Breathing in Anesthetized Animals and Man," J.Ap.Physiol., Vol.7, pp 225-229, 1954.
- Comroe, J.H. (Jr), Foster (II), R.E., Dubois, A.B., Briscoe, W.H. and Carlson, E., The Lung: Clinical Physiology and Pulmonary Function Tests, (2nd edit.), Year Book Pub. Co., Chicago, 1962.
- Cook, C.D., Sutherland, J.M., Segal, S., Cherry, R.B., Mead, J., McIlroy, M.B. and Smith, C.A., "Studies of Respiratory Physiology in the Newborn Infant. III Measurements of Mechanics of Respiration," J.Clin.Invest., Vol.36, pp 440-448, 1957.
- Cops, M.H. and Moore, J.H., "Electronic Petrol Systems Utilizing Corona Discharge Air Mass Flow Transducers," Lucas Engineering Review, paper first read to the S.A.E. International Automotive Engineering Congress, Detroit, in February, 1977.
- Cournand, A., Motley, H.L., Werko, L. and Richards, D.W., "Physiological Studies of the Effects of Intermittent Positive Pressure Breathing on Cardiac Output in Man," Ame.J.of Physiol., Vol.52, pp 162-174, 1948.
- Cox, L.A., Almeida, A.P., Robinson, J.S. and Horsely, J.K., "An Electronic Respirometer," B.J.Anaesth., Vol.46, pp 302-310, 1974.
- Cox, P., Miller, L. and Petty, T.L., "Clinical Evaluation of a New Electronic Spirometer," Chest, Vol.63(4), pp 517-519, 1973.
- Crane, R.A. and Stuttard, B., "A Digital Technique for Linearising the Output of a Turbine Anemometer," Biomed.Eng., January, 1976.
- CRC Handbook of Chemistry and Physics, 58th Edit., Chemical Rubber Pub.Co., Cleveland, Ohio, 1977.
- Cromwell, L., Weibell, F.J., Pfeiffer, E.A. and Usselman, L.B., "Tests and Instrumentation for the Mechanics of Breathing, pp 185-187, in Biomedical Instrumentation and Measurements, Prentice-Hall, New Jersey, 1973.
- Cross, K.W., "The Respiratory and Ventilation in the Newborn Baby," J.Physiol., Vol.109, pp 459-474, 1949.
- Cross, K.W., "Respiration and Oxygen Supplies in the Newborn" Ch.52, Handbook of Physiology: Respiration, Vol.2, pp 1329-1343, (eds.) Fenn, W. and Rahn, H., Baltimore, Waverley Press, Inc., 1965.
- Cross, K.W. and Oppe, T.E., "The Respiratory Rate and Volume in the Premature Infant," J.Physiol., Vol.116, pp 168-174, 1952.
- Deal, C., Osborn, J.J., Ellis, E. and Gerbode, F., "Chest Wall Compliance," Annals of Surgery, Vol.167, pp 73-77, 1967.
- Dekker, E., "Transition between Laminar and Turbulent Flow in Human Trachea," J.Ap.Physiol., Vol.16(6), pp 1060-1064, 1961.
- de Oliveira, W.A., "Uncertainty in the Sensitivity of Thermistor Ebulioscopes," Rev.Sci.Instrum., Vol.43(7), pp 1273-1280, 1977.
- de Villiers, J.F. and Diep, G.B., "Hot-Wire Measurements of Gas Mixture Concentrations in a Supersonic Flow," Disa Inf. No.14, pp 29-36, March, 1973.

Disa Elektronik Type 55M25 Lineariser, Technical Publication No. 5901E, Disa Elektronik, Skovlunde, Denmark, 1975.

Disa Inf.11, "Improvements in Frequency Response," p 42, May, 1971.

Dornette, W., "Monitoring in Anesthesia," Clinical Anesthesia, Vol.9(2 and 3), F.Davis, Co., 1973.

Dosman, J., Bode, F., Urbanetti, J., Antic, R., Martin, R.R., Macklem, P.T., "Role of Inertia in Measurement of Dynamic Compliance," J.Ap.Physiol, Vol.38, pp 64-69, 1975.

Douma, J.H. and Wammes, L.J.A., "The Influence of the Composition and the State of the Gas on a Fleisch Pneumotachograph," Bull.Europ.Physio-path., Resp., Vol.14(4), pp 68-70, 1978.

Downes, J.J., "Mechanical Ventilation in the Newborn," Editorial, Anaesthesiol., Vol.34(2), pp 116-117, 1971.

du Bois, A.B., Brody, A.W., Lewis, D.H. and Burgess, B.F., "Oscillation Mechanics of Lungs and Chest in Man," J.Ap.Physiol., Vol.8, pp 587-594, 1956.

Dubois, A.B., "Resistance to Breathing," Handbook of Physiol.: Respiration, Vol.1, Fenn, W.O. and Rahn, H. (Eds), pp 451-461, American Physiol.Soc., Washington, 1964.

Duffy, W.T., McCormick, J.B., Hamilton, D.J. and Kerwin, W.J., "Distortion and Noise-Induced D.C. Offsets in Operational Amplifiers," IEEE Journal of Solid State Circuits, Vol.S.C.10(3), pp 161-167, June, 1967.

Egbert, L.D., Laver, M.B. and Bendixen, H.H., "Intermittent Deep Breaths and Compliance during Anaesthesia in Man," Anaesthesiol., Vol.24(1), pp 57-60, 1963.

Elliot, S.E., Shore, J.H., Barnes, C.W., Lindauer, J. and Osborn, J.J., "Turbulent Airflow Meter for Long-Term Monitoring in Patient-Ventilator Circuits," J.Ap.Physiol.; Respirat.Environ. Exercise Physiol., Vol.42(3), pp 456-460, 1977.

Elsner, J. and Gundlach, W.R., "Some Remarks on the Thermal Equilibrium Equation of Hot-Wire Probes," Disa Inf.14, pp 21-24, March, 1973.

Engelman, F.A., Jr., and Cook, A.M., "Digital Electronic Control of Automatic Ventilators," IEEE Trans. on Biomed.Eng., Vol.BME-24, pp 188-190, March, 1977.

Engström, C. G. and Norlander, O.P., "A New Method for Analysis of Respiratory Work by Measurements of the Actual Power as a Function of Gas Flow, Pressure and Time," Acta anaesth. Scand., Vol.6, pp 49-51, 1962.

Engström, I., Karlberg, P. and Swarts, C.L., "Respiratory Studies in Children: IX Relationships between Mechanical Properties of the Lungs, Lung Volume and Ventilatory Capacity in Healthy Children 7-15 years of Age," Acta Paediatrics, Vol.51, pp 68-80, Jan.1962.

Envil Spiroflo Lung Respiration Monitor, Tech-Spec 5005-74, data sheet, Envil Ltd, Summers Group, London.

Epstein, M.A.F. and Epstein, R.A., "Airway Flow Patterns during Mechanical Ventilation of Infants: A Mathematical Model," IEEE Trans. on Biomed.Eng., Vol.BME-26(5), pp 299-306, 1979.

Eyles, J.G. and Pimmel, R.L., "Estimating Respiratory Mechanical Parameters in Parallel Compartment Models," IEEE Trans.on Biomed.Eng., BME-28(4), pp 313-317, 1981.

- Fairley, H.B. and Blenkarn, G.D., "Effect on Pulmonary Gas Exchange of Variation in Respiratory Flow Rate during Intermittent Positive Pressure Ventilation," Brit.J.Anaesth., Vol.38, pp 320-328, 1966.
- Fenn, W.O. and Rahn, H. (Eds), Handbook of Physiol. : Respiration, Vol.I, American Physiol.Soc., Washington, 1964.
- Fenn, W.O. and Rahn, H. (Eds), Handbook of Physiol. : Respiration, Vol.II, American Physiol.Soc., Washington, 1965.
- Ferris, B.G., Jr, Mead, J. and Opie, L.H., "Partitioning of Respiratory Flow Resistance in Man," J.Ap.Physiol., Vol.19(4), pp 653-658, 1964.
- Finucane, K.E., Egan, B.A. and Dawson, S.V., "Linearity and Frequency Response of Pneumotachographs," J.Ap.Physiol., Vol.32(1), pp 121-126, 1972.
- Fischer and Porter Liquid Vortex Meter type IOLV data sheet, Fischer and Porter, Co., Pennsylvania, U.S.A., May, 1976.
- Fisher, A.B., Du Bois, A.B. and Hyde, R.W., "Evaluation of the Forced Oscillation Technique for the Determination of Resistance to Breathing," J.Clin.Invest., Vol.47, pp 2045-2057, 1968.
- Fishman, A., (ed.), Assessment of Pulmonary Function, New York, McGraw Hill, 1980.
- Fitzgerald, M.X., Smith, A.A. and Goensler, E.A., "Evaluation of Electronic Spirometers," New Eng. J.Med., Vol.289, pp 1283-1388, 1973.
- Fleisch, A., "Der Pneumotachograph : die Apparatur zur Geschwindigkeitsregistrierung der Atemluft" Plügers Arch. ges. Physiol., Vol.209, pp 713-722, 1925.
- Fleisch, Dr A., "The Pneumotachograph," data sheet from Instrumentation Associates, New York.
- Fleischer, L.S. and Bridge, J.F., "An Analytical Model of Inspiratory Gas Flow within the Human Bronchial Tree," ASME, Biomech.Div., Winter Annual Meeting, 17-22 November, 1974.
- Fletcher, G. and Bellville, J.W., "On-Line Computation of Pulmonary Compliance and Work of Breathing," J.Ap.Physiol., Vol.21, pp 1321-1327, 1965.
- Flora, C.M., "Process Measurement for Energy Management," Pulse, pp 25-29, March, 1979.
- Frank, N.R., Mead, J., Ferris, B.G., Jr, "The Behaviour of the Lungs in Healthy Elderly Persons," J.Clin.Invest., Vol.36, pp 1680-1687, 1957.
- Fredberg, J.J., "A Model Perspective of Lung Response," J.Acoust.Soc.Amer., Vol.63(3), pp 962-966, Mar.1978.
- Freitag, J.J. and Miller, L.W., "Acute Respiratory Failure," Manual of Medical Therapeutics, (23 ed.) pp 143-158, Dept. of Medicine, Washington School of Medicine, Little Brown Pub.Co., 1980.
- Frey-mouth, P., "Feedback Control Theory for Constant-Temperature Hot-Wire Anemometers," Rev.Sci.Instrum., Vol.38(5), pp 677-681, 1967.
- Frey-mouth, P., "Compensation for the Thermal Lag of a Thin-Wire Resistance Thermometer by means of a Constant-Temperature Hot-Wire Anemometer," J.Phys.E.Sci.Instrum., Vol.2, pp 1001-1002, 1969.
- Frey-mouth, P., "Nonlinear Control Theory for Constant-Temperature Hot-Wire Anemometers," Rev.Sci.Instrum., Vol.40(2), pp 258-262, 1969.

Freyemouth, P., "Improved Linearisation for Hot-Wire Anemometers," J. Phys. E. Sci. Instrum., Vol. 5, pp 533-534, 1972.

Froebel, E., "A New Lineariser Unit for Hot-Wire Anemometry," DFVLR-Institut für Turbulenz Forschung, Berlin, Reports (as quoted by Bruun, [1151]), 1969.

Frost and Sullivan, Inc., Report 625, Frost and Sullivan, Inc., 106 Fulton Street, New York, NY 10038, as quoted in Medical and Biological Engineering and Computing, March, 1980.

Fry, D.L., Hyatt, R.E., McCall, C.B. and Mallos, A.J., "Evaluation of Three Types of Respiratory Flowmeters," J. Ap. Physiol., Vol. 10(2), pp 210-214, 1957.

Fry, D.L. and Hyatt, R.E., "A Unified Analysis of the Relationship between Pressure, Volume and Gasflow in the Lungs of Normal and Diseased Human Subjects," Ame. J. Med., Vol. 22, pp 672-689, October, 1960.

Fung, Y.-C., "Does the Surface Tension Make the Lung Inherently Unstable?" Circulation Research, Vol. 37, pp 497-502, October, 1975.

Gerbode, F., "Computerised Monitoring of Seriously Ill Patients," J. Thoracic and Cardiovascular Surgery, Vol. 66(2), pp 167-174, August, 1973.

Gerrard, J.H., "The Mechanics of the Formation Region of Vortices behind Bluff Bodies," J. Fluid Mech., Vol. 25(2), pp 401-413, 1966.

Geubelle, F. and de Rudder, P., "Respiratory Studies in Children: II Functional Residual Capacity in Healthy Children," Acta Paediatrica, Vol. 50, pp 277-282, May, 1961.

Glauser, E.M., Cook, C.D. and Bougas, T.P., "Pressure Flow Characteristics and Dead Spaces of Endotracheal Tubes Used in Infants," Anaesthesiol., Vol. 22(3), pp 339-341, 1961.

Goldman, M., Knudson, R.J., Mead, J., Peterson, N., Schwaber, J.R., and Wohl, Mary E., "A Simplified Measurement of Respiratory Resistance by Forced Oscillation," J. Ap. Physiol., Vol. 28(1), pp 113-116, January, 1970.

Graeme, J.G., Applications of Operational Amplifiers: Third Generation Techniques, McGraw Hill, New York, 1973.

Graeme, G., Tobey, G. and Huelsman, L., Operational Amplifiers: Design and Applications, McGraw Hill, Kogakusha, Tokyo, 1971.

Grahn, A.R., Paul, M.H. and Wessel, H.U., "Design and Evaluation of a New Linear Thermistor Velocity Probe," J. Ap. Physiol., Vol. 24(2), pp 236-246, 1968.

Grahn, A.R., Paul, M.H. and Wessel, H.U., "A New Direction-Sensitive Probe for Catheter-tip Thermal Velocity Measurements," J. Ap. Physiol., 27(3), pp 407-412, 1969.

Grant, W., Medical Gases, their Properties and Use, H.M. and M. Publishers.

Grant, H.P. and Kronaver, R.E., "Fundamentals of Hot-Wire Anemometry," Trans. ASME Symposium on Measurements in Unsteady Flow, pp 44-53, Worc. Mass., 1962.

Grenvik, A., "Respiratory, Circulatory and Metabolic Effects of Respirator Treatment," Acta anaesth. Scand., Suppl. 19, pp 1-121, 1966.

Grenvik, A., Hedstrand, U. and Sjögren, H., "Problems in Pneumotachography," Acta anaesth. Scand., Vol. 10, pp 147-155, 1966.

Grenvik, A. and Hedstrand, U., "The Reliability of Pneumotachography in Respirator Ventilation," Acta anaesth. Scand., Vol. 10, pp 157-167, 1966.

Haddad, C. and Richards, C.C., "Mechanical Ventilation of Infants: Significance and Elimination of Ventilator Compression Volume," Anesthesiol., Vol. 29(2), pp 365-370, 1968.

- Haddy, Theresa B. and Haddy, Francis J., "The Effect of Acute Pulmonary Edema upon Lung Compliance," Pediatrics, Vol. 33, pp 55-62, January, 1964.
- Hald, A. and Stigsby, B., "Computerised Hot-Wire Anemometry - Principles of Calculation," Computer Programs in Biomedicine 11, pp 113-118, 1980.
- Hall, K.D. and Reeser, F.H. (Jr), "Calibration of Wright Spirometer," Anaesthesiol., Vol. 23(1), pp 126-129, 1962.
- Harrison, V.C., Hyaline Membrane Disease: A Study of Function and Treatment, (Doctor of Medicine Thesis), University of Cape Town, August, 1967.
- Heaf, P.J.D. and Prime, F.J., "The Compliance of the Thorax in Normal Human Subjects," Clin.Sci., Vol. 15, pp 319-327, 1956.
- Hedley-Whyte, J., Laver, M.B. and Bendixen, H.H., "Effect of Changes in Tidal Ventilation on Physiologic Shunting," Am.J.Physiol., Vol. 206, pp 891-897, 1964.
- Helliesen, P.J., Cook, C.D., Friedlander, M.D. and Agathon, S., "Studies of Respiratory Physiology in Children: I. Mechanics of Respiration and Lung Volumes in 85 Normal Children 5 to 17 years of Age," Pediatrics, Vol. 30, pp 80-93, December, 1962.
- Herzog, P. and Norlander, O.P., "A Precision Method for the Dynamic Volume-Flow Calibration During Pneumotachography," Acta anaest.Scand., Supp. 24, pp 119-126, 1966.
- Hewlett Packard Model 8816A Respiratory Analyser Data Sheet, printed U.S.A. 2/75.
- Hewlett-Packard, Medical Products Group, Catalogue, Respiratory Care Products, printed U.S.A. 5/75.
- Hilberman, M. Schill and Peters, K.M., "Respiratory Mechanics and Respirator Control," J.Thoracic and Cardiovascular Surg., Vol. 58(6), pp 821-828. December, 1969.
- Hilberman, M., "Monitoring in the Operating Room: Current Techniques and Future Requirements," Med.Instrum., Vol. 11(5), pp 283-287, 1977.
- Hill, D.W., "The Rapid Measurement of Respiratory Pressures and Volumes," Brit. J.Anaesth., Vol. 31, pp 352-358, 1959.
- Hill, D.W., Electronic Measurement Techniques in Anaesthesia and Surgery, 2nd edit, London, Butterworth, 421 pp, 1973.
- Hill, D.W., Physics Applied to Anaesthesia, 3rd edit., London, Butterworth, 411 pp, 1976.
- Hill, D.W. and Moore, V., "The Action of Adiabatic Effects on the Compliance of an Artificial Thorax," Br.J.Anaesth., Vol. 37, pp 19-22, 1965.
- Hingorani, B.K., "The Resistance to Airflow of Tracheotomy Tubes, Connections, and Heat and Moisture Exchangers," Brit.J.Anaesth., Vol. 37, pp 454-462, 1965.
- Hyatt, R.E., Shilder, D.P. and Fry, D.I., "Relationship between Maximum Expiratory Flow and Degree of Lung Inflation," J.Ap.Physiol., Vol. 13, pp 331-336, 1958.
- Hughes, T.J., "Measuring 'Instantaneous' Active and Reactive Power - Part I: Active Power," University of Cape Town, Dept.Elec.Eng.Research Review, Vol. 1, No. 3, pp 22-24, 1 June, 1977.
- Hughes, T.J., "Measuring 'Instantaneous' Active and Reactive Power - Part II: Reactive Power," University of Cape Town, Dept.Elec.Eng.Research Review, Vol. 2, No. 1, pp 25-27, February, 1978.

Karlberg, P., Cherry, R.B., Escardó, F.E. and Koch, G., "Respiratory Studies in Newborn Infants: II. Pulmonary Ventilation and Mechanics of Breathing in the First Minutes of Life, including the Onset of Respiration," Acta Paediatrica, Vol.51, pp 121-128, March, 1962.

Karlberg, P. and Koch, G., "Respiratory Studies in Newborn Infants: III Development of Mechanics of Breathing during the First Week of Life. A Longitudinal Study," Acta Paediatrica, Suppl.135, pp 121-129, 1962.

Keuskamp, D.H.G., (ed.), Neonatal and Pediatric Ventilation, International Anesthesiology Clinics, Vol.12(4), Little, Brown, Co., Boston, 1974.

King, J.V., "On the Convection of Heat from Small Cylinders in a Stream of Fluid: Determination of the Convection Constants of Small Platinum Wires with Application to Hot-Wire Anemometry," Phil.Trans.R.Soc., A.214, pp 563-570, 1914.

Koch, F.A. and Gartsshore, I.S., "Temperature Effects on Hot-Wire Anemometer Calibrations," J.Phys.E.Sci.Instrum., Vol.5, pp 58-61, 1972.

Kovacs, L.S.G. and Chevray, R., "Temperature Compensated Linearizer for Hot-Wire Anemometer," Rev.Sci.Instrum., Vol.40(1), pp 91-94, 1969.

Kramers, H., "Heat Transfer from Spheres to Flowing Media," Physica, Vol.12(2-3), pp 61-80, 1946.

Krieger, I., "Studies on Mechanics of Respiration in Infants," Am.J.Of Diseases of Children, Vol.105, pp 439-449, 1963.

Krieger, I., "Mechanics of Respiration in Bronchiolitis," Pediatrics, Vol.33, pp 45-54, 1964.

Hyatt, R.E., Zimmerman, I.R., Peters, G.M. and Sullivan, W.J., "Direct Writeout of Total Respiratory Resistance," J.Ap.Physiol., Vol.28(5), pp 675-678, May, 1970.

International Electrotechnical Commission Publication 601-1, Safety of Medical Electrical Equipment, Geneva, 1977.

International Telephone and Telegraph Corporation Catalogue 6513/2066E, Ed.III, 1978, "Thermistor Data 1978/9".

Jackson, A.C., Butler, J.P. and Pyle, R.W., Jr, "Acoustic Input Impedance of Excised Dogs Lungs," J.Acoust.Soc.Am., Vol.64(4), pp 1020-1026, October, 1978.

Jaeger, M.J. and Matthys, H., "The Pattern of Flow in the Upper Human Airways," Resp.Physiol., Vol.6, pp 113-127, 1968/69.

Jain, N.K., "Optimal Respiration Settings in Assisted Respiration," Med.Biol.Eng., Vol.12, pp 425-430, 1974.

Janney, C.D., "Super Syringe," Anesthesiol., Vol.20(5), pp 709-711, Sept./Oct., 1959.

Johansson, H., "Effects of Different Inspiratory Gas Flow Patterns on Thoracic Compliance during Respiration Treatment," Acta anaesth.Scand., Vol.19, pp 89-95, 1975.

Kanevče, G. and Oka, S., "Correcting Hot-Wire Readings for Influence of Fluid Temperature Variations," Disa Inf. 15, pp 21-24, October, 1973.

Kann, T., Hald, A. and Jørgensen, F.E., "A New Transducer for Respiratory Monitoring," Acta anaesth.Scand., Vol.23, pp 349-358, 1979.

- Landser, F.J., Nagels, J., Demedts, M., Billiet, L. and van de Woestijne, K.P., "A New Method to Determine Frequency Characteristics of the Respiratory System," J.Ap.Physiol., Vol.41(1), pp 101-106, July, 1976.
- Laurence, J.C. and Sandborn, V.A., "Heat Transfer from Cylinders," Trans. ASME Symposium on Measurements in Unsteady Flow, Worc.Mass, 1962.
- Lilly, J.C., "Flowmeter for Recording Respiratory Flow in Human Subjects," in Methods in Medical Research, Silverman, L. and Whittenberger, J.L. (Eds), Year Book Publishing Co., Chicago, 1950.
- Lindahl, S. and Okmian, L., "Experimental Studies on Artificial Ventilation using a Tidal Volume Ventilator," Acta anaesth.Scand., Vol.23, pp 359-369, 1979.
- Lindahl, S., Kugelberg, J. and Okmian, L., "The Circulatory Response to Specific Ventilatory Patterns using a Tidal Volume Ventilator," Acta anaesth.Scand., Vol.23, pp 370-378, 1979.
- Lindahl, S., Arborelius, M. and Okmian, L., "Influence of Ventilatory Frequencies and Ventilator Volume/Pressure Quotients on Pulmonary Ventilation using a Tidal Volume Ventilator," Acta anaesth.Scand., Vol.23, pp 379-394, 1979.
- Lindahl, S., Okmian, L. and Thomson, D., "Artificial Ventilation in Children during Anaesthesia using Tidal Volume Ventilator," Acta anaesth.Scand., Vol.23, pp 587-595, 1979.
- Loeber, N.V. and Downes, J.J., "Lung Function in Chronic Respiratory Failure in Infancy," Anesthesiol., Vol.51(3), ASA Abstract 328, 1978.
- Lu, S.S., "Dynamic Characteristics of a Simple Constant-Temperature Hot-Wire Anemometer," Rev.Sci.Instrum., Vol.50(6), pp 772-775, 1979.
- Lumley, J.L., "The Constant Temperature Hot-Thermistor Anemometer," ASME Symposium on Measurement in Unsteady Flow, Worc., Mass., 1962.
- Lunn, J.N., Molyneux, L. and Pask, E.A., "A Device for the Measurement of Ventilation in Young Children under General Anaesthesia," Anaesthesia, Vol.20, pp 135-144, 1965.
- Machattie, L.E., "A Transistor Anemometer," J.Phys.E : Sci.Instrum., Vol.14, pp 80-82, 1981.
- Macklem, P.T., "Physiology of the Peripheral Airways," EuroMech.lecture, 1977. Draft obtained from author.
- Mahajan, R.L. and Gebhart, B., "Hot-Wire Anemometer Calibration in Pressurised Nitrogen at Low Velocities," J.Phys.E : Sci.Instrum., Vol.13, pp 1110-1118, 1980.
- Man Moon, I., "Direction-Sensitive Hot-Wire Anemometer for Two Dimensional Flow Study near a Wall," Trans. ASME Symposium on Measurements in Unsteady Flow, pp 71-74, Worc.Mass., 1962.
- Mansell, A., Levison, H., Kruger, K. and Tripp, T.L., "Measurement of Respiratory Resistance in Children in Forced Oscillations," Am.Rev.Resp.Dis., Vol.106, pp 710-714, 1972.
- Marshall, R., McIlroy, M.B. and Christie, R.V., "The Work of Breathing in Mitral Stenosis," Clin.Sci., Vol.13, pp 137-146, 1954.
- Marshall, R., "Objective Tests of Respiratory Mechanics," Handbook of Physiol. : Respiration, Vol.II, Fenn, W.O. and Rahn, H. (Eds), pp 1399-1411, American Physiol.Soc., Washington, 1965.
- Mattila, M.A.K., "The Role of the Physical Characteristics of the Respiator in Artificial Ventilation of the Newborn," Acta anaesth.Scand., Suppl.56, pp 1-107, 1974.

- McCall, C.B., Hyatt, R.E., Noble, F.W. and Fry, D.L., "Harmonic Content of Certain Respiratory Flow Phenomena of Normal Individuals," J.Ap.Physiol., Vol.10, pp 215-218, 1957.
- McIlroy, M.B., Marshall, R. and Christie, R.V., "The Work of Breathing in Normal Subjects," Clin.Sci., Vol.13, pp 127-136, 1954.
- McIlroy, M.B. and Christie, R.V., "The Work of Breathing in Emphysema," Clin.Sci., Vol.13, pp 147-154, 1954.
- McIlroy, M.B., Tierney, D.F. and Nadel, J.A., "A New Method for Measurement of Compliance and Resistance of Lungs and Thorax," J.Ap.Physiol., Vol.17, pp 424-427, 1963.
- Mead, J. and Agostini, E., "Dynamics of Breathing," Handbook of Physiol. : Respiration, Vol.1, Fenn, W.O. and Rahn, H. (Eds), pp 411-427, American Physiol.Soc., Washington, 1964.
- Mead, J. and Milic-Emili, "Theory and Methodology in Respiratory Mechanics with Glossary of Symbols," Handbook of Physiol. : Respiration, Vol.1, Fenn, W.O. and Rahn, H. (Eds), pp 363-376, American Physiol.Soc., Washington, 1964.
- Mead, J. and Whittenberger, J.L., "Physical Properties of Human Lungs Measured during Spontaneous Respiration," J.Ap.Physiol., Vol.5, pp 779-796, 1953.
- Measurement and Control, "Vortex Shedding applied to Flow Metering," Vol.6, p 179, May, 1973.
- Meier, A. and Baum, M., "The Influence of the Internal Compliance of a Resistor on the Alveolar Gas Distribution," Acta anaesth.Scand., Suppl.63, pp 1-20, 1976.
- Meijer, H., "Intrinsic Safety," Pulse, July, 1979.
- Mennen Greatback, Israel, Respiratory Mechanics Monitoring System Data Sheet : "Concepts and Techniques - Respiratory Mechanics Monitoring."
- Mercury Lung Function Analysers Data Sheet, (Models LA 2 to LA 5), Mercury Electronics, Glasgow, Scotland.
- Meriam Laminar Flow Elements, Bulletin File No.501-215-3 from Meriam Instrument, Cleveland, Ohio.
- Micro Medical MM10 Digital Thermistor Spirometer Operator's Manual, Micro Medical, U.S.A.
- Miller, J.H. and Simmons, D.H., "Rapid Determination of Dynamic Pulmonary Compliance and Resistance," J.Ap.Physiol., Vol.15, pp 967-974, 1960.
- Milner, A.D., "Assessment of Respiratory Function in Childhood and Infancy," Recent Advances in Paediatrics, 4th edit., Gairdner, D., Hull, D. (Eds), pp 217-244, Churchill, London, 1971.
- Minato AS-700 Autospirometer Manual, Minato Med.Sc., Co., Osaka, Japan.
- Mithoefer, J.C., Bossman, D.G., Thibeault, D.W. and Mead, G.D., "The Clinical Estimation of Alveolar Ventilation," Am.Rev.Resp.Dis., Vol.98, pp 868-871, 1968.
- Miyakawa, M., Yamamoto, K. and Mikami, T., "Acoustic Measurement of the Respiratory System - An Acoustic Pneumograph," Med.and Biol.Eng., pp 653-659, November, 1976.
- Miyamoto, Y. and Mikami, T., "An On-Line Device for the Continuous Measurement of Airways Resistance," Med.and Biol.Eng., pp 631-636, September, 1975.
- Mollee, C.S. and Vitale, P., "Thermistors make Good Thermometers - if you know how to linearize the Operation of these Semiconductor Elements to make them fit your Temperature Range," Electronic Design 8, pp 90-92, April, 1978.

- Morrison, G.L., "Effects of Fluid Property Variations on the Response of Hot-Wire Anemometers," J. Phys. E. Sci. Instrum., pp 434-436, 1974.
- Morrison, G.L., "Errors in Heat Transfer Laws for Constant-Temperature Hot-Wire Anemometers," J. Phys. E. Sci. Instrum., Vol. 9, pp 50-52, 1976.
- Munson, E.S., Farnham, M. and Hamilton, W.K., "Studies of Respiratory Gas Flows: A Comparison using Different Anaesthetic Agents," Anaesthesiol., Vol. 24(1), pp 61-67, 1963.
- Murphy, B.G., Dosman, J., Bode, F. and Macklem, P.T., "A Dynamic Compliance Computer: Comparison of On-Line Results with Manual Calculations in Man," J. Ap. Physiol., Vol. 36(5), pp 629-633, 1974.
- Mushin, W.W., Mapleson, W.W. and Lunn, J.N., "Problems of Automatic Ventilation in Infants and Children," Brit. J. Anaesth., Vol. 34, pp 514-522, 1962.
- Mushin, W.W., Rendall-Baker, L.K., Thompson, P.W. and Mapleson, W.W., Automatic Ventilation of the Lungs, 2nd edit., London: Blackwell Scientific Publications, 1969.
- Nada, M.D. and Linkens, D.A., "An Adaptive Analogue Tracker for Automatic Measurement of Lung Parameters," Med. and Biol. Eng., pp 609-615, November, 1976.
- National Semiconductor Data Book on Transducers, Pressure and Temperature, National Semiconductor, Santa Clara, California, 1974.
- National Semiconductor Pressure Transducer Handbook, National Semiconductor, Santa Clara, California, 1977.
- Neergaard, K., "Neue Auffassungen über einen Grundbegriff der Atemmechanik. Die Retraktionskraft der Lunge abhängig von der Oberflächenspannung in den Alveolen," Z. Ges. Exptl. Med., pp 373-394, 1929.
- Neergaard, K. and Wirz, K., "Über eine Methode zur Messung der Lungenlastizität am Lebenden Menschen insbesondere beim Emphysem," Z. Klin. Med., 105, pp 51-82, 1927.
- Nelson, C., "Monolithic Amp Delivers Instrument Precision," Electronic Design, pp 95-102, 9th July, 1981.
- Nelson, N.M., Prod'hom, L.S., Cherry, R.B., Lipsitz, P.J. and Smith, C.A., "Pulmonary Function in the Newborn Infant: I. Methods - Ventilation and Gaseous Metabolism," Pediatrics, Vol. 30, pp 963-974, December, 1962.
- Nelson, N.M., Prod'hom, L.S., Cherry, R.B., Lipsitz, P.J. and Smith, C.A., "Pulmonary Function in the Newborn Infant: II. Perfusion - Estimation by Analysis of the Arterial Carbon Dioxide Difference," Pediatrics, Vol. 30, pp 975-989, December, 1962.
- Nemerovskii, L.I., "Modeling of the Amplitude-Frequency Response of the Pulmonary Air Tract," Sov. Phys. Acoust., Vol. 24(3), pp 215-217, May-June, 1978.
- Neuerburg, W., "Directional Hot-Wire Probe," Disa Inf. No. 7, January, 1969.
- Nisell, O. and Ehrner, L., "The Resistance to Breathing Determined from Time-Marked Respiratory Pressure Volume Loops," Acta med. Scand., Vol. CLXI, pp 427-434, 1958.
- Nisell, O. and Ehrner, L., "A Simple Apparatus for Measurement of Pressure Volume Relationship in Respiration," J. Ap. Physiol., Vol. 8, pp 565-567, 1956.
- Norlander, O.P., "Functional Analysis of Force and Power of Mechanical Ventilators," Acta anaesth. Scand., Vol. 8, pp 57177, 1964.

- Raemer, D.B., Westenskow, D.R., Gehmlich, D.K., Richardson, C.P. and Jordan, W.S., "A Method for Measurement of Oxygen Uptake in Neonates," J.Ap.Physiol., Respirat.Environ.Exercise Physiol., Vol.46(6), pp 1200-1204, 1979.
- Rashad, K.F., "The Mechanical Respirator and the Pediatric Patient," Surg.Clin.N.Am., Vol.50(4), pp 781-785, 1970.
- Rattenborg, C.C. and Holaday, D.A., "Constant Flow Inflation of the Lungs: Theoretical Analysis," Acta anaesth.Scand., Suppl.23, 211-223, 1966.
- Richards, C.C. and Bachman, L., "Lung and Chest Wall Compliance of Apnoeic Paralyzed Infants," J.Clin.Invest., Vol.40, pp 273-278, 1961.
- Rolfe, P., "Instruments for the Care of Ill Newborn Babies," Electronics and Power, Vol.23, pp 32-39, January, 1977.
- Ross, A.J., Raber, M.B., Kirk, B.W. and Goldstein, D.H., "Direct Readout of Respiratory Impedance," Med.and Biol.Eng., pp 558-564, September, 1976.
- Ruiz, J.G. and Hernandez, M.J.G., "Problems and Solutions with Ultrasonic Pneumotachographs," XII International Conf. on Med. and Biol. Eng., Jerusalem, Israel, August, 19-24, 1979.
- Sakao, F., "Constant-Temperature Hot Wires for Determining Velocity Fluctuations in an Air Flow accompanied by Temperature Fluctuations," J.Phys.E.Sci.Instrum., Vol.6, pp 913-916, 1973.
- Sakao, F., "Two Point Calibration of the Lineariser for a Hot-Wire Anemometer," J.Phys.E : Sci.Instrum., Vol.13, pp 1278-1279, 1980.
- Saklad, M. and Weyerhaeuser, R., "The Construction of Linear Resistances for the Testing of Ventilators," Lab.Report, Anesthesiology, Vol.52, pp 71-73, 1980.
- Saklad, M.D., Sullivan, M., Pallotta, J. and Lipsky, M., "Pneumotachography: A New, Low-Dead-Space, Humidity-Independent Device," J.Phys.E : Sci.Instrum., Vol.14, pp 149-153, 1981.
- Schmid-Schoenbein, G.W. and Fung, Y.C., "Forced Perturbation of Respiratory System, B. A Continuum Mechanics Analysis," Annals of Biomed.Eng., Vol.6, pp 367-398, 1978.
- Schultz, D.L., Tunstall-Pedoe, D.S., Der J.Lee, G., Gunning, A.J. and Bellhouse, B.J., "Velocity Distribution and Transition in the Arterial System," pp 172-202 in Circulatory and Respiratory Mass Transport, (Eds) Wolstenholme, G.E.W. and Knight, J., Messrs J.A.Churchill, Ltd, pub., London, 1969.
- Schultz, D.L., Tunstall-Pedoe, D.S., Lee, G.de J., Gunning, A.J. and Bellhouse, B.J., "Velocity Distribution and Transition in the Arterial System," Internal Report, Oxford Univ.Dept.Eng. Sc. and Cardiac and Surgery Depts., Radcliffe Infirmary.
- Schwaber, J.R. and Mead, J., "Use of a Modified Thunberg Barospirator to Determine Airway Resistance in Man," J.Ap.Physiol., Vol.25(3), pp 328-332, September, 1968.
- Shaffer, T., "Limitations of Frequency Dependence as a Measure of Airways Obstruction," IEEE Trans.on Biomed.Eng., Vol.BME-22(4), pp 317-321, July, 1975.
- Sharp, J.T., Henry, J.P., Sweeney, S.K., Meadows, W.R. and Pictros, R.J., "Total Respiratory Inertance and Its Gas and Tissue Components in Normal and Obese Men," J.Clin.Invest., Vol.43(3), pp 503-509, 1964.

- Pedley, T.J., Schroter, R.C. and Sudlow, M.F., "The Prediction of Pressure Drop and Variation of Resistance within the Human Bronchial Airways," Respiration Physiology, 9, pp 387-405, 1970, North Holland Pub.Co., Amsterdam.
- Peslin, R., Papon, J., Duvivier, C. and Richalet, J., "Frequency Response of the Chest : Modeling and Parameter Estimation," J.Ap.Physiol., Vol.39(4), pp 523-534, October, 1975.
- Peslin, R., Jardin, P. and Hannhart, B., "Modeling of the Relationship between Volume Variations at the Mouth and Chest," J.Ap.Physiol., Vol.41(5), pp 659-667, November, 1976.
- Peters, R.M. and Hilberman, M., "Respiratory Insufficiency : Diagnosis and Control of Therapy," Surgery 70(2), pp 280-287, 1971.
- Peters, R.M., Hilberman, M., Hogan, J.S. and Cranford, D.A., "Objective Indications for Respirator Therapy in Post-Trauma and Post-Operative Patients," Am.J.Surg., Vol.124, pp262-269, 1972.
- Phoenix T.M.F. Spirometer Data Sheet, Phoenix Abboflex and Instruments, Ltd, Abercainid, Merthyr, Tydfil, South Wales (Senior Engineering Group, Ltd).
- Pichon, J., "Comparison of Some Methods of Calibrating Hot-Film Probes in Water," Disa Inf. 10, pp 15-21, October, 1970.
- Pimmel, R.L., Sunderland, R.A., Robinson, D.J., Williams, H.B., Hamlin, R.L. and Bromberg, P.A., "Instrumentation for Measuring Respiratory Impedance by Forced Oscillations," IEEE Trans.on Biomed.Eng., Vol.BME-24(2), pp 89-93, March, 1977.
- Pimmel, R.L., Wintor, D.C. and Bromberg, P.A., "Forced Oscillatory Parameters of the Canine Respiratory System with Altered Vagal Tone," IEEE Trans.on Biomed.Eng., Vol.BME-27(3), pp 146-149, March, 1980.
- Pimmel, R.L., Williams, S.P., Fullton, J.M., Tsai, M.J., Wintor, D.C. and Collier, A.M., "Respiratory Impedance and Derived Parameters in Small Children," University of North Carolina, An.Conf. for Eng. in Med. and Biol., pp 97-99, 1978.
- Plaut, D.I. and Webster, J.G., "Ultrasonic Measurement of Respiratory Flow," IEEE Trans.on Biomed. Eng., Vol.BME-27(10), pp 549-558, October, 1980.
- Plaut, D.I. and Webster, J.G., "Design and Construction of an Ultrasonic Pneumotachometer," IEEE Trans. on Biomed.Eng., BME-27(10), pp 590-597, October, 1980.
- Polgor, G. and Promadhat, V., Pulmonary Function Testing in Children : Techniques and Standards, W. Saunders Co., 1972.
- Precision Monolithics Full Line Catalogue, 1979, Precision Monolithics, Santa Clara, California.
- Primiano, F.P.(Jr), "Measurement of the Respiratory System," in Medical Instrumentation, Application and Design, Webster, J.G. (Ed), pp 434-510, Houghton Mifflin, Co., Boston, 1978.
- Prosser Scientific Instruments AVM 500 Series Air Velocity Meters Data Sheet.
- Radford, E.P., Jr, "Theory of Mechanical Artificial Respiration," in Artificial Respiration Theory and Applications, Wittenberger, J.I. (ed.), pp 156-172, Hoeber, New York, 1962.
- Radford, E.P.(Jr), "Static Mechanical Properties of Mammalian Lungs," Handbook of Physiol. : Respiration, Vol.I, Fenn, W.O. and Rahn, H;(Eds), pp 429-449, American Physiol. Soc., Washington, 1964.

- Norlander, O., Herzog, P., Nordén, I., Hossli, G., Schaefer, H. and Gattiker, R., "Compliance and Airway Resistance during Anaesthesia with Controlled Ventilation," Acta anaesth. Scand., Vol. 12, pp 135-152, 1968.
- Nunn, J.F., "A New Method of Spirometry Applicable to Routine Anaesthesia," Br. J. Anaesth., Vol. 28, pp 440-449, 1956.
- Okmian, L., "Artificial Ventilation by Respirator for Newborn Infants during Anaesthesia: A Method using a New Formula and a New Nomogram," Acta anaesth. Scand., Vol. 7, pp 31-57, 1963.
- Okmian, L., Wallgren, G. and Wahlin, A., "Artificial Ventilation by Respirator for Newborn and Small Infants during Anaesthesia: III. Mechanics of Ventilation," Acta anaesth. Scand., Vol. 10, pp 181-202, 1966.
- Okmian, L., Wallgren, G. and Wahlin, A., "Artificial Ventilation by Respirator for Newborn and Small Infants during Anaesthesia: IV. A Study of Two Methods for the Determination of the Pulmonary Ventilation and an Appraisal of the Ventilatory Standards Used," Acta anaesth. Scand., Vol. 10, pp 203-217, 1966.
- Okmian, L., "Artificial Ventilation by Respirator for Newborn and Small Infants during Anaesthesia," Acta anaesth. Scand., Suppl. 20, Vol. 10, 1966.
- Oliver, T.K., Demis, J.A. and Bates, G.D., "Serial Blood-Gas Tension and Acid-Base Balance during the First Hour of Life in Human Infants," Acta Paediatrica, Vol. 50, pp 346-359, May, 1961.
- Osborn, J.J., Elliot, S.E., Segyer, F.J. and Gerbode, F., "Continuous Measurement of Lung Mechanics and Gas Exchange in the Critically Ill," Medical Research Engineering, pp 19-23 and p 32, May-June, 1969.
- Osborn, J.J., "Cardiopulmonary Monitoring in the Respiratory Intensive Care Unit," Med. Instrum., Vol. 11(5), pp 278-282, 1977.
- Ostrander, L.E., Chester, E.H. and Franck, J.-B., "Fundamental Frequency Analysis of Pulmonary Mechanical Resistance and Compliance," J. Ap. Physiol., Vol. 35(4), pp 526-537, October, 1973.
- Otis, A.B., Fenn, W.O. and Rahn, H., "Mechanics of Breathing in Man," J. Ap. Physiol., Vol. 2, pp 592-607, 1950.
- Otis, A.B., "The Work of Breathing," Physiol. Rev., Vol. 34, pp 449-458, 1954.
- Otis, A.B., "The Work of Breathing," Handbook of Physiol. : Respiration, Vol. I, pp 463-476, Fenn, W.O. and Rahn, H. (Eds), American Physiol. Soc. Washington, 1964.
- Owen-Thomas, J.B., Ulan, O.A. and Swyer, P.R., "The Effect of Varying Inspiratory Gas Flow Rate on Arterial Oxygenation during IPPV in the Respiratory Distress Syndrome," Brit. J. Anaesth., Vol. 40, pp 493-501, 1968.
- Parker, G.A. and Hay, A.E., "A Planar Fluidic Flowmeter Applicable to Respiratory Flows," Trans. of ASME : J. Dynamic Systems, Measurement and Control, pp 293-299, December, 1977.
- Paton, J.S., Shaw, A. and MacDonald, T.H., "A Comprehensive Treatment Unit for the Respiratory Distress Syndrome in the Newborn," Biomed. Eng., pp 214-216, June, 1976.
- Pedley, T.J., Schroter, R.C. and Sudlow, M.F., "Energy Losses and Pressure Drop in Models of Human Airways," Respiration Physiology, 9, pp 371-386, 1970, North Holland Pub. Co., Amsterdam.

Singh, R. and Schary, M., "Acoustic Impedance Measurement using Sine Sweep Excitation and Known Volume Velocity Technique," J. Acoust. Soc. Am., Vol. 64(4), pp 995-1003, October, 1978.

Smith, P.C., Schach, E. and Daily, W.J., "Mechanical Ventilation of Newborn Infants : II. Effects of Independent Variation of Rate and Pressure on Arterial Oxygenation of Infants with Respiratory Distress Syndrome," Anesthesiology, Vol. 37(5), pp 498-502, 1972.

Smith, R.M., Anaesthesia for Infants and Children, 2nd edit. 1963, and 3rd edit. 1968, C.V. Mosby, Pub. Co.

Smith, W.D.A., "The Effects of External Resistance to Respiration, Part I : General Review," Brit. J. Anaesth., Vol. 33, pp 549-554, 1961.

Smith, W.D.A., "The Effects of External Resistance to Respiration, Part II : Resistance to Respiration due to Anaesthetic Apparatus," Brit. J. Anaesth., Vol. 33, pp 610-627, 1961.

Smits, A.J. and Perry, A.E., "The Effect of Varying Resistance Ratio on the Behaviour of Constant-Temperature Hot-Wire Anemometers," J. Phys. E : Sci. Instrum., Vol. 13, pp 451-456, 1980.

Sonderquist, D., "Minimisation of Noise in Operational Amplifier Applications," Precision Monolithics Application Note 15, 1979. Precision Monolithics, Santa Clara, California.
Statham Pressure Transducers, Model P23 series, Data Sheet, Statham Instruments, California, February, 1967.

Stockert, J. and Nave, E.R., "Operational Amplifier Circuit for Linearizing Temperature Readings from Thermistors," IEEE Trans. on Biomed. Eng., Vol. BME-21, pp 188-190, March, 1974.

Strang, L.B., "Alveolar Gas and Anatomical Dead-Space Measurements in Normal Newborn Infants," Clin. Sci., Vol. 21, pp 107-114, 1961.

Swyer, P.R., Rulman, R.C. and Wright, J.J., "Ventilation and Ventilatory Mechanics in the Newborn," J. Ped., Vol. 56(5), pp 612-622, 1960.

Taroni, A. and Zanarini, G., "Dynamic Behaviour of Thermistor Flowmeters," IEEE Trans. on Industrial Electronics and Control Instrum., Vol. IECI-22, No. 3, pp 391-396, August, 1975.

Taylor, A., "Flow Measurement as an Afterthought," Measurement and Control, Vol. 9, pp 207-208, June, 1976.

Taylor, G., Larson, P. and Prestwich, R., "Unexpected Cardiac Arrest during Anaesthesia and Surgery," JAMA, Vol. 236(24), pp 2758-2760, December, 1976.

Thermometrics Thermistor Product Data, Thermometrics Inc., Edison, New Jersey.

Thermo-Systems Incorporated Technical Information Brochure, Minneapolis-St Paul, Minnesota.

Thung, N., Herzog, P., Christlieb, I.I., Thompson, W.M., Jr. and Dammann, J.F., "The Cost of Respiratory Effort in Postoperative Cardiac Patients," Circulation, Vol. XXVIII, pp 552-559, October, 1963.

Todres, I.D., Rodgers, M.C., Shannon, D.C., Moylan, F.M.B. and Ryan, J.F., "Percutaneous Catheterisation of the Radial Artery in the Critically Ill Neonate," J. Paediatrics, Vol. 87(2), pp 273-275, 1975.

Torri, G., Damia, G., Ravagnon, R. and Levi, E., "A Graphical Analysis of the Respiratory Mechanics during I.P.P.R. and I.P.P.N.R.," Acta anaesth. Scand., Suppl. 23, pp 224-232, 1966.

Tsai, M.-J. and Pimmel, R.L., "Computation of Respiratory Resistance, Compliance and Inertance from Forced Oscillatory Impedance Data," IEEE Trans. on Biomed. Eng., Vol. BME-26(8), pp 492-493, August, 1979.

van der Hegge Zijnen, B.G., "Modified Correlation Formulae for the Heat Transfer by Natural and Forced Convection from Horizontal Cylinders," Ap.Sci.Res., Vol.A.6, pp 129-140, 1956.

van de Woestijne, K.P., "The Human Respiratory System," CRC Handbook of Engineering in Medicine and Biology, Sect.B., Instruments and Measurements, pp 93-116, Chemical Rubber Co., 1978.

Varene, P. and Jacquemin, Ch., "Airways Resistance : A New Method of Computation," in Airways Dynamics Physiology and Pharmacology, Bouhays, A., (Ed), Charles C. Thomas, Springfield, Illinois, 1970, p 99. (Not seen. As quoted in reference [30].)

Victory Engineering Catalogue MGP 681 REV 6-78 Condensed Catalogue : Thermistors/Varistors, Victory Engineering, Springfield, New Jersey, U.S.A., 1978.

Visick, W.D., Fairley, H.B. and Hickey, R.F., "Evaluation of a New Electronic Spirometer," Anaesthesiol., Vol.34, pp 475-478, 1971.

Walker, C.H.M., "Impedance Respiratory Monitoring in the Newborn Infant," Biomed.Eng., pp 454-459, October, 1978.

Weidman, P.D. and Browand, F.K., "Analysis of a Simple Circuit for Constant Temperature Anemometry," J.Phys.E : Sci.Instrum., Vol.8, pp 553-560, 1975.

Westgate, H.D., Gordon, J.R. and van Bergen, F.H., "Changes in Airway Resistance Following Intravenously Administered d.Tubocurrarine," Anaesthesiol., Vol.25(1), pp 65-73, 1962.

Wever, A.M.J., Britton, M.G. and Hughes, D.D.T., "Evaluation of Two Spirometers," Chest, Vol.70(2), pp 244-250, August, 1976.

White, D.F., Rodely, A.E. and McMurtrie, C.L., "The Vortex Shedding Flowmeter," Symposium on Flow, pp 967-974, 2-16-187, Pittsburgh, Pa, 1971.

Wilson, F.J. and Bone, R.C., "Monitoring Respiratory Function in Acute Respiratory Failure," Pulmonary Disease Reviews, (Ed.) R.C. Bone, Vol.1, pp 431-447, John Wiley, 1980.

Wilson, R.S., "Monitoring the Lung : Mechanics and Volume," Anesthesiology, Vol.45(2), August, 1976.

Wittenberger, J.L. (Ed.), Artificial Respiration Theory and Applications, Hoeber, New York, 1962.

Wright, B.M., "A Respiratory Anemometer," J.Physiol., Vol.127, (25 p from Proc.Physiol.Soc. 12-13 Nov., 1954), 1955.

Wright, P.H., "The Coanda Meter - a Fluidic Digital Gas Flowmeter," J.Phys.E : Sci.Instrum., Vol.13, pp 433-436, 1980.

Wohl, M.E.B., Stigal, L.C. and Mead, J., "Resistance of the Total Respiratory System in Healthy Infants and Infants with Bronchiolitis," Pediatrics, Vol.43(4), pp 495-509, 1969.

Yoo, J.H.K., Hander, E.W. and Petroff, P.A., "Implementation of Computation Algorithms for Pulmonary Mechanics on a Programmable Calculator," Med.and Biol.Eng. and Computing, pp 528-533, September, 1977.

Zanker, K.J., "Flare Gas Flow Measurement," - the Agar FM 700 series flowmeters, Pulse, pp 26-28, August, 1979.

Zwart, A., Seagrave, R.C. and van Dieren, A., "Ventilation-Perfusion Ratio obtained by a Non-Invasive Frequency Response Technique," J.Ap.Physiol., Vol.41(3), pp 419-424, September, 1976.